



Kay, Emily (2020) *An epigenetic switch links stromal pyruvate dehydrogenase activation to extracellular matrix production via proline synthesis*. PhD thesis.

<https://theses.gla.ac.uk/79034/>

Copyright and moral rights for this work are retained by the author

A copy can be downloaded for personal non-commercial research or study, without prior permission or charge

This work cannot be reproduced or quoted extensively from without first obtaining permission in writing from the author

The content must not be changed in any way or sold commercially in any format or medium without the formal permission of the author

When referring to this work, full bibliographic details including the author, title, awarding institution and date of the thesis must be given

Enlighten: Theses

<https://theses.gla.ac.uk/>
research-enlighten@glasgow.ac.uk

An epigenetic switch links stromal pyruvate dehydrogenase activation to extracellular matrix production via proline synthesis

Emily Kay (MSci)

Submitted in fulfilment of the requirements for the degree
of Doctor of Philosophy

Cancer Research UK Beatson Institute
College of Medical, Veterinary and Life Sciences
University of Glasgow
September 2019



University
of Glasgow

Abstract

Cancer associated fibroblasts (CAFs) are known to influence tumour progression through the secretion of factors which influence tumour growth and invasion. Collagen production is a major aspect of the secretory CAF phenotype. High collagen content in breast cancer is a marker of poor prognosis and is known to promote tumour growth and metastasis, as well as impeding drug delivery to the tumour through reduced perfusion. Tumour metabolism is also well established as a hallmark of cancer, however, how the metabolism of CAFs influences their pro-tumourigenic phenotype is not yet well understood.

We investigated metabolic differences between paired CAFs and normal fibroblasts (NFs) from breast tissue. Using an unbiased phosphoproteomic analysis, we identified pyruvate dehydrogenase kinase 2 (PDK2) as the most downregulated kinase in CAFs. PDK2 phosphorylates and deactivates pyruvate dehydrogenase (PDH), which is a key metabolic protein that converts pyruvate to acetyl-CoA in the mitochondria, providing a key link between the major metabolic pathways of glycolysis and the TCA cycle. However, extensive metabolic profiling of CAFs and NFs did not reveal metabolic differences that could be attributed to PDH activity.

Acetyl-CoA is also used for protein acetylation, and, using an MS-proteomic approach, we discovered increased histone acetylation in CAFs, which has epigenetic implications for how CAFs regulate their activated phenotype. Using a combination of proteomics, metabolomics, in vitro assays and imaging analyses we investigated the role of PDH-mediated histone acetylation in CAFs and uncovered the importance of histone acetylation in regulating collagen and ECM production by CAFs. PDH activity also regulated PYCR1 expression in CAFs, and we further discovered that proline production by PYCR1 is further required to maintain PDH-activity induced collagen synthesis in CAFs. Our findings open up new possibilities for targeting the desmoplastic stroma to reduce tumour growth and metastasis, and improve drug delivery.

Table of Contents

List of Tables	6
List of Figures	7
Acknowledgements	10
Author's declaration.....	11
Abbreviations	12
Chapter 1 Introduction.....	14
1.1 Cancer associated fibroblasts in the tumour microenvironment	14
1.1.1 The tumour microenvironment.....	14
1.1.2 The origins and definition of cancer associated fibroblasts.....	16
1.1.3 The pro-tumourigenic phenotype of CAFs	18
1.1.4 CAFs in breast cancer.....	23
1.2 The role of CAF-derived ECM in cancer	28
1.2.1 Properties of the extracellular matrix	28
1.2.2 An overview of collagen.....	29
1.2.3 Features and properties of CAF-derived ECM	30
1.2.4 CAF-derived ECM sustains and promotes tumour development	31
1.3 Epigenetic control of collagen and ECM production.....	36
1.3.1 Epigenetics	36
1.3.2 Regulation of CAF activation and fibrotic collagen production by epigenetics.....	37
1.4 CAF metabolism	40
1.5 The role of metabolism in collagen production.....	46
1.6 An overview of PDH and PYCR1 and their roles in cancer	49
1.6.1 Pyruvate dehydrogenase	49
1.6.2 Regulation of PDH phosphorylation.....	52
1.6.3 Regulation of PDH activity by acetylation	54
1.6.4 The varied roles of PDH	54
1.6.5 PDH activity in cancer	59
1.6.6 PYCR1 and proline metabolism.....	61
1.6.7 PYCR1 in cancer	64
1.8 Objectives	69
Chapter 2 Materials and Methods	70
2.1 Materials.....	70
2.1.1 Reagents and kits	70
2.1.2 Buffers and solutions	73
2.1.3 Antibodies.....	74

2.1.4 Primers.....	75
2.1.5 Small interfering RNA	76
2.1.6 Short hairpin RNA.....	77
2.1.7 Plasmids.....	78
2.2 Methods	79
2.2.1 Cell lines and culture	79
2.2.1.1 iCAFs and iNFs	79
2.2.1.2 pCAFs and pNFs	79
2.2.1.3 Cell culture.....	80
2.2.2 Cell based assays	80
2.2.2.1 EdU proliferation assay (Immunofluorescence)	80
2.2.2.2 EdU proliferation assay (Flow Cytometry)	81
2.2.2.3 PDH activity assay	81
2.2.2.4 Seahorse assay	81
2.2.2.5 Bioanalyzer assay.....	82
2.2.2.6 Flow cytometry analysis of mitochondrial probes	82
2.2.3 Transient transfection and lentiviral infection.....	83
2.2.3.1 Fibroblast transfection	83
2.2.3.3 Stable expression of shRNA in fibroblasts.....	83
2.2.3.4 ECM production	83
2.2.5 Western blotting analysis.....	84
2.2.5.1 Protein quantification	84
2.2.5.2 SDS Page and Western blotting	84
2.2.6 Immunofluorescence	85
2.2.6.1 2D cell cultures	85
2.2.6.2 Xenograft tumour sections	85
2.2.7 Image analysis.....	85
2.2.8 Bacterial transformation and plasmid generation	86
2.2.9 CNA35-mCherry purification	86
2.2.10 RNA extraction and RT-PCR.....	87
2.2.10.1 RNA extraction	87
2.2.10.2 cDNA synthesis.....	87
2.2.10.3 RT-PCR.....	88
2.2.11 MS-Metabolomics analysis.....	88
2.2.11.1 Sample preparation for intracellular metabolomics	88
2.2.11.2 Q-Exactive acquisition.....	88
2.2.11.3 Analysis of metabolomics data	89

2.2.12 Sample preparation for MS-proteomics	89
2.2.12.1 In solution digestion	89
2.2.12.2 In gel digestion	90
2.2.12.2 StageTip desalting.....	91
2.2.12.2 SILAC labelling	91
2.2.12.3 Acetylome enrichment	91
2.2.13 Mass spectrometer set up	92
2.2.13.1 Nano liquid chromatography.....	92
2.2.13.2 Q-Exactive HF acquisition	93
2.2.13.3 Orbitrap Fusion Lumos acquisition.....	93
2.2.14 Proteomic data analysis	93
2.2.14.1 Data processing with MaxQuant	93
2.2.14.2 Perseus data analysis	94
2.2.15 Xenografts of MCF10DCIS.com cells and CAFs.....	97
Chapter 3 Pyruvate dehydrogenase activity is upregulated in mammary CAFs.....	98
3.1 Characterisation of CAFs and NFs.....	98
3.2 Predicting kinase activity in iCAF and iNF.....	102
3.3 Pyruvate dehydrogenase is less phosphorylated in CAFs	106
3.4 PDK2 regulates PDH phosphorylation.....	108
3.4.1 PDK2 expression is downregulated in CAFs	108
3.4.2 PDK2 expression regulates PDH phosphorylation	109
3.5 PDH is more active in CAFs	114
3.5.1 The PDH complex is more active in CAFs in an <i>in vitro</i> assay	114
3.5.2 CAFs produce more acetyl-coA in a PDH phosphorylation-dependent manner	114
3.6 Investigation of PDK2 regulation in CAFs	118
3.7 Conclusions.....	124
Chapter 4 PDH activity regulates histone acetylation in CAFs	126
4.1 PDH is localised in the mitochondria	126
4.2 There is no difference in glycolysis or oxidative phosphorylation between CAFs and NFs	128
4.2.1 There are no differences in uptake or secretion of major metabolites between CAF and NFs.....	128
4.2.2 MS-metabolomic tracing experiments show few differences between CAFs and NFs	133
.....	139
4.2.3 Glutamine is the main source of TCA cycle metabolites in CAFs and NFs ...	140

4.2.4 CAFs have decreased mitochondrial functionality and are more autophagic than NFs	143
4.2.5 PDH activity does not affect mitochondrial functionality	147
4.3 ATP-citrate lyase is active in CAFs	150
4.4 PDH derived acetyl-coA is not used to fuel increased lipid synthesis	152
4.5 Histones are more acetylated in iCAF s	154
4.6 H3K27 acetylation is regulated by PDH dependent acetyl-coA production	159
4.6.1 H3K27 is more acetylated in CAFs than NFs	159
4.6.2 H3K27 acetylation is regulated by acetyl-coA availability	159
4.6.3 PDH activity regulates H3K27 acetylation	160
4.7 Discussion	167
Chapter 5 H3K27 acetylation regulates collagen production in CAFs	174
5.1 MS-proteomic analysis of c646 treated CAFs	174
5.2 c646 regulates collagen expression in CAFs	179
5.3 Acetyl-coA availability regulates collagen production in CAFs	185
5.3.1 ACLY inhibition reduces collagen production in CAFs	185
5.3.2 Acetate increases collagen production in NFs	190
5.4 PDH activity regulates collagen production in fibroblasts	193
5.5 Discussion	196
Chapter 6 6 Upregulated proline synthesis in CAFs promotes collagen production	201
6.1 c646 regulates PYCR1 expression	201
6.2 PYCR1 expression is regulated by acetyl-coA	205
6.3 PYCR1 expression is regulated by PDH activity	208
6.4 PYCR1 expression regulates proline production	210
6.4.1 PYCR1 knockdown reduces intracellular proline	210
6.4.2 Acetyl-coA regulates proline production	211
6.5 PYCR1 produces proline for collagen production	216
6.6 PYCR1 regulates collagen production	218
6.7 <i>in vivo</i> co-transplantation of CAFs and MCF10DCIS.com cells	224
6.8 Discussion	227
Chapter 7 7 Discussion and Future work	233
7.1 Discussion	233
7.2 Future Work	248
Chapter 8 References	253

List of Tables

Table 2-1 Reagents and kits.....	69
Table 2-2 Buffers and solutions.....	72
Table 2-3 Antibodies and dilutions.....	73
Table 2-4 Primers.....	74
Table 2-5 Small interfering RNAs.....	75
Table 2-6 Small hairpin RNAs	76
Table 2-7 Plasmids.....	77

List of Figures

Figure 1-1 CAFs are highly secretory cells	21
Figure 1-2 Reaction catalysed by PDC.....	51
Figure 1-3 Acetyl-coA is a central metabolite	58
Figure 1-4 Proline synthesis pathway.....	62
Figure 1-5 Metabolic impact of proline synthesis.....	67
Figure 3-1 Patient derived CAFs express the fibroblast marker vimentin.....	100
Figure 3-2 CAFs express more α SMA than NFs.....	101
Figure 3-3 Visualisation of predicted kinase activity in iCAF and iNFs	104
Figure 3-4 Phosphoproteomic data of iCafs and iNFs highlighting PDH phospho-sites ..	105
Figure 3-5 PDHA1 phosphorylation in CAFs and NFs.....	107
Figure 3-6 PDK expression in CAFs and NFs.....	111
Figure 3-7 PDK2 regulated PDH phosphorylation	112
Figure 3-8 PDK expression in normal and tumour-associated stroma.....	113
Figure 3-9 PDH complex activity in CAF and NFs	116
Figure 3-10 PDH activity regulates acetyl-coA in fibroblasts	117
Figure 3-11 TGFB and cancer cell conditioned media do not activate PDH	120
Figure 3-12 Akt inhibitor increases PDH phosphorylation	121
Figure 3-13 CAF ECM decreases PDH phosphorylation	122
Figure 3-14 CAF ECM decreases PDK2 expression.....	123
Figure 4-1 PDH is mitochondrial in CAFs.....	127
Figure 4-2 Metabolic flux of CAFs and NFs in normoxia/high glucose conditions	130
Figure 4-3 Metabolic flux of CAFs and NFs in hypoxia	131
Figure 4-4 Metabolic flux of CAFs and NFs cultured in low glucose media	132
Figure 4-5 13 C-Glucose labelling of glycolytic metabolites.....	135
Figure 4-6 13 C-Glucose labelling of TCA cycle metabolites.....	136
Figure 4-7 13 C-Glucose labelling of non-essential amino acids	137
Figure 4-8 13 C-Glucose labelling of acetylated metabolites.....	138
Figure 4-9 NADH:NAD ⁺ ratio in CAFs and NFs	139
Figure 4-10 13 C labelling of glycolytic metabolites.....	141
Figure 4-11 13 C labelling of TCA cycle metabolites.....	142
Figure 4-12 Mitochondrial content of CAFs and NFs.....	145
Figure 4-13 LCB-II accumulation in iCafs and iNFs.....	146
Figure 4-14 Oxygen consumption rate (OCR) of CAFs and NFs.....	149
Figure 4-15 p-ACLY levels in NFs and CAFs	151
Figure 4-16 Lipid metabolism in iNFs and iCafs	153
Figure 4-17 iCAF vs iNF acetylome	156

Figure 4-18 One-dimension enrichment analysis of acetylome data	157
Figure 4-19 Regulatory acetylated sites	158
Figure 4-20 H3K27 is more acetylated in CAFs	162
Figure 4-21 H3K27 acetylation is regulated by ACLY inhibition	163
Figure 4-22 H3K27 acetylation is regulated by PDK2 expression.....	164
Figure 4-23 H3K27 acetylation is regulated by PDK2 expression.....	166
Figure 5-1 c646 reduces H3K27 acetylation.....	176
Figure 5-2 c646 downregulates collagen proteins.....	177
Figure 5-3 Collagens are highly abundant in iCAF ECM.....	178
Figure 5-4 c646 reduces collagen expression at the mRNA level	181
Figure 5-5 c646 reduces collagen levels in the ECM	182
Figure 5-6 c646 reduces collagen production by CAFs	183
Figure 5-7 c646 reduces collagen production in CAF/Cellaria-Wood co-cultures	184
Figure 5-8 BMS303141 reduces collagen in CAF-derived ECM	187
Figure 5-9 BMS303141 reduces collagen production in CAF/Cellaria-Wood co-cultures	188
Figure 5-10 BMS303141 reduces collagen expression at the mRNA level	189
Figure 5-11 Acetate increases H3K27 acetylation in NFs	191
Figure 5-12 Acetate increases collagen expression in NFs.....	192
Figure 5-13 PDK2 expression regulates collagen production in fibroblasts.....	194
Figure 5-14 PDK2 expression regulates collagen mRNA in fibroblasts.....	195
Figure 5-15 c646 downregulates ECM proteins	199
Figure 5-16 c646 downregulates proteins involved in proline and collagen synthesis..	200
Figure 6-1 c646 reduces PYCR1 expression	203
Figure 6-2 Proline synthesis enzymes are upregulated in tumour-associated stroma ..	204
Figure 6-3 PCYR1 expression is regulated by extra-mitochondrial acetyl-coA.....	206
Figure 6-4 PCYR1 expression is regulated by extra-mitochondrial acetyl-coA.....	207
Figure 6-5 PYCR1 expression is regulated by PDK2 levels.....	209
Figure 6-6 Proline synthesis is regulated by PYCR1 expression	212
Figure 6-7 PYCR2 does not compensate for PYCR1	213
Figure 6-8 Proline synthesis is regulated by PYCR1 expression	214
Figure 6-9 Proline synthesis is regulated by acetyl-coA levels.....	215
Figure 6-10 PCYR1 produces proline for collagen synthesis	217
Figure 6-11 Collagen production is regulated by PCYR1 expression.....	220
Figure 6-12 Collagen production is regulated by PYCR1 expression.....	221
Figure 6-13 Collagen production is regulated by PYCR1 expression.....	222
Figure 6-14 PYCR1 is required for PDH activity-induced collagen production	223
Figure 6-15 Stromal PYCR1 promotes tumour growth	225
Figure 6-16 PCYR1 promotes collagen production in vivo	226

Figure 6-17 Proline synthesis pathway is upregulated in ovarian stroma	231
Figure 6-18 Proline synthesis pathway is upregulated in TGF-B treated fibroblasts	232
Figure 7-1 Sources of alpha-ketoglutarate	241
Figure 7-2 Expression of PDK, proline synthesis and collagen genes in CAF subpopulations	247

Acknowledgements

First and foremost I would like to thank my supervisor, Prof. Sara Zanivan, for giving me the opportunity to work on this project and for all her invaluable guidance, support and discussion throughout my PhD. Many thanks also go to the members of our lab, past and present, for their support and assistance: Lisa Neilson, Dr. Sam Atkinson, Dr. Alice Santi, Ilaria Puoti, Dr. Dave McGarry, Claudia Boldrini Fernanda Kugeratski, Steven Reid and Dr. Juan Ramon Hernandez-Fernaud. In particular, I would like to thank Juan who carried out the original phosphoproteomics study that inspired this project, Lisa for her work in isolating the patient derived fibroblasts and Claudia who contributed to the MS-acetylomics study.

I would like to thank my second supervisor, Dr. Karen Blyth for her helpful discussions and input, and also for her assistance with the *in vivo* experiment, along with Sandeep Dhayade. I would also like to thank Dr. Sergio Lilla and Kelly Hodge for their assistance with the MS-proteomics experiments, and to Dr. David Sumpton, Dr. Gio Rodriguez-Blanco and Dr. Gillian Mackay for their assistance with the MS-metabolomics experiments. Thanks to Grace McGregor and Dr. Jurre Kamphorst for their contribution to the lipidomics experiments, and to Dr. Frederic Fercoq and Ewan McGhee for their assistance with imaging tumour sections. Thanks to all of the Beatson services that have supported my research. Thanks also go to our external collaborators who have provided data for this thesis: Enio Gjerga, Dr. Julio Saez-Rodriguez and Dr. Morag Park.

I would like to thank Cancer Research UK for providing the funding for this PhD and to the University of Glasgow for giving me the opportunity to work here. Finally, I would like to thank my family and friends for all the support and encouragement they have given me throughout the course of my studies. Particular thanks go to Coffee Club for the chat and cake-based support.

Author's declaration

I declare that this thesis is the result of my own work, unless otherwise stated, and no part of this work has been submitted for any other degree at the University of Glasgow, or any other institution

Emily Kay

Abbreviations

ACN	Acetonitrile
AcCoA	Acetyl coA
ACLY	ATP citrate lyase
AKT	Protein kinase B
ALDH18A1	Aldehyde Dehydrogenase 18 Family Member A1
α SMA	Alpha smooth muscle actin
ATP	Adenosine triphosphate
BRD	Bromodomain
BSA	Bovine serum albumin
CAF	Cancer associated fibroblast
CAV-1	Caveolin-1
cDNA	Complementary Deoxyribonucleic acid
COL1A1	Collagen I A1
COL6A1	Collagen VI A1
CNA35	Collagen adhesion binding protein 35
DAPI	4',6-diamidino-2-phenylindole
DMEM	Dulbecco's Modified Eagle Medium
DMSO	Dimethyl sulfoxide
DNA	Deoxyribonucleic acid
DTT	Dithiothreitol
E. Coli	Escherichia Coli
ECM	Extracellular matrix
EdU	5-ethynyl-2'-deoxyuridine
EMT	Epithelial to mesenchymal transition
EP300	E1A Binding Protein P300
FBS	Foetal bovine serum
FDR	False discovery rate
FN	Fibronectin
GAPDH	Glyceraldehyde 3-phosphate dehydrogenase
GC-MS	Gas chromatography tandem mass spectrometry
H3	Histone 3
H3K27	Histone 3 lysine 27
H3K27ac	Histone 3 lysine 27-acetylated
HAT	Histone acetylase
HDAC	Histone deacetylase
HPLC	High performance liquid chromatography
hTERT	Human Telomerase reverse transcriptase
IDH	Isocitrate dehydrogenase
IPTG	Isopropyl β -D-1-thiogalactopyranoside
KO	Knockout
LC-MS	Liquid chromatography tandem mass spectrometry
MEF	Mouse embryonic fibroblast
MMP	Matrix metalloprotease

MOPS	(3-(N-morpholino)propanesulphonic acid)
MS	Mass spectrometry
NAD ⁺	Nicotinamide adenine dinucleotide (oxidised)
NADH	Nicotinamide adenine dinucleotide (reduced)
NF	Normal fibroblast
OAT	Ornithine aminotransferase
OXPPOS	Oxidative phosphorylation
PBS	Phospho-buffered saline
PDAC	Pancreatic ductal adenocarcinoma
PDH	Pyruvate dehydrogenase
PDHA1	Pyruvate dehydrogenase subunit A1
pPDHA1	Phosphorylated Pyruvate dehydrogenase subunit A1
PDC	Pyruvate dehydrogenase complex
PDGF	Platelet derived growth factor
PDK1	Pyruvate dehydrogenase kinase 1
PDK2	Pyruvate dehydrogenase kinase 2
PDK3	Pyruvate dehydrogenase kinase 3
PDK4	Pyruvate dehydrogenase kinase 4
PDP1	Pyruvate dehydrogenase phosphatase 1
PDP2	Pyruvate dehydrogenase phosphatase 2
PE	PBS containing EDTA
PFA	Paraformaldehyde
PRODH	Proline dehydrogenase
PYCR1	Pyrroline-5-Carboxylate Reductase 1
PYCR2	Pyrroline-5-Carboxylate Reductase 2
RNA	Ribonucleic acid
ROS	Reactive oxygen species
RT	Room temperature
RT-PCR	Real time-polymerase chain reaction
SDS	Sodium dodecyl sulphate
siRNA	Small interfering RNA
shRNA	Short hairpin RNA
TBP2	Tata binding protein 2
TCA cycle	Tricarboxylic acid cycle
TFA	Trifluoroacetic acid
TGF- β	Transforming growth factor beta
TME	Tumour microenvironment
TMRE	Tetramethylrhodamine ethyl ester
TNBC	Triple negative breast cancer

Chapter 1 Introduction

1.1 Cancer associated fibroblasts in the tumour microenvironment

1.1.1 The tumour microenvironment

Tumours do not exist only as an isolated mass of tumour cells, but must exist in an already present complex body; indeed tumours utilise their surrounding tissues to provide them with a wide range of factors which they require to grow and progress. Whereas initial research on cancer as a disease focussed on targeting the tumour cells themselves, in more recent decades it has become clear that the cells and tissue surrounding the tumour, known as the 'tumour microenvironment' (TME), is a key targetable feature of the tumour. The TME is inseparably intertwined with the fate of the tumour through a complex array of interactions and crosstalk between different cell types and extracellular matrix (ECM), such that a tumour can be considered as a new and separate organ, albeit an abnormally functioning one (Egeblad et al., 2010).

Tumour cells recruit and activate cells from their surrounding tissue via the secretion of growth factors, chemokines and cytokines. For example, VEGF secreted by tumour cells stimulates blood vessel sprouting (Carmeliet, 2005), which is a critical step in tumour vascularization. Intratumoural blood vessels are important for tumour development because in order to grow the tumour needs to develop its own supply of oxygen and nutrients, as well as providing tumour cells with a means of dissemination into the blood stream to form distant metastases. Tumours also create an immunosuppressive environment to evade being targeted by the immune system. For example, secretion of cytokines, such as IL-23, CXCL5, CXCL7, IL-1 β , IL-6, CCL2 and CCL9, recruit immunosuppressive macrophages, neutrophils and CD4⁺ T cells to the tumour, while repelling immunoactive NK, B and CD8⁺ T cells (Koyama et al., 2016, Rabinovich et al., 2007, Kortlever et al., 2017). Additionally, tumours secrete factors including IL-4 and IL-13 to polarise macrophages from the immunoactive M1 phenotype to the immunosuppressive M2 (Aras and Zaidi, 2017). Finally, cancer associated fibroblasts (CAFs) are highly abundant in the TME. CAFs have a highly secretory phenotype themselves that

promotes tumour growth, progression, and metastasis, and have been shown to be recruited and activated through a combination of growth factors and cytokines including TGF- β , TNF- α , PDGF and FGF2 (LeBleu and Kalluri, 2018), as well as signalling proteins such as Wnt (Avgustinova et al., 2016) and integrin mediated interactions with the ECM (Franco-Barraza et al., 2017).

Therapeutically, targeting the TME has a number of advantages. Since cells of the TME are more genetically stable than tumour cells, they are less likely to gain resistance to therapies. Furthermore, the tumour microenvironment may provide support to tumour cells which enables them to overcome traditional cytotoxic therapies, and also reduces efficient drug delivery due to the leaky vasculature and increased interstitial fluid pressure (Joyce, 2005). Combination therapies combining standard chemotherapy with tumour microenvironment targeting drugs have been particularly successful in the clinic. For example, using the anti-VEGF antibody Avastin to normalise the tumour vasculature in combination with standard chemotherapy has shown benefits and is an approved line of treatment in some colorectal, breast and non-small cell lung cancers (Sini et al., 2016, Hurwitz, 2004, Sandler et al., 2006), and the anti B1-integrin antibody P5, which targets interactions between tumour cells and the ECM, has reached stage III clinical trials in combination with cisplatin for treatment of non-small cell lung cancer (Kim et al., 2016). Of recent years, targeting the immune response in tumours has been a breakthrough in cancer treatment, with the recent completion of several phase II or III trials combining checkpoint inhibitors with standard chemotherapy in lung, HNSCC and breast cancers (Gandhi et al., 2018, Bauml et al., 2017, Schmidt, 2019). Two immunotherapies have also recently been approved for treatment of acute myeloid leukaemia and diffuse-large B cell lymphoma (Maude, 2018, Schuster and Investigators, 2019). Therefore understanding the mechanisms that regulate the pro-tumourigenic microenvironment has led to the development of important anti-cancer therapies, and is vital to gain insight into potential vulnerabilities of the tumour. During my PhD I focussed on how the pro-tumourigenic phenotype of CAFs is regulated, and therefore in the following sections I will describe in more detail the fundamental role of CAFs in the TME and the myriad of ways in which they promote tumour progression.

1.1.2 The origins and definition of cancer associated fibroblasts

Fibroblasts are found throughout the body as cells whose primary function is to continuously secrete ECM to maintain the structure of connective tissues. Fibroblasts secrete components of the fibrillar ECM and basement membrane, including collagens, fibronectin and laminin (Tomasek et al., 2002, Rodemann and Muller, 1991), as well as matrix metalloproteases (MMPs) to regulate ECM turnover (Simian et al., 2001). Fibroblasts are also mediators of the wound healing response, providing new ECM deposition to act as a scaffold for wound closure, contractile forces to close the wound, pro-angiogenic factors to promote blood vessel formation and growth factors to promote cell proliferation (Darby et al., 2014). In order to carry out these functions, fibroblasts in a wound become 'activated', a state which is most often characterised by an increase in the cytoskeletal protein α -smooth muscle actin (α SMA) expression. A chronic wound healing response is also found in diseases of fibrosis and in tumours, since the continuously growing tumour causes persistent injury in the surrounding tissue. This has led to the description of tumours as 'wounds that do not heal' (Dvorak, 2015). In accordance with this, activated fibroblasts make up a significant component of tumours, where their wound healing phenotype is co-opted by the tumour to provide a stroma that promotes tumour growth and development.

The activation of quiescent fibroblasts into CAFs has been the subject of much study, with many different pathways being implicated. Undoubtedly the most widely known activating factor is transforming growth factor beta (TGF- β), which is produced initially by cancer cells and binds to the type 2 TGF- β receptor on CAFs, stimulating ECM production and secretion of paracrine signalling factors. TGF- β activation then is maintained by autocrine CAF signalling, creating a positive feedback loop of CAF activation (Ronnov-Jessen and Petersen, 1993, Kojima et al., 2010, Colak and Ten Dijke, 2017). Platelet derived growth factor (PDGF) is another CAF activating factor frequently secreted by tumour cells and has been shown to stimulate ECM production and fibroblast proliferation (Shao et al., 2000, Cadmuro et al., 2013). CAFs have also been shown to be activated by other secreted proteins including Wnt7a signalling (Avgustinova et al., 2016), and inflammatory TNF α , IL-1 β and IL-6 signalling (Giannoni et al., 2010, Katanov et al., 2015). In recent years, several studies have shown that tumour derived micro-

RNAs, which are transferred to CAFs via exosomes, also play a role in CAF activation (Fang et al., 2018, Pang et al., 2015, Dror et al., 2016). The physical alterations that occur in the tumour microenvironment can further contribute to CAF activation, such as increased mechanical stress, hypoxia and oxidative stress (Calvo et al., 2013, Toullec et al., 2010, Chiavarina et al., 2010, Martinez-Outschoorn et al., 2010a). Interestingly, hypoxia has also been shown to deactivate fibroblasts via loss of PHD2 (Madsen et al., 2015), so the role of hypoxia in fibroblast activation has yet to be elucidated. Therefore there is no single pathway that activates CAFs from normal fibroblasts, and the specific mechanism may depend on the tumour cells and other factors of the TME for each individual cancer.

In addition to being activated through a combination of different signalling pathways, CAFs can also be derived from a variety of different cell types. Although the majority of CAFs are likely to be derived from resident quiescent fibroblasts from the tissue of origin of the cancer, other cell types can also be recruited by the cancer and develop a CAF-like phenotype. Bone marrow mesenchymal stem cells are a popular source of CAFs, with reports showing that up to 20-25% of CAFs originate from the bone marrow in mouse models of pancreatic and gastric cancer (Ishii et al., 2003, Quante et al., 2011). In breast cancer models, bone marrow derived CAFs can form a separate CAF subpopulation which may even be more aggressive than CAFs derived from resident fibroblasts (Raz et al., 2018). Furthermore, Jotzu et al. demonstrated that adipocyte stem cells, which are known to interact with tumour cells, develop an α SMA positive, myofibroblast-like phenotype when treated with cancer cell conditioned media (Jotzu et al., 2010). TGF- β treatment of endothelial cells can induce a myofibroblastic phenotype (Zeisberg et al., 2007), and it has even been suggested that epithelial cells can develop into CAFs or activated fibroblasts through undergoing epithelial to mesenchymal transition (EMT) (Petersen et al., 2001, Iwano et al., 2002).

With such a varied array of origins and activation pathways, it is unsurprising that there is no common consensus for defined markers of CAFs. α SMA is the most commonly used CAF marker, both because it is a hallmark of upregulated TGF- β signalling, which as mentioned previously is one of the most well-defined pathways of CAF activation, and because α SMA expression is often equated with

the contractile, ECM producing myofibroblast phenotype. However, it has been demonstrated that not all contractile fibroblasts are α SMA positive (Sun et al., 2016). There are many other markers associated with activated fibroblasts including upregulation of vimentin, PDGFR α , fibroblast activating protein (FAP) and fibroblast specific protein (FSP-1), and downregulation of caveolin-1 (CAV1) and CD36. These markers do not always appear concurrently, and none of them are specific for cancer associated fibroblasts as they also label other cell types. Even α SMA is also highly expressed in pericytes (Kalluri, 2016). Therefore CAFs are a broad and heterogeneous group of cells, which can be recruited from a number of different cell types and activated by a combination of many different mechanisms. Perhaps this reflects the heterogeneity of the tumours themselves, as different tumours are likely to be able to utilise different pathways of CAF activation.

1.1.3 The pro-tumourigenic phenotype of CAFs

A multitude of studies have demonstrated that CAFs promote tumour progression, growth and metastasis. Early studies showed that isolated CAFs support tumour formation in vivo whereas normal fibroblasts do not (Olumi et al., 1999, Orimo et al., 2005) and are also more pro-invasive and pro-angiogenic (Dimanche-Boitrel et al., 1994, Fukumura et al., 1998) One of the key features of CAFs that distinguishes them from normal fibroblasts is their highly secretory phenotype which influences both tumour cells and other cell types of the TME (Fig. 1-1). CAFs have been shown to secrete several growth factors which stimulate tumour proliferation and metastasis. Among these are HGF, which has also been shown to promote chemoresistance, CTGF, EGF and IGF, secretion of which is upregulated under hypoxic conditions (Straussman et al., 2012, Ding et al., 2018, Tyan et al., 2011, Ren et al., 2015, Rozenchan et al., 2009) (Unger et al., 2017, Hirakawa et al., 2016). CAFs can also fuel tumour growth through secretion of metabolites such as lactate, ketones and amino acids (Martinez-Outschoorn et al., 2010) and stimulate growth, EMT and cell migration through cytokines such as IL-6 (Wu et al., 2017, Kinoshita et al., 2013).

A key group of secreted factors by CAFs is pro-angiogenic factors. CAFs are a major regulator of angiogenesis in the TME, which is vital to provide tumours with a

supply of oxygen and nutrients for growth, and also a means of metastasis. The excess of pro-angiogenic factors in the TME also creates a leaky and irregular network of blood vessels, which further promotes metastasis and impairs drug and oxygen delivery creating more aggressive tumours (Carmeliet and Jain, 2000). CAFs induce angiogenesis through secretion of VEGF, the most potent and well-known pro-angiogenic factor, as well as TGF- β , PDGF, SDF-1 and IL-6 (Nagasaki et al., 2014, Ferrara, 2010, Gomes et al., 2013). ECM remodelling due to the increased contractility of CAFs also increases vascularisation (Sewell-Loftin et al., 2017). Interestingly, stromal angiogenesis can preclude response to anti-VEGF treatment. A study found that tumours with blood vessels predominantly within the tumour cells responded better to the VEGF antibody bevacizumab either as a single therapy or in combination with traditional chemotherapy, as opposed to tumours with predominantly stromal blood vessels (Smith et al., 2013), suggesting that blood vessels stimulated by CAFs are more resistant to anti-angiogenic therapies.

CAF protein secretion also influences the immune response. Secretome and proteomic analyses of CAFs have revealed a highly immunomodulatory secretome (Torres et al., 2013, Ge et al., 2012). More in depth studies have shown that secretion of growth factors, cytokines and chemokines such as TGF- β , CCL2, CCL5, CXCL14, CXCL12, SDF1 and IL-6 promote M2 macrophage differentiation, recruit neutrophils and inhibit cytotoxic T-cells and natural killer cells (Comito et al., 2014, Takahashi et al., 2017, Castriconi et al., 2003, Ziani et al., 2018). Upregulated production and secretion of the prostaglandin PGE₂ also inhibits the anti-tumour immune response (Kalinski, 2012). Moreover, CAFs may account for the failure of some patients to respond to immunotherapy. In a mouse model of pancreatic ductal adenocarcinoma (PDAC), it was found that CXCL12 produced by FAP⁺ CAFs was preventing response to two checkpoint inhibitor therapies, despite the presence of tumour suppressive CD8⁺ T cells. Simultaneously treating tumours with a CXCL12 receptor inhibitor and the checkpoint inhibitor α -PD-L1 caused rapid recruitment of T-cells to the tumour and reduced tumour size (Feig et al., 2013). This study highlights the advantages of using combination therapies targeting the tumour microenvironment alongside the tumour cells to increase tumour sensitivity and response to drugs.

Another important aspect of the TME influenced by CAF secretion is the ECM, which I will expand upon in later sections. Briefly, CAFs upregulate secretion of ECM components including collagens, fibronectin and laminin, resulting in a thicker and stiffer desmoplastic stroma that promotes tumour growth and invasiveness (Naba et al., 2014, Alexander and Cukierman, 2016, Kai et al., 2019). Conversely, CAFs also secrete matrix metalloproteases (MMPs) which degrade the matrix and enable angiogenesis and tumour cell migration (Boire et al., 2005, Deryugina and Quigley, 2015). ECM also confers drug resistance through adhesion of cancer cells to the ECM and through compressing blood vessels so that perfusion is limited in the tumour (Hazlehurst and Dalton, 2001, Chauhan et al., 2013).

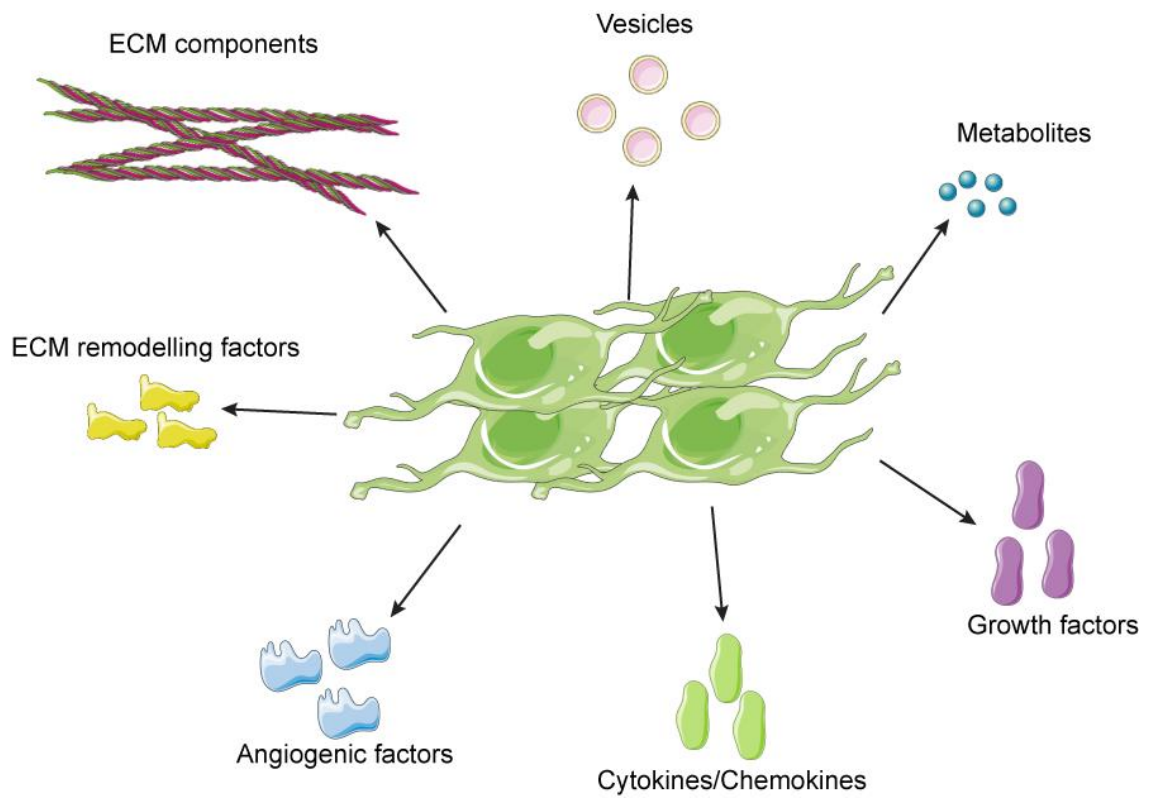


Figure 1-1 CAFs are highly secretory cells

Diagram showing the wide variety of secreted factors from CAFs. Images were adapted from <https://smart.servier.com/>

Although the majority of studies on CAFs demonstrate that they are pro-tumourigenic, several works have also demonstrated an anti-tumour effect of CAFs. Two studies in PDAC demonstrated a tumour suppressive role for CAFs. Depleting sonic hedgehog, which is a CAF activator, in a mouse model of PDAC actually increased tumour aggressiveness and vascularisation, showing that a high stromal content is not necessarily pro-tumourigenic (Rhim et al., 2014). Similarly, depleting α SMA⁺ cells in PDAC also increased tumour aggressiveness, (Ozdemir et al., 2014) suggesting that α SMA is not necessarily a marker of the pro-tumourigenic CAF phenotype. Patient derived mammary fibroblasts have been shown to express high levels of SLIT-2, which suppresses breast cancer cell invasion and is a predictor of better clinical outcome in patients (Chang et al., 2012). Once again, the heterogeneity of CAFs is evident in their functionality in addition to their origins and activation mechanisms.

In recent years, the heterogeneity of CAFs has been further expanded by the discovery of different subpopulations of CAFs which may co-exist in the same tumour. For example, Ohlund et al. distinguished between two spatially distinct subpopulations of contractile, α SMA high myCAF^s and proinflammatory iCAF^s in KPC tumours (Ohlund et al., 2017). Subsequent studies have identified four subpopulations in CAFs derived from breast tumours through the more high-throughput analysis techniques of single cell RNA-sequencing and flow cytometry analysis (Costa et al., 2018, Bartoschek et al., 2018). Still, α SMA expression and modulation of the immune response remain key distinguishing features between the different subtypes. In the Costa et al. study, it was shown that enrichment in breast tumours for either or both of two of their four defined subtypes was a predictor for subsequent metastasis, demonstrating the prognostic power of the stroma. Another recent study identified a subset of CAFs driving tumour growth as well as promotion of cancer stem cells and chemoresistance in lung and breast cancer. Usefully, these CAFs could be identified by the cell surface markers CD10 and GPR77, and were successfully targeted by an anti-GPR77 antibody, providing evidence that it may be possible to target specific tumour promoting CAF subpopulations (Su et al., 2018). There is also evidence to suggest that CAFs derived from different cell types contribute to functionally different subpopulations, as bone marrow derived CAFs and resident CAFs formed two distinct subpopulations defined by PDGFR expression in the MMTV-PyMT model

(Raz et al., 2018). In a review on CAFs, Kalluri postulates that there may be many subtypes including tumour restraining, tumour promoting, secretory and ECM-remodelling CAFs (Kalluri, 2016). As this is a relatively recent field of CAF research, it will be interesting to see what future developments there are in identification of CAF subpopulations, and what the implications are for trying to pharmacologically target the CAF phenotype.

So far, no drugs have been developed specifically to target CAFs, although pirfenidone has been approved to treat fibrotic fibroblasts, which have a similar activated, wound healing phenotype (Takeda et al., 2014). Drugs have also been developed that target aspects of the TME known to be regulated by CAFs, such as suramin, which targets ECM turnover and blocks FGF and PDGF signalling and has shown promising results in breast and prostate cancers (Cheng et al., 2019). Yet drugs specifically targeting CAF activation, such as Shh inhibitors and the anti-FAP antibody sibrotuzumab, have so far failed to show benefits in clinical trials. However, new therapies are constantly being developed. A vitamin D analogue which has been shown to deactivate CAFs in pancreatic cancer (Sherman et al., 2014) is currently being tested in clinical trials in combination with standard chemotherapy. CAFs have also been targeted with nanoparticles which both deactivate the CAFs and cause apoptosis of surrounding tumour cells (Miao et al., 2015). Therefore there is still much to be discovered about the pro-tumourigenic CAF phenotype and vulnerabilities for potential therapeutic treatment.

1.1.4 CAFs in breast cancer

During my PhD I focussed on mammary CAFs. Breast cancer is the most common cancer in women worldwide, and according to the world health organisation (WHO) over 600,000 women died from breast cancer in 2018. In high income countries such as Japan or the USA, the survival rate is around 80% due to early detection programmes as well as advances in diagnosis and treatment, whereas in low income countries the survival rate is halved to around 40%. However, even with up to 80% of patients able to be successfully treated, the 20% who are not are still make up a considerable number. In the UK, breast cancer accounts for 7% of all cancer deaths and worldwide for 15% of all cancer deaths, with the rate of breast cancer incidence and mortality increasing most rapidly in the developing

world. Therefore there is still a need for new targets and therapies, and for a greater understanding of the molecular mechanisms driving breast cancer.

The current system of patient classification for therapy is based on the standard clinical factors of tumour size, grade and presence of metastases, but also on breast cancer specific molecular markers. These consist of three receptors: the oestrogen receptor (ER), the progesterone receptor (PR) and the human epidermal growth factor receptor 2 (HER2). The system of classification was developed about twenty years ago by comparing gene expression data with clinical data from patient tumours (Perou et al., 2000, Sorlie et al., 2001). Five subtypes were identified: Normal-like (ER+ PR+ HER2-), Luminal A (ER+ PR+ HER2-), Luminal B (ER+ PR+ HER2+/-), HER2-amplified (ER- PR- HER2+) and Triple negative (ER- PR- HER2-). The ER+ and PR+ tumours have the best predicted outcome (Dunnwald et al., 2007) and usually respond to hormonal therapies, such as tamoxifen. Triple negative breast cancer (TNBC) has the worst prognosis, and there are currently no targeted therapies; the only options are standard chemotherapy, radiotherapy and surgery.

The stroma is an extremely important aspect of breast cancer. Breast cancers have a particularly high stromal component with up to 80% of fibroblasts being activated as defined by high α SMA expression (Sappino et al., 1988) and the presence of α SMA positive myofibroblasts is further correlated with decreased survival and higher proliferation of tumour cells in breast cancer (Surowiak et al., 2007). Other studies have also shown a correlation with a higher proportion of stroma in breast tumours with a poorer clinical outcome, especially in TNBC (de Kruijf et al., 2011, Moorman et al., 2012, Kramer et al., 2019). Furthermore, the gene signature of breast cancer stroma can serve as a prognostic marker. Using microdissected stroma from 53 breast cancer patients, Finak et al. formulated a set of 26 prognostic genes which, when applied to other data from independent studies, successfully predicted patient outcome (Finak et al., 2008). Further stromal prognostic markers in breast cancer have been identified, such as PDGFR expression (Paulsson et al., 2009) and ERK phosphorylation, which predicts tamoxifen resistance (Busch et al., 2012). Interestingly, one of the studies on CAF subpopulations also connected different CAF subpopulations with the different molecular subtypes of breast cancer, with enrichment of the immunosuppressive

CAF-S1 subtype in TNBC and enrichment of the myofibroblastic CAF-S4 subtype in HER2+ tumours (Costa et al., 2018). This suggests that, for example, the CAF-S1 subtype could be targeted to improve response to immunotherapies such as anti-PD-L1 treatment. Another intriguing recent study suggested that the stroma may play an active role in determining the molecular subtype of breast cancer. Targeting the signalling between PDGF producing basal-like carcinoma cells and the corresponding PDGF-receptor expressing CAFs transformed the cancers into a hormone receptor positive state, increasing their sensitivity to hormone therapy that they had previously shown resistance to (Roswall et al., 2018). Therefore breast cancer stroma plays a significant role in controlling patient outcome and is a potential therapeutic target.

The molecular mechanisms underpinning the pro-tumourigenic aspects of mammary CAFs have been studied in some detail. The classic tropes of high α SMA expression and TGF- β signalling are key features of mammary CAFs. Overexpression of TGF- β or HGF in mammary fibroblasts stimulated breast cancer initiation in mice (Kuperwasser et al., 2004), and TGF- β treatment of mammary fibroblasts resulted in increased expression of many ECM-remodelling and pro-tumourigenic proteins, including hyaluron synthase 2, fibulin-5, CTGF, podocalyxin and EphA2 in a proteomic study (Groessler et al., 2014). As well as being activated by TGF- β secreted by tumour cells, CAFs also produce their own TGF- β , and it has been shown that Wnt7a produced by breast cancer cells stimulates TGF- β production and signalling in CAFs (Avgustinova et al., 2016). After activation by TGF- β , mammary CAFs can maintain their myofibroblast activation through autocrine TGF- β and SDF1 signalling (Kojima et al., 2010). TGF- β signalling by mammary CAFs is an important aspect of their pro-tumourigenic phenotype. For example, TGF- β signalling is known to upregulate α SMA expression; and mammary CAFs overexpressing miR-200 to reduce α SMA expression and contractility formed smaller tumours in vivo (Tang et al., 2016). In co-culture experiments, TGF- β production by CAFs also stimulated EMT in breast cancer cell lines (Yu et al., 2014), which increased their metastatic potential. Furthermore, TGF- β activation in mammary CAFs stimulated CAF metabolic reprogramming, with an increase in oxidative stress, autophagy and a more glycolytic metabolism, which in turn promoted tumour growth (Guido et al., 2012). TGF- β signalling has been further associated with regulating production of MMPs and chemokines in mammary CAFs

(Moore-Smith et al., 2017, Fang et al., 2015). However, targeting TGF- β in CAFs can simply lead to compensation by HGF, which also promotes tumour growth and invasion (Cheng et al., 2008).

Mammary CAFs have been implicated in all of the pro-tumourigenic effects of CAFs on the TME. They promote angiogenesis through upregulation of VEGF signalling (Kugeratski et al., 2019), through deformation of the ECM (Sewell-Loftin et al., 2017), and through secretion of factors such as the oxidoreductase CLIC3, which acts via TGM2 (Hernandez-Fernaud et al., 2017), and SDF-1, which additionally promotes tumour growth via CXCR4 (Orimo et al., 2005). Mammary CAFs also contribute to an immunosuppressive microenvironment (Cohen et al., 2017, Liao et al., 2009) and promote chemoresistance (Mao et al., 2014). They have been further shown to promote breast cancer invasion and metastasis through a variety of secreted factors, including CLIC3, CXCL12, and IL-32 (Hernandez-Fernaud et al., 2017, Dvorak et al., 2018, Wen et al., 2019).

In addition to secreting protein factors and metabolites, there is a growing field of research showing that CAFs, including mammary CAFs, also modulate the TME through secretion of extracellular vesicles containing proteins, metabolites and nucleic acids. Luga et al. first showed that CAFs from breast cancer patients produced CD81⁺ exosomes which increased breast cancer cell motility and metastasis through Wnt signalling activation (Luga et al., 2012). The transfer of Wnt10b by CAF-derived exosomes was also shown to increase breast cancer cell invasion (Chen et al., 2017). In addition to protein transfer, one of the key ways in which vesicles from mammary CAFs are able to influence cancer cells is through miRNA transfer. The miR221/222 secreted by CAFs was shown to induce hyperactive MAPK signalling in breast cancer cells, which is known to be associated with a higher risk of recurrence and poorer survival (Shah et al., 2015). Similarly, a combination of three miRNAs contained in CAF-derived exosomes promoted cancer cell stemness and EMT in breast cancer (Donnarumma et al., 2017). Mammary CAF-derived exosomes can also contain mitochondrial DNA, which has been shown to restore oxidative phosphorylation to breast cancer cells with impaired metabolism and enable therapy resistance (Sansone et al., 2017).

Therefore CAFs in breast cancer stroma play an extremely important role in tumour progression, and understanding the mechanisms involved in how CAFs create a pro-tumourigenic microenvironment could provide important information on how to therapeutically target breast cancer. In the following sections I will go into more detail about the crucial roles that CAF derived ECM and CAF metabolism play in creating a pro-tumourigenic TME.

1.2 The role of CAF-derived ECM in cancer

1.2.1 Properties of the extracellular matrix

The ECM is made up of a variety of proteins, glycoproteins, proteoglycans and polysaccharides (Ozbek et al., 2010). There are two types of ECM: the basement membrane and the interstitial matrix. The basement membrane separates epithelium from stromal cells and is very compact, whereas the interstitial matrix contributes to the tensile strength of tissues and is more porous. The basement membrane is composed primarily of collagen IV, fibronectin, laminins and linker proteins. The interstitial matrix also contains a high proportion of fibronectin and collagens, but additionally contains a greater amount of glycoproteins and proteoglycans (Egeblad et al., 2010). The ECM therefore contains a high degree of biophysical and biochemical diversity.

Physically, the ECM's orientation, stiffness, porosity and ability to act as a barrier determine the scaffolding and integrity of tissues. The orientation of fibres, the physical barrier and the availability of proteins for cell adhesion also regulate cell migration (Lu et al., 2012). Furthermore, ECM elasticity and stiffness is a key environmental regulator of cell behaviour. Focal adhesion complexes, which are plasma membrane-associated multi-protein complexes that interact with the ECM through receptors such as integrins, act as mechanosensing links between ECM stiffness and the cytoskeleton and cell signalling pathways. Their components can change conformation depending on the applied force (Sawada et al., 2006, del Rio et al., 2009). This leads to functional consequences for the cell, including regulation of cell fate, cell contractility, and conventional cell signalling pathways (Engler et al., 2006, Gehler et al., 2009, Maeda et al., 2011).

Biochemically, the ECM is rich in signalling cues, acting as a reservoir of signalling molecules such as the growth factors FGF and VEGF, which bind to proteoglycans. It has been suggested that this can create growth factor gradients, which are important for determining cell fate in development, or that these growth factor reserves can be released when required by ECM degradation (Hynes, 2009). Integrins provide cells with the ability to anchor themselves to the ECM, and are

also key mediators of signalling pathways regulating cell growth and proliferation, metabolism and migration, such as the MAPK cascade (Ata and Antonescu, 2017, Schwartz and Assoian, 2001).

Tissues can constantly make new ECM, degrade existing ECM via MMPs and rearrange or realign ECM fibres via crosslinking and covalent modifications, making the ECM a highly dynamic structure that is able to stimulate rapid changes in cell behaviour.

1.2.2 An overview of collagen

Collagen accounts for approximately a third of all proteins in humans and other animals, and is furthermore the most abundant protein in the ECM. Approximately 28 different collagens have been identified in vertebrates (Gordon and Hahn, 2010). It is primarily a structural protein, and all collagens contain three polypeptide α -chains which fold together to form a rod-like triple helix. Each chain consists of a repeating Gly-X-Y triplet amino acid motif, in which X and Y are most commonly proline or hydroxyproline, which is a derivative of proline produced by prolyl hydroxylases. This is because small, flexible amino acids are required to fit into the helix conformation, and in particular glycine is the only amino acid small enough to fit into the centre of the triple helix. Furthermore, the hydroxyproline residues can form hydrogen bonds along the helix to stabilise it. Some collagens contain interruptions or imperfections in the Gly-X-Y motif which destabilise the helix and thus give them increased flexibility. Collagens are heavily post-translationally modified in the endoplasmic reticulum where lysyl hydroxylases and prolyl hydroxylases create hydroxylysine and hydroxyproline respectively on the nascent polypeptide. The hydroxylysine residues can be further glycosylated. After folding, the full length collagen chain or 'procollagen' consists of a collagenous NC1 domain and a non-collagenous NC2 domain, which keeps the NC1 domain soluble in the cell. Upon secretion, the NC2 domain is cleaved by procollagen N-proteases, which causes a sudden decrease in solubility and the collagens form aggregates. Lysyl oxidases can further stabilise the fibrillar aggregates by covalently crosslinking adjacent fibrils (Boot-Handford and Tuckwell, 2003, Kadler et al., 2007).

There are three classes of collagens: fibrillar collagens which make up the interstitial matrix, network-forming collagens which are found in the basement membrane, and transmembrane collagens which are involved in cell adhesion (Shoulders and Raines, 2009, Franzke et al., 2003). Collagen I is the archetypal fibrillar collagen, although collagens II, III, V and VI are also common fibrillar collagens, while collagen IV is the most abundant network-forming collagen.

1.2.3 Features and properties of CAF-derived ECM

As discussed previously, the main function of quiescent fibroblasts is to maintain the ECM of connective tissue. Under normal activation in wound healing, ECM production is enhanced in order to produce new ECM to heal the wound and create a scaffold for the cells migrating and proliferating to close the gap. Therefore it is unsurprising that one of the main outputs of fibroblasts activated in the context of cancer is ECM production. Indeed CAFs are the main source of ECM in tumours (Bhowmick et al., 2004). CAF-derived ECM differs from normal ECM in its composition, turnover and stiffness, and in the alignment of fibres.

One of the major differences between CAF and normal fibroblast (NF) derived ECM is simply that they make more of it. CAFs deposit large quantities of ECM proteins including fibronectin, hyaluronic acid and collagen, which is the most abundant ECM protein and makes up to 30% of the total protein mass of animals (Frantz et al., 2010). Many collagens are enriched in tumour ECM, including collagen I, II, III, IV, V, VI and XI (Kauppila et al., 1998, Nissen et al., 2019). In addition to producing more collagen, CAFs also induce higher rates of ECM turnover and remodelling of the basement membrane through increased expression of ECM degrading enzymes, the most prominent of which are the MMPs, paving the way for cancer cells to proliferate, migrate and for new blood vessel formation (Kessenbrock et al., 2010). Furthermore, the presence of collagen degradation products in serum can distinguish between healthy and breast or ovarian cancer patients (Bager et al., 2015).

In addition to increasing ECM production and turnover, CAF-derived ECM is also stiffer, in part because there is more of it but also due to increased crosslinking of fibrillar proteins such as collagens and elastin by lysyl oxidase and

transglutaminase, expression of both of which are upregulated in CAFs (Levental et al., 2009, Lucero and Kagan, 2006). Fibres in the ECM produced by CAFs are also more directionally aligned and bundle together to create gaps in the basement membrane. Indeed, the alignment of collagen fibres in the ECM can be used to predict patient outcome in breast cancer (Bredfeldt et al., 2014, Conklin et al., 2011). Ao et al. showed that the mechanical forces that CAFs exert on the ECM also cause alignment of fibronectin fibres (Ao et al., 2015). Interestingly, high Cav-1 expressing mouse fibroblasts also showed more fibronectin and collagen alignment via increased Rho-mediated contractile force (Goetz et al., 2011), despite the fact that other studies have claimed that loss of Cav-1 in CAFs is a marker of the TGF- β induced myofibroblastic phenotype (Guido et al., 2012, Martinez-Outschoorn et al., 2010a), again highlighting fibroblast heterogeneity and the many different opposing signalling pathways that fibroblasts can use to create a pro-tumourigenic microenvironment. Similarly, it was shown that CAFs expressing Snail-1, which induces RhoA and α SMA mediated contractility, increased anisotropic fibre organisation and matrix stiffness (Stanisavljevic et al., 2015). CAF contractility was also shown to be necessary for matrix remodelling in gastric cancer, where cancer cells were able to invade matrigel that was being remodelled by CAFs (Yamaguchi et al., 2014). Therefore it seems that the myofibroblastic, contractile, α SMA positive CAF phenotype is key to ECM remodelling in the TME.

1.2.4 CAF-derived ECM sustains and promotes tumour development

Taken together, the increased ECM deposition and turnover as well as increased matrix stiffness and remodelling create a highly pro-tumourigenic environment. One of the hallmarks of cancer is sustained proliferation, and CAF-derived ECM sustains proliferation through several pathways. Firstly, as mentioned previously, the increased ECM deposition by CAFs enables integrin adhesion by cancer cells, which sustains proliferative signalling through Fak activation leading to Erk/PI3K signalling and cell cycle progression (Schwartz and Assoian, 2001). The increased stiffness of the ECM further upregulates integrin-mediated Fak phosphorylation and accelerates cell cycle progression (Bae et al., 2014, Provenzano and Keely, 2011). Equally, integrin mediated adhesion to the ECM can inhibit tumour growth suppressors such as BRCA1 and p21 and allow cancer cells to circumvent these

pathways (Kim et al., 2008, O'Connell and Martin, 2000), as well as inducing anti-apoptotic factors and blocking p53-mediated apoptosis to promote cell survival (Gilmore et al., 2000, Lewis et al., 2002). Furthermore, as discussed previously, the ECM can act as a reservoir of growth factors and signalling molecules such as FGF and Wnt. Enhanced degradation of the ECM by MMPs produced by CAFs can release these factors, stimulating tumour growth. Additionally, TGF- β , which is a key factor promoting tumour progression, is secreted in an inactive form and is subsequently activated by MMP cleavage or by mechanical stress, both of which are enhanced by CAFs (ten Dijke and Arthur, 2007). Interestingly, it has recently been shown that cancer cells can use the ECM for metabolic fuel; taking up and degrading collagen to satisfy their demand for amino acids and promote tumour growth and survival (Gouirand and Vasseur, 2018). In vivo, the effects of the ECM on tumour growth have been assessed in several studies. Ablation of Col6a1 or Col5a3 in the MMTV-PyMT mammary tumour model resulted in reduced hyperplasia and primary tumour growth (Iyengar et al., 2005, Huang et al., 2017). Conversely, mice which have been engineered to produce more collagen (Col1a1^{tm1jae}) showed increased tumour growth in the MMTV-PyMT model (Esbona et al., 2016, Provenzano et al., 2008). Inhibition of production of other ECM components such as hyaluronan, fibronectin and tenascin-C also suppresses tumour initiation and growth (Udabage et al., 2005, Lingasamy et al., 2019).

In addition to promoting tumour growth and survival, CAF-derived ECM is a key factor in determining the metastatic ability of tumours by promoting EMT, inducing invadopodia formation and providing cancer cells with escape routes. Increased ECM stiffness has been shown to promote hallmarks of EMT in cancer cells, such as TWIST1 activation, vimentin expression and β -catenin nuclear localisation (Wei et al., 2015, Rice et al., 2017). One of the many roles of TGF- β signalling is to promote EMT, and so the combination of increased matrix stiffness and enhanced MMP activity can further drive EMT through release and activation of TGF- β (Leight et al., 2012). Integrin binding to proteins enriched in CAF-derived ECM, such as collagen and laminins, also promotes EMT in tumour cells (Scott et al., 2019). The combination of increased ECM stiffness and integrin receptor binding to the ECM also regulates formation of invadopodia, which are membrane protrusions which enable cell migration and invasion. Increased stiffness caused by collagen crosslinking promoted integrin clustering in cancer cells to stimulate

focal adhesion assembly and promote PI3K signalling, which is required for invadopodia formation (Levental et al., 2009). Increased MMP remodelling, which can be stimulated by integrin signalling at focal adhesion complexes, also enables invadopodia formation (Jacob and Prekeris, 2015). Alternatively, CAFs can combine MMP remodelling with increased collagen directionality due to Rho-ROCK mediated contractile forces to create 'tracks' for cancer cells to migrate along (Gaggioli et al., 2007). This allows cancer cells to migrate while still maintaining epithelial properties so that there is no need for them to undergo EMT. Similarly, it was observed that CAFs invaded first into matrigel using MMPs, and the cancer cells followed the path taken by the CAFs (Li et al., 2016). In addition to providing paths for tumour cells to migrate along, the forces exerted by CAFs on the basement membrane create holes, increasing the leakiness of blood vessels and allowing cancer cells to escape the tumour boundary and enter the bloodstream (Egeblad et al., 2010, Glentis et al., 2017).

Another important aspect of the CAF ECM is to induce angiogenesis, which also affects tumour metastasis by providing the tumour cells with a means of extravasation into the blood stream. As well as acting as a reservoir of factors that induce tumour growth, the ECM also stores VEGF and other pro-angiogenic factors, which can be released by matrix deformation and MMP remodelling. Both MMP-7 and MMP-9 have been implicated in promoting angiogenesis in tumours (Littlepage et al., 2010). Conversely, anti-angiogenic factors could be released by the same means, so the ECM can also inhibit angiogenesis in some cases. Increased ECM stiffness was also shown to promote endothelial cell MMP activity and endothelial VEGF expression, which is required for blood vessel branching and growth (Bordeleaux et al., 2017, Mammoto et al., 2009). Stiffness-induced ROCK activation in cancer cells further promotes angiogenesis (Croft et al., 2004).

CAF derived ECM also affects the immune response of the tumour. Integrin signalling can mediate avoidance of the anti-tumour immune response (Weaver et al., 2002). Collagen I has been specifically implicated in inhibiting T-cell proliferation and activation, and a collagen rich ECM promotes the immunosuppressive M2 macrophage phenotype, although conversely fibronectin rich ECM can promote M1 macrophage polarisation (Meyaard, 2008, Wesley et al., 1998, Perri et al., 1982). This is perhaps in part due to collagen rich ECM being

stiffer due to collagen crosslinking, as a stiffer ECM has also been shown to promote M2 macrophage polarisation and T-cell activation (Patel et al., 2012, O'Connor et al., 2012). Collagen assembly has also been recently shown to impede T-cell access to the tumour (Mariathasan et al., 2018). This may explain why immune checkpoint inhibitors often fail to produce a response in stroma-rich tumours, and, indeed, combining checkpoint inhibitors with targeting CXCL12 production by myofibroblastic CAFs has shown success in a mouse model of PDAC (Feig et al., 2013). The ECM can also regulate cytokine availability. MMPs such as MMP-12 can cleave and inactivate cytokines which would recruit neutrophils and inflammatory monocytes (Dean et al., 2008). TGF- β release and activation by the ECM can further modulate the immune environment by influencing T-cell differentiation to being pro or anti-inflammatory in a concentration dependent manner (Li and Flavell, 2008).

Drug response and resistance in tumours is also affected by the ECM. The increased stiffness of tumour associated ECM increases interstitial fluid pressure, which has been shown to reduce the efficiency of drug delivery. Matrix composition and organisation also affects drug delivery as increased collagen content and alignment in ECM have been shown to impede drug transport (Heldin et al., 2004, Netti et al., 2000). Further to this, normalisation of tumour stroma has been shown to improve response to therapy (Liu et al., 2012a). Cancer cell-ECM interactions also play a key role in drug resistance. Integrin mediated fibronectin attachment has been shown to enhance drug resistance and integrin β 1 has been implicated in resistance to radiotherapy and chemotherapy in head and neck, breast and lung cancer (Damiano, 2002, Eke et al., 2012, Huang et al., 2011). Cancer stem cells expressing integrins β 4 and β 3 have also all been found to be enriched after chemotherapy treatment and in relapsed tumours, suggesting that integrin-ECM interactions may mediate drug resistance through promoting cancer stem cell survival (Zheng et al., 2013, Seguin et al., 2015).

Therefore the increase in ECM output by CAFs and the increase in stiffness due to collagen crosslinking and fibre alignment creates a pro-tumourigenic microenvironment by promoting tumour cell growth and survival, invasion and metastatic potential, angiogenesis, an immunosuppressive immune response and also contributes to drug resistance and tumour relapse. The ECM plays a key role

in breast cancer pathology, and in particular increased collagen deposition and crosslinking have been shown to contribute to breast cancer progression (Kaushik et al., 2016).

1.3 Epigenetic control of collagen and ECM production

1.3.1 Epigenetics

Epigenetics is defined as the heritable modification of gene function without alterations in the DNA sequence, either by DNA or histone modification or by changes in chromatin structure. Histone modification is a major source of epigenetic regulation in cells. Histones are the core component of nucleosomes, which compact chromatin by wrapping DNA around them. In general, nucleosome compaction is obstructive to gene transcription as it reduces DNA accessibility to the transcriptional machinery. However, post translational histone modification can further regulate chromatin accessibility as well as recruiting specific transcription factors. So far, observed histones modifications include methylation, acetylation, phosphorylation, ubiquitination, deamination, ribosylation and sumoylation (Lawrence et al., 2016). Lysine acetylation and methylation are the most widely studied histone modifications and as far as we know have the greatest impact on chromatin accessibility and regulation of gene transcription (Bartova et al., 2008). In general, it is thought that acetylation neutralises the positive charge on lysine, destabilising bonds with negatively charged DNA and causing chromatin to form a more open conformation, enabling transcription machinery access. Conversely, methylation is associated with increased chromatin compaction and repression of transcription (Margueron et al., 2005). There are several exceptions to this, for example, H3K4me3 is known to be a transcriptional activator marking transcriptional start sites (Schneider et al., 2004). Furthermore, lysine residues can be modified with up to 3 methyl groups, and different numbers of methyl groups can have different effects. For example, H3K27me3 represses transcription whereas H3K27me1 promotes transcription (Ferrari et al., 2014). Methylation and acetylation have been further shown to influence recruitment and binding of transcription factors and the transcriptional machinery to gene promoters (Vettese-Dadey et al., 1996, Wysocka, 2006, Lawrence et al., 2016). DNA itself can also be methylated, and methylation of CpG dinucleotides at transcriptional start sites is a marker of transcriptional repression (Edwards et al., 2017, Jones, 2012).

1.3.2 Regulation of CAF activation and fibrotic collagen production by epigenetics

Many factors have been shown to contribute to increased collagen synthesis by activated fibroblasts in fibrotic tissue, including cytokines such as TGF- β , IL-3 and IL-4, growth factors such as CTGF and PDGF and the Wnt and Notch signalling pathways, and miRNA mediated post-transcriptional regulation (Bhogal et al., 2005, Leask, 2010, Beyer et al., 2013, Dees et al., 2011, Nijhuis et al., 2014). However, in recent years epigenetic regulation of fibroblast activation and fibrosis through altering histone modification patterns or DNA methylation has been shown to be an important and targetable point of regulation of collagen synthesis.

Since CAF activation is accompanied by dramatic alterations in gene and protein expression, which leads to increased production and secretion of many factors, it is to be expected that epigenetic alterations underpin at least a part of the process of CAF activation. Furthermore, the fact that the CAF phenotype is self-sustaining in culture (Kojima et al., 2010) and does not require the presence of cancer cells to maintain activation suggests that an epigenetic switch supports CAF activation. Initial studies showed that CAF DNA was overall hypomethylated in comparison to NF DNA, suggesting an overall increase in active transcription (Jiang et al., 2008, Hu et al., 2005, Vizoso et al., 2015). Recently, a more in depth analysis of global DNA methylation in paired prostate CAFs and NFs using whole genome bisulphite sequencing revealed that CAFs had many consistent differences in methylation compared to NFs, particularly in genes involved in stromal-epithelial signalling and tissue development. These genes tended to be hypomethylated in comparison with NFs, which implies that they are more actively transcribed (Pidsley et al., 2018).

TGF- β signalling is a hallmark of activated, ECM producing myofibroblasts and a potent fibrotic activator. The major downstream effectors of TGF- β are the transcriptional modulators Smad2 and Smad3, which translocate into the nucleus and recognise Smad binding elements to promote transcription of target genes (Feng and Derynck, 2005). Blocking Smad signalling reduces collagen transcription (Ding et al., 2013). In addition to regulating transcription factor translocation to the nucleus to regulate collagen transcription, TGF- β signalling has also been

found to promote expression of fibrotic genes via regulating histone modifications. In rat mesangial cells, TGF- β activation upregulated expression of fibrotic genes, including collagen I, by increasing H3K4 trimethylation, a marker of active transcription, and decreasing repressive H3K9 methylation at the promoters of these genes. Furthermore, TGF- β upregulated the expression and recruitment of the H3K4 methyltransferase SET7/9 to the collagen I promoter, again to activate its transcription (Sun et al., 2010). Additionally, the combination of the cytokines TGF- β , TNF α and IL1- β induced alterations in histone modification at the promoters of fibrotic genes in fibroblasts, including hyperacetylation of histone 3 and hypermethylation of histone 4 at the Col1a2 promoter, increasing its expression at the mRNA level (Sadler et al., 2013). TGF- β signalling has also been implicated in decreasing DNA CpG methylation at collagen promoters and thereby activating transcription via downregulation of the DNA methyltransferases DNMT1 and DNMT3 (Pan et al., 2013). Other studies have also demonstrated a decrease in DNA methylation in activated fibroblasts at the promoters of fibrotic genes including collagens due to DNMT inhibition (Hu et al., 2010, Ko et al., 2013). However, increased DNA methylation of certain genes stimulates CAF activation. For example, a study by Albregues et al. demonstrated that methylation of the gene encoding protein phosphatase SHP-1 resulted in activated JAK1/STAT3 signalling in fibroblasts, leading to a pro-invasive CAF phenotype (Albregues et al., 2015). Therefore upregulation of the fibrotic response in CAFs, as stimulated by TGF- β , involves epigenetic alterations, and epigenetic regulation of collagen transcription is a key aspect of this.

Many studies have shown that increased expression of collagen by fibroblasts activated during fibrotic diseases is also regulated at the epigenetic level. H3K27me3 is a well-known marker of transcriptional repression that recruits polycomb group proteins to target genes, creating repressive polycomb complexes. In fibrotic sclerosis, H3K27me3 was shown to be decreased in fibroblasts, causing loss of transcriptional repression of collagen (Kramer et al., 2013). In glioma cells, increased collagen expression was associated with the presence of H3K4me2, H3 hyperacetylation, and a reduction in H3k27me3, showing that epigenetic regulation of collagen production at the histone modification level is not limited to fibroblasts (Chernov et al., 2010). At the DNA methylation level, Gotze et al. explored the role of DNA methylation in

fibrogenesis of hepatic stellate cells and found an increase in hypomethylated genes, similar to the findings in CAF activation, although collagen was not specifically studied (Gotze et al., 2015).

Epigenetic therapies have had some success at treating collagen production in fibrosis and in CAFs. DNA methylation inhibition reduced collagen I and collagen III in human fibroblasts and in spontaneously hypertensive rats (Watson et al., 2016). BET inhibitors and histone deacetylase (HDAC) inhibitors have been investigated as an effective combination therapy in mouse models of PDAC, and BET inhibitors were further shown to effectively target PDAC stroma (Mazur et al., 2016). BET inhibitors inhibit BRD transcription factors, which bind acetylated histone motifs and recruit further transcription factors and chromatin remodellers. Kumar et al. showed that in pancreatic stellate cells and in an in vivo model of PDAC, BET inhibition reduced collagen I expression through inhibition of BRD4 (Kumar et al., 2017). BET inhibitors or BRD4 knockdown have also been shown to decrease fibrosis-driven collagen production in lung and renal fibroblasts (Tang et al., 2013, Xiong et al., 2016). This further shows that histone acetylation is required for activation of collagen production in fibroblasts. BRD4 is strongly associated with the H3K27ac motif, which is found at enhancer regions and is a powerful activator of transcription (Raisner et al., 2018, Lee et al., 2017). As mentioned earlier, loss of H3K27me3 and hyperacetylation of histone 3 are also associated with increased collagen production, suggesting that a switch from methylation to acetylation of H3K27 could be a key epigenetic alteration stimulating collagen production in CAFs. On the other hand, HDAC inhibitors also have shown effectiveness in reducing fibrotic ECM. In cardiac fibrosis, HDAC1 and HDAC2 inhibition reduced collagen I, III and fibronectin (Nural-Guvener et al., 2015). Similarly, the HDAC inhibitor SAHA effectively inhibited fibrotic collagen production in lung fibroblasts (Wang et al., 2009). Thus, it is clear that epigenetic alterations are a crucial aspect of CAF activation, particularly with regard to collagen and ECM production, and can be targeted with already existing inhibitors, several of which have undergone testing in clinical trials.

1.4 CAF metabolism

In the past decade, there has been increasing research into how the metabolic rewiring of CAFs contributes to their pro-tumourigenic phenotype. The majority of this research focusses on how CAFs produce metabolites which can be taken up by tumour cells and used as fuel to promote growth and invasion.

One of the first observations about CAF metabolism was an increase in glycolysis in CAFs. This was initially demonstrated in mammary fibroblasts by the Lisanti group (Pavlidis et al., 2009). Proteomic analysis of fibroblasts activated upon knockdown of caveolin-1 (Cav-1) showed a general upregulation of glycolytic proteins. Downregulation of Cav-1 has been further shown to be a marker of CAFs, and to promote tumour growth and metastasis. Cav-1 is downregulated in CAFs due to increased oxidative stress and HIF1 α stabilisation, which are caused both by TGF- β activation in CAFs and by the reactive oxygen species (ROS) and the hypoxic microenvironment created by tumour cells (Martinez-Outschoorn et al., 2010a). The authors hypothesised that the increase in lactate produced by glycolytic CAFs could be used to fuel oxidative phosphorylation in cancer cells. This metabolic cross talk has been termed ‘the Reverse Warburg effect’ because the stromal cells are highly glycolytic instead of the tumour cells, as was initially discovered by Otto Warburg. Transcriptomic analysis of breast tumours also showed evidence of upregulation of glycolytic enzymes in the stroma (Pavlidis et al., 2010c), and it was shown that Cav-1 knockdown in mammary fibroblasts led to increased glycolysis (Pavlidis et al., 2010b). TGF- β activation of mammary fibroblasts leading to oxidative stress, upregulated autophagy, HIF-1 α stabilisation and Cav-1 loss caused increased glucose uptake and lactate secretion (Guido et al., 2012). Furthermore, in co-cultures with the MCF7 breast cancer cell line, fibroblasts upregulated the expression of the lactate transporter MCT4, and this was shown to be a result of increased oxidative stress. This was coupled with corresponding expression of the lactate importer MCT1 in the MCF7 cells, suggesting that they are able to utilise the fibroblast-produced lactate. The upregulation of MCT4 in the fibroblasts protected the cancer cells against cell death, showing that the metabolic reprogramming of CAFs is important for tumour cell survival (Whitaker-Menezes et al., 2011b). Other studies have also demonstrated that cancer cells rely on lactate from the tumour microenvironment

(Sonveaux et al., 2008), and that a similar transfer of lactate occurs between glycolytic hypoxic and oxidative normoxic tumour cells, suggesting that this metabolic coupling is a common mechanism promoting tumour survival (Allen et al., 2016). Furthermore, treatment of xenografts containing Cav-1 (-/-) fibroblasts cotransplanted with MDA-MB-231 breast cancer cells with glycolysis inhibitors reduced the positive effect on tumour growth of the Cav-1 (-/-) fibroblasts. However, whether the glycolysis inhibitors would have had a similar effect on tumours containing normal fibroblasts was not assessed (Bonuccelli et al., 2010). A Cav-1 independent pathway stimulating glycolysis in mammary CAFs was discovered by Yu et al. in which the G-protein coupled Oestrogen receptor (GPER) was translocated to the cytoplasm in CAFs, where it promoted glycolysis via PKB and CREB signalling. Pyruvate and lactate produced by the CAFs were then used to fuel mitochondrial metabolism in tumour cells (Yu et al., 2017). A recent study also showed that MYC driven breast cancers stimulated glycolysis in CAFs via miR-105, which was secreted in tumour cell-derived extracellular vesicles. miR-105 caused fibroblasts to upregulate genes involved in glycolysis and glutaminolysis (Yan et al., 2018).

Another aspect of the reverse Warburg effect hypothesis is that oxidative stress drives increased autophagy in CAFs, leading to mitochondrial breakdown and secretion of autophagic breakdown metabolites, such as ketones and amino acids, which can also be used to drive oxidative phosphorylation in cancer cells. Therefore CAFs should show evidence of mitochondrial dysfunction whereas cancer cells should show evidence of upregulated mitochondrial activity. In sections of breast cancer tissue, it was demonstrated that the stroma had little mitochondrial activity as measured by cytochrome C oxidase, NADH and succinate dehydrogenase staining whereas adjacent cancer cells were highly positive (Whitaker-Menezes et al., 2011a). In vitro, co-cultures of mammary fibroblasts and MCF7 cells demonstrated that CAFs had decreased levels of intact mitochondria whereas the MCF7 cells increased their levels of intact mitochondria (Martinez-Outschoorn et al., 2010b). In support of an autophagic CAF phenotype catabolically producing metabolites, metabolic analysis of mammary fat pad fibroblasts from Cav-1 (-/-) mice demonstrated upregulated production of ketone bodies, amino acids and markers of the breakdown of collagen and other proteins (Pavlides et al., 2010a). It was further demonstrated that MDA-MB-231 breast

cancer cells take up and use lactate and ketone bodies to fuel mitochondrial metabolism, growth and metastasis (Bonucci et al., 2010). Cav-1 loss has been shown to promote mitophagy by enabling accumulation of nitric oxide (NO). NO accumulation inhibits cytochrome c oxidase which causes mitochondrial uncoupling and triggers mitophagy (Pavlidis et al., 2010b). Interestingly, Cav-1 (-/-) mammary fibroblasts showed increased expression of the matrix remodelling factors PAI1 and PAI2, which activate plasmin and MMPs to degrade ECM proteins. Fibroblasts overexpressing PAI1/2 also demonstrated an increase in autophagy, suggesting that ECM remodelling and degradation may have an unexplored role in regulating stromal metabolism. It is possible that either the protein break down products or pro-autophagic factors released from the degraded ECM stimulate autophagy in mammary CAFs (Castello-Cros et al., 2011). Other ECM related proteins such as the growth factors CTGF and MSF, which is a truncated form of fibronectin, have also been shown to promote the reverse Warburg effect in mammary CAFs. CTGF led to HIF1 α stabilisation and thereby increased autophagy and glycolysis, whereas MSF stimulated Akt and mTOR signalling to promote glycolysis in mammary CAFs (Capparelli et al., 2012, Carito et al., 2012). Interestingly the reverse Warburg effect has been further shown to enable drug resistance in breast cancer cells. Increased oxidative phosphorylation mediated by TIGAR enabled tamoxifen resistance in MCF7 cells. The cells could be resensitised to tamoxifen by treating them with anti-mitochondrial drugs such as metformin (Martinez-Outschoorn et al., 2011a).

All the above studies were carried out using only mammary CAFs, however, aspects of the reverse Warburg effect, namely increased glycolysis and autophagy in CAFs, have been observed in other cancers. In prostate cancer, a similar coupling of lactate metabolism was observed with CAFs expressing high levels of MCT4 and tumour cells expressing MCT1. Also in fibroblasts derived from prostate cancer, activation by TGF- β or PDGF was demonstrated to increase glycolysis by causing downregulation of isocitrate dehydrogenase 3 α (IDH3 α). This led to an imbalance in the α -ketoglutarate-succinate ratio, causing inhibition of PDH2 and HIF1 α stabilisation, thus mimicking the upregulation of glycolysis caused by the hypoxic response. IDH3 α downregulation was also seen in the stroma of prostate cancer patients, suggesting that this mechanism occurs in vivo (Zhang et al., 2015). In ovarian cancer, BRCA mutated ovarian cancer cells were shown to

produce hydrogen peroxide, stimulating oxidative stress and thereby autophagy, mitophagy and increased glycolysis including higher MCT4 expression in ovarian CAFs via upregulation of NF κ B signalling (Martinez-Outschoorn et al., 2012). In pancreatic tumours, PDAC tumour cells stimulated autophagy in pancreatic stellate cells leading to stromal alanine secretion. Alanine was then used in preference to glucose and glutamine, which can be limited in the tumour microenvironment, to fuel the TCA cycle and amino acid and lipid synthesis in the tumour cells and also rescued the growth of PDAC cells under nutrient deprived conditions (Sousa et al., 2016). In another study, pancreatic CAFs had increased expression of glycolytic enzymes such as LDHA, MCT4 and PKM2 compared to NFs, and conditioned media from CAFs both stimulated mitochondrial biogenesis and upregulated expression of MCT1 and TCA cycle enzymes fumarate dehydrogenase and succinate dehydrogenase in pancreatic cancer cell lines (Shan et al., 2017).

Upregulated glycolysis is not a feature of all CAFs, however. Although many of the aforementioned studies in breast cancer demonstrated the existence of the reverse Warburg effect in breast tumours, many of the co-culture and xenograft experiments were carried out using MCF7 cancer cells. ER⁺ breast cancer cells, such as MCF7, have previously been shown to rely more on mitochondrial metabolism whereas the more aggressive HER2⁺ and TNBC subtypes are more glycolytic (Choi et al., 2013, Lanning et al., 2017). The study by Choi et al. classified stromal-tumour metabolic relationships by using immunohistochemistry to determine whether the stromal and tumour compartments used predominantly glycolytic or oxidative metabolism. The authors found a mixture of traditional Warburg, reverse Warburg, mixed (both tumour and stroma are glycolytic) or null (both tumour and stroma are oxidative) metabolic relationships between tumour and stroma. Lower grade ER⁺ tumours displayed the highest proportion of the reverse Warburg phenotype, and TNBC and HER2⁺ tumours constituted the majority of traditional Warburg and mixed metabolism phenotypes. Therefore, targeting the reverse Warburg effect in breast cancer stroma might be more effective in ER⁺ patients. In support of this, a study showed that CAFs from the more aggressive basal-like breast cancers stimulated glucose uptake in both basal and luminal cancer cells, whereas CAFs derived from luminal breast cancers suppressed glucose uptake in cancer cells, which is more reminiscent of the reverse Warburg effect (Brauer et al., 2013).

Several other studies have demonstrated that the Reverse Warburg effect is not a feature of all CAFs. In prostate cancer, one study found that p62 is downregulated in prostate cancer stroma. The authors showed that p62 loss was involved in increased ROS production by the CAFs, which is consistent with the reverse Warburg effect, but that this was mediated through metabolic reprogramming involving a decrease in glutamine metabolism, as well as a decrease in glucose uptake and lactate secretion, which is directly in contradiction with the catabolic metabolism of the Reverse Warburg effect theory (Valencia et al., 2014). Another recent study demonstrated that in head and neck squamous cell carcinoma CAFs actually induced a more glycolytic phenotype in the tumour cells, and utilised the lactate produced by the glycolytic tumour cells for oxidative phosphorylation, which again is in opposition to the reverse Warburg effect (Kumar et al., 2018). Similarly, in co-cultures of lung cancer cells and fibroblasts, the fibroblasts were found to upregulate pyruvate dehydrogenase and the lactate importer MCT1, suggesting a more oxidative metabolism, whereas the tumour cells upregulated lactate dehydrogenase and decreased pyruvate hydrogenase activity which is in accordance with the glycolytic tumour phenotype of the traditional Warburg effect (Koukourakis et al., 2017). In a mass-spectrometry based analysis of metabolism in lung derived CAFs and NFs, although it was found that CAFs had metabolic markers of increased autophagy, such as dipeptides, the levels of these markers correlated with the glycolytic capacity of the tumour which the CAFs were derived from. Therefore in this study, increased autophagy in the CAFs did not seem to be related to mitochondrial metabolism in the tumours, and instead verified the original Warburg effect theory that more glycolytic tumours are more aggressive. Even without promoting a switch to mitochondrial metabolism in cancer cells, CAF autophagy can still provide cancer cells with nutrients, such as amino acids, lipids and nucleic acids, as well as protecting against oxidative damage (Kimmelman, 2011).

Therefore although autophagy does seem to be a common feature of the CAF phenotype, providing tumour cells with metabolites to fuel growth and metastasis, the question of whether CAFs develop a glycolytic metabolism to fuel oxidative metabolism in tumour cells via lactate transfer has not been resolved. Given the high levels of heterogeneity in CAFs previously discussed, it is likely that the

reverse Warburg effect is present in some tumours but further stratification is needed to determine which tumours might respond to therapies targeting this aspect of tumour-stroma crosstalk. In breast cancer, it is likely that the reverse Warburg effect occurs predominantly in lower grade, ER+ tumours.

Other mechanisms of metabolic coupling between CAFs and tumour cells have been discovered. In ovarian cancer, CAFs were shown to upregulate synthesis of glutamine, which was then taken up and used by the tumour cells to fuel glutamate synthesis. By simultaneously targeting glutamine synthase in CAFs and glutaminase in cancer cells in an orthotopic mouse model of ovarian CAFs the authors were able to reduce both tumour growth and metastasis (Yang et al., 2016). Another study in ovarian cancer showed that glutathione and cysteine released by CAFs promotes resistance to platinum-based chemotherapy (Wang et al., 2016). In PDAC, activation of pancreatic stellate cells was recently shown to induce production and secretion of lipids, including lysophosphatidylcholines, which were used by the tumour cells to produce components of cell membranes, facilitating proliferation, and also to support migration and Akt activation (Auciello et al., 2019). CAFs can further provide tumour cells with nutrients through secretion of exosomes. In PDAC, pancreatic stellate cells produce exosomes containing amino acids including alanine, which, as discussed above, has been shown to be an important metabolite driving mitochondrial metabolism in PDAC cells (Zhao et al., 2016). The exosomes also contained glucose, glutamine, lactate, acetate, TCA cycle metabolites and lipids, all of which can be used to fuel tumour growth.

Taken together, all of these studies show that, as with most other aspects of their phenotype, CAFs are metabolically highly diverse and promote tumour growth, metastasis and chemoresistance through upregulation of a variety of metabolic pathways. However, there is a common thread running through them in that the highly secretory phenotype of CAFs clearly extends to their metabolism, as all of these studies focus on how CAFs secrete metabolites to promote tumour progression.

1.5 The role of metabolism in collagen production

Since both metabolism and upregulated ECM production have been shown to be vitally important aspects of the CAF phenotype, an interesting question that has been little explored is whether alterations in CAF metabolism regulate ECM production. The many studies discussed in the previous section on how CAFs rewire their metabolism predominantly focus on how this enables CAFs to secrete metabolites, which can be taken up and used as fuel by cancer cells, but little research has been done on how fibroblast metabolism might underpin other aspects of their activated phenotype. Since collagen is such a major part of the protein output of activated fibroblasts, it is reasonable to suggest that there may be energetic requirements necessary to maintain this, or requirements for amino acids to support the translational output. In recent years, a few studies have shown this to be the case. It was shown that fibroblasts require an increase in glucose uptake and glycolysis to maintain TGF- β -induced collagen production in fibrosis, demonstrating a need for increased energy to fuel protein synthesis (Nigdelioglu et al., 2016). At the amino acid level, two recent studies have demonstrated that upregulation of glycine and serine production is required to maintain upregulated collagen synthesis in fibrotic disease. As discussed previously, collagen is predominantly made up of the Gly-X-Y motif, meaning that approximately 1/3 of collagen amino acid residues are glycine. The first study demonstrated that TGF- β treatment of fibroblasts caused upregulation of enzymes involved in de novo synthesis of glycine and serine from glucose, such as PHDGH and SHMT2. PHDGH and SHMT2 are also upregulated in lungs from patients with idiopathic pulmonary fibrosis, and inhibition of PHDGH or SHMT2 by genetic or pharmacological means led to reduced collagen production by fibroblasts. Since glycine is synthesised from serine, this implies that upregulation of glycolysis in fibrosis is used to fuel the serine/glycine synthesis pathway and increased glycine production is required for collagen synthesis (Nigdelioglu et al., 2016). More recently, Selvarajah et al. elucidated the mechanism of this pathway and showed that canonical TGF- β signalling through Smad3 in fibroblasts enhanced expression of glycine synthesis enzymes via activation of mTORC1 leading to upregulation of the transcription factor ATF4. ATF4 induced transcription of the glucose importer GLUT1 and enzymes for synthesising serine and glycine from glucose. Inhibition of this pathway reduced glycine incorporation into collagen (Selvarajah et al., 2019).

These two studies demonstrated a need for amino acid synthesis to maintain the increased collagen output of activated fibroblasts, and discovered a further role for TGF- β activation of glycolysis in activated fibroblasts: to produce glycine for collagen synthesis. Although these studies were carried out in the context of lung fibrosis, since CAFs and fibroblasts in fibrotic disease share many similarities in the upregulation of ECM production the mechanism is likely to be relevant for CAFs as well.

A requirement for glycine for collagen synthesis by fibroblasts has therefore been demonstrated, but a requirement for proline, the second most abundant amino acid in collagen, has been little studied. Some nutritional studies have shown that a diet supplemented with proline improves growth in young animals, which could be linked to an increased ability to synthesise proline-rich proteins such as collagens (Wu et al., 2011). A recent study of collagen synthesis in chondrocytes showed that supplementing media with proline, lysine or glycine, but not other amino acids, stimulated an increase in collagen production, although interestingly both proline and lysine had a greater effect at lower doses whereas glycine supplementation maintained a consistent level of collagen production at higher doses, suggesting that an excess of proline and lysine might adversely affect the cells (de Paz-Lugo et al., 2018).

Another metabolic aspect of collagen synthesis is the requirement for prolyl and lysyl hydroxylases, which convert α -ketoglutarate to succinate as a by-product of the hydroxylation reaction. The α -KG:succinate ratio is therefore very important for prolyl hydroxylase function as an excess of α -KG activates the enzymes whereas an excess of succinate is inhibitory (Gorres and Raines, 2010). The impact of the α -KG:succinate ratio on prolyl hydroxylases has mostly been studied in the context of HIF-1 α , which is targeted for degradation when hydroxylated (MacKenzie et al., 2007, Selak et al., 2005, Zhang et al., 2015). The requirement for α -KG by prolyl hydroxylases has also been linked to amino acid sensing by mTOR, since α -KG is a degradation product of several amino acids and the product of glutamine deamination (Duran et al., 2013). As previously discussed, mTOR activation has also been linked to collagen production through activation of glycine synthesis. It has further been shown that α -KG promotes collagen formation by fibroblasts, both by activation of mTOR and by proline hydroxylation

of procollagen (Ge et al., 2018). A more recent study demonstrated that HIF-1 α activation in chondrocytes led to increased glutaminolysis and thereby accumulation of α -KG. This enhanced proline and lysine hydroxylation on collagen, making the matrix more resistant to degradation by MMPs and ultimately resulting in skeletal dysplasia (Stegen et al., 2019). Since HIF-1 α signalling is also often activated in CAFs, this mechanism could also be relevant for increased collagen modification in the tumour microenvironment. Another recent study demonstrated that breast cancer cells require extracellular pyruvate to fuel α -KG synthesis and thus maintain activation of the prolyl hydroxylase P4HA. Inhibition of the pyruvate transporter MCT2 resulted in decreased collagen hydroxylation and functionality in vivo, and this could be rescued by α -KG. Furthermore succinate, which inhibits P4HA, also inhibited pyruvate driven proline hydroxylation. The authors also demonstrated that collagen hydroxylation was dependent on pyruvate and the α -KG:succinate ratio in CAFs but not in normal fibroblasts (Elia et al., 2019).

Therefore, metabolic rewiring in CAFs is an important factor to maintain the increase in collagen synthesis that accounts for the majority of CAF-derived ECM. CAFs both increase the synthesis of specific amino acids to support translation of collagen and maintain the α -KG:succinate ratio to promote the activity of prolyl and lysyl hydroxylases, which are essential for the correct folding and stabilisation of collagen proteins.

1.6 An overview of PDH and PYCR1 and their roles in cancer

1.6.1 Pyruvate dehydrogenase

In my thesis, the first of the two key metabolic enzymes I investigated was pyruvate dehydrogenase (PDH). Pyruvate dehydrogenase is an extremely important metabolic enzyme because it sits at the centre of glucose and oxidative metabolism, connecting the two major metabolic pathways in the cell: glycolysis and the TCA cycle. For this reason it has been named the ‘mitochondrial gatekeeper’. Inhibition of PDH generally results in a more glycolytic metabolism and activation leads to oxidative, mitochondrial metabolism. The reaction catalysed by PDH involves the reduction of 3-carbon pyruvate to 2-carbon acetyl-coA, with the release of carbon dioxide and the reduction of NAD⁺ to NADH. The pyruvate dehydrogenase complex (PDC) is made up of three subunits: E1 (Pyruvate dehydrogenase or PDH), E2 (Dihydrolipoyl transacetylase or DLAT) and E3 (Dihydrolipoyl dehydrogenase or DLD). The E1 subunit catalyses the rate limiting step, which is the decarboxylation of pyruvate into an acetyl group and CO₂, with vitamin B6 as a cofactor. The acetyl group reduces a lipoyl moiety linked to the E2 subunit. The E2 subunit then catalyses the transacylation reaction transferring the acetyl group to the thiol of coenzyme A producing acetyl-coA. Finally, the E3 subunit restores the complex to the resting state by reoxidising the lipoyl moieties, mediated by the reduction of NAD⁺ to NADH with FAD as a cofactor (Fig. 1-1).

The conversion of pyruvate to acetyl-coA is irreversible, and therefore the flux through the pyruvate dehydrogenase complex is tightly regulated (Patel and Korotchkina, 2006). Since the E1 subunit catalyses the rate limiting reaction, it has been the most highly studied and is the subunit subject to most regulation at the post translational level and by allosteric binding. Allosterically, the products of the reaction, acetyl-coA and NADH, both inhibit PDH activity. At the post-translational level, the major way that the E1 subunit is regulated is through inhibitory phosphorylation (Harris et al., 2001). The PDC has four regulatory phosphorylation sites. Three of these are on the E1 alpha subunit (PDHA1) and are

regulated by pyruvate dehydrogenase kinases (PDKs): S293, S232 and S300. The fourth, Y301, is on the E2 subunit and is thought to be phosphorylated by epidermal growth factor (EGF) and other tyrosine kinases (Fan et al., 2014), causing obstruction of pyruvate binding. The S293 site is the most well-studied and is also the most potent, as phosphorylation reduces PDH activity by over 97% by blocking the active site (Patel and Korotchkina, 2006).

1.6.2 Regulation of PDH phosphorylation

There are four PDKs in mammals, named PDK1-4, which share ~70% homology. The different PDKs preferentially phosphorylate different sites. PDK1 is the only PDK known to phosphorylate all three sites of PDHA1, but all PDKs will phosphorylate S293 and S300 in vitro (Patel and Korotchkina, 2001). S293 is the site most rapidly phosphorylated in PDH isolated from mammalian tissues (Yeaman et al., 1978). PDK2 exhibits the highest affinity for the S293 phosphorylation site, followed by PDK4, PDK1 and PDK3 and therefore PDK2 activity has the greatest effect on PDH inhibition, at least in vitro. The different PDK isoforms further show differences in tissue distribution. In rat tissue, PDK1 and PDK4 are predominantly found in heart and skeletal muscle, PDK2 is expressed in most tissues and PDK3 is most highly expressed in the testes and lungs (Bowker-Kinley et al., 1998). In mouse tissues, PDK1 and PDK2 were ubiquitously expressed whereas PDK3 and PDK4 were more limited. PDK3 was found only in testes, lung, brain and heart. PDK4 was only expressed at very low levels in muscular tissues (Klyuyeva et al., 2019).

Regulation of the PDKs is as diverse as the differential tissue expression. In general, all the PDKs can be activated by the outputs of the PDH-catalysed reaction: mitochondrial acetyl-coA and NADH. They can be additionally activated by ATP, as are many kinases. Conversely, pyruvate, NAD⁺ and ADP inhibit the PDKs (Pratt and Roche, 1979, Hansford, 1976, Cate and Roche, 1978). However, the combination of NADH and acetyl-coA increases the activity of PDK1 and PDK2 by 200-300 fold, whereas PDK3 is unresponsive to NADH and PDK4 is unresponsive to acetyl-coA and only increases its activity 2 fold with NADH stimulation (Bowker-Kinley et al., 1998). PDK1 has been shown in several studies to be upregulated by HIF1 α signalling in hypoxia to promote a more glycolytic metabolism by blocking flux into the TCA cycle. This maintains ATP production whilst blocking ROS accumulation (Kim et al., 2007, Kim et al., 2006a, Papandreou et al., 2006). Another study demonstrated that under hypoxia, Akt accumulates in the mitochondria and phosphorylates PDK1 to activate it (Chae et al., 2016). Therefore hypoxia appears to be a major regulator of PDK1 activity. PDK3 has also been shown to be upregulated by hypoxia (Lu et al., 2008). Both PDK2 and PDK4 have been shown to be upregulated by starvation and in diabetes (Huang et al., 2002) and insulin decreases the expression of both PDK2 and PDK4 (Kim et al.,

2006c). Little is known about how PDK2 is regulated by insulin, but the PDK4 promoter contains insulin response sequences which are binding sequences for the FOXO1 and FOXO3 transcription factors, which have been shown to upregulate PDK4 transcription (Furuyama et al., 2003). The nuclear hormone receptors PPARs have also been associated with increased expression of PDK2, PDK3 and PDK4, possibly via FOXO activity, however the evidence suggests that PDK2 is probably not a direct target of PPARs (Degenhardt et al., 2007, Holness and Sugden, 2003). Other nuclear hormone receptors and factors that have been shown to upregulate PDK4 expression include the glucocorticoid receptor, Estrogen-related receptors and Thyroid hormone receptors (Huang et al., 2002, Zhang et al., 2006, Attia et al., 2010, Connaughton et al., 2010). However, none of these pathways have conclusively been shown to also upregulate PDK2 expression. Interestingly, p53 has been shown to repress PDK2 activity which could contribute to metabolic alterations and increased glycolysis in tumours with p53 mutations (Contractor and Harris, 2012). Therefore PDK1 and PDK3 appear to be predominantly activated by hypoxia, whereas PDK2 and PDK4 are more responsive to metabolic stimuli such as starvation and insulin. The regulation of PDK4 is better understood than that of PDK2, despite PDK2 being the more ubiquitously expressed throughout the body.

PDH phosphorylation by the PDKs is opposed by pyruvate dehydrogenase phosphatases of which there are two isoforms: PDP1 and PDP2. Little is known about their regulation in comparison to the PDKs. Both PDPs are activated by insulin, in contrast to the inhibitory effect of insulin on PDK2 and PDK4 (McLean et al., 2008). PDP1 activity is also known to be stimulated by Ca^{2+} ions, but PDP2 is not. As with the PDKs, the PDPs are expressed in a tissue specific manner. PDP1 is the predominant isoform in skeletal muscle, whereas PDP2 is more abundant in the liver and in adipocytes (Huang et al., 1998). PDHA1 phosphorylation has further been shown to be downregulated by PI3K/Akt signalling, although it is unclear which PDKs and/or PDPs are responsible for this (Cerniglia et al., 2015).

1.6.3 Regulation of PDH activity by acetylation

Due to the high concentration of acetyl-coA, which is the substrate for protein acetylation, in the mitochondria, many proteins are auto-acetylated and this can impact on their activity. Acetylation in the mitochondria is predominantly regulated by deacetylases, the major mitochondrial deacetylase being SIRT3 (Lombard et al., 2007). Although not so highly characterised as PDH phosphorylation, a few studies have investigated the role of PDH acetylation. K321, which is the lysine residue that binds the FAD cofactor, has been identified as a regulatory acetylation site on the E1 subunit that inhibits PDH activity when acetylated. Deacetylation by SIRT3 restored PDH activity (Ozden et al., 2014). Treatment with a SIRT3 inhibitor increased PDH acetylation and decreased its activity in myocardial tissue (Zhang et al., 2018). In a further study, both PDH and PDP1 were shown to be regulated by acetylation. Again, K321 acetylation was shown to inhibit PDH activity by recruiting PDK1, and PDP1 acetylation on K202 caused PDP1 to dissociate from PDH, leading to an overall increase in glycolytic metabolism (Fan et al., 2014). PDH was also shown to be more acetylated in mice fed a high fat diet; it is possible that acetylation decreased PDH activity so that fatty acid oxidation could take over as the main source of acetyl-coA in the mitochondria (Thapa et al., 2017). Therefore acetylation, like phosphorylation, is an inhibitory modification for PDH, and can furthermore provide a mechanism to reduce PDH activity if there is an excess of acetyl-coA that is not converted to citrate, maintaining metabolic homeostasis.

1.6.4 The varied roles of PDH

The acetyl-coA produced by the PDH complex is a highly versatile metabolite. It consists of an acetyl group joined by a thioester bond to Coenzyme A, which is a derivative of vitamin B5 and cysteine. The thioester bond is high in energy, and therefore the acetyl group can easily be transferred to acceptor molecules such as metabolites or proteins. Acetyl-coA from PDH is one of two routes that pyruvate

can take to enter the TCA cycle and therefore controls the flux into the TCA cycle from glycolysis. Acetyl-CoA can then be exported out of the mitochondria either via citrate or acetylcarnitine, where it can be used for fatty acid, sterol and ketone body synthesis. PDH thus links glucose, oxidative and lipid metabolism (Fig. 1-2). It is vital for an organism to be able to adapt nutrient usage to nutrient availability, that is, to be able to rapidly switch between using carbohydrates or lipids depending on supply, because the inability to do this leads to diseases such as diabetes, obesity and metabolic syndrome. PDH therefore sits at a central metabolic point. Finally, acetyl-coA is the substrate for protein acetylation which is a key post-translational modification, especially in the nucleus where histone acetylation can drastically alter the epigenetic code.

The majority of the studies on PDH activity have focussed on its ability to switch cell metabolism from glycolytic to oxidative and vice versa. The PDKs play a vital role in the metabolic flexibility of different organs, particularly PDK2 and PDK4. PDK4 is upregulated in skeletal muscle during and after exercise to inactivate the PDH complex and promote glycolysis. This enables increased ATP production during exercise to meet the higher energy demands and subsequently allows the cells to replenish glycogen stores to restore metabolic homeostasis (Pilegaard and Neufer, 2004). The PDH complex is also a crucial enzyme in the liver, which regulates blood glucose levels and the supply of other nutrients to tissues. In fasting conditions, the liver must produce glucose from non-carbohydrate sources by gluconeogenesis. Inactivation of PDH by upregulating PDK4 enables pyruvate derived from glucose to directly enter the TCA cycle via oxaloacetate rather than being used for fatty acid synthesis. This promotes the use of lipids for gluconeogenesis (Randle, 1986). In the liver, conversion of glucose to lipids is also important for storing energy. PDH knockdown decreased fatty acid synthesis in the liver. Interestingly, PDH knockdown also decreased expression of lipid synthesis genes, suggesting that acetyl-coA is not only a building block for lipid synthesis but also a regulator of gene expression, possibly through altering histone acetylation (Mahmood et al., 2016). As mentioned earlier, PDH plays an important role in the switch to glycolytic metabolism in hypoxia, via HIF-1 α upregulation of PDK1 to phosphorylate and inhibit PDH activity. This is important to block access to the TCA cycle and initiate the switch to lactate production, increasing ATP

synthesis and reducing toxic ROS production in the mitochondria to prevent hypoxia-induced apoptosis (Kim et al., 2006a).

Failure to correctly regulate PDH activity leads to disease. Pyruvate dehydrogenase deficiency leads to a build-up of lactate leading to acidosis and genetic disorders such as encephalopathy, demonstrating the importance of PDH in regulating oxidative metabolism (Asencio et al., 2016). PDH activity also plays an important role in insulin resistance, which is characterised by an inability to switch from lipid to glucose oxidation when stimulated. Insulin resistant patients have increased PDK2 and PDK4 expression, and fail to reduce PDK4 expression in response to insulin, demonstrating the importance of regulating PDH activity to maintain metabolic flexibility (Kim et al., 2006c). Metabolic flexibility is also important in the heart, because the heart has to be able to rapidly oxidise glucose to meet energy demands. PDK4 is upregulated in cardiomyopathy, and overexpression of PDK4 in cardiac tissue in mice led to a decrease in glucose catabolism and increased hypertrophy and death (Zhao et al., 2008). Interestingly, PDH activity has also been linked to neurological disorders. The brain relies primarily on glucose oxidation for energy, which requires an active PDH. Alzheimers disease has been linked to dysfunctional glucose metabolism involving a reduction in PDH activity (Yao et al., 2009), and the expression of PDK1 and PDK2 is upregulated in the aging brain (Nakai et al., 2000).

Although the PDH complex is a major source of acetyl-coA in cells and it is known that acetyl-coA is the substrate for protein acetylation, there are few studies showing that PDH activity has a direct impact on protein acetylation. Mitochondria are known to have a disproportionately high level of acetylated proteins, and this is thought to occur due to the high concentration of acetyl-coA in the mitochondria which stimulates autoacetylation of lysine residues (Baeza et al., 2016). Acetylation of mitochondrial proteins is generally inhibitory (Anderson and Hirschey, 2012). PDH activity could therefore regulate mitochondrial acetylation to control mitochondrial metabolism. Although PDH is typically a mitochondrial protein, studies have shown that PDH can be located in the nucleus in lung fibroblasts, where the acetyl-coA it produces is used to acetylate specific lysine residues on histones to enable cell cycle progression (Sutendra et al., 2014, Chen et al., 2018). Mitochondrial acetyl-coA production can also affect histone

acetylation. Recently, studies have shown that mitochondrial dysfunction leads to decreased histone acetylation. Under conditions of mitochondrial DNA depletion, the pool of mitochondrial acetyl-coA was reduced, leading to loss of histone acetylation, and particularly of H3K9 and H3K27 acetylation (Lozoya et al., 2019). However whether this is due specifically to loss of PDH activity or is a general response to mitochondrial dysfunction is unclear. Similarly, loss of the transcription factor TFAM, which is important for transcription of mitochondrial genes, led to decreased mitochondrial metabolism and a corresponding decrease in histone acetylation in erythroid cells (Liu et al., 2017). However, at present there is still no direct link between mitochondrial PDH activity and nuclear histone acetylation in the literature.

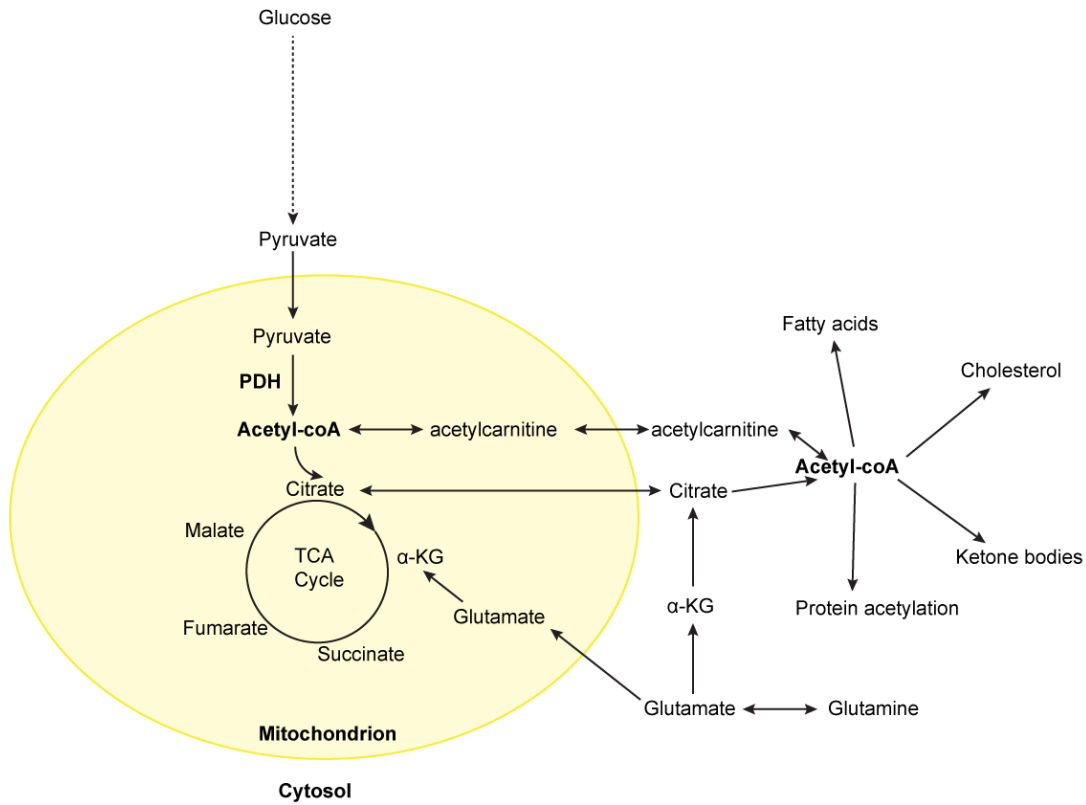


Figure 1-3 Acetyl-coA is a central metabolite

Diagram showing the production of acetyl-coA by PDH and the varied metabolic and acetylation pathways that acetyl-coA can be used for both inside and outside the mitochondria.

1.6.5 PDH activity in cancer

In addition to regulating metabolic diseases, PDH activity has been shown to play a critical role in cancers in many studies. One of the most well-known metabolic alterations in tumour cells is the Warburg effect, in which cancer cells become more glycolytic. PDH is a key player in this, and PDKs are upregulated in many cancers in order to inhibit oxidative metabolism and promote glycolysis. PDK1 is upregulated in several types of cancer and high PDK2 expression in cervical cancer cells is a prognostic factor for metastasis and poor survival (Lyng et al., 2006). PDK3 expression is increased in colorectal cancer and is associated with drug resistance and tumour relapse (Lu et al., 2011). PDK4 has been shown to be both up and downregulated in various cancers including lung, ovarian, breast and prostate tumours (Grassian et al., 2011, Ross et al., 2000). Therefore in some tumours an increase in PDH activity is required, possibly to produce acetyl-coA for fatty acid synthesis, which can be upregulated in cancer cells. Furthermore, as discussed previously, in the reverse Warburg effect some tumours rely more on lactate uptake to fuel oxidative phosphorylation than on glycolysis. This would require a more active PDH and therefore reduced PDK4 expression would be beneficial. The role of PDK1 in mediating metabolic adaptation to hypoxia is also important in the context of cancer, where hypoxia is a commonly occurring stress in the tumour microenvironment due to poor oxygenation by dysfunctional blood vessels. PDK-mediated inhibition of PDH activity has also been associated with metastasis. PDK4 upregulation enhanced the ability of mammary cancer cells to resist matrix detachment-induced apoptosis, otherwise known as anoikis, which is a barrier to metastasis (Kamarajugadda et al., 2012).

Targeting PDH to increase its activity and reduce the Warburg effect has been proposed as a metabolic therapy for cancer. Several studies have shown that increasing PDH activity reduces cancer aggressiveness. For example, in BRAF driven melanoma, senescence was shown to be mediated by PDK1 downregulation and induction of PDP2 to activate PDH activity. Furthermore, PDK1 knockdown in BRAF^{V600E} cell lines made them more sensitive to BRAF inhibitors (Kaplon et al., 2013). Dichloroacetate (DCA), which activates PDH by inhibiting the PDKs, is the most well studied drug targeting PDH. It is already used clinically to target lactic acidosis, and was shown to have anti-tumour properties, causing apoptosis in

several cancer cell lines and reducing tumour growth in xenografts (Bonnet et al., 2007, Michelakis et al., 2008). In breast and non-small cell lung cancer xenografts, inhibition of PDK2 with DCA also reduced angiogenesis and suppressed pseudohypoxic HIF signalling (Sutendra et al., 2013). DCA has shown additive or synergistic effects in pre-clinical experiments in combination with already existing therapies, including radiation, metformin, cisplatin and bevacizumab (Cao et al., 2008, Florio et al., 2018, Kumar et al., 2013a, Kumar et al., 2013b). As a cancer therapy, DCA has been effective in treating some individual cases (Flavin, 2010a, Flavin, 2010b). In clinical trials however, its effectiveness has not been conclusively demonstrated so far. In a trial on glioblastoma patients, some patients showed a response, but a phase II clinical trial on breast and non-small cell lung cancer had to be halted due to safety concerns and DCA had no effect on head and neck cancer in phase II trials (Powell, 2015, Dunbar et al., 2014, Garon et al., 2014). Conversely, inhibiting PDH has shown great effectiveness in some cancers. CPI-613, which inhibits both PDH and α -ketoglutarate dehydrogenase to block mitochondrial metabolism, has been shown to improve response and enhance sensitivity to chemotherapy in AML, T-cell lymphoma and pancreatic cancer, and is currently in stage II and III clinical trials for treatment of pancreatic cancer patients (Pardee et al., 2018, Alistar, 2018, Lamar, 2016). Therefore it appears that PDH activity can have both positive and negative effects on tumour progression, and further investigation is needed in order to determine which tumours would benefit from PDH-targeting therapy and whether to inhibit or activate PDH.

Although there has been much research on PDH activity in cancer cells, little is known about its role in the stroma. As discussed earlier, the metabolism of the stroma is often the opposite to that of the tumour, creating a metabolic symbiosis. Therefore if tumour cells have an inactive PDH to promote glycolysis, it is possible that PDH is more active in the stroma and promoting a more oxidative metabolism. In support of this, one study has found that PDH expression is upregulated in lung fibroblasts co-cultured with cancer cells, and, conversely, the cancer cells upregulate PDK1 expression to reduce PDH activity and promote glycolysis (Koukourakis et al., 2017). On the other hand, one of the studies demonstrating the existence of the reverse Warburg effect, PDH expression was found to be downregulated in CAFs in response to oxidative stress as part of the switch to

glycolytic metabolism (Martinez-Outschoorn et al., 2010). Therefore the role of PDH in the stroma is still an open question, and may depend on whether the tumour the CAFs are derived from has a more glycolytic or oxidative metabolism.

1.6.6 PYCR1 and proline metabolism

Pyrroline-5-carboxylate reductase 1 (PYCR1) is the second metabolic enzyme that I discovered regulated in mammary CAFs during my PhD. PYCR1 catalyses the final, rate limiting step in proline production from glutamate or ornithine in cells: the NAD(P)H dependent conversion of pyrroline-5-carboxylate (P5C) to proline. P5C is the intermediate linking the two pathways of proline synthesis, and is synthesised from glutamate by P5C synthase (P5CS or ALDH18A) or from ornithine by ornithine aminotransferase (OAT) (Fig. 1-4). Proline is an unusual amino acid because its α -amino group is contained within its pyrrolidine ring, and therefore its metabolic pathways of synthesis and degradation are distinct from those of other amino acids. For example proline does not undergo decarboxylation, deamination and other pyridoxal phosphate (vitamin B6) catalysed reactions typical of other amino acids (Adams and Frank, 1980).

There are three homologous PYCR genes: PYCR1, PYCR2 and PYCR3. De Ingeniis et al. showed that PYCR1 and PYCR2 are mitochondrial, whereas PYCR3 is cytoplasmic. The authors also suggested that PYCR1 and PYCR2 mainly use glutamate as a source of proline whereas PYCR3 participates only in the conversion of ornithine to proline. However, these results were only demonstrated in melanoma cells, so whether they are also relevant in other cell lines is unknown. Other studies suggest that P5C is derived from either glutamate or ornithine in the mitochondria and can then be exported for conversion to proline by PYCR3 (Tanner et al., 2018). The three isoforms also differ in their response to product inhibition: PYCR2 is the most highly inhibited by proline, followed by PYCR1, and PYCR3 is not inhibited by proline within a physiological range (De Ingeniis et al., 2012). PYCR3 could therefore maintain a baseline level of proline synthesis even when cytosolic proline levels are high.

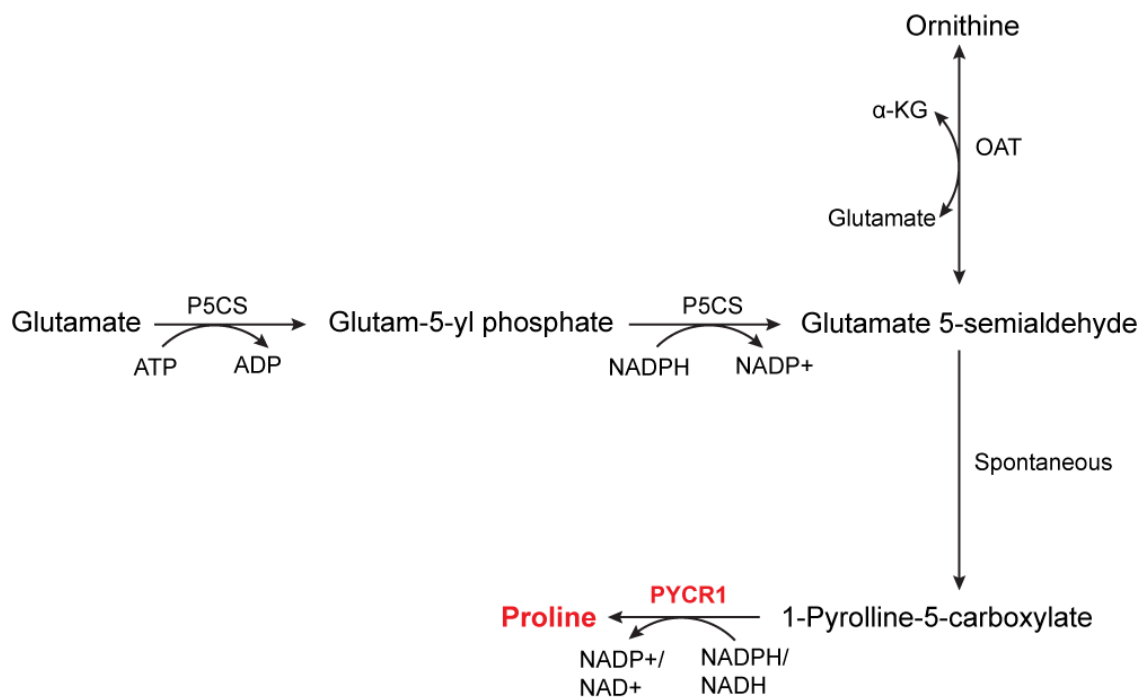


Figure 1-4 Proline synthesis pathway

Diagram showing the production of proline from both ornithine and glutamate, with the final step being catalysed by PYCR1

Proline synthesis plays an important role in protecting cells from stress. The production of proline by PYCR1 oxidises NADPH or NADH to NADP⁺/NAD⁺, which can support glycolysis and the pentose phosphate pathway (Liu et al., 2015). Equally, the interconversion of P5C and PYCR1 creates a shuttle of the redox equivalents NADPH/NADP⁺ between the mitochondria and cytosol, meaning that proline production plays a role in maintaining redox homeostasis (Hagedorn and Phang, 1983). Furthermore, the proline molecule itself protects against ROS via the secondary amine of the pyrrolidine ring and has also been reported to protect against photooxidative UVA damage (Wondrak et al., 2005). The importance of proline production to protect against ROS has been demonstrated in several studies. For example, treatment of mammalian cell lines with hydrogen peroxide resulted in increased PYCR1 expression, and higher PYCR1 expression was then found to protect cells from ROS-induced apoptosis. Conversely, overexpression of proline dehydrogenase (PRODH) resulted in decreased intracellular proline levels and decreased resistance to ROS (Krishnan et al., 2008). Interestingly, both PYCR1 and PYCR2 have been found to interact with and promote the activity of RRM2B, a protein which promotes DNA damage repair in response to oxidative stress, in fibroblasts, showing that the anti-oxidant properties of PYCR1 are not solely due to its role in proline production but that it also plays a role in the wider cellular response to oxidative stress (Kuo et al., 2016). Further demonstrating the diverse roles of PYCR1 as a protection against cellular stresses are studies showing that proline produced by PYCR1 can protect against protein misfolding *in vitro* and in *E. coli* and plants by acting as a molecular chaperone (Samuel et al., 2000). This is due to its properties as an osmolyte, which is a substance that can change the physical properties of biological fluids such as the viscosity or ionic strength, and can therefore influence protein stability, folding rate and aggregation (Fisher, 2006).

As an amino acid, a major role of proline is to contribute to protein synthesis, and another important aspect of proline synthesis is the fact that it makes up a considerable proportion of collagen, the most abundant protein in the body, as discussed earlier in this chapter. Although there is little evidence so far in the literature connecting proline synthesis to collagen production, it is interesting to note that collagen production is downregulated in response to oxidative stress caused by ROS, and this can be rescued by treating cells with reducing agents

(Tanaka et al., 1993). It is therefore possible that collagen can be a means of getting rid of excess reducing potential in the form of proline, again demonstrating the importance of proline as a reducing equivalent.

Clinically, PYCR1 mutations are one of the causes of cutis laxa, a disorder with symptoms including wrinkled skin, premature aging, and developmental delay, showing the importance of maintaining proline levels during development, and in fibroblasts for maintenance of skin elasticity and turnover. Research into the role of proline in cutis laxa showed that PYCR1 mutant fibroblasts did not display a reduction in intracellular proline, although patients had slightly lower levels of proline in their serum. However, the morphology of mitochondria in the fibroblasts was abnormal and they were more susceptible to ROS induced apoptosis, again showing the importance of PYCR1 in maintaining redox balance across the mitochondrial membrane (Reversade et al., 2009). The presence of abnormal collagen fibres and a decrease in collagen bundle compactness, along with a significant decrease in elastin fibres, has also been reported in the ECM of some patients with PCYR1 mutations (Kretz et al., 2011). Additionally, a study on *pycr1* KO zebrafish found that the zebrafish had reduced ECM content and decreased levels of proline and hydroxyproline in their tissues (Liang et al., 2019). Although none of these studies conclusively linked proline levels to collagen production, it is reasonable to hypothesise that a reduction of proline production can affect collagen production since proline is such a crucial component of collagen.

Therefore aside from its role as an amino acid for protein synthesis, proline is a highly important molecule for maintaining redox balance and protecting cells from stresses such as ROS or protein misfolding. Since these factors are critical in tumours, where there are higher levels of ROS and oxidative stress, it is unsurprising that PYCR1 expression is dysregulated in many cancers.

1.6.7 PYCR1 in cancer

Increased PYCR1 expression is a common feature of tumours. In a meta-analysis of the mRNA profiles of 2000 tumours spanning 19 types of tumour, PYCR1 was found to be one of the most consistently upregulated metabolic genes (Nilsson et

al., 2014). This is at least in part due to the fact that PYCR1 is a known target of cMyc and has also been shown to be linked to PI3K signalling; both of which are oncogenes that are commonly activated in cancer. In tumours where PYCR1 is upregulated by cMyc, there also is a corresponding increase in intracellular proline, showing that PYCR1 overexpression has a functional output. (Liu et al., 2015, Liu et al., 2012b). Increased proline production by tumour cells has been reported in other studies. In a study profiling central carbon metabolism in breast cancer, a significant increase in proline synthesis was the main metabolic alteration observed in metastatic cells when compared to non-metastatic cells (Richardson et al., 2008). PYCR1 and proline synthesis upregulation is not merely a side effect of oncogenic tumour formation, however, but also contributes significantly to tumour development. PYCR1 knockdown inhibited tumour formation by xenografts *in vivo* (Possemato et al., 2011). In both prostate and non-small cell lung cancer, PYCR1 is overexpressed and has been shown to promote proliferation and inhibit apoptosis (Cai et al., 2018). PYCR1 appears to be the main regulator of tumourigenesis out of the PYCR enzymes, since a study comparing PYCR1 and PYCR2 expression in data from 2535 breast cancer patients found that PYCR1, but not PYCR2, was upregulated in breast cancer and corresponded with poor survival and metastasis (Ding et al., 2017). The pro-tumourigenic effects of PYCR1 have mostly been found to involve maintaining redox homeostasis. In glioma cells, IDH1 mutations, which cause loss of reducing potential and alter the NADPH:NADP⁺ ratio, were shown to upregulate PYCR1 expression. This provided a mechanism of NAD(P)H reduction to maintain redox balance, and the increased production of proline from glutamate led to partial TCA cycle uncoupling from respiration. This enabled oxygen-independent synthesis of TCA cycle-derived metabolites, such as citrate and aspartate, which would give the cells a metabolic advantage under hypoxia (Hollinshead et al., 2018). PYCR1 has further been shown to contribute to the adaptation of cancer cells to hypoxia by promoting HIF-1 α signalling. In hepatocellular carcinoma, HIF1 α signalling under hypoxia stimulated proline production, leading to increased hydroxyproline production. Increased levels of hydroxyproline stabilised HIF1 α and enhanced hypoxia-driven signalling (Tang et al., 2018). PYCR1 has also been shown to be important for the broader metabolic rewiring of tumours. Because proline production is a source of NAD⁺/NAPDH⁺, it can stimulate glycolysis through GAPDH activity and nucleotide synthesis through the pentose phosphate pathway, both of

which enable increased proliferation of cancer cells. Because proline is derived from glutamine, proline production by PYCR1 thus links the frequently observed reliance on glutamine by tumours with nucleotide synthesis and the Warburg effect to promote proliferation (Liu et al., 2015) (Fig. 1-5).

Tumour cells are also dependent on proline for protein synthesis. Ribosome profiling revealed that proline was a limiting factor for protein synthesis in both kidney and breast cancers, and that this was dependent on high expression of PYCR1. Loss of PYCR1 increased ribosome stalling and inhibited tumour growth (Loayza-Puch et al., 2016). Proline synthesis was also shown to be required for protein synthesis in melanoma cells, where P5C synthase knockdown inhibited protein synthesis via EIF2AK4 activation (Kardos et al., 2015). The necessity for tumour cells to maintain proline levels is also highlighted by the fact that tumours have recently been shown to use degraded collagen from the ECM as a source of proline to maintain protein synthesis and redox homeostasis. In PDAC, upregulation of MMPs, which are involved in collagen degradation, and PRODH, the proline catabolism enzyme, enabled tumour cells to scavenge and utilise collagen from the tumour microenvironment in times of nutrient scarcity (Gouirand and Vasseur, 2018, Olivares et al., 2017). This again highlights the importance of CAF-derived collagen in the ECM to promote tumour growth and metastasis. Additionally, upregulated expression of PRODH in breast cancer cells supported growth by maintaining ATP levels in 3D culture and promoted the formation of lung metastases in orthotopic mouse models (Elia et al., 2017). This could mean that breast cancer cells are also able to scavenge collagen from their environment as a source of proline. However, in this study the PYCR enzymes were still required even with exogenous proline treatment; therefore although cancer cells may degrade proline as a source of energy, it is probably still necessary to continue synthesising proline to maintain the cellular redox balance.

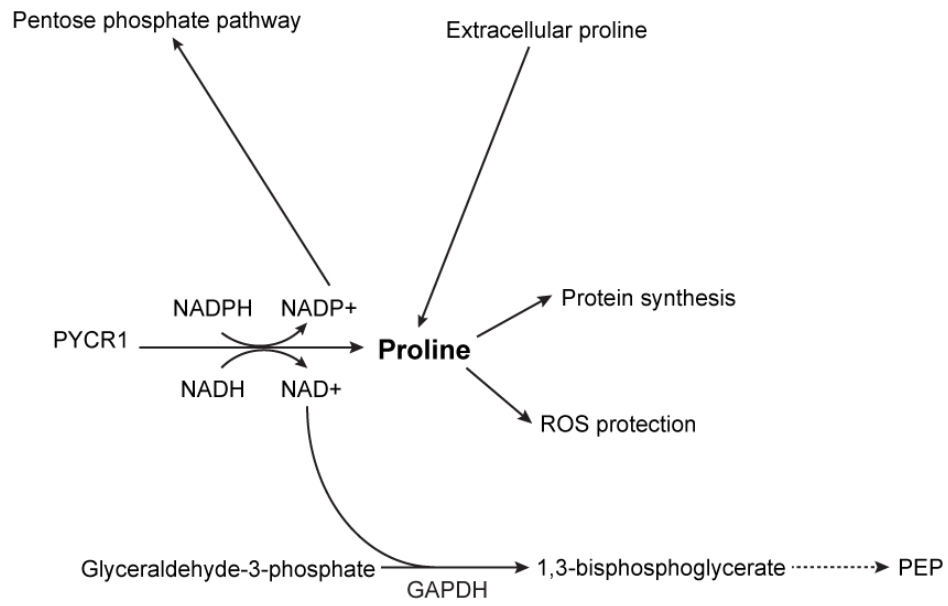


Figure 1-5 Metabolic impact of proline synthesis

Diagram showing the pathways affected by the products of the PYCR1-catalysed reaction

Despite the aforementioned significance of proline metabolism and synthesis in tumour development and progression, until recently there were no drugs or other therapeutic agents targeting PYCR1, so the relevance of these findings to the clinic has been untested. However, very recently a small molecule inhibitor has been developed against PYCR1 which reduced intracellular proline and inhibited growth in breast cancer cell lines (Milne et al., 2019). Although the drug is metabolised rapidly in mice, and therefore is unlikely to be suitable for clinical studies, it is a good starting point for the development of treatments targeting PYCR1. Much of the initial work on targeting tumour metabolism was done on 'core' metabolic pathways such as glucose or glutamine metabolism, which are indeed highly dysregulated in tumours. However, targeting these pathways has proved difficult, since they are also vital pathways for all cells in the body, so pharmacological inhibition produced severe side effects. Therefore targeting metabolic pathways which are not universally required but are dysregulated in tumour cells and therefore provide therapeutic vulnerabilities has become a more promising strategy, and proline production by PYCR1 falls under this category.

Finally, although many studies have linked PYCR1 expression to poor clinical outcome in tumours and demonstrated the relevance of PYCR1 in cancer cells, little research has been done on the role of PYCR1 in the tumour microenvironment. PYCR1 has been shown to be important for fibroblast functionality in the context of cutis laxa caused by PYCR1 mutations, but so far no studies have investigated whether PYCR1 is relevant in CAFs or, indeed, in any other cells of the TME. As any drug targeted towards the cancer cells will naturally also have an impact on the stroma, to determine if PYCR1 is a viable therapeutic target it is also important to know what effect, if any, it has in the stroma.

1.8 Objectives

The primary objective of this study was to gain further insight into how the metabolic rewiring of CAFs contributes to their pro-tumourigenic function, with the aim of discovering new potential targets for therapies targeting the tumour microenvironment, or to inform on existing lines of treatment. Many studies have shown that CAFs rewire their metabolism to secrete metabolites to fuel tumour cells. However, how CAF metabolic rewiring might affect other aspects of the CAF phenotype has been little explored. In particular, ECM production, which is a major function of CAFs, is known to be affected by metabolite availability but as yet few studies have investigated ECM production from a metabolic perspective in CAFs. Targeting ECM production in the stroma can improve tumour perfusion and drug delivery as well as reducing tumour growth and metastasis. Furthermore, as metabolic targets and therapies are being discovered for tumour cells, it is important to have an understanding of whether these will also target the CAF phenotype and if so whether they might have a pro or anti-tumourigenic effect. To uncover metabolic differences between CAFs and NFs which contribute to the pro-tumourigenic CAF phenotype, I used a combination of mass spectrometry-based proteomics and metabolomics and *in vitro* assays. Based on these results, I selected candidate metabolic enzymes that were differentially regulated between CAFs and NFs. In order to characterise these targets and determine how they affected pro-tumourigenic phenotype of CAFs I carried out further proteomic and metabolomic experiments as well as characterising the effects of overexpression and pharmacological or RNAi mediated inhibition of these targets, both using *in vitro* assays and *in vivo* characterisation of xenografts containing CAFs with impaired metabolism.

Chapter 2 Materials and Methods

2.1 Materials

2.1.1 Reagents and kits

Table 2-1 Reagents and kits

Reagent	Supplier	Catalogue #
Acetic acid	Sigma	32009
Acetonitrile	Sigma	34967
Alexa Fluor 647 azide	Life Technologies	A10277
Amaya nucleofector kit R	Lonza	VCA-1001
Ammonium bicarbonate	Sigma	11213
Ampicillin	Sigma	A0166
Bradford reagent	Biorad	500-0205
BSA	Sigma	A2153
BSA standard	Biorad	500-0206
Calcium phosphate transfection kit	Invitrogen	K278001
Chloroacetamide	Sigma	C0267
Click-iT™ EdU Alexa Fluor™ 647 Flow Cytometry Assay Kit	Life Technologies	C10419
D-Glucose	Sigma	G7021
D-Glucose U- ¹³ C ₆	Cambridge Isotope laboratories	CLM-1396
Dialysed FBS	Sigma	F0392
DMEM	Gibco	11960044
DMEM 1g/l glucose (low glucose)	Gibco	21885025
DMEM no glucose	Gibco	11966025
DMEM no pyruvate	Gibco	11960044
DMSO	Fisher	10080110
DNase I recombinant, RNase free	Roche	4716728001
DTT	Sigma	43819
Empore solid phase extraction disk (C18)	3M	2215
F12 medium	Gibco	21765029
FBS	Gibco	10270
Fluorescent mounting medium	Dako	S3032
Fungizone	Gibco	15290018
Glutamine	Life technologies	25030-024
Glutamine U- ¹³ C ₅	Cambridge Isotope Laboratories	CLM-182
Glycine	Sigma	G7126
HEPES	Sigma	H3537

Horse serum	Gibco	26-050-070
Hygromycin	Sigma	H3274
iScript cDNA synthesis kit	Biorad	170-8891
iTaq Universal SYBR green supermix	Biorad	172-5121
Kanamycin sulphate	Sigma	11815024
L-Arginine hydrochloride 13C6 15N4 (Arg10)	Cambridge laboratories	Isotope CNLM-539-H-PK
L-Lysine hydrochloride 13C6 15N2 (Lys8)	Cambridge laboratories	Isotope CNLM-291-H-PK
L-Arginine hydrochloride (Arg0)	Sigma	A6969-25
L-Lysine monohydrochloride	Sigma	L8662
LysC		
Growth factor reduced Matrigel	Corning	15585729
Methanol	Sigma	32213
Methanol (HPLC grade)	Sigma	34860
MitoSOX Red Mitochondrial Superoxide Indicator	Life Technologies	M36008
Nicotinamide	Sigma	72340
Nitrocellulose transfer membrane 0.45 µm	GE Healthcare	10600003
Non-fat milk	Marvel	5000354167508
NP-40	Sigma	NP40S
NuPage 4-12% Bis-tris polyacrylamide gel	Life Technologies	NW04120
NuPage LDS sample buffer	Life Technologies	NP0007
NuPage running buffer (MOPS)	Life Technologies	NP0001
NuPage running buffer (MES)	Life Technologies	NP0002
NuPage transfer buffer	Life Technologies	NP0006-1
Optiblot Bradford reagent	abcam	ab119216
Palmitate U- ¹³ C ₁₆	Sigma	605573
Paraformaldehyde	Sigma	441244
PBS with Mg ²⁺ and Ca ²⁺	Sigma	D8662
Penicillin/Streptomycin	Life Technologies	15140122
Phalloidin	Life Technologies	A12379
Ponceau Red	Sigma	P7170
Puromycin	Gibco	A1113802
PVDF transfer membrane 0.45 µm	Thermo Scientific	88518
Pyruvate dehydrogenase enzyme activity microplate assay	abcam	ab109902
Qiashredder kit	Qiagen	79656
RNase free DNase	Qiagen	79254
RNEasy mini kit	Qiagen	74904
Saponin	Sigma	84510
Seahorse XF base medium	Agilent	102353-100
Seahorse XF24 Fluxpak	Agilent	100867-100

SILAC DMEM (no Arg/Lys)	Gibco	A14431-01
Sodium acetate	Sigma	241245
Sodium butyrate	Sigma	B5887
Sodium chloride	Fisher	S/3160/60
Sodium deoxycholate	Sigma	D6750
Sodium dodecyl sulphate (SDS)	Fisher	S/P530/53
Sodium hydroxide	Sigma	S5881
Sodium pyruvate	Gibco	11360070
Sodium pyruvate (U- ¹³ C ₃)	Sigma	490733
Sulforhodamine B	Sigma	230162
TCEP	Sigma	C4706
TFA	Sigma	T6508
Thiourea	Sigma	T8656
TMRE	Life Technologies	T669
Tris	Melford	B2005
Triton-X-100	Sigma	X100
Trypsin	Life Technologies	15090
Trypsin (MS-grade)	Promega	V5280
Urea	Sigma	U5128
Western blotting detecting reagent Amersham ECL	GE Healthcare	RPN2109
Western blotting detecting reagent Amersham ECL Prime	GE Healthcare	RPN2232

2.1.2 Buffers and solutions

Table 2-2 Buffers and solutions

Name	Composition
Buffer A	0.5% (v/v) formic acid in HPLC water
Buffer A*	2% (v/v) ACN, 0.1% (v/v) TFA in HPLC water
Buffer B	80% (v/v) ACN, 0.5% (v/v) formic acid in HPLC water
IAP buffer	50 mM MOPS, 10 mM sodium phosphate, 50 mM sodium chloride in HPLC water
PBS	0.8 % (w/v) Sodium chloride, 0.02 % (w/v) potassium chloride, 0.115 % (w/v) di-sodium hydrogen phosphate, 0.02 % (w/v) potassium dihydrogen phosphate, pH 7.3
RIPA	50 mM Tris-HCl pH 7.5, 150 mM sodium chloride, 1 mM EDTA, 1% (v/v) NP-40, 0.1% (w/v) sodium deoxycholate
SDS buffer	2% (w/v) SDS, 100 mM Tris-base pH 7.4
TBST	Tris buffered saline with 0.05 % Tween-20
Urea buffer	6M Urea, 2M thiourea, 40 μ M CAA, 10 μ M TCEP

2.1.3 Antibodies

Table 2-3 Antibodies and dilutions used

Antibody	Supplier	Catalogue #	Dilution
α SMA	Sigma	A5288	1:10,000 WB, 1:1000 IF
Acetylated H3K27	Abcam	ab4729	1:1000
ACLY	CST	4332S	1:1000
B-tubulin	abcam	ab6046	1:1000
GAPDH	Santa Cruz	sc-47724	1:1000
CD31	BioRad	MCA1370Z	1:100
PDHA1	Abcam	ab110334	1:1000 WB, 1:100 IF
Phospho-ACLY (S455)	CST	4331S	1:1000
Phospho-PDHA1 (S293)	Abcam	177461	1:2000
Phospho-Smad 2	CST	3108	1:1000
PYCR1	ProteinTech	22150-1-ap	1:1000
Vimentin	Santa Cruz	sc-7557	1:2000
Vinculin	Sigma	V9131	1:1000
Anti-mouse HRP	CST	7076S	1:5000
Anti-rabbit HRP	CST	7074S	1:5000
Anti-mouse Alexa fluor 555	Life Technologies	A32773	1:500
Anti-rabbit Alexa Fluor 555	Life Technologies	A32794	1:500
Anti-mouse Alexa fluor 647	Life Technologies	A32787	1:500
Anti-rabbit Alexa Fluor 647	Life Technologies	A32795	1:500
Anti-hamster Alexa Fluor 647	Life Technologies	A-21451	1:200

2.1.4 Primers

Table 2-4 List of primers

Gene name	Forward (5'-3')	Reverse (3'-5')
18S	AGGAATTGACGGAAGGGCAC	GGACATCTAAGGGCATCACA
ACTB	GGCATGGGTCAGAAGGATT	ACATGATCTGGGTCATCTTCTC
COL1A1	TGAAGGGACACAGAGGTTTCAG	GTAGCACCATCATTTCACGA
COL6A1	AGCAAGTGTGCTGCTCCTTC	CTTCCAGGATCTCCGGCTTC
GAPDH	AGCCACATCGCTCAGACA	GCCCAATACGACCAAATCC
PDK1	GAATGTTACTCAATCAGCACTCTT	CCTAGCATTTTTCATAGCCATCTTT
PDK2	CGGGGACCACAACCAAAGTC	GCTGGATCCGAAGTCCAGAAA
PYCR1	CCCCGCCTACGCATTCA	GCGCGTTGGAAGTCCCATCT
PYCR2	GTACACTGTAGCGCCTTCCTG	GTACACTGTAGCGCCTTCCTG
TBP2	AGTGACCCAGCATCACTGTTT	TAAGGTGGCAGGCTGTTGTT

2.1.5 Small interfering RNA

Table 2-5 List of small interfering RNAs

Gene name	Sequences (5'-3')	Supplier	Catalogue #
Control pool	UGGUUUACAUGUCGACUAA, UGGUUUACAUGUUGUGUGA, UGGUUUACAUGUUUUCUGA, UGGUUUACAUGUUUCCUA	Dharmacon	D-001810-10-05 (On Target plus non-targeting pool)
PDK2	CCACGUACCGCGUCAGCUA, AAGGCGUGCUUGAGUACAA, CAACGUCUCUGAGGUGGUC, UGGCUAAGCUCCUGUGUGA	Dharmacon	LQ-005020-00- 0002 (Set of 4)
PYCR1	GACCAACACUCCAGUCGUG, GAUGUGCUCUCCUGGCUG, GCCACAAGAUAAUGGCUA, GCGCCGACAUUGAGGACAG	Dharmacon	LQ-012349-00- 0002 (Set of 4)

2.1.6 Short hairpin RNA

Table 2-6 Short hairpin RNAs and their targets

Target Gene	Sequence (5'-3')	Supplier	Catalogue #
Control	CCGGCAACAAGATGAAGAGCACCA ACTCGAGTTGGTGCTCTTCATCTT GTTGTTTTT	Sigma	SHC002
PDK2	ACTATATACACAGAAGGTC	Dharmacon	V2LHS_169815
PYCR1-a	CCGGGAGGGTCTTCACCCACTCCT ACTCGAGTAGGAGTGGGTGAAGAC CCTCTTTTTG	Sigma	TRCN000003898 1
PYCR1-b	CCGGTGAGAAGAAGCTGTCAGCGT TCTCGAGAACGCTGACAGCTTCTT CTCATTTTTG	Sigma	TRCN000003898 3

2.1.7 Plasmids

Table 2-7 Plasmids

Name	Source	Catalogue #
WT PDK2	Prof. Angus McQuibben	
N255A PDK2	Prof. Angus McQuibben	
hTERT (Lentivirus)	Dr. Fernando Calvo	
pET28a-mCherry-CNA35	Addgene	61607

2.2 Methods

2.2.1 Cell lines and culture

2.2.1.1 iCAFs and iNFs

iCAFs and iNFs were kindly provided by Prof. Akira Orimo (Kojima et al., 2010). The iNFs are normal human mammary fibroblasts derived from reduction mammoplasty tissue and immortalised with a construct containing hTERT, GFP and puromycin resistance. hTERT is the catalytic subunit of human telomerase, which prevents telomere shortening and thereby the induction of telomere controlled senescence. hTERT expression has been shown to effectively immortalise cells without causing phenotypic changes or making the cells cancerous (Lee et al, 2004). A subsection of iNFs were transformed into iCAFs by two rounds of co-injection subcutaneously with MCF7-hRAS cells into mice and subsequent reisolation of the fibroblasts by culturing the isolated tumours with puromycin for 5 days.

2.2.1.2 pCAFs and pNFs

pCAFs and pNFs were isolated in house by Lisa Neilson from matched normal and breast cancer tissue from patients obtained through NHS Greater Glasgow and Clyde Biorepository. All participants gave specific consent to use their tissue samples for research. The fat surrounding the tissue was removed before cutting the tissue into small pieces. The tissue was then treated with 10 mg collagenase A in DMEM (10% FBS, 2 mM glutamine, 1% penicillin/streptomycin, 1% fungizone) overnight, after which the fibroblasts were the only surviving cells. The following day, fibroblasts were isolated using a cell strainer and plated on a cell culture dish coated with 35 mg/ml collagen I. The isolated fibroblasts were either expanded and frozen down or used for subsequent immortalisation. Fibroblasts become senescent after several passages, so in order to continue using them for experiments, the pCAFs and pNFs were immortalised using an hTERT lentiviral construct (pIRES-hygro-hTERT) kindly provided by Dr. Fernando Calvo. HEK293T cells were used to generate the hTERT lentivirus. 2×10^6 HEK293T cells were plated in a 10 cm dish. The next day, the HEK293T were transfected with 10 μ g of pIRES-hygro-hTERT as well as 4 μ g VSVG and 7.5 μ g psPAX as packaging plasmids by calcium phosphate transfection. The following morning the medium was replaced

with DMEM with 1 mM sodium butyrate. After 24h, the medium containing the virus was collected and 4 µg/ml polybrene was added. The virus was filtered through a 0.45 µm membrane to remove HEK293T cells and transferred onto the primary fibroblasts. This step was repeated the following day. After 48h, the immortalised fibroblasts were selected with 100 µg/ml hygromycin.

2.2.1.3 Cell culture

iCAFs, iNFs, pCAFs, pNFs, MCF7 and HEK293T cells were cultured in DMEM supplemented with 10% FBS, 2 mM glutamine, and 1% penicillin/streptomycin. MCF10DCIS.com cells were cultured in F12 medium supplemented with 5% horse serum, 2 mM glutamine, 1% penicillin/streptomycin and 0.1% fungizone. For SILAC experiments, cells were cultured in DMEM supplemented with 10% FBS, 2 mM glutamine, 1% penicillin/streptomycin and either 84 mg/l $^{13}\text{C}_6^{15}\text{N}_4$ L-arginine and 175 mg/l $^{13}\text{C}_6^{15}\text{N}_2$ L-lysine or 84 mg/l $^{12}\text{C}_6^{14}\text{N}_4$ L-arginine and 175 mg/l $^{12}\text{C}_6^{14}\text{N}_2$ L-lysine for 'heavy' and 'light' labelled cells respectively. All cells were cultured at 37°C, 5% CO₂, 21% O₂ and harvested with trypsin (0.025% in PE).

2.2.2 Cell based assays

2.2.2.1 EdU proliferation assay (Immunofluorescence)

EdU (5-ethynyl-2'-deoxyuridine) is an analogue of thymidine which is incorporated into newly synthesised DNA strands during S-phase. EDU incorporation can be detected using a fluorophore conjugated to an azide which is covalently cross-linked to EdU via a Click-iT reaction. It can therefore be used as a readout for the rate of cell proliferation. 5×10^5 cells were seeded on 13 mm coverslips. After 24h, EdU was added at a concentration of 1 mM and incubated for 2h at 37°C. Cells were fixed in 4% PFA for 15min, washed twice in PBS and simultaneously blocked and permeabilised with 1% BSA and 0.5% Triton-X100 in PBS. The Click-iT reaction was performed using Alexa-fluor 647 azide according to the manufacturers' protocol and the cells were counterstained with DAPI. Images were taken using a Zeiss 710 confocal microscope, and the percentage of cells that had incorporated EdU was calculated using an Image J macro.

2.2.2.2 EdU proliferation assay (Flow Cytometry)

EdU was added to medium at a concentration of 1 mM and incubated with the cells for 2h at 37°C. Cells were harvested and fixed in 4% PFA for 15 min, washed twice in PBS and simultaneously blocked and permeabilised with 1% BSA and 0.5% Triton-X100 in PBS. The Click-iT reaction was performed using Alexa-fluor 647 azide according to the manufacturers' protocol. The cells were washed x3 in PBS and resuspended in PBS with 1% BSA before analysis by flow cytometry using an Attune NxT (RL1 channel). The percentage of cells that had incorporated EdU was calculated using FloJo software.

2.2.2.3 PDH activity assay

Pyruvate dehydrogenase (PDH) activity was measured using the Pyruvate dehydrogenase enzyme activity microplate assay kit (abcam). The kit contains 96 wells coated with an antibody which captures the intact pyruvate dehydrogenase complex. PDH activity is then measured by following the reduction of NAD⁺ to NADH, which is a by-product of the conversion of pyruvate to acetyl-coA by PDH. This reduction is coupled to a reporter dye which produces a yellow reaction product, the concentration of which can be detected by measuring the absorbance at OD450. 5x15 cm dishes of CAFs and NFs at 80-90% confluency were harvested for each reaction and the assay was carried out following the manufacturers' protocol. OD450 absorbance was measured over 30 mins to determine the rate of reaction.

2.2.2.4 Seahorse assay

5x10⁴ cells were seeded in each well of the Seahorse xf24 cell culture plates and cultured for 48h. 30 mins before the assay the medium was replaced with the Seahorse base medium supplemented with 1% FBS, 2 mM glutamine and 1% penicillin/streptomycin and the cell culture plate was placed in a CO₂ free incubator at 37°C. The Seahorse xf24 assay plate was prepared according to the manufacturers' protocol. Using the Seahorse xf24, the oxygen concentration in the wells was measured 3 times over 12 minutes at basal levels, then following stepwise addition of 1 µM oligomycin, 1 µM CCCP and 1 µM of both Antimycin A and rotenone. Oligomycin inhibits ATP synthase by blocking the proton channel

(F0 subunit) thus reducing oxygen consumption. CCCP uncouples the electron transport chain from ATP synthesis by making the inner mitochondrial membrane permeable to protons, forcing the cells to consume oxygen at their maximum capacity. Finally Antimycin A and Rotenone inhibit cytochrome C and Complex I in the electron transport chain respectively to reduce oxygen consumption to almost nothing. The oxygen consumption was normalised to the protein content of the wells using SRB (Sulphurhodamine B). The cells were fixed in 10% TCA (Trichloroacetic acid) at 4°C overnight. The wells were washed with water, dried at RT and incubated with 0.04% SRB in 1% (v/v) acetic acid for 1 hr at RT. The wells were washed in 1% acetic acid and dried at RT. 200 µl of Tris-HCl pH 10.5 was added to each well and incubated at RT for 30 min to resolubilise the dye. The OD for each well was measured at 510 nm and the cell number for each well was calculated by comparing the results to a standard curve of 20,000-100,000 cells

2.2.2.5 Bioanalyzer assay

8x10⁴ fibroblasts were seeded in each well of 6 well plates. A control plate was included with media but no cells. Every 24h for 96h, 1 ml of media was taken from 3 wells for each biological replicate, centrifuged at 16000xg for 5 min and the supernatant was stored at -80°C. The cells from the wells were harvested and counted and the cell number was used to make a growth curve for each replicate. After all samples had been collected, 200 µl of each sample was analysed using the YSI 2950 Biochemistry Analyzer. The concentration of glucose, lactate, glutamine and glutamate was measured for each sample. The data was subsequently normalised to the metabolite concentrations from the control plate and to the number of cells in each well. The rate of metabolite exchange between the cells and the media was calculated with the following equation:

$$\frac{\text{Media from cells} - \text{control media}}{\text{area under growth curve}}$$

2.2.2.6 Flow cytometry analysis of mitochondrial probes

Cells were incubated for 30 min at 37°C with 100 nM MitoTracker Red CMXRos or 100 nM TMRE in FBS free DMEM. Cells were harvested and fixed in 4% PFA for 15 mins, washed twice in PBS and analysed by flow cytometry with the Attune NxT (YL1 or BL2 channel). The staining intensity was calculated using FloJo software.

2.2.3 Transient transfection and lentiviral infection

2.2.3.1 Fibroblast transfection

For transient expression or siRNA knockdown, 2×10^6 fibroblasts were harvested and used in each transfection. Cells were transfected with a Nucleofector device (Lonza) according to the manufacturer's protocol using the program T-20 and the Amaxa kit R. Cells were transfected with 1-3 nM non-targeting siRNA as a control or with siRNAs targeting PDK2 and PYCR1, or with $5 \mu\text{g}$ pGCA-PDK2^{N255A} or pGCA-PDK2^{WT} plasmids (kindly provided by Dr. Angus McQuibban, Shi et al. 2017). Cells were used for experiments 48-72h after transfection.

2.2.3.3 Stable expression of shRNA in fibroblasts

HEK293T cells were used to generate lentivirus expressing shRNA constructs. 2×10^6 HEK293T cells were plated in a 10 cm dish. The next day, the HEK293T were transfected by calcium phosphate with $10 \mu\text{g}$ of DNA as well as $4 \mu\text{g}$ VSVG and $7.5 \mu\text{g}$ psPAX as packaging plasmids. The following morning the medium was replaced with DMEM with 1 mM sodium butyrate. After 24h, the medium containing the virus was collected with the addition of $4 \mu\text{g}/\text{ml}$ polybrene, filtered through a $0.45 \mu\text{m}$ membrane and transferred onto the fibroblasts. This step was repeated the following day. After 48h, the fibroblasts were selected with $1 \mu\text{g}/\text{ml}$ puromycin. Untreated fibroblasts were also placed under puromycin selection to ensure that all uninfected fibroblasts were killed.

2.2.3.4 ECM production

Cells were seeded at confluence and cultured for 3-7 days. Cells were lysed by incubating with extraction buffer (20mM NH_4OH , 0.5% Triton X-100 in PBS) until no intact cells were visible but the ECM remained on the dish. The ECM was washed in PBS with Ca^{2+} and Mg^{2+} , then residual DNA was digested with $10 \mu\text{g}/\text{ml}$ RNase free recombinant DNase I for 30 mins at 37°C . ECM was either stored at 4°C in PBS with Ca^{2+} and Mg^{2+} and used to plate cells on, or collected and lysed with 2% SDS buffer for western blot analysis.

2.2.5 Western blotting analysis

2.2.5.1 Protein quantification

Unless otherwise stated, cells were lysed in 2% SDS buffer, boiled at 95 °C for five minutes, sonicated with a metal probe and centrifuged at 16000xg for 10 mins. The supernatant was quantified by Bradford assay. Up to 2 µl of each sample was added to 1 ml Optiblot Bradford reagent in triplicate, mixed and left to react for 5 mins at RT. The absorbance at 595 nm was quantified with a spectrophotometer (Biophotometer plus, Eppendorf) and the absolute protein quantification was determined by comparison with a standard curve generated using 1-5 mg/ml BSA and an equal amount of SDS buffer.

2.2.5.2 SDS Page and Western blotting

Loading buffer containing 1M DTT was added to equal quantities of each sample and the samples were boiled for 5 mins at 95 °C. Proteins were then separated on a 4-12% NuPage Bis-Tris polyacrylamide gel in MES or MOPS running buffer. Proteins were transferred onto methanol activated PVDF or nitrocellulose membrane at 100V for 60 mins in transfer buffer. The membrane was blocked in 3% BSA or milk in TBST for 1 hr at RT, then incubated with the primary antibody diluted in the blocking solution overnight at 4 °C. Excess antibody was removed with 3 x 10 min washes in TBST, followed by incubation with horseradish peroxidase conjugated secondary antibodies diluted 1:5000 in TBST for 45 mins at RT. Excess secondary antibody was removed with 3 x 10 min washes in TBST, and the western blots were imaged using chemiluminescence with a MyECL imager (Thermo Fisher Scientific). Image analysis was performed using Image Studio Lite software (LICOR). Western blots were stripped using 150 mM NaCl, 50 mM Glycine, 1% NP-40, pH2 in PBS for 1 hr at RT. Stripping buffer was removed with 5 x 10 min washes in TBST, followed by re-blocking the membrane and probing with further primary antibodies.

2.2.6 Immunofluorescence

2.2.6.1 2D cell cultures

Cells were cultured on 13 mm coverslips and fixed in 4% PFA for 15 mins. The coverslips were washed x3 in PBS and simultaneously permeabilised and blocked for 1 hr at RT with 1% BSA in PBST. Incubation with the primary antibody diluted in blocking solution was performed for 1 hr at RT. Excess antibody was removed with 3 x 10 min washes in PBS and coverslips were then incubated with Alexa Fluor conjugated secondary antibodies diluted 1:500 in blocking solution for 1 hr at RT. Coverslips were counterstained with DAPI, washed with 3 x 10 min washes in PBS and mounted on glass slides in DAKO fluorescence mounting medium. Images were acquired using a Zeiss 710 confocal microscope.

2.2.6.2 Xenograft tumour sections

Tumours from xenografts containing shCtl or shPYCR1 pCAFs (Chapter 2.2.15) were sliced into 400 μm sections using a vibratome. The sections were blocked and permeabilised using blocking buffer (0.3% Triton-X, 0.05% Azide, 1% BSA, and 10% donkey serum in PBS) for 24h at RT. The primary antibody was diluted in blocking and incubated with the sections for 72h at RT, followed by an overnight wash in blocking buffer. The secondary antibody and DAPI were diluted in blocking buffer and incubated with the sections for 48h at RT. The sections were washed twice for 12h with blocking buffer, followed by a 1h wash in PBS. The sections were cleared with Ce3D solution for approximately 2h or until transparent (Li et al., 2017) and mounted in Ce3D solution. Images were taken using a Zeiss 880 multiphoton microscope with single harmonic generation imaging to detect collagen.

2.2.7 Image analysis

Quantification of collagen area and density or cell number in immunofluorescent images or tumour sections was carried out using ImageJ software. Quantification of cell number was achieved by splitting the image into red, green and blue channels, then keeping the blue channel which contained the DAPI stain. The number of nuclei were counted using the 'Particle analysis' function. To quantify

collagen overlapping with CAFs, the image was split into red, green and blue channels, with the red channel containing the collagen stain and the green channel for the CAFs. The area of CAFs was selected based on an appropriate threshold. In the case of the images acquired using the xenograft tumour sections, the selection was expanded by 0.05 inches to ensure that all collagen produced by the CAFs was included. The selection area was then applied to the red channel and the density of collagen staining within the selection or the percentage of the selection that was positive for collagen was calculated. For the analysis of collagen produced by non-CAF cells and therefore not overlapping with the CAFs, the selection of the CAF area was inverted and then applied to the red channel and analysed as described above.

2.2.8 Bacterial transformation and plasmid generation

Competent *E. coli* bacteria (DH5 α or BL21-DE3) were thawed on ice and incubated with 2 μ l plasmid for 30 mins on ice. The bacteria were then incubated for 1 min at 42°C before immediately being placed on ice for 2 mins. The transformed bacteria were then incubated in 1 ml LB broth for 1 hr at 37°C before being spread on an agar plate containing ampicillin or kanamycin and incubated overnight at 37°C. One colony was subsequently picked and expanded in LB broth containing ampicillin or kanamycin for 24h at 37°C and 250 rpm. Bacteria were pelleted at 4000xg for 20 min and the pellet was frozen. The plasmid was subsequently isolated from the pellet using a Qiagen maxiprep kit.

2.2.9 CNA35-mCherry purification

pET28a-mCherry-CNA35 was a gift from Maarten-Merx (Aper et al., 2014). The CNA35-mCherry plasmid was transformed into *E. coli* BL21-DE3. A single colony was expanded in LB broth containing 30 μ g/ μ l kanamycin until the optical density at 600 nm reached circa 0.6 in 4 x 1 L flasks. CNA35-mCherry expression was induced by addition of 0.5 mM Isopropyl β -D-1-thiogalactopyranoside (IPTG). Expression was induced for 20 h at 25°C and 250 rpm. Bacteria were pelleted by centrifugation for 15 min at 10000xg and 4°C. The pellet was resuspended in Buffer 1 (20mM Tris-HCl pH 7.9, 0.5M NaCl) and the bacteria were lysed using a

High Pressure Homogeniser. The suspension was then centrifuged for 35 min at 20000xg at 4 °C and the supernatant containing the solubilised protein was purified by Ni²⁺-affinity chromatography since the protein has an N-terminal 6 x His-tag. A 5 ml His-trap HP column (GE Healthcare) was used for purification in conjunction with an Akta flow system. The protein solution was loaded onto the column and CNA35-mCherry was eluted using an increasing imidazole gradient created by mixing Buffer 1 with an increasing proportion of Buffer 2 (20mM Tris-HCl pH 7.9, 0.5M NaCl, 500 mM imidazole). The fractions containing the protein were easily identifiable as they were purple, and these were concentrated to 5 mL using Amicon Ultra-4 Centrifugal Filter Units. The protein was further purified using size exclusion chromatography. The protein containing fractions were concentrated to 5 mL again and the concentration was determined by Bradford assay. 1 µl was added in triplicate to 1 ml Bradford reagent and allowed to react for 5 min at RT. The absorbance at 595 nm was measured using a spectrophotometer and absolute protein quantification was determined by comparison with a standard curve generated using 1-5 mg/ml BSA. Aliquots of the protein were snap frozen in liquid nitrogen and stored at -80.

2.2.10 RNA extraction and RT-PCR

2.2.10.1 RNA extraction

RNA was extracted from cells grown to 80% confluence in 6 well plates. Cells were lysed in RLT buffer (Qiagen) and the cell lysate was either frozen immediately at -80 °C or used immediately for RNA extraction. RNA was extracted using the Qiagen RNEasy mini kit according to the manufacturers protocol, eluted from the RNEasy spin column with 30 µl RNase free H₂O and 1 µl was used for quantification with a nanodrop.

2.2.10.2 cDNA synthesis

1 µg RNA was used for DNA synthesis. RNA was mixed with iScript reverse transcriptase and reverse transcription-reaction mix (BioRad) and RNase free water was added to bring the total volume for each reaction to 20 µl. cDNA was generated using the following programme: 5 min at 25 °C, 30 min at 42 °C, 5 min at 85 °C.

2.2.10.3 RT-PCR

cDNA was diluted 1:5 for RT-PCR. 10 µl iTAQ Universal SYBR Green supermix (BioRad) was mixed with 2 µl cDNA and 400 nM forward and reverse primers diluted in 8 µl nuclease free H₂O for each reaction. Each sample was analysed in triplicate, and, in addition to the target(s) of interest, primers for at least two reference genes were included for normalisation of each sample. Non-template controls were also run alongside each experiment. The RT-PCR reaction was carried out on a Quant Studio 3 RT-PCR machine (Thermo Scientific) using their Standard programme.

2.2.11 MS-Metabolomics analysis

2.2.11.1 Sample preparation for intracellular metabolomics

2x10⁵ fibroblasts were seeded in each well of 6 well plates. For each biological replicate 3 separate wells were used in each condition. For tracing experiments, cells were cultured in DMEM 10% FBS supplemented with either 25 mM U-¹³C₆ Glucose, 2 mM U-¹³C₅ Glutamine, 1 mM U-¹³C₃ Pyruvate or 100 µM U-¹³C₁₆ Palmitate. After 48h of culture, the cells were washed x3 in ice cold PBS to remove the media, then 400 µl ice cold extraction buffer (50% methanol, 30% acetonitrile, 20% water) was added to each well and incubated at 4°C for 5 min. The extracted metabolites were collected and centrifuged at 16000xg for 5 min at 4°C. 200 µl from each sample was transferred to an LC-MS vial and stored at -80°C until analysis by LC-MS.

2.2.11.2 Q-Exactive acquisition

LC-MS was carried out using a previously described method (Mackay et al., 2015). A Q-Exactive Orbitrap mass spectrometer (Thermo Scientific) was used in combination with a Thermo Ultimate 3000 HPLC system. The HPLC system was set up with a Zic-pHILIC 5 µm polymer column, 150 x 2.1 mm (SeQuant, Merck) and a ZIC-pHILIC guard column, 20 x 2.1 mm (SeQuant, Merck). A volume of 5 µl of cell extract was injected and the metabolites were separated over a 15 min mobile phase gradient from an initial ACN content of 80% ACN with 20% ammonium bicarbonate (pH 9.2) decreasing to 20% ACN. The flow rate was 200 µL/min and

the column temperature was 45°C. The metabolites were detected over a period of 25 min using the Q-Exactive mass spectrometer across a mass range of 75-1000 m/z and at a resolution of 35,000 (at 200 m/z). Electrospray ionisation and polarity switching enabled both positive and negative ions to be detected in the same run. Lock masses were used and the mass accuracy for each metabolite was less than 5 ppm. To detect acetyl-coA, a single ion monitoring (SIM) method was employed. The Q-Exactive mass spectrometer was used to monitor the three masses for acetyl-coA labelled M0, M1 or M2 (810, 811 and 812 m/z) with an isolation window of 1 m/z for each isotope. The resolution was 70,000 and the ion trap fill time was 100 ms. The automatic gain control (AGC) target value was $5e^4$. Only positive ions were detected as single polarity was used rather than polarity switching. Thermo Xcalibur software was used for data acquisition.

2.2.11.3 Analysis of metabolomics data

Data analysis was carried out using TraceFinder 4.0 software to determine the peak area of each metabolite of interest. The spectra were queried against a curated compound database created from analysis of commercial standards of each metabolite run previously on this LC-MS system and pHILIC column. Metabolites were identified based on the exact mass of the singly charged ion and the retention time on the column. Predicted retention times were manually adjusted based on those of a standard metabolite mix which was run on the LC-MS system alongside the samples. The relative total metabolite levels and ¹³C labelling patterns were determined based on the peak area for the accurate mass of each isotopologue for each metabolite. The peak areas were normalised to total protein content for each sample. Proteins were collected from each cell culture well after the metabolite extraction and quantified by Bradford assay.

2.2.12 Sample preparation for MS-proteomics

2.2.12.1 In solution digestion

Proteins were denatured in urea buffer. The lysate was diluted 1:2 in 25 mM Tris-HCl pH 8.5. For every 50 µg of protein, 1 µg of LysC was added and the mixture was incubated for 3h at RT. LysC partially digests the protein at the C terminus of

lysine residues, which enables more efficient trypsin digestion. The lysate was then further diluted 1:2 in 25 mM Tris-HCl pH 8.5 to give a final dilution of 1:4 lysate:buffer, and 1 µg trypsin was added for every 50 µg of protein. The proteins were left to digest overnight at RT. The digestion reaction was then terminated by acidifying the sample with TFA (trifluoroacetic acid) to a final concentration of 1%.

2.2.12.2 In gel digestion

Each sample was denatured in SDS buffer and run on a 4-12% SDS page gel to separate the proteins. The gel was stained with Coomassie blue for 1 hr and washed x3 in HPLC water. Each lane of the gel was cut into identical bands and each band was further chopped into small pieces and placed in a 1.5 ml Eppendorf tube. The Coomassie stain was removed with 3 x 20 min washes of a 1:1 mixture of 50 mM ABC and absolute ACN. The gel was then dehydrated in ACN for 10 min, and this step was repeated until the gel pieces were hard and white. The gel was then dried in a Speed-Vac for 5 min. The gel was rehydrated in 10 mM DTT and incubated for 1 hr at 56°C to reduce cysteines. The reduced cysteines were then alkylated in 55 mM IAA at RT for 45 min in the dark. The gel pieces were washed in 50 mM ABC for 20 min and dehydrated with ACN for 10 min. The wash and dehydration steps were repeated. The gel was then dried in a Speed-Vac for 5 mins. The proteins in the gel were digested with 625 ng trypsin for each sample. The trypsin was diluted in 50 µl of 50 mM ABC and allowed to rehydrate the gel pieces for 15 min. Then, a further 70 µl of 50 mM ABC was added, or enough to cover the gel pieces. The samples were incubated overnight at 37°C. The following day, the peptides were extracted from the gel pieces by alternating 10 min incubations of the extraction buffer (3% TFA, 30% ACN in water) with ACN to dehydrate the samples. The supernatant from each incubation step was kept and transferred to a new tube. After two rounds of extraction and dehydration, the supernatant was reduced in the Speed-Vac to a volume of approximately 100 µl. Samples were then desalted by StageTip before MS analysis.

2.2.12.2 StageTip desalting

StageTips were prepared by loading 1 x C18 membrane for every 5 µg protein into a 200 µl pipette tip. The StageTip was activated for protein binding by adding 50 µl methanol and centrifugation for 1.5 min at 600xg by which point all the methanol had passed through the membranes. Subsequently, 50 µl buffer B was passed through the membranes by centrifugation at 600xg, followed by 50 µl buffer A*. The digested peptides were then loaded onto the membranes and centrifuged at 200xg for 5 min. The bound peptides were washed with 50 µl buffer A at 600xg and eluted with 2 x 20 µl buffer B. The eluted peptides were stored at -80°C until MS-proteomic analysis, at which point the ACN was evaporated using a speed vacuum until ~3 µl remained and an equal volume of buffer A* was added.

2.2.12.2 SILAC labelling

SILAC (Stable isotope labelling of amino acids in cell culture) labelled cells were generated by culturing the cells in SILAC media (DMEM supplemented with light or heavy arginine and lysine) for 3 passages or until the cells were at least 95% labelled. The percentage of SILAC labelled proteins was determined by MS-proteomics. Cells were lysed in urea buffer. The lysate was sonicated on ice with a metal probe and centrifuged at 16000xg for 10 mins. The supernatant was digested by in solution digestion followed by StageTip desalting and MS analysis. Incorporation of SILAC labels was determined using the peptides.txt output file from MaxQuant software analysis with R software. The incorporation of Arg10 and Lys8 were calculated separately with the equation

$$Incorporation = 1 - \left(\frac{1}{ratio\ H:L} \right) * 100$$

Once the incorporation was $\geq 95\%$, the cells were used for further MS-proteomic experiments.

2.2.12.3 Acetylome enrichment

SILAC labelled iCAFs and iNFs were grown to 80% confluence in 10 x 15 cm dishes for each cell line. The cells were lysed on ice in RIPA buffer supplemented with 10 mM nicotinamide and 1 µM Trichostatin A to inhibit deacetylases. 1/10th of the volume of 5M NaCl was added to improve recovery of chromatin bound proteins and the lysates were incubated for 15 min on ice. The lysates were sonicated with a metal probe and centrifuged at 4800 x g. 4 volumes of ice cold acetone were

added and the lysates were incubated overnight at -20°C to precipitate proteins. The precipitate was pelleted at $4800 \times g$ for 20 min at 4°C and washed with ice cold acetone. The pellets were resuspended in urea buffer and the protein concentration was determined by Bradford assay. Equal amounts of heavy and light labelled lysate were mixed and the samples were digested by in solution digestion. The samples were desalted by C18 SepPak column. The SepPak was activated by allowing 5 ml ACN to run through via gravitational flow and equilibrated with 2×5 ml 0.1% TFA. The sample was then loaded and allowed to flow through the column. The peptides were washed with 0.1% TFA and then with water. Peptides were eluted stepwise with an increasing gradient of ACN in 0.1% TFA (10, 15, 20, 25, 30, 40, 60% ACN). The eluates were pooled and evaporated by speed vacuum to a volume of approximately 1 ml. The sample was then mixed with $10 \times$ IAP buffer to make a $1 \times$ IAP buffer solution. The sample was brought to pH 7. $50 \mu\text{l}$ slurry containing agarose beads conjugated to anti-Acetyllysine antibody were centrifuged at $2000 \times g$ for 30 sec and the supernatant was removed. The beads were washed $\times 4$ in PBS and resuspended in $40 \mu\text{l}$ PBS. The peptides were added to the beads and incubated on a rotation wheel overnight at 4°C . The following day, the beads were centrifuged at $2000 \times g$ for 1 min at 4°C . The beads were washed $\times 4$ with IAP buffer and $\times 3$ with water. The acetylated peptides were eluted with $50 \mu\text{l}$ 0.1% TFA and incubated at RT for 10 min before centrifugation at $2000 \times g$. The elution step was repeated twice and the combined supernatant was desalted by StageTip before MS analysis.

2.2.13 Mass spectrometer set up

2.2.13.1 Nano liquid chromatography

All samples were further fractionated to separate the peptides by reverse-phase chromatography at high resolution. After StageTip desalting, the peptides were resuspended in buffer A* and injected into an EASY-nLC system coupled online to a mass spectrometer (Thermo Fisher Scientific). The peptides were separated on a 20 cm fused silica emitter column (New Objective) packed in-house with reverse-phase Reprosil Pur Basic $1.9 \mu\text{m}$ (Dr. Maisch GmbH). The peptides were eluted with a flow rate of 300 nL/min over a 60 min linear gradient from 5% to 30% of

buffer B. The eluted peptides were ionised and injected into the mass spectrometer by electrospray ionisation.

2.2.13.2 Q-Exactive HF acquisition

The full MS scan was acquired with a mass range of 375-1500 m/z, a resolution of 60,000 and an AGC of $3e^6$. The top 15 most intense peaks from the full MS scan were isolated for fragmentation and MS/MS analysis with an AGC target of $5e^4$ ions at a resolution of 15,000. Singly charged ions were excluded, and those ions that were selected for MS/MS analysis were subsequently added to a list of excluded ions to prevent the same ion from being fragmented multiple times. MS data were acquired using XCalibur software (Thermo Fisher Scientific).

2.2.13.3 Orbitrap Fusion Lumos acquisition

The full MS scan was acquired with a mass range of 350-1550 m/z, a resolution of 60,000 and an AGC of approximately 5×10^5 . The top 15-20 most intense peaks from the full MS scan were isolated for fragmentation and MS/MS analysis with an AGC target of 50-100,000 ions at a resolution of 15,000. The included charge range was 2-7 and those ions that were selected for MS/MS analysis were subsequently added to a list of excluded ions to prevent the same ion from being fragmented multiple times. MS data were acquired using XCalibur software (Thermo Fisher Scientific)

2.2.14 Proteomic data analysis

2.2.14.1 Data processing with MaxQuant

The raw MS data files were processed for peptide and protein identification and quantification using MaxQuant software coupled to the Andromeda search engine (Cox and Mann, 2008, Cox et al., 2011). MaxQuant versions 1.6.0.7 or 1.6.3.3 were used. The data was queried against the human UniProt database (www.uniprot.org) to identify the presence of peptides and proteins based on their MS and MS/MS spectra. The following settings were used across all experiments: Acetyl (N-term) and Oxidation (M) were set as variable modifications and Carbamidomethyl (C) as a fixed modification and the digestion mode was Trypsin (P). Up to 2 missed cleavages were allowed. An initial mass deviation of

4-5 ppm for the parent mass and 20 ppm for the fragment ion was allowed. Matching between runs was enabled when fractions with similar chromatography were compared. The false discovery rate was set to 1% for identification of peptides and proteins, and only unique peptides, i.e. peptides that are not found in any other protein, were used for quantification. For the acetylome experiment (2.2.11.3), I added Acetyl (K) as an additional variable modification.

For SILAC experiments, MaxQuant can accurately quantify the relevant abundance of protein between samples based on the intensities of identified SILAC pairs. The additional MaxQuant settings for SILAC experiments were as follows: The multiplicity of the experiment was set to 2, with the light labels set as Arg0 and Lys0 and heavy labels Arg10 and Lys8.

In the absence of isotopic labels, MaxQuant can still quantify differential peptide and protein amounts between samples using Label Free Quantification (LFQ) (Cox et al., 2014). Briefly, the normalisation of the fractions is delayed until all the peptide ion intensities across the fractions are summed and the normalisation factor for each fraction is then calculated in order to produce the least amount of variation between samples, based on the assumption that the majority of the proteome does not change between two conditions. For label free experiments, the LFQ setting was enabled in MaxQuant.

MaxQuant software generates a set of output tables. For further analysis, I used the proteingroups.txt file and, if relevant, the Acetyl (K)Sites.txt file for further analysis with Perseus software (Tyanova et al., 2016).

2.2.14.2 Perseus data analysis

Perseus versions 1.5.5.3, 1.6.0.7 or 1.6.2.2 were used to carry out statistical analysis of the proteomic data. For all experiments, analysis of the proteingroups.txt file was as follows: For SILAC experiments, the SILAC ratios H/L were uploaded as main columns and for LFQ experiments the normalised LFQ intensities were uploaded as main columns. The data was then filtered by removing potential contaminants, such as keratins and trypsin derived peptides. Reverse peptides, which are identified by querying them against a decoy database (Elias and Gygi, 2010) were also removed. Finally peptides only identified by site,

meaning only the modified version of the peptide was identified, were also removed. Only proteins identified in at least two biological replicates were considered for analysis. For SILAC experiments, the SILAC ratio for the 'Reverse' experiment was inverted to make the comparison between Forward and Reverse labelled experiments consistent. SILAC ratios were then transformed by \log_2 and the intensities and LFQ intensities were transformed by \log_{10} . The distribution of the SILAC data was assessed using a histogram, and if the data did not follow a normal distribution centred on zero, the median ratio was subtracted from all the ratios for each sample. Proteins that were significantly different between conditions were identified by performing a two sample t-test ($p \leq 0.05$) for the label free experiments.

For the acetylome experiment, the Acetyl (K)Sites.txt file was analysed as follows: The data was filtered for contaminants and reverse peptides as described previously. Only peptides with a score differential > 0.5 and a localisation probability of > 0.75 were kept for the analysis. The site table was expanded to separate peptides with the same sequence but different numbers of acetylated sites. All acetylated peptides with a SILAC ratio in at least one biological replicate were used for the analysis to extract the maximum amount of data from the experiment. The acetylation sites were annotated with the following information about modification sites derived from the PhosphoSitePlus database (www.phosphositeplus.org): linear motifs, known sites, regulatory sites and sequence features. The SILAC ratios were transformed by \log_2 and the intensities by \log_{10} , and the Reverse ratios inverted. The data was then normalised to the total proteome by subtracting the SILAC ratio for each protein from the proteingroups.txt analysis from the SILAC ratio for each acetylated peptide. If the unmodified protein was not identified in the total proteome, a SILAC ratio of 0 was imputed so as not to lose information about modifications. Significantly regulated peptides were identified using a one sample t-test, with an $S0 \leq 0.1$ and a Benjamini-Hochberg false discovery rate (FDR) ≤ 0.05 . The proteins were further annotated with information from the Gene Ontology Cellular Compartment (GOCC), Gene Ontology Biological Function (GOBF), Gene Ontology Molecular Function (GOMF), Kyoto encyclopaedia of genes (KEGG) and Protein families (Pfam) databases. A one dimension category enrichment analysis was then carried out to identify which categories from these databases were enriched for

acetylated peptides in the different conditions (Cox and Mann, 2012). The enrichment factor was calculated using the Fisher exact test with a Benjamini-Hochberg $FDR \leq 0.02$:

$$\textit{Enrichment factor} = \frac{\textit{intersection size} \times \textit{total size}}{\textit{selection size} \times \textit{category size}}$$

An enrichment factor of > 1 denotes an enriched category and < 1 a depleted category.

2.2.15 Xenografts of MCF10DCIS.com cells and CAFs

MCFDCIS.com breast cancer cells were combined with either the shCtl or shPYCR1 pCAF cell lines in a 1:3 ratio and resuspended in 50% growth factor reduced matrigel and 50% PBS. 200 μ l of the matrigel mixture containing 0.5×10^6 MCF10DCIS.com cells and 1.5×10^6 CAFs was injected subcutaneously into the mammary fat pad of 12 Balb-C nude mice for each condition. The tumours were measured by calliper every 2-3 days. After 2 weeks, six mice from each condition with the largest tumours as measured by the calliper were culled and the tumours were collected. The tumours were weighed and cut in half. One half was fixed in 4% PFA overnight and transferred to 70% ethanol before being embedded in paraffin blocks for immunohistochemical analysis. The other half was fixed in 4% PFA for 1 hr and subsequently sliced into 400 μ m sections which were used for single harmonic generation imaging to detect collagen. The remaining mice were allowed to reach endpoint as determined by the tumours reaching a length of 15 mm or the presence of ulceration. Each mice was culled at endpoint and the tumours were collected. The injection, monitoring and tumour collection were carried out by Sandeep Dhayade from the Beatson Institute.

Chapter 3 Pyruvate dehydrogenase activity is upregulated in mammary CAFs

3.1 Characterisation of CAFs and NFs

In this study I used paired CAFs and NFs derived in two different ways. The first are the iCAF and iNF which were kindly provided by Professor Akiro Orimo (Chapter 2.2.1.1). The iCAFs and iNFs have been characterised by the Orimo group and the iCAFs were shown to have an activated, myofibroblastic phenotype in comparison to the iNFs (Kojima et al., 2010), and this phenotype is maintained in culture in an autocrine manner through TGF- β and SDF-1 signalling. The iCAFs and iNFs have also been well characterised by our group (Hernandez-Fernaud et al., 2017) (Kugeratski et al., 2019) and the iCAFs have been demonstrated to be more pro-invasive, pro-angiogenic and pro-tumourigenic than the iNFs, all of which are important characteristics of the CAF phenotype.

The second type of CAFs and NFs are the pCAFs/pNFs which are derived from human breast cancer patients and which I immortalised (Chapter 2.2.1.2). I immortalised 3 matched pairs of CAFs and NFs where both cell types came from the same patient (pCAFs/NFs 1-3), and one unmatched CAF and NF cell line (pCAF 4, pNF 5). All of the fibroblast lines expressed the mesenchymal cell marker vimentin as shown by immunofluorescence (Figure 3-1). Furthermore, our group has checked by flow cytometry analysis that the patient derived fibroblasts are uncontaminated with endothelial, immune or epithelial cells. In order to verify the activation of all the CAF cell lines I measured the levels of α SMA expression, which is the most commonly used marker of the activated myofibroblast phenotype, by western blot. Overall CAFs expressed more α SMA than NFs, although pNF 5 had relatively high α SMA levels (Figure 3-2). I regularly monitored α SMA levels in both the iCAFs/iNFs and pCAFs/pNFs during this study in order to be sure that they were maintaining their respective CAF and NF phenotypes. In this way I could carry out my experiments both using the iCAFs/iNFs, which have been extensively characterised, and the pCAFs/pNFs, which have been less well characterised and are likely to be more heterogeneous since we do not know what

cells the CAFs originate from, but are patient derived and therefore more clinically relevant.

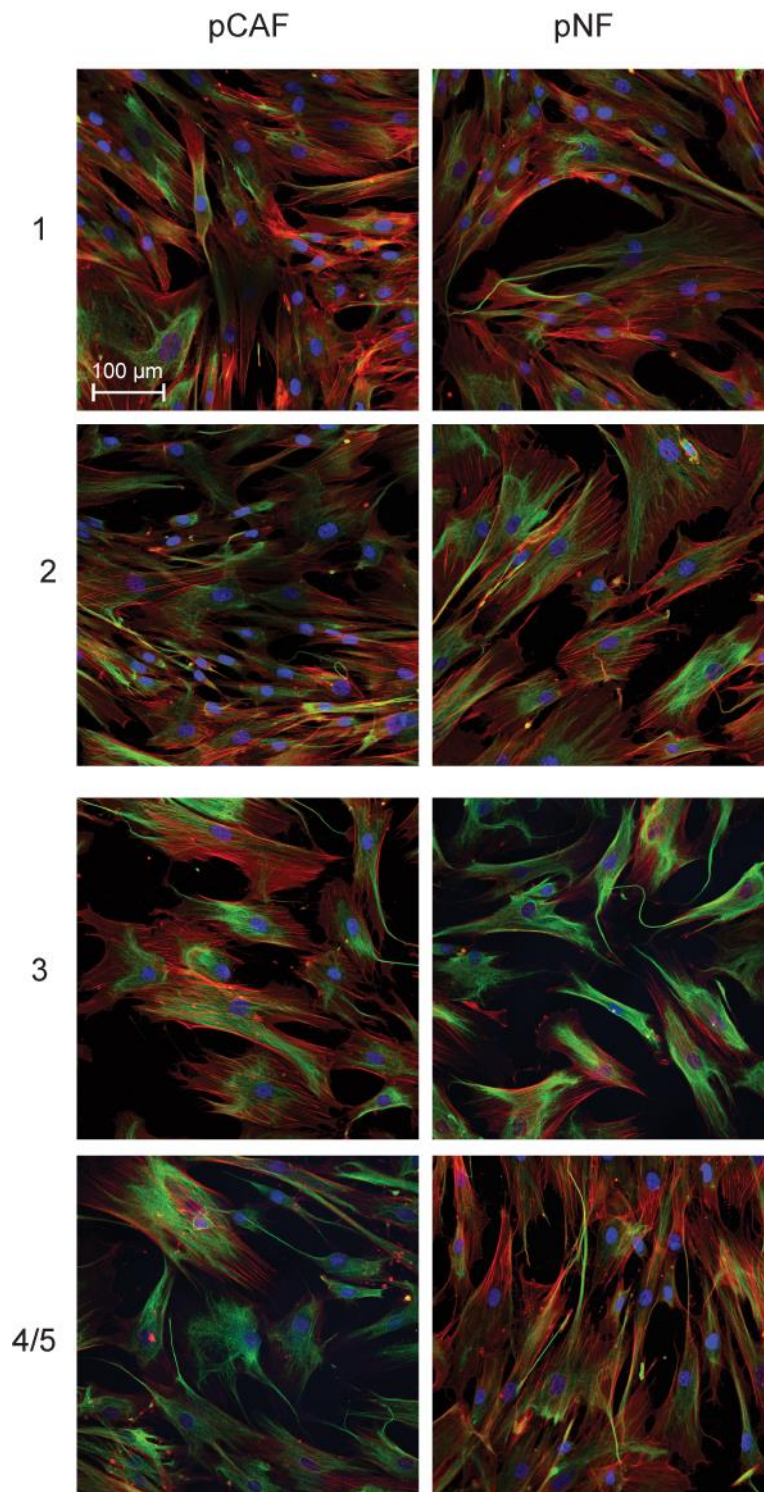


Figure 3-1 Patient derived CAFs express the fibroblast marker vimentin

Representative images of the pCAFs post-immortalisation stained for vimentin (green), phalloidin (red) to visualise the actin cytoskeleton and DAPI (blue). Images were acquired using the Zeiss 710 at 20x magnification. Representative images of $n \geq 3$ replicates

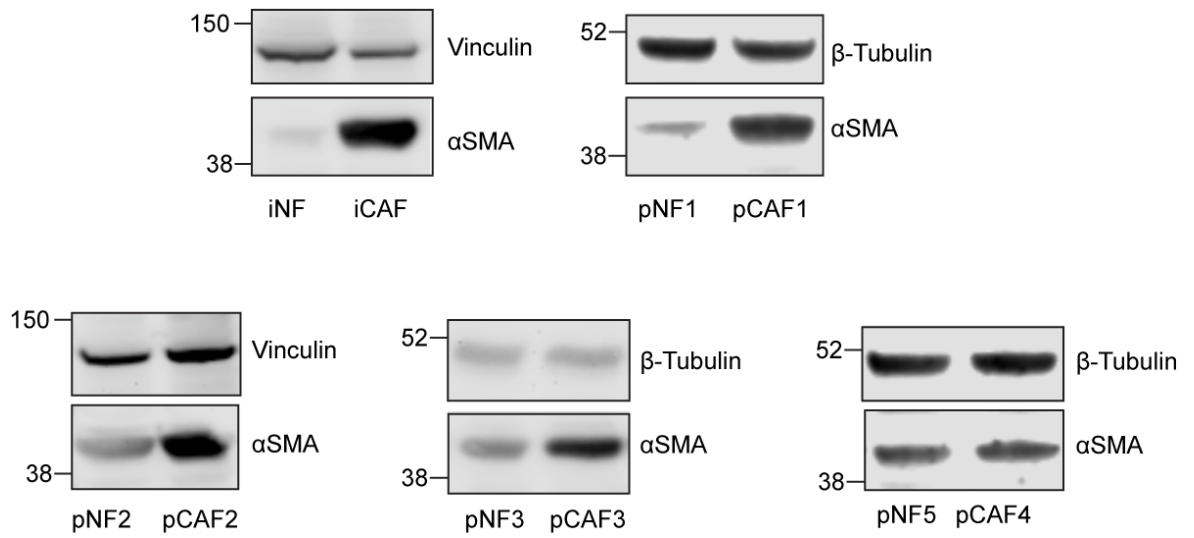


Figure 3-2 CAFs express more α SMA than NFs

Representative western blots of $n \geq 3$ biological replicates of α SMA levels in all the pairs of fibroblasts. Vinculin or β -tubulin was used as a loading control. Positions of molecular weight markers are shown.

3.2 Predicting kinase activity in iCAFs and iNFs

Many key signalling pathways in cells are driven by changes in phosphorylation due to altered kinase activity. In particular, kinase dysregulation is a common feature of cancer cells. To further probe into how CAFs maintain their activated phenotype, we collaborated with Dr. Julio Saez-Rodriguez and Enio Gjerga from RWTH Aachen University (Germany) to elucidate changes in kinase activity from the phosphoproteomes of the iCAFs and iNFs. The MS-phosphoproteomic data was previously acquired and analysed by Juan Ramon Hernandez-Fernaud from our group. Samples from SILAC labelled iCAFs and iNFs were enriched for phosphorylated peptides and analysed by MS-proteomics. The experiment was performed with both forward and reverse labelled cells (i.e. heavy CAFs with light NFs and light CAFs with heavy NFs) to give two total experiments. The Saez-Rodriguez group then used the differences between iCAFs and iNFs in the \log_2 SILAC ratios of phosphosites known to be targeted by specific kinases to predict which kinases were more or less active in the iCAFs. From this modelling, only five kinases were predicted to have significantly different activity between iCAFs and iNFs: MAPK1, MAPK3, AKT3, CDK2 and PDK2 (Figure 3-3). Of these, I decided to focus on PDK2 (Pyruvate dehydrogenase kinase), the activity of which was downregulated in the iCAFs, because it was predicted to have the greatest difference in activity between iCAFs and iNFs. Furthermore, it has only one main target: Pyruvate dehydrogenase (PDH), although it has recently been shown to also phosphorylate PARL (Shi and McQuibban, 2017). The pyruvate dehydrogenase complex is made up of three subunits, of which the PDH subunit catalyses the rate limiting step of pyruvate decarboxylation and is therefore subject to the most regulation at the post-translational level. The PDC is a key metabolic enzyme because it converts pyruvate to acetyl-coA in the mitochondria, thus connecting the two major metabolic pathways of glycolysis and the TCA cycle. Acetyl-coA produced by the PDC can also be used for a variety of other metabolic pathways including cholesterol and fatty acid synthesis, as well as for protein acetylation, making it a versatile and central metabolite. Therefore changes in PDH activity could have a profound impact on the CAF phenotype. PDH was also the most highly regulated protein at the phosphorylation level in the phosphoproteomics data; three out of its four phosphorylation sites on the A1 subunit were highly downregulated in the iCAFs, including S293 which is the site that PDK2 has the

highest affinity for (Figure 3-4). Phosphorylation of any of these three sites is known to inhibit PDH activity by blocking binding of pyruvate to the active site. Therefore, since PDH phosphorylation was less phosphorylated in the iCAFs I hypothesised that PDH activity was downregulated due to a decrease in PDK2 activity.

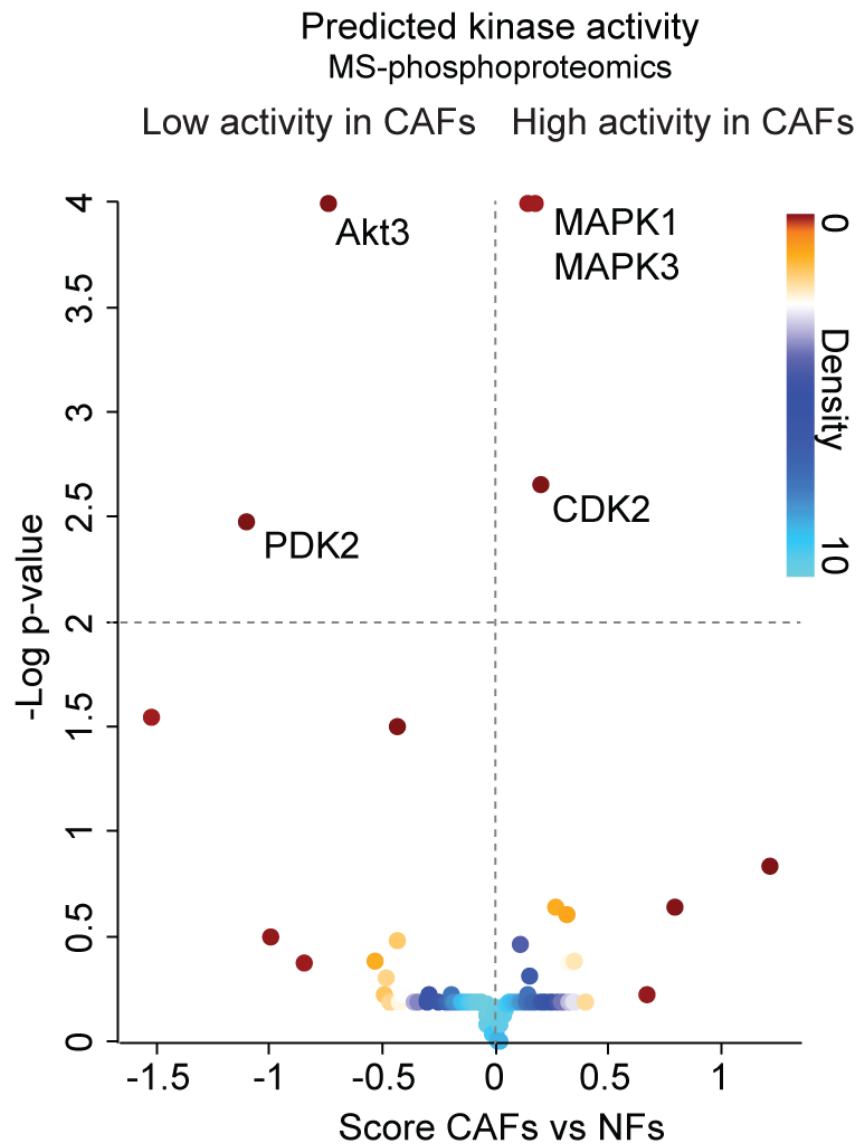


Figure 3-3 Visualisation of predicted kinase activity in iCAFs and iNFs

Plot showing the score for the predicted difference in kinase activity in iCAFs compared to iNFs based on phosphoproteomic data from the iCAFs and iNFs. Data from two experiments with both forward and reverse labelled fibroblasts was used for the modelling. Each dot represents a kinase used in the analysis. Kinases with a significant p-value are named.

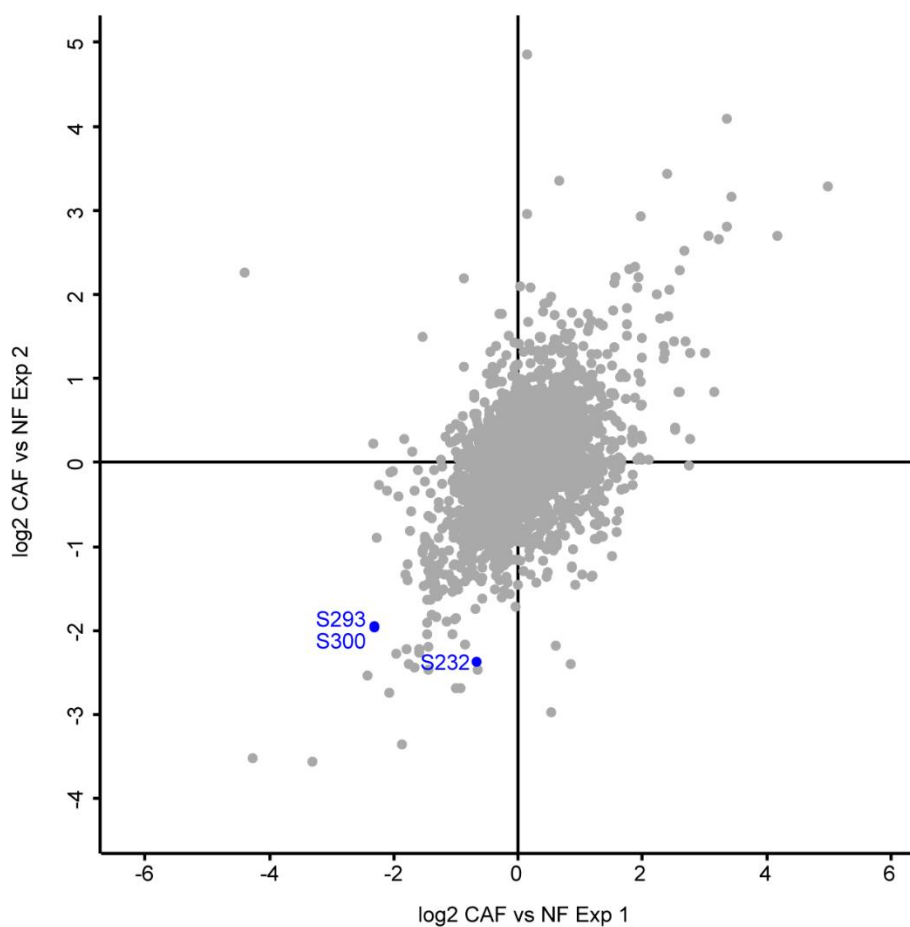


Figure 3-4 Phosphoproteomic data of iCAFs and iNFs highlighting PDH phospho-sites

Scatter plot showing the log₂ difference of phosphorylated proteins between iCAFs and iNFs in two independent SILAC experiments. For each experiment both forward and reverse labelled experiments were averaged. Each dot represents a phosphorylation site. The three identified phosphorylation sites on PDH are highlighted in blue

3.3 Pyruvate dehydrogenase is less phosphorylated in CAFs

To verify the results of the phosphoproteomic data, I assessed the levels of PDH phosphorylation in CAFs and NFs by western blot. I chose the S293 phosphorylation site to study because this is the site with the highest affinity for PDK2. I compared PDH phosphorylation levels between the iCAF and iNF as well as two pCAF and pNF pairs: pCAF2/pNF2 and pCAF3/pNF3. I selected these two pairs because both had a good regulation of α SMA between NFs and CAFs and because the pCAF2/NF2 fibroblasts are from an ER positive patient whereas the pCAF3/pNF3 are from a triple negative patient and I wanted to demonstrate that the regulation of PDH phosphorylation is not specific to CAFs from one subtype of breast cancer. I then used these pCAF/pNF pairs in all subsequent experiments involving pCAFs and pNFs. In all the fibroblast pairs, PDH was significantly less phosphorylated in the CAFs as shown by western blot analysis (Figure 3-5). The total amount of PDH did not decrease, showing that PDH phosphorylation is being regulated rather than the protein expression. This supports the phosphoproteomic data from the iCAFs and iNFs and shows that PDH regulation is not specific to the iCAFs but also occurs in patient derived CAFs.

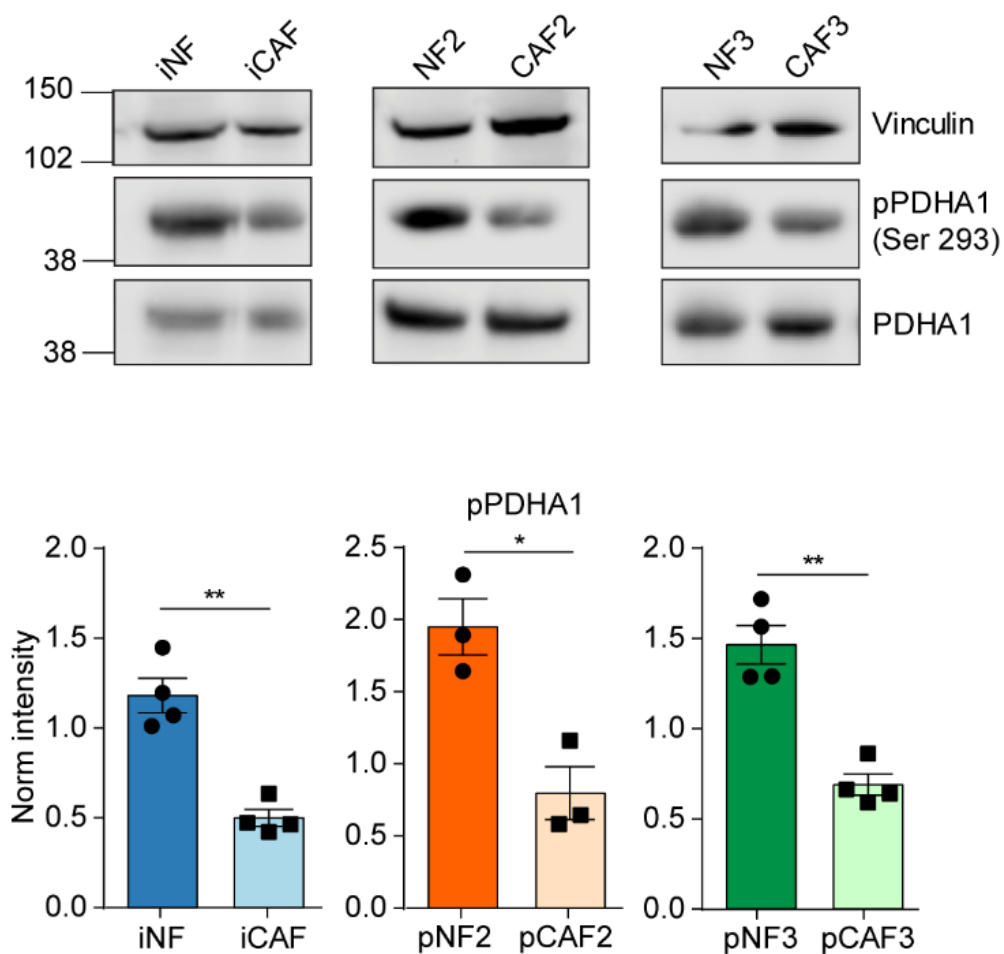


Figure 3-5 PDHA1 phosphorylation in CAFs and NFs

Representative western blots and quantification of pPDHA1 levels in CAFs and NFs. Graphs show SEM and mean of 3 independent experiments. Quantification represents pPDHA1 intensity normalised to both total PDHA1 intensity and vinculin intensity. Molecular weight markers are indicated next to the blots. Significance was calculated using an unpaired student t-test with Welch's correction: $p \leq 0.05$ *, $p \leq 0.01$ **

3.4 PDK2 regulates PDH phosphorylation

3.4.1 PDK2 expression is downregulated in CAFs

Although PDK2 was the only pyruvate dehydrogenase kinase predicted to be regulated in the iCAF by the modelling of the phosphoproteomic data, there are in fact four pyruvate dehydrogenase kinases that can phosphorylate and inactivate PDH: PDK1, PDK2, PDK3 and PDK4. These are isoforms which share ~70% homology. Of these, PDK3 is predominantly found in heart and skeletal muscle tissue in humans and detected only in lung, brain, kidney and testes in mice, so I discounted PDK3 from being the main driver of changes in PDH phosphorylation in the mammary CAFs. PDK1 and PDK4 are also only expressed highly in heart and skeletal muscle, however, they are overexpressed in several cancers (Grassian et al., 2011) (Hsieh et al., 2008) (Kaplon et al., 2013) (Pate et al., 2014) and PDK1 is known to be upregulated in response to hypoxia (Kim et al., 2006a), which is a common feature of the tumour microenvironment. PDK2 however is ubiquitously expressed in all tissues. In addition there are two pyruvate dehydrogenase phosphatases: PDP1 and PDP2 which can regulate PDH phosphorylation and activity. There are few studies on the PDPs, although there is evidence suggesting they are regulated at the post translational level in some cancers (Fan et al., 2014) (Shan et al., 2014). However, neither PDP has ever been investigated as a drug target in the context of cancer or any other disease, whereas PDKs can be targeted with several drugs including dichloroacetate (DCA) which has so far been shown to be well tolerated in Phase I clinical trials involving cancer patients (Dunbar et al., 2014). I therefore wanted to assess whether PDK2 was indeed the main kinase or phosphatase responsible for the difference in PDH phosphorylation. I designed and tested primers for PDK1, PDK2 and PDK4. PDK4 could not be detected by qPCR, but PDK2 was significantly downregulated at the mRNA level in CAFs compared to NFs and PDK1 was significantly downregulated in the pCAF2s (Figure 3-6a). PDK2 was much more highly expressed in the fibroblasts than PDK1, so I concluded that the regulation of PDK2 in CAFs would have a greater effect on PDH phosphorylation. Although PDK4 could not be detected at the mRNA level, the protein expression of PDK4 in lysates from iCAF and iNF could be detected by western blot, but there was no difference in expression between iCAF and iNF.

I also tried to detect PDP1 and PDP2 by western blot, however, PDP1 expression was not upregulated in the iCAFs and I could not detect PDP2 (Figure 3-6b). Furthermore, treatment of the iNFs with DCA, the PDK inhibitor, greatly reduced PDH phosphorylation as shown by western blot (Figure 3-7a). This suggests that a PDK is driving increased PDH phosphorylation in NFs rather than a PDP driving increased dephosphorylation of PDH in CAFs.

To see if PDK2 was also downregulated in CAFs in a clinical context, the expression of the PDKs was measured in laser capture microdissected sections of normal or tumour associated stroma from triple negative breast cancer patients in collaboration with Dr. Morag Park. This data showed that both PDK2 and PDK4 are downregulated in tumour associated stroma, whereas PDK1 and PDK3 are not (Figure 3-8). Although PDK4 was also highly downregulated in the tumour-associated stroma, since it was not highly expressed or regulated between my CAFs and NFs whereas PDK2 consistently was, I focussed on PDK2 in my future experiments.

I therefore concluded from these experiments that PDK2 expression was downregulated in CAFs and that this was likely to be the cause of the observed decrease in PDH phosphorylation

3.4.2 PDK2 expression regulates PDH phosphorylation

To confirm that PDK2 was controlling PDH phosphorylation in CAFs, I modulated the expression of PDK2 in the iCAFs and iNFs and quantified the level of PDH phosphorylation by western blot (Figure 3-7b). The iNFs were transfected with an siRNA pool against PDK2 to transiently knock down PDK2. The efficiency of the knock down was verified by RT-qPCR and showed that 48h after transfection there was a reduction in phosphorylated PDH in siPDK2 transfected iNFs compared to the siCTL. Conversely, the iCAFs were transfected with a plasmid to transiently overexpress either wild-type PDK2 or PDK2 with the mutation N255A which abrogates its kinase activity (Shi and McQuibban, 2017). Expression of PDK2^{WT} was sufficient to increase PDH phosphorylation in comparison to PDK2^{N255A} 48h after transfection. Therefore PDK2 is indeed a major regulator of PDH phosphorylation

in fibroblasts, and I am able to control PDH phosphorylation in both CAFs and NFs by overexpression or siRNA knock down of PDK2.

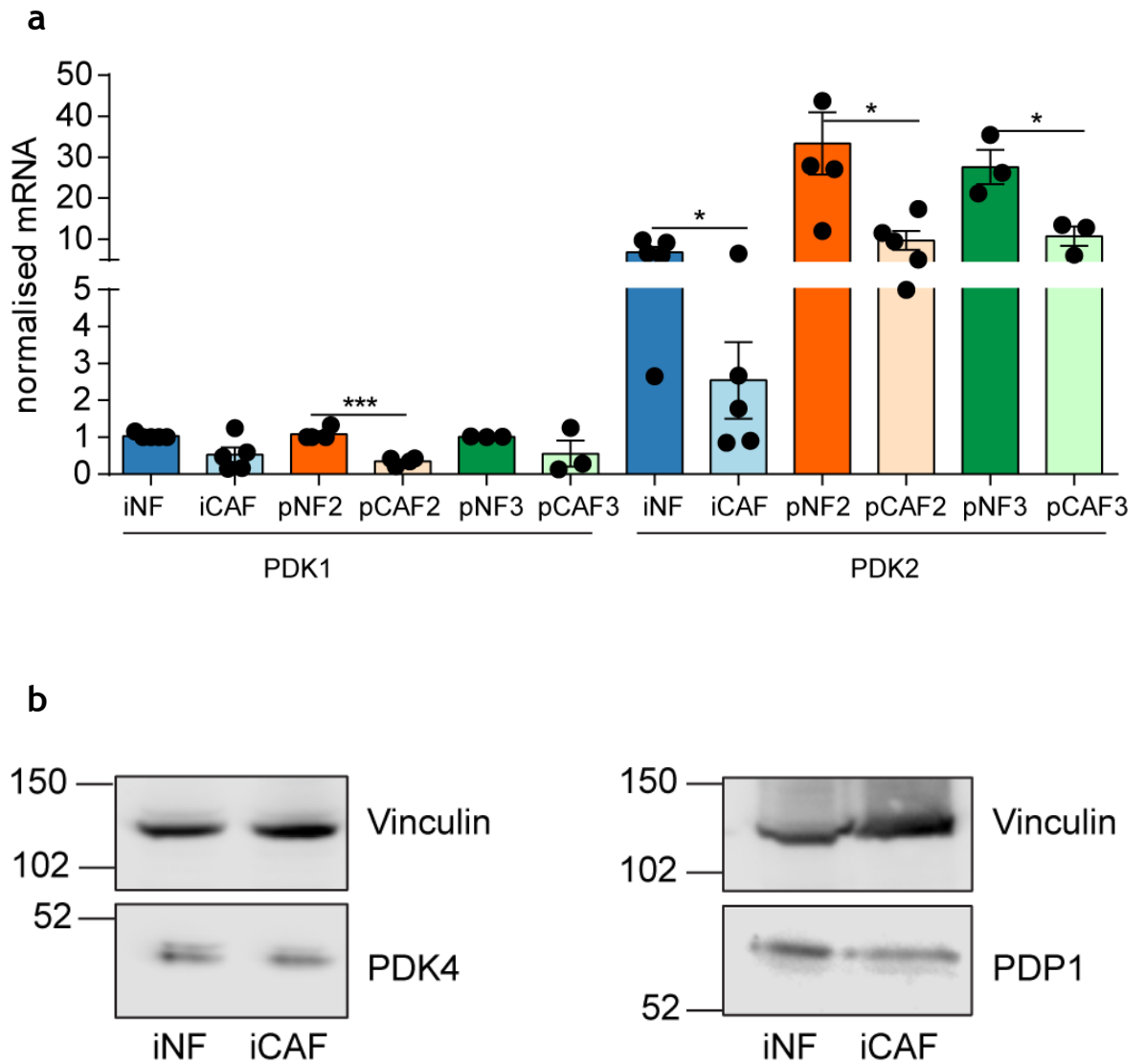


Figure 3-6 PDK expression in CAFs and NFs

a: mRNA expression of PDK1 and PDK2 in CAFs and NFs as measured by RT-qPCR. The mean and SEM of at least 3 independent experiments are shown. PDK1 and PDK2 expression was normalised to GAPDH expression for each cell line. $n \geq 3$ biological replicates. Significance was calculated using an unpaired student t-test test with Welch's correction: $p \leq 0.05$ *, $p \leq 0.01$ **, $p \leq 0.001$ ***

b: Western blots showing the levels of PDK4 and PDP1 in the iCAFs and iNFs. Molecular weight markers are shown next to the blots. Representative images of $n \geq 3$ biological replicates

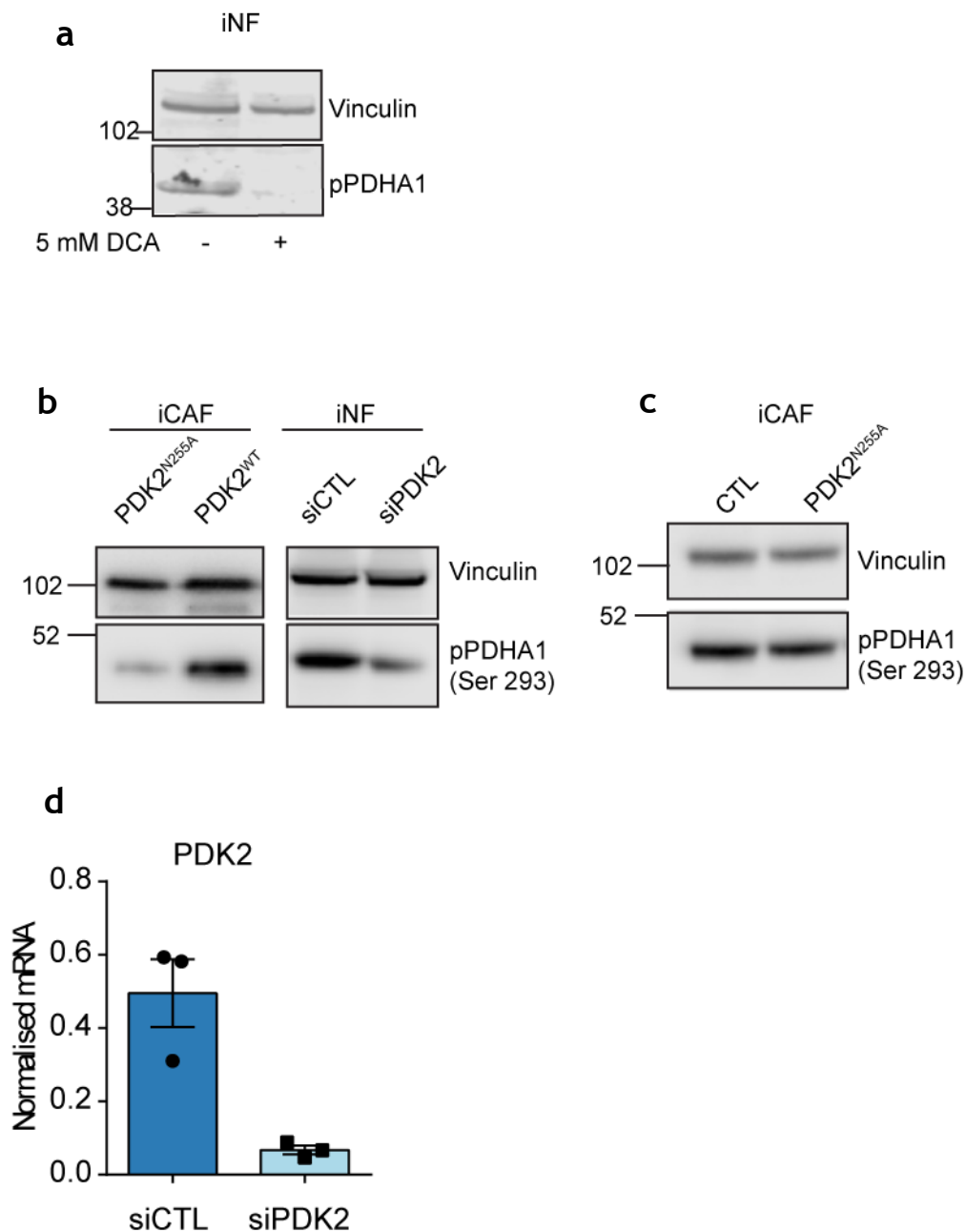


Figure 3-7 PDK2 regulated PDH phosphorylation

a: Western blot showing the levels of phospho-PDHA1 in iNFs after 24h of treatment with 5 mM DCA or DMSO control. Molecular weight markers are shown next to the blots. **b:** Western blot showing the levels of phospho-PDHA1 in iCAFs transfected for 48h with PDK2^{N255A} or PDK^{WT} and iNFs transfected for 48h with siCTL or siPDK2. **c:** Western blot showing phospho-PDHA1 levels are not altered in CAFs transfected for 48h with the inactive PDK2^{N255A} compared to an empty vector control. **d:** PDK2 expression measured by RT-qPCR in iNFs transfected for 48h with siCTL or siPDK2. PDK2 mRNA levels were normalised to TBP2. Graph shows mean and SEM of 3 biological replicates. Significance was calculated using an unpaired student t-test with Welch's correction: $p \leq 0.05$ *

All Western blots are representative images of $n \geq 3$ biological replicates

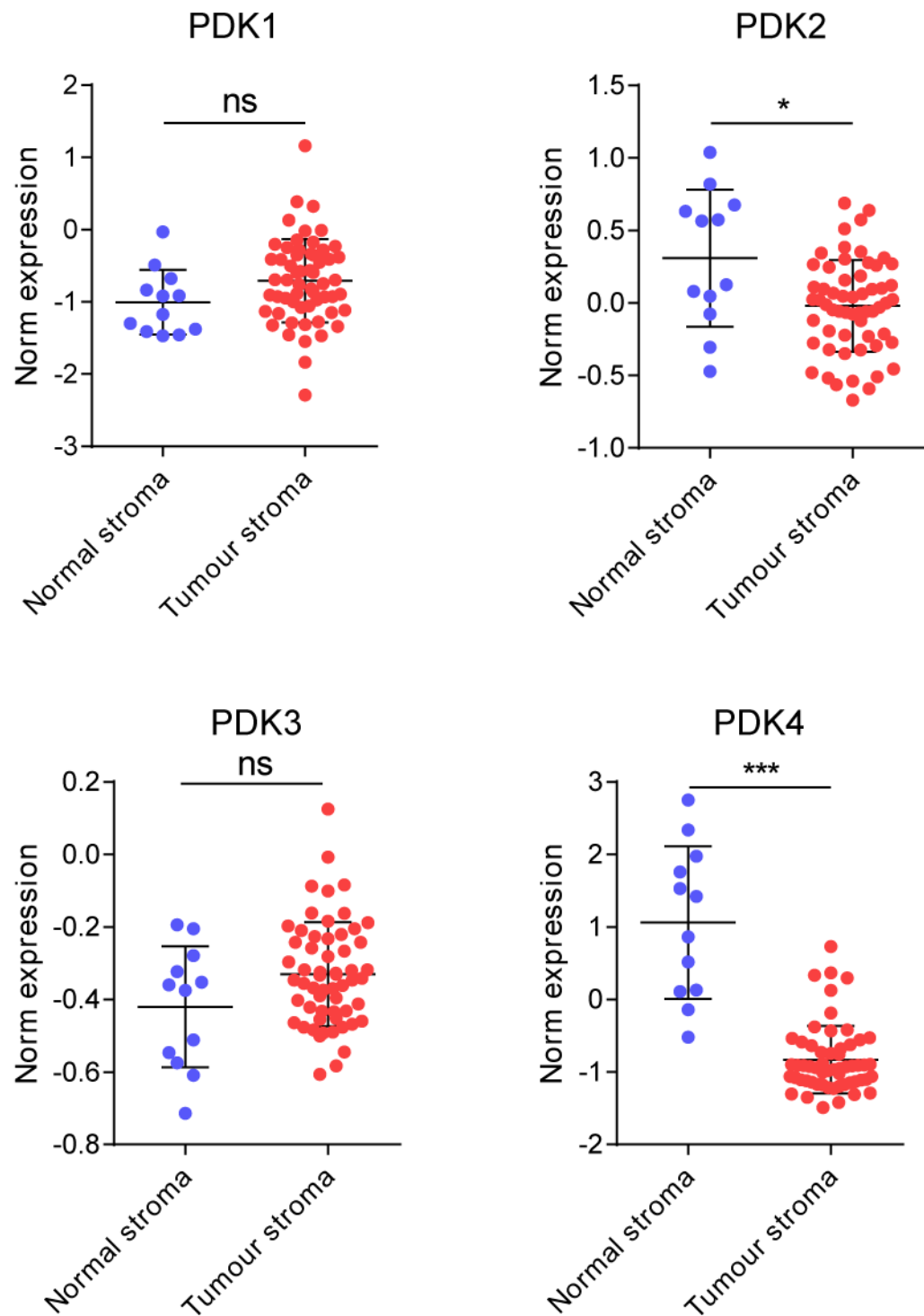


Figure 3-8 PDK expression in normal and tumour-associated stroma

Expression of PDK1,2,3 and 4 mRNA in microdissected sections of normal and tumour associated stroma from triple negative breast cancer patients. Each dot represents 1 patient. Data was provided by Morag Park (McGill University). Error bars show mean and SEM. Significance was calculated using an unpaired student t-test: $p \leq 0.05$ *, $p \leq 0.01$ **, $p \leq 0.001$ ***

3.5 PDH is more active in CAFs

3.5.1 The PDH complex is more active in CAFs in an *in vitro* assay

It is well known that phosphorylation of PDH decreases its activity. Therefore the decrease in phosphorylated PDH in CAFs should mean that PDH is more active. To confirm that PDH is in fact more active in CAFs, I used an enzymatic assay to measure PDH activity in CAFs and NFs. The assay can be used to measure the rate of NADH production by immunocaptured PDH from cell lysates using a reporter dye which gives a yellow reaction product. The rate of NADH production was significantly higher in all CAF cell lines compared to their paired NFs, showing that PDH was indeed more active in CAFs than NFs (Figure 3-9).

3.5.2 CAFs produce more acetyl-coA in a PDH phosphorylation-dependent manner

The role of PDH is to convert pyruvate to acetyl-coA; in order to show that the decrease in PDH phosphorylation increased its activity in the CAFs I used MS-metabolomics to quantify the amount of intracellular acetyl-coA in CAFs and NFs. The total amount of acetyl-coA in the CAFs was significantly higher than in NFs across all three pairs of fibroblasts, suggesting that CAFs do produce more acetyl-coA (Figure 3-10a). However, acetyl-coA can be derived from several pathways. In addition to PDH, acetyl-coA can be produced from beta-oxidation of fatty acids, or from TCA cycle metabolites via citrate. I therefore performed a metabolomics tracing experiment to find out what proportion of acetyl-coA in CAFs was actually produced by PDH. The fibroblasts were labelled for 48h with media containing either $^{13}\text{C}_6$ -glucose or $^{13}\text{C}_3$ -pyruvate to trace acetyl-coA through PDH, $^{13}\text{C}_5$ -glutamine for acetyl-coA produced via the TCA cycle or $^{13}\text{C}_{16}$ -palmitate for acetyl-coA coming from fatty acids (Figure 3-10b). The intracellular metabolites were then harvested and analysed using LC-MS, and the percentage of heavy labelled metabolites incorporated into acetyl-coA was determined. This experiment showed that about 70% of acetyl-coA in the CAFs is derived from glucose and pyruvate combined, meaning that PDH is the main source of acetyl-coA in CAFs. To investigate whether PDH phosphorylation levels were responsible for the difference in acetyl-coA production between CAFs and NFs, I transfected the iNFs

with siPDK2 or siCTL and the iCAFs with PDK2^{WT} or PDK2^{N255A} to increase PDH phosphorylation in iNFs and decrease it in the CAFs, respectively. The intracellular metabolites were extracted from the fibroblasts 48h after transfection and the relative total amount of acetyl-coA was quantified (Figure 3-10c). Increasing PDH phosphorylation decreased intracellular acetyl-coA and vice versa. Therefore PDH activity is increased in CAFs as shown by the increase in acetyl-coA production, and this is dependent on the level of PDH phosphorylation, which is controlled by PDK2 expression.

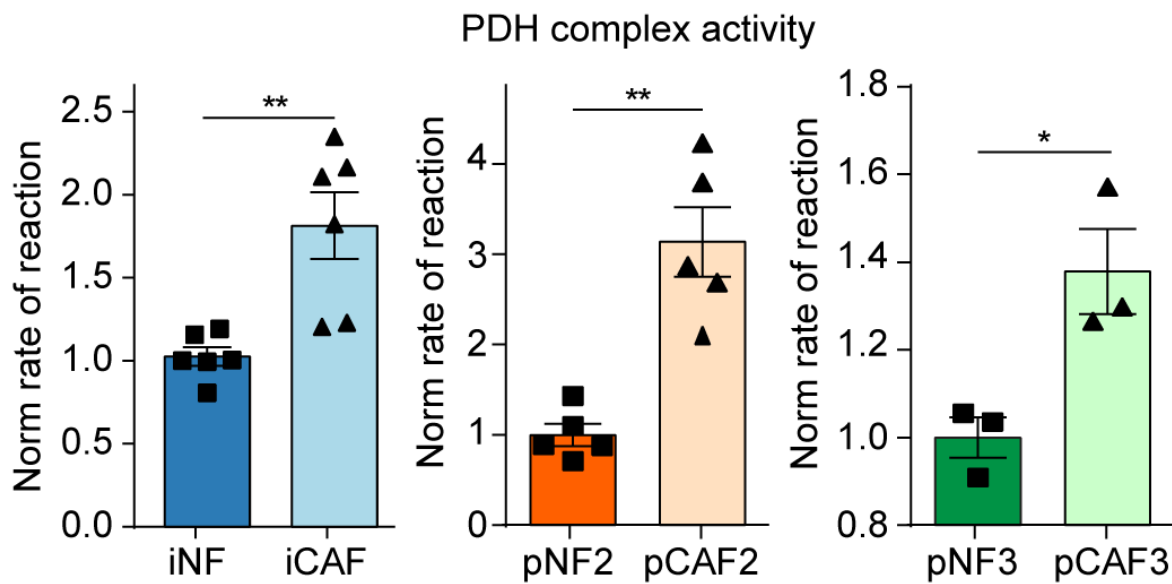


Figure 3-9 PDH complex activity in CAF and NFs

Rate of pyruvate to acetyl-coA conversion by immunocaptured PDH. Rate of reaction was measured as the change in absorbance at OD405 nm and normalised to the rate of reaction in the NFs. Graphs show the mean and SEM of at least 3 independent experiments. Significance was calculated using an unpaired student t-test test with Welch's correction: $p \leq 0.05$ *, $p \leq 0.01$ **

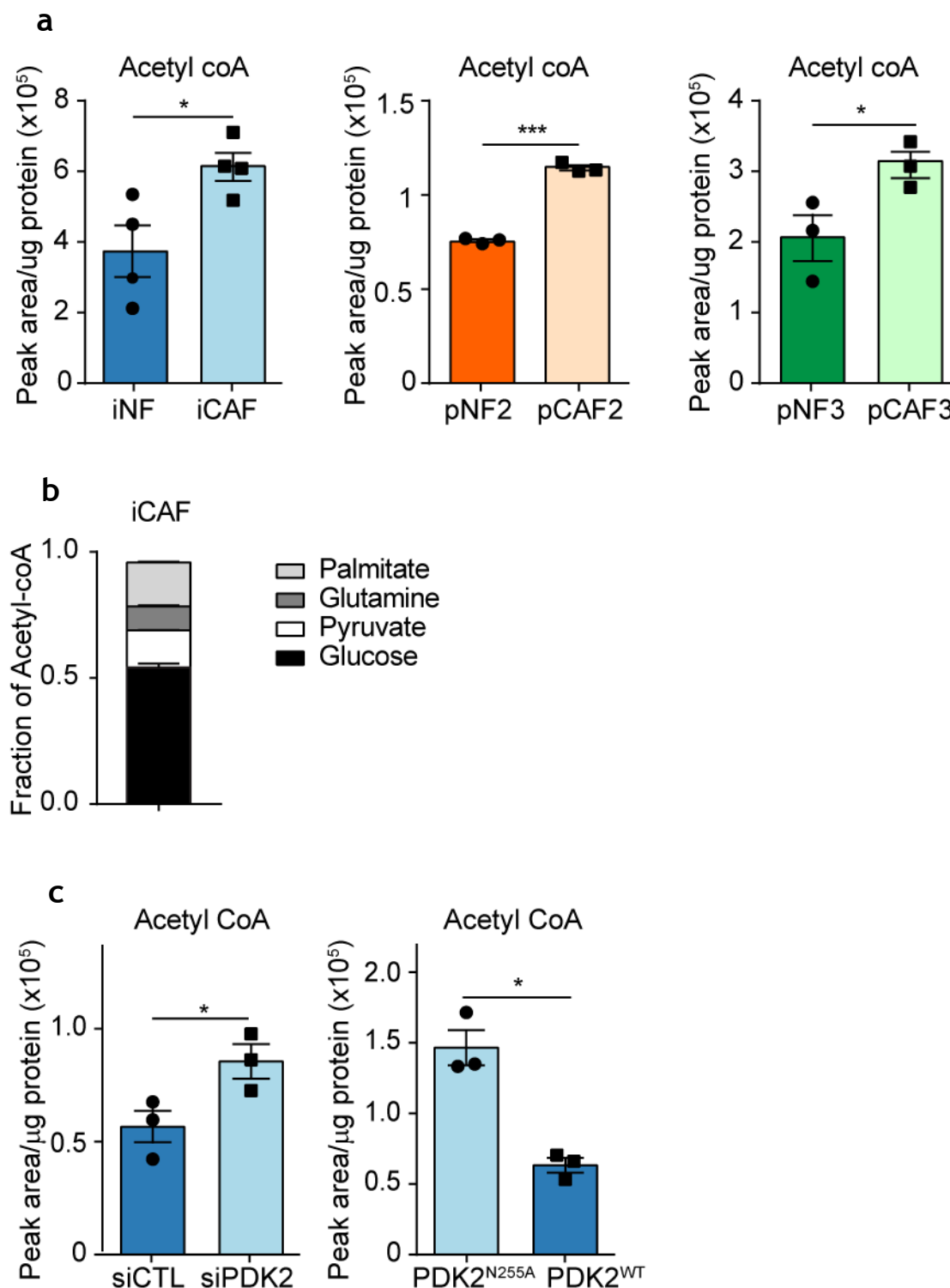


Figure 3-10 PDH activity regulates acetyl-coA in fibroblasts

a: Total intracellular acetyl-coA in NFs and CAFs measured by LC-MS and normalised to protein content. **b:** Fraction of acetyl-coA labelled by glucose, glutamine, pyruvate and palmitate in iCAFs. Acetyl-coA was measured by LC-MS and normalised to protein content. **c:** Total intracellular acetyl-coA in iCAFs transfected for 48h with PDK2^{N255A} or PDK2^{WT} and iNFs transfected for 48h with siCTL or siPDK2. Acetyl-coA was measured by LC-MS and normalised to protein content.

Graphs show the mean and SEM of at least 3 independent experiments. Significance was calculated using an unpaired student t-test test with Welch's correction: $p \leq 0.05$ *, $p \leq 0.01$ **, $p \leq 0.001$ ***

3.6 Investigation of PDK2 regulation in CAFs

I have shown that the decrease in PDH phosphorylation in CAFs is regulated by PDK2 expression, however, it is unknown what pathway in the CAFs leads to decreased PDK2 expression. I reasoned that there must be some aspect of the activated CAF phenotype that was linked to PDK2 expression. Upregulated TGF- β signalling is a hallmark of activated CAFs, so initially I investigated the impact of TGF- β on PDH phosphorylation. I treated the iNFs with recombinant human TGF- β 1 for 48h. This caused an increase in the levels of phospho-Smad2, a readout of activated TGF- β signalling, showing that the treatment was effective (Figure 3-11). However, it did not decrease phospho-PDH, in fact, it slightly increased phospho-PDH levels. It is also well known that CAF activation is stimulated by factors produced by cancer cells. Therefore I also cultured the iNFs with conditioned media from MDA-MB-231 cells, which are a highly aggressive and invasive triple negative breast cancer cell line, for 48h (Figure 3-11). However, this also failed to reduce PDH phosphorylation in the iNFs.

It has been previously shown that PI3K/Akt signalling stimulates decreased PDH phosphorylation on S293 by PDKs in head and neck cancer (Cerniglia et al., 2015). From the phosphoproteomic data from the iCAF and iNF there was evidence to suggest that Akt signalling is upregulated in iCAF and other works have shown that PI3K-Akt signalling is active in CAFs (Sun et al., 2019). I therefore treated the CAFs with the Akt inhibitor MK2066 to investigate the effect of Akt signalling on PDH activity in the CAFs. The Akt inhibitor effectively reduced phospho-Akt, i.e. active Akt, levels after 24h of treatment, and correspondingly increased phospho-PDHA1 levels in both the iCAF and pCAF3s, although not in the pCAF2s (Fig. 3-12). As PI3K/Akt signalling is stimulated by integrin signalling in response to extracellular matrix (ECM) adhesion and CAFs produce a very different ECM to NFs, both in terms of amount of protein and of composition, I investigated whether CAF and NF ECM produced a different response in regard to PDH phosphorylation. Both CAFs and NFs were seeded at confluence and allowed to produce ECM for 7 days. Then, the ECM was decellularised, and CAFs or NFs were seeded on the fibroblast-derived ECM and cultured for 48h. Each pair of CAFs and NFs was seeded on ECM derived from the same pair. By western blot, CAF ECM significantly decreased phospho-PDH levels in NFs relative to NF ECM or plastic (Fig. 3-13). I also analysed

the expression of PDK2 in response to iCAF and iNF derived ECM by RT-PCR and again found that PDK2 expression decreased more in response to being cultured on iCAF derived ECM than iNF ECM or plastic (Fig. 3-14). I therefore concluded that there is a component of CAF derived ECM that stimulates a pathway leading to decreased PDK2 expression and thereby decreased PDH phosphorylation, probably via integrin mediated Akt signalling.

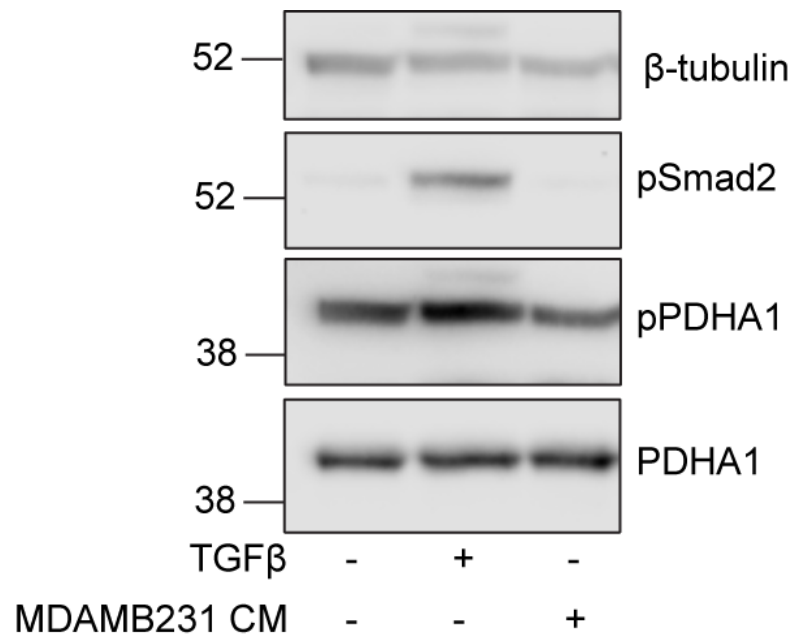


Figure 3-11 TGFβ and cancer cell conditioned media do not activate PDH

Western blot showing phospho-Smad, phospho-PDHA1 and total PDHA1 levels in iNFs after 48h treatment with either recombinant TGFβ or conditioned media from MBAMB231 cancer cells. β-tubulin was used as a loading control. Molecular weight markers are shown next to the blots. Representative image of $n \geq 3$ biological replicates

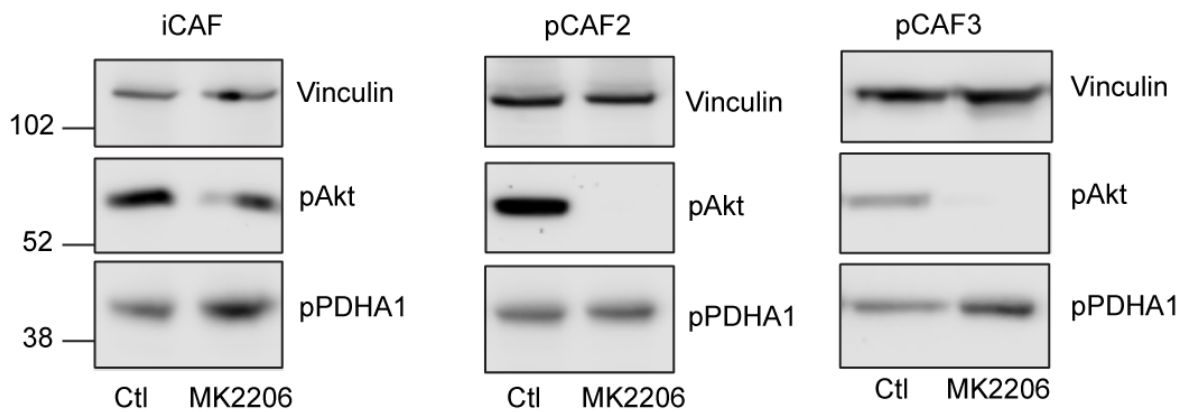


Figure 3-12 Akt inhibitor increases PDH phosphorylation

Western blot showing phospho-Akt and phospho-PDHA1 levels in CAF cell lines after 24h treatment with MK2206. Vinculin was used as a loading control. Molecular weight markers are shown next to the blots. Representative image of $n \geq 2$ biological replicates

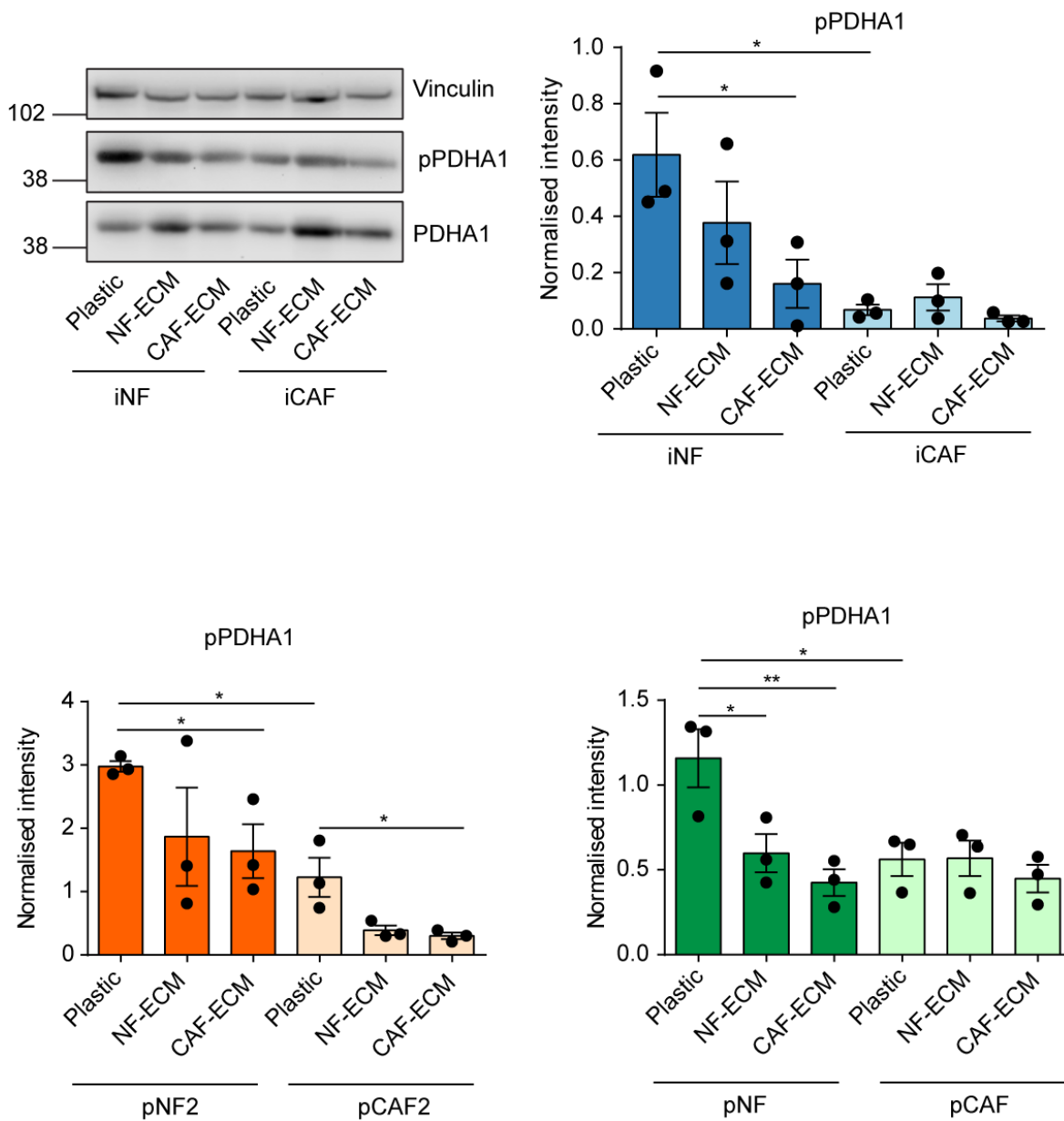


Figure 3-13 CAF ECM decreases PDH phosphorylation

Representative Western blot and quantification of pPDHA1 levels in CAFs and NFs cultured on plastic or on CAF or NF-derived ECM for 48h. The pPDHA1 intensity was normalised to total PDHA1 intensity and loading control intensity. Molecular weight markers are shown next to the blots.

Graphs show mean and SEM of 3 independent experiments. Significance was calculated using a one-way ANOVA with Tukey's multiple comparisons test $p \leq 0.05$ *, $p \leq 0.01$ **, $p \leq 0.001$ ***

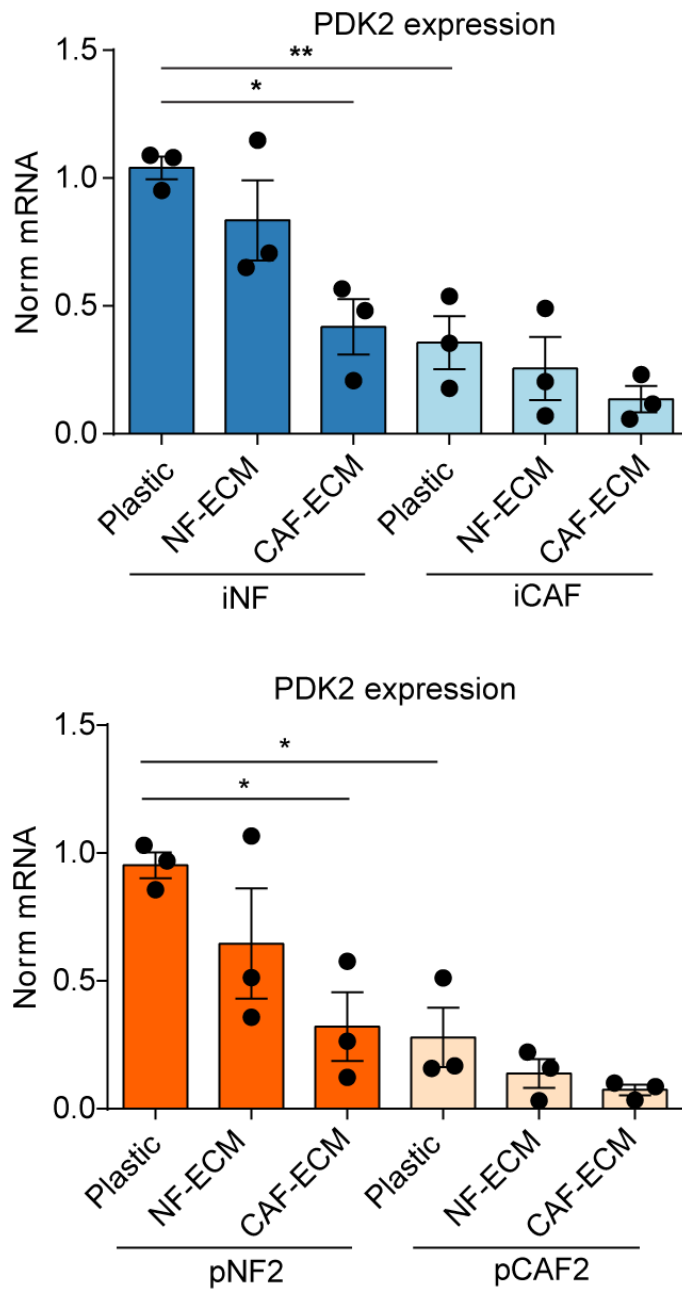


Figure 3-14 CAF ECM decreases PDK2 expression

RT-qPCR quantification of PDK2 expression on CAFs and NFs cultured on plastic or CAF or NF-derived ECM for 48h. PDK2 expression was normalised to 18S expression. Graphs show mean and SEM of 3 independent experiments. Significance was calculated using a one-way ANOVA $p \leq 0.05$ *, $p \leq 0.01$ **, $p \leq 0.001$ ***

3.7 Conclusions

The key finding of this chapter is that pyruvate dehydrogenase, a central metabolic enzyme which produces the versatile metabolite acetyl-coA, is more active in CAFs. The most common way that PDH activity is regulated in cells is by inhibitory phosphorylation, and this is decreased in CAFs compared to NFs. This decrease in phosphorylation was predicted to be regulated by PDK2 based on phosphoproteomic data from the iCAFs and iNFs and I then confirmed this prediction by showing that PDK2 is downregulated in the three CAF cell lines I am using, as well as in microdissected sections of tumour associated stroma from patients, and that PDK2 expression regulates PDH phosphorylation in the fibroblasts. Although there are other enzymes that modify PDH phosphorylation, the fact that PDH phosphorylation is drastically reduced by the PDK inhibitor DCA in NFs points towards the kinases rather than the phosphatases being responsible for regulating PDH phosphorylation in the fibroblasts. Furthermore, PDK2 is the only PDK that was consistently regulated both in my fibroblast cell lines and in stroma from patient samples, and was overall more highly expressed than the other PDKs. Finally, I could significantly alter PDH phosphorylation simply by modulating PDK2 expression in the fibroblasts, again pointing towards PDK2 as the major regulator of PDH phosphorylation in CAFs and NFs. Interestingly, a study found that PDH levels were increased in lung fibroblasts when co-cultured with tumour cells, although there was no difference in phosphorylation, showing that upregulated PDH activity could be a general mechanism across different types of CAFs and not specific to breast cancer stroma. Furthermore, increased levels of PDH in fibroblasts stimulated tumour cell migration, demonstrating that increased PDH activity has a functional effect in the tumour microenvironment (Koukourakis et al., 2017).

There have been few studies investigating pathways that regulate PDK2 expression (Cerniglia et al., 2015, Contractor and Harris, 2012). I began to investigate possible upstream pathways regulating PDK2 expression and showed that CAF derived ECM decreases PDK2 expression. Integrin receptors mediate cellular responses to the ECM, suggesting that this is an integrin regulated pathway. Integrin signalling has been shown to play an important role in the CAF phenotype; integrins $\alpha\beta3$, $\alpha3$ and $\beta6$ have all been shown to stimulate CAF activation (Jang

and Beningo, 2019). Integrins activate signalling pathways mainly through recruiting kinases to the membrane where they are activated. One such kinase is PI3K which activates Akt signalling. This was a good candidate for PDK2 regulation as we know Akt signalling is upregulated in the iCAFs and it has previously been shown to impact PDH phosphorylation. An Akt inhibitor effectively increased PDH phosphorylation in only two out of my three CAF cell lines however, so there may be different regulatory mechanisms happening. I did not pursue investigation into the upstream factors controlling PDK2 expression further, preferring instead to concentrate on the impact that increased PDH activity has on the CAF phenotype, which will be discussed in the following chapters.

The output of increased PDH activity is an increase in acetyl-coA production, which I have demonstrated occurs in my CAF cell lines and that this is regulated by PDK2 dependent PDH phosphorylation. The next question was therefore what this increase in acetyl-coA levels is used for in the CAFs. PDH is primarily a mitochondrial protein, although it has been observed in the nucleus (Sutendra et al., 2014). The metabolic impact of PDH activity has been widely studied in tumour cells, although not in the tumour microenvironment. PDH has been called the 'mitochondrial gatekeeper' as it connects glycolysis to mitochondrial metabolism and many studies on PDH activity have shown that altering PDH phosphorylation and activity pushes cancer cells towards either glycolytic or oxidative metabolism, and that this impacts on tumour progression (McFate et al., 2008, Kaplon et al., 2013, Saunier et al., 2017, Yonashiro et al., 2018). However, acetyl-coA can be exported from the mitochondria into the cytoplasm via citrate, and it has been shown that PDH activity affects cytoplasmic lipid synthesis (Rajagopalan et al., 2015). Acetyl-coA is also a substrate for protein acetylation, and PDH activity has also been shown to affect protein acetylation (Sutendra et al., 2014, Lozoya et al., 2019). An increase in acetyl-coA could therefore modulate a wide variety of pathways contributing to aspects of the activated CAF phenotype either through altered metabolism or through protein acetylation.

Chapter 4 PDH activity regulates histone acetylation in CAFs

4.1 PDH is localised in the mitochondria

In this chapter, I investigated how the acetyl-coA produced by PDH is used by the CAFs, since acetyl-coA is a highly versatile metabolite and can be used for a wide variety of metabolic and acetylation pathways (Pietrocola et al., 2015). PDH is typically known as a mitochondrial enzyme, however, studies have shown that PDH can relocate to the nucleus and produce acetyl-coA there to promote histone acetylation (Sutendra et al., 2014, Shi et al., 2017). The localisation of PDH could impact on how the acetyl-coA it produces is used, although acetyl-coA can be shuttled between the cytosol and mitochondria or nucleus via citrate or acetyl-carnitine. Therefore, there is no barrier to acetyl-coA being produced in one compartment and being used in another. Even so, as a starting point to investigating the function of acetyl-coA in CAFs, I first determined the localisation of PDH. iCAF and iNF were labelled in culture with MitoTracker, which stains mitochondria. The cells were then fixed and probed by immunofluorescence with an antibody against PDHA1, which is the regulatory subunit of the PDH complex (Fig. 4-1a). The PDHA1 staining overlapped entirely with the mitochondrial staining and there was no detectable PDHA1 in the nucleus. To further verify these results, I fractionated lysate from iCAF into nuclear, mitochondrial and cytosolic fractions using a cell fractionation kit. The efficacy of the fractionation was assessed by western blot of each fraction using an antibody cocktail for nuclear, mitochondrial, cytosol and plasma membrane markers: histone 3, ATP5A, GAPDH and Na⁺/K⁺ ATPase respectively. The localisation of PDHA1 in each fraction was determined by western blot and this showed that the PDHA1 band was only visible in the mitochondrial fraction (Fig 4-1b). Therefore, I have conclusively shown that PDH is localised in the mitochondria in the fibroblasts.

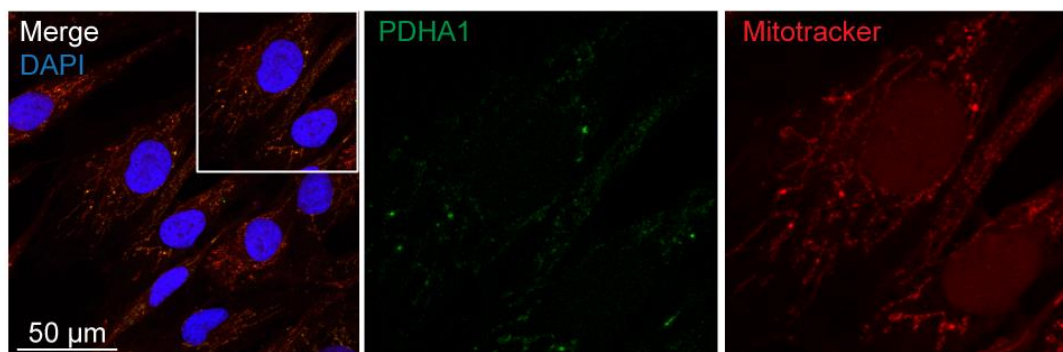
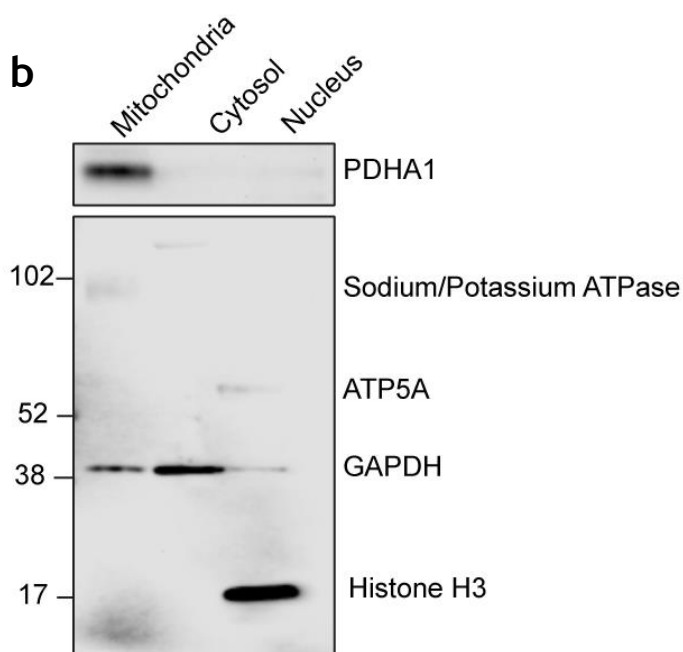
a**b**

Figure 4-1 PDH is mitochondrial in CAFs

a: Representative image of CAFs stained for PDHA1 (green), MitoTracker Red (red) and DAPI (blue). Images were acquired at 40x magnification. Representative image of $n \geq 3$ biological replicates **b:** Western blot of mitochondria, cytosol and nuclear fractions from iCAF lysate showing expression of PDHA1 (top) and mitochondrial, plasma membrane, cytosol and nuclear markers (bottom). Molecular weight markers are shown beside the blots. Representative image of $n = 2$ biological replicates

4.2 There is no difference in glycolysis or oxidative phosphorylation between CAFs and NFs

4.2.1 There are no differences in uptake or secretion of major metabolites between CAF and NFs

The majority of pathways that use acetyl-coA are metabolic pathways. Therefore when investigating the role of increased PDH activity in CAFs, the first step was to discover if there were any metabolic differences between CAFs and NFs. In order to obtain a basic overview of CAF and NF metabolism and to find out if there were major differences between them, I used the YSI 2900 biochemistry analyser to calculate the rate of uptake or secretion of four key metabolites: glucose, lactate, glutamine and glutamate. These metabolites account for most of the metabolic uptake and secretion by cells and are the main carbon sources for the two major metabolic pathways of glycolysis and the TCA cycle.

I took samples of media from CAFs and NFs after 48h of culture and used the biochemistry analyser to measure the concentration of glucose, lactate, glutamine and glutamate in the media. The concentration of each metabolite was normalised to cell number and the rate of uptake or secretion per hour was calculated relative to media that had not been cultured with cells (Fig. 4-2). There were no consistent differences between the CAFs and NFs, which was surprising given that several studies have shown that mammary CAFs are more glycolytic than NFs (Guido et al., 2012, Pavlides et al., 2009, Yu et al., 2017) so I would have expected differences in glucose uptake and lactate secretion. I did however normalise for the increase in cell number over 48h, which would remove any differences in glycolysis due to differences in proliferation rate.

The results of the above experiment were taken from cells under standard cell culture conditions, in media with a plentiful supply of metabolites. However in the tumour microenvironment cells can be under different stresses, including hypoxia and nutrient deprivation. To investigate whether stressing the fibroblasts would elucidate metabolic differences and possible vulnerabilities in the CAFs, I repeated the previous experiment with the CAFs and NFs, however the cells were either cultured in hypoxic conditions with 1% oxygen (Fig 4-3) or with 'low glucose' media (Fig 4-4), which contains 1 g/l glucose instead of 5 g/l and is more similar

to the glucose concentration in a tumour. Again, I took media after 48h of culture and measured the concentration of glucose, lactate, glutamine and glutamate using the biochemistry analyzer. Although the rate of glucose uptake and lactate secretion increased under hypoxia and decreased under low glucose conditions, there were still no consistent differences between CAFs and NFs. However, there were differences in individual metabolites between CAFs and NFs from the same pair, highlighting the heterogeneity of the patient derived CAFs compared to the iCAF. For example, the pCAF2 line takes up a high amount of glutamine and secretes a high amount of glutamate under low glucose conditions.

However, these experiments show that there are no metabolic differences between the mammary CAFs and NFs at the basic level of conversion of glucose to lactate and the glutamine/glutamate cycle. In order to discover whether the increased PDH activity in CAFs had any metabolic effects, it was necessary to gain a more in depth understanding of the metabolism of the CAFs and NFs.

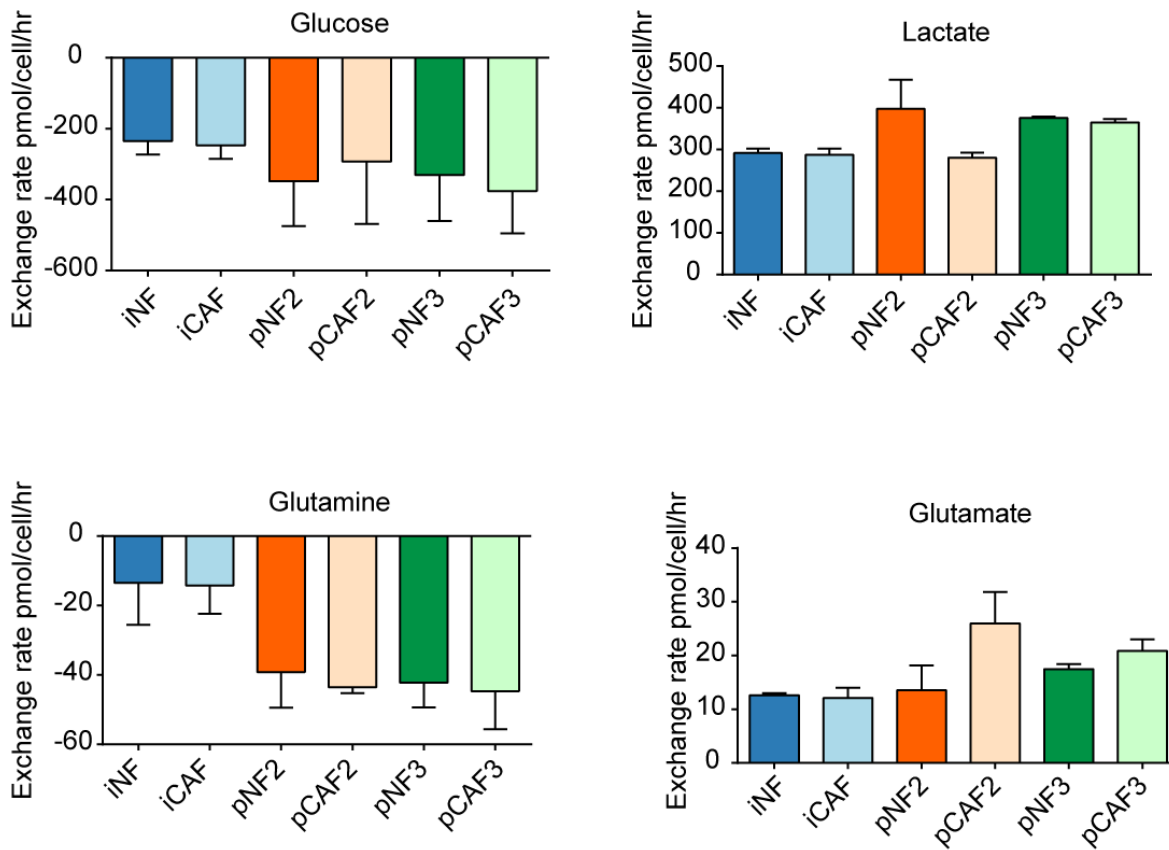


Figure 4-2 Metabolic flux of CAFs and NFs in normoxia/high glucose conditions

Graphs showing the exchange rate between fibroblasts and media of glucose, lactate, glutamine and glutamate. Bars show the mean and SEM of three independent experiments. Significance between CAFs and NFs of the same pair was calculated using a students t-test with Welch's correction

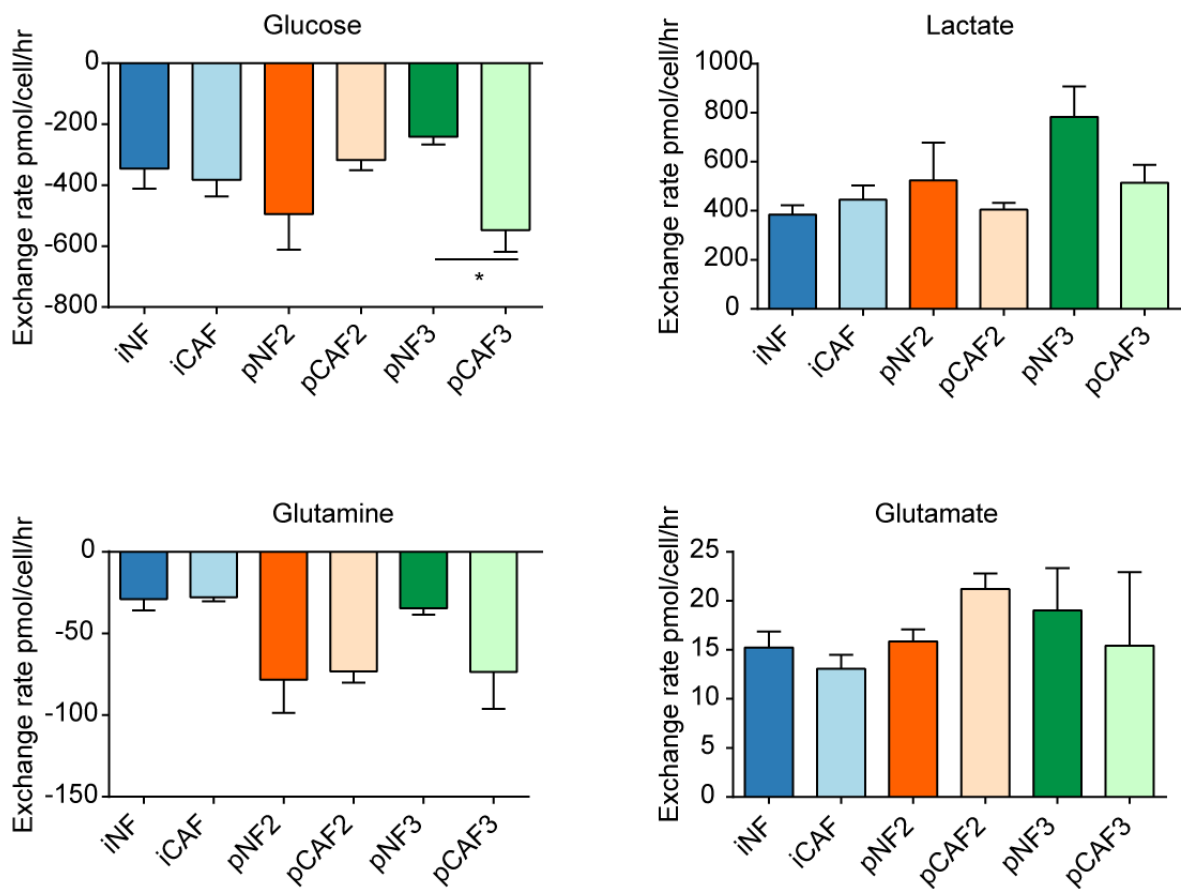


Figure 4-3 Metabolic flux of CAFs and NFs in hypoxia

Graphs showing the exchange rate between fibroblasts and media of glucose, lactate, glutamine and glutamate. Cells were cultured in 1% O₂ for the duration of the experiment. Bars show the mean and SEM of three independent experiments. Significance between CAFs and NFs of the same pair was calculated using a student's t-test with Welch's correction: *p≤0.05, ** p≤0.01, *** p≤0.001

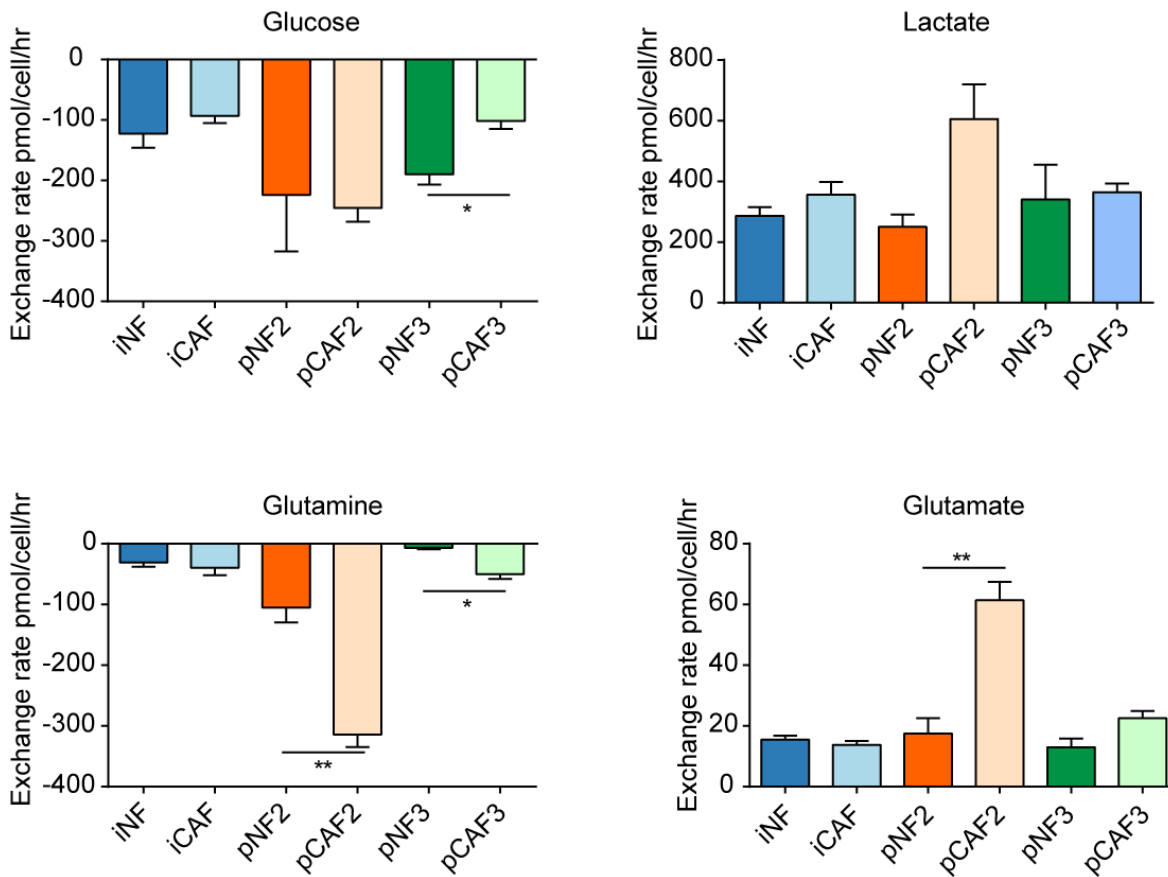


Figure 4-4 Metabolic flux of CAFs and NFs cultured in low glucose media

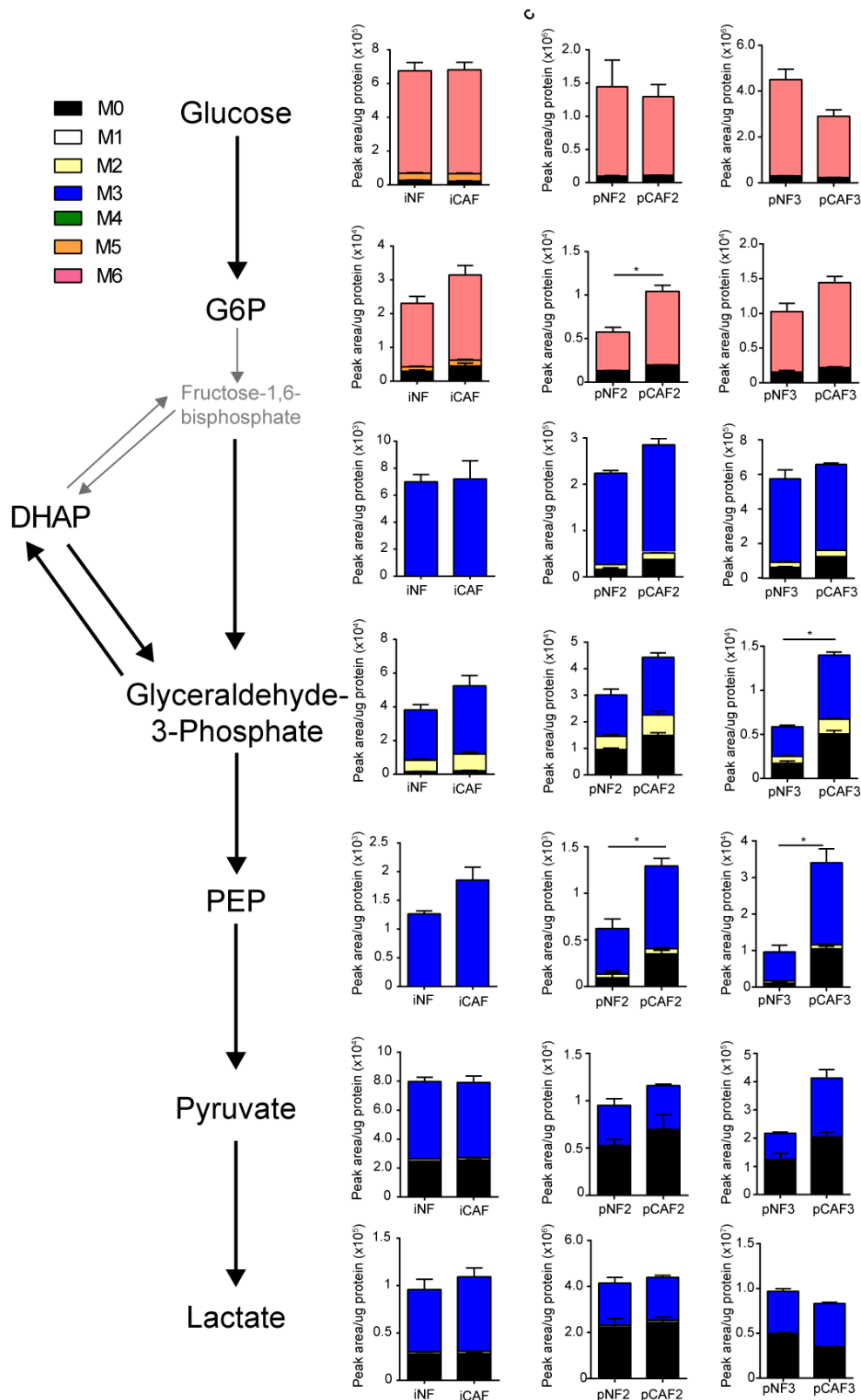
Graphs showing the exchange rate between fibroblasts and media of glucose, lactate, glutamine and glutamate. Cells were cultured in media containing 1 g/l glucose for the duration of the experiment. Bars show the mean and SEM of three independent experiments. Significance between CAFs and NFs of the same pair was calculated using a students t-test with Welch's correction: * $p \leq 0.05$, ** $p \leq 0.01$, *** $p \leq 0.001$

4.2.2 MS-metabolomic tracing experiments show few differences between CAFs and NFs

The most obvious route for acetyl-coA produced in the mitochondria is to enter the TCA cycle. Indeed, the majority of studies on increased PDH activity show that it is used to fuel and promote oxidative metabolism in cells. In addition to fuelling oxidative phosphorylation, TCA cycle metabolites have many other roles including as precursors for amino acid and nucleotide synthesis and as signalling molecules. In order to obtain a more in depth overview of the metabolism of CAFs and NFs, I performed metabolomic tracing experiments with the iCAFs and iNFs as well as the pCAFs and pNFs. I cultured the fibroblasts with media containing $^{13}\text{C}_6$ -glucose for 48h before extracting the metabolites and analysing heavy glucose incorporation and relative levels of metabolites by LC-MS.

Although in individual CAF and NF pairs there were significant differences in some metabolites, overall there were few consistently regulated metabolites between CAFs and NFs. N-acetyl-aspartate levels were higher in CAFs than in NFs in 2 out of 3 pairs, and incorporated heavy glucose at M+2, which could come from acetyl-coA since the acetyl group has two carbons (Fig. 4-8). Additionally, intracellular proline and asparagine levels were consistently higher in CAFs than in NFs (Fig. 4-7). I found that glycolytic metabolites were highly labelled, showing that the cells effectively took up the labelled glucose (Fig. 4-5), and that glucose labelled about 25% of intracellular citrate. There was an increase in labelled citrate in CAFs compared to NFs. However, there was minimal labelling in the other TCA cycle metabolites (Fig 4-6), and in amino acids derived from them (Fig 4-7). This strongly suggested that acetyl-coA produced by PDH is converted to citrate, but is then exported out of the mitochondria where it can be converted back to acetyl-coA by ATP-citrate lyase (ACLY). Interestingly, a high proportion of heavy glucose was incorporated into acetylcarnitine in CAFs (Fig. 4-8). Acetylcarnitine is another pathway that can be utilised to export acetyl-coA out of the mitochondria. Mitochondrial carnitine O-acetyltransferase (CRAT) catalyses the reversible transfer of the acetyl group of acetyl-coA onto carnitine, which is shuttled out of the mitochondria and can again be converted back to acetyl-coA and carnitine in the cytosol. This has been shown to act as means of maintaining a steady state of oxidative phosphorylation by removing excess acetyl-coA from the mitochondria

(Davies et al., 2016). Taken together, the metabolomics tracing data suggests that acetyl-coA produced by PDH has a role outside of the mitochondria and is not used to fuel the TCA cycle.



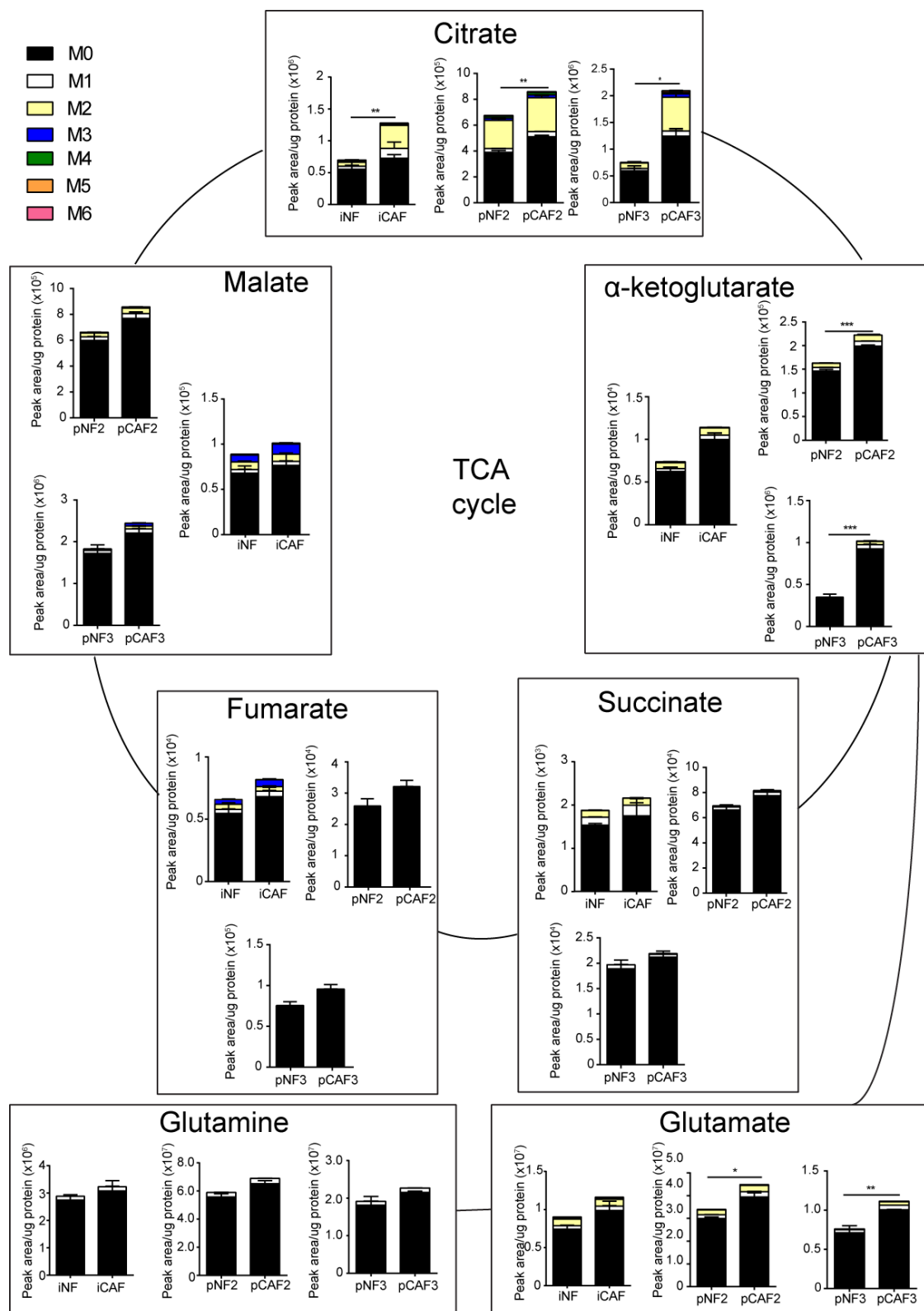


Figure 4-6 ^{13}C -Glucose labelling of TCA cycle metabolites

Graphs show the total intracellular TCA cycle metabolites with the proportion of labelled carbons incorporated into each metabolite after 48h of labelling with ^{13}C -glucose. NFs and CAFs were compared for each pair of fibroblasts. For each isotope, the peak area was normalised to the protein content of the cells from which the metabolites were harvested. Error bars show the mean and SEM for each isotope from 3 independent experiments. Significance was calculated using a student's t-test with Welch's correction: * $p < 0.05$, ** $p < 0.01$, *** $p < 0.001$

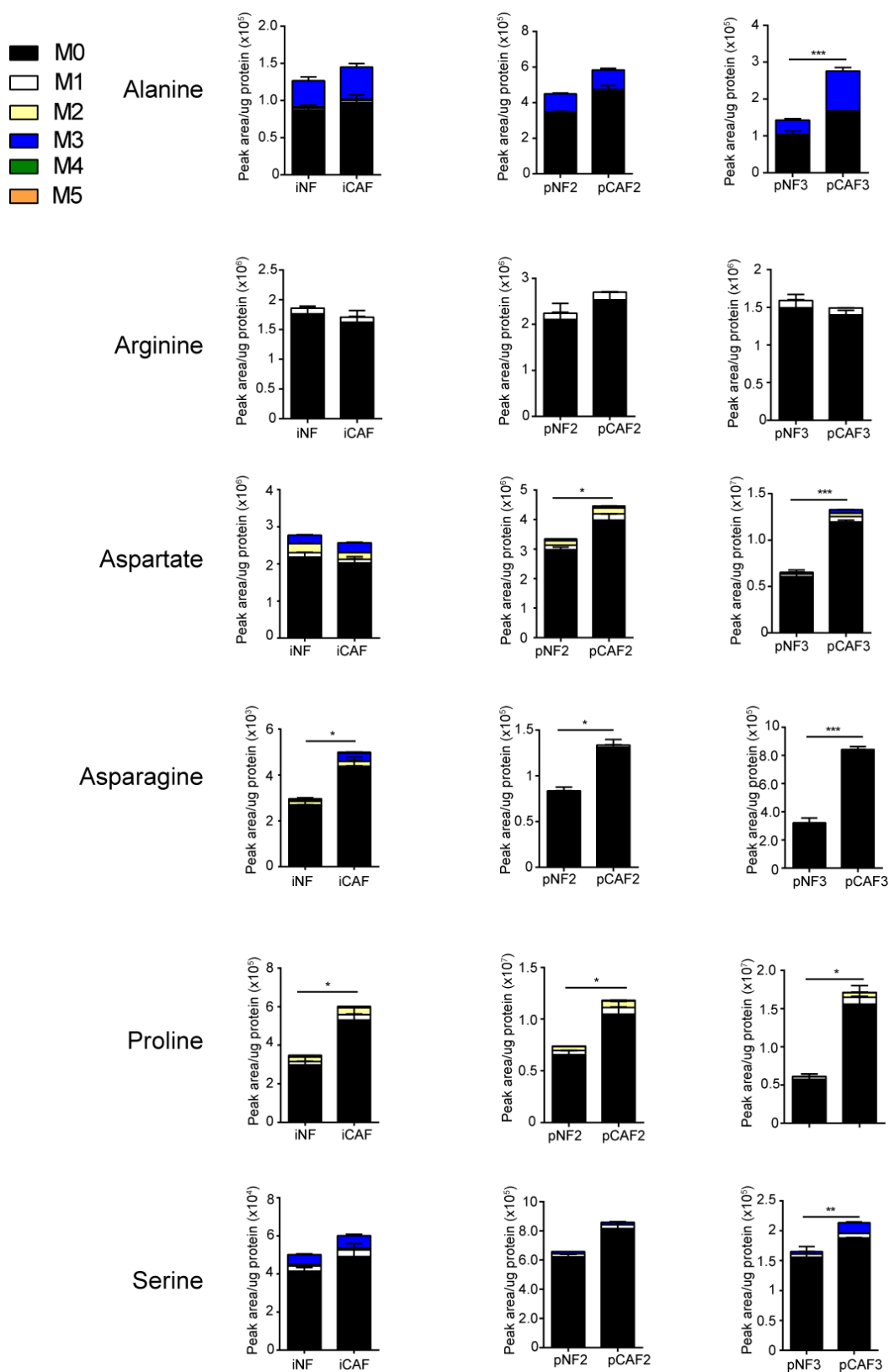


Figure 4-7 13C-Glucose labelling of non-essential amino acids

Graphs show the total intracellular non-essential amino acids with the proportion of labelled carbons incorporated into each metabolite after 48h of labelling with 13C-glucose. NFs and CAFs were compared for each pair of fibroblasts. For each isotope, the peak area was normalised to the protein content of the cells from which the metabolites were harvested. Error bars show the mean and SEM for each isotope from 3 independent experiments. Significance was calculated using a student's t-test with Welch's correction: *p<0.05, ** p<0.01, *** p<0.001

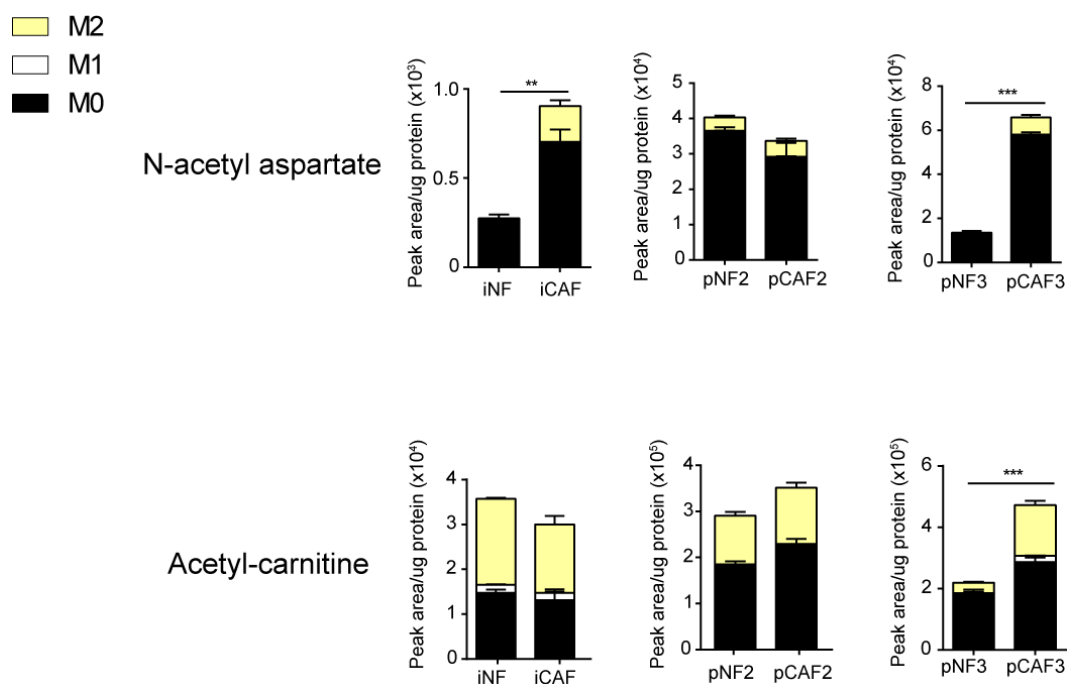


Figure 4-8 ¹³C-Glucose labelling of acetylated metabolites

Graphs show the total intracellular acetylated metabolites with the proportion of labelled carbons incorporated into each metabolite after 48h of labelling with ¹³C-glucose. NFs and CAFs were compared for each pair of fibroblasts. For each isotope, the peak area was normalised to the protein content of the cells from which the metabolites were harvested. Error bars show the mean and SEM for each isotope from 3 independent experiments. Significance was calculated using a student's t-test with Welch's correction: * $p \leq 0.05$, ** $p \leq 0.01$, *** $p \leq 0.001$

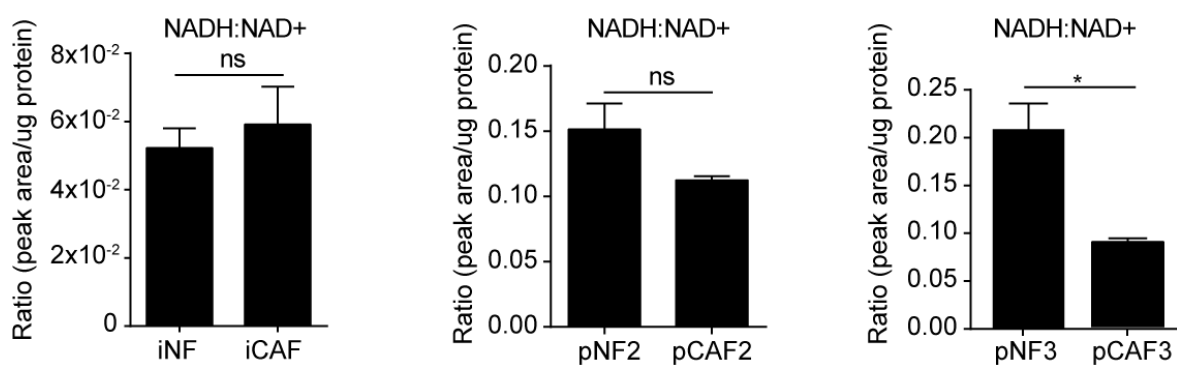


Figure 4-9 NADH:NAD⁺ ratio in CAFs and NFs

Graphs show the NADH:NAD⁺ ratio calculated based on the total intracellular metabolite. NFs and CAFs were compared for each pair of fibroblasts. The peak area was normalised to the protein content of the cells from which the metabolites were harvested. Error bars show the mean and SEM for each isotope from 3 independent experiments. Significance was calculated using a student's t-test with Welch's correction: *p<0.05, ** p<0.01, *** p<0.001

4.2.3 Glutamine is the main source of TCA cycle metabolites in CAFs and NFs

To further verify that acetyl-coA derived from PDH was not an important source of TCA cycle metabolites, I performed additional metabolomics tracing experiments with the iCAFs and iNFs. The fibroblasts were labelled for 48h with either $^{13}\text{C}_6$ -glucose, $^{13}\text{C}_5$ -glutamine or $^{13}\text{C}_{16}$ -palmitate. Glutamine can enter the TCA cycle via conversion to glutamate (glutaminolysis) and palmitate can enter the TCA cycle through conversion to acetyl-coA (fatty acid oxidation). I then extracted the intracellular metabolites and analysed the incorporation of heavy carbon by MS-metabolomics (Fig. 4-10, Fig. 4-11). Once again, there were no differences in the total proportion of heavy carbon incorporation into glycolysis or TCA cycle metabolites between CAFs and NFs. However, it was clear from this experiment that the majority of TCA cycle metabolites are derived from glutamine and not from glucose or palmitate. Glutamine labelled around 70% of TCA cycle metabolites, whereas glucose and palmitate gave around 5-10% label incorporation, with the exception of citrate as shown in the previous experiment. This experiment further supported my previous metabolomics data in showing that increased PDH activity does not increase oxidative phosphorylation in CAFs.

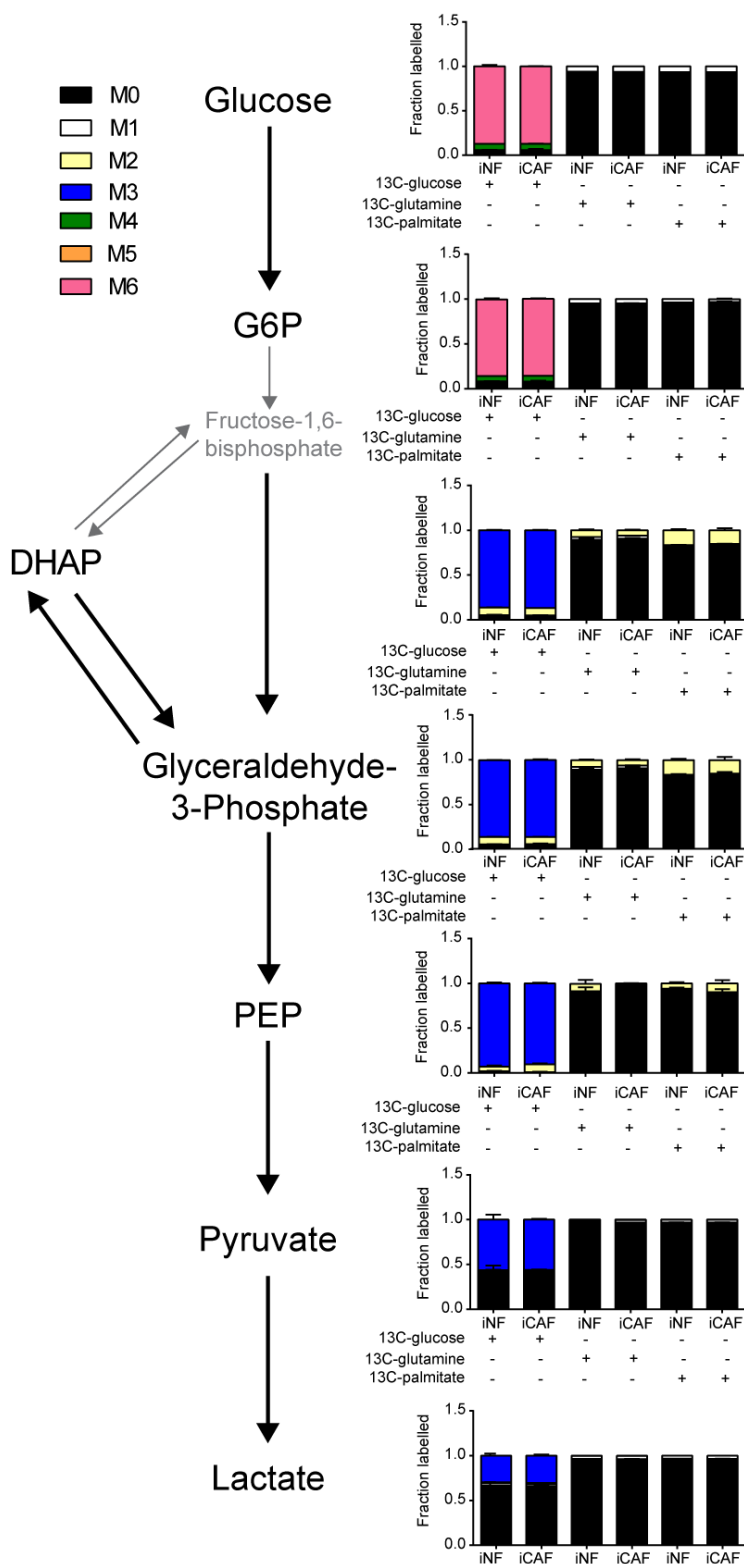


Figure 4-10 ^{13}C labelling of glycolytic metabolites

Graphs show the proportion of labelled carbons incorporated into each metabolite after 48h of labelling with ^{13}C -glucose, glutamine or palmitate in the iNFs and iCAFs. For each isotope, the peak area was normalised to the protein content of the cells from which the metabolites were harvested. Error bars show the mean and SEM for each isotope from 3 independent experiments. Significance was calculated using a student's t-test with Welch's correction: * $p \leq 0.05$, ** $p \leq 0.01$, *** $p \leq 0.001$

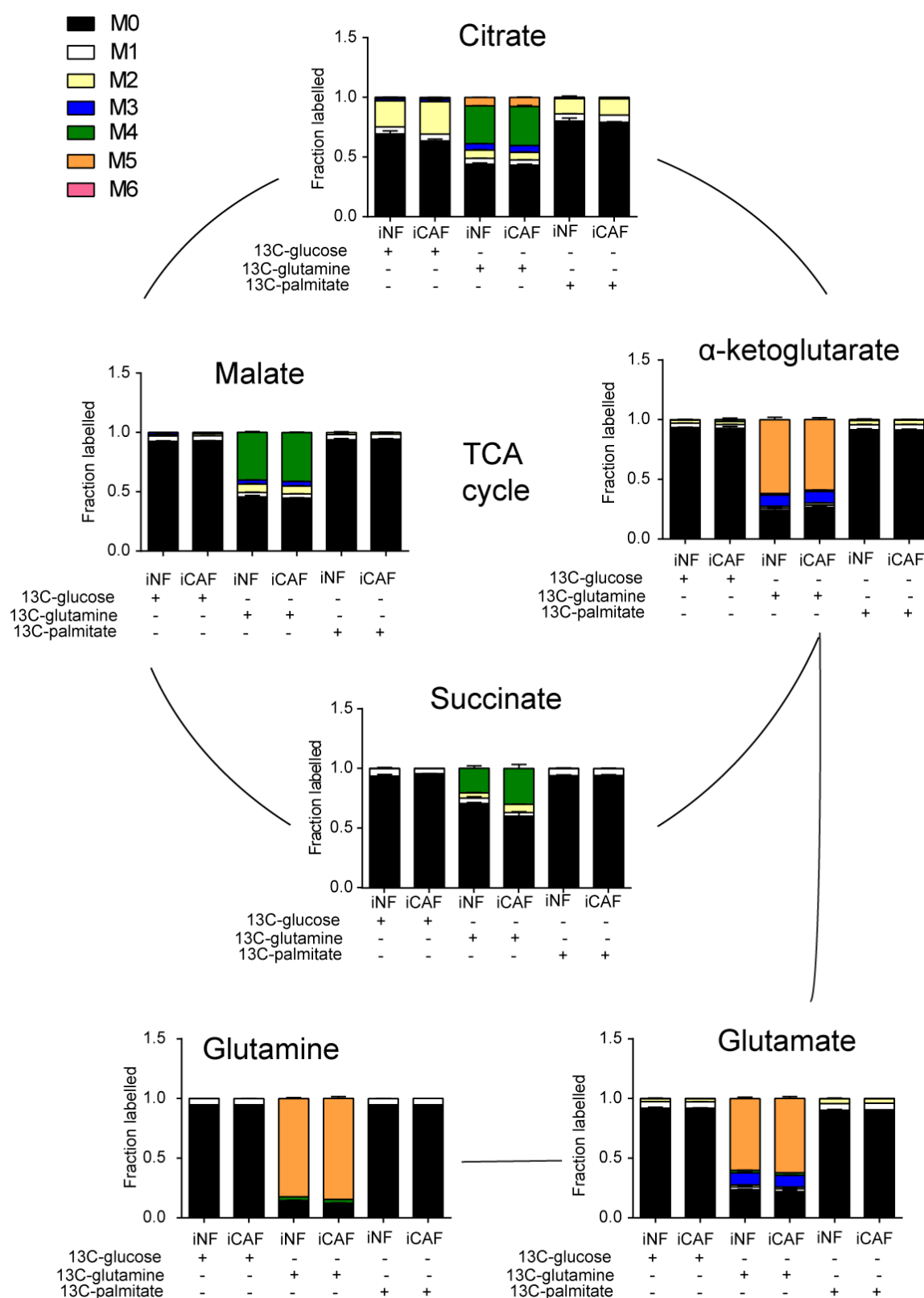


Figure 4-11 ^{13}C labelling of TCA cycle metabolites

Graphs show the proportion of labelled carbons incorporated into each metabolite after 48h of labelling with ^{13}C -glucose, glutamine or palmitate in the iNFs and iCAFs. For each isotope, the peak area was normalised to the protein content of the cells from which the metabolites were harvested. Error bars show the mean and SEM for each isotope from 3 independent experiments. Significance was calculated using a student's t-test with Welch's correction: * $p \leq 0.05$, ** $p \leq 0.01$, *** $p \leq 0.001$

4.2.4 CAFs have decreased mitochondrial functionality and are more autophagic than NFs

To further investigate whether there are mitochondrial differences between CAFs and NFs, I stained the cells with MitoTracker or TMRE. MitoTracker labels mitochondria, thus giving a readout of the total mitochondrial content of the cells. TMRE, however, labels mitochondria in a membrane potential dependent manner, and therefore only labels functional mitochondria. After labelling the fibroblasts with the mitochondrial dyes in culture, the cells were harvested and fixed, and the intensity of the staining was quantified using flow cytometry. I could not detect significant differences in the total amount of mitochondria using MitoTracker staining between iCAF/iNF or pCAF3s/pNF3s, although pCAF2s had a significantly decreased mitochondrial content (Fig. 4-11a). However, both the iCAF and the pCAF2s had a significantly lower amount of TMRE labelling after normalisation to the total mitochondrial content, indicating that their mitochondria are less functional (Fig. 4-12b).

It has previously been reported that CAFs are more autophagic than NFs due to increased accumulation of reactive oxygen species (ROS), and it has been shown that the degradation products of autophagic CAFs provide tumour cells with key nutrients and building blocks for their faster rate of biosynthesis and metabolic turnover (Capparelli et al., 2012, Pavlides et al., 2012, Pavlides et al., 2010a). Mitochondrial dysfunction is a key aspect of autophagy, as dysfunctional mitochondria which cannot carry out oxidative phosphorylation accumulate ROS due to their dissipated membrane potential and thus stimulate autophagy (Ding and Yin, 2012). To assess whether the CAFs were more autophagic than NFs, I quantified the expression of LC3BII after treatment of the iCAF and iNF with bafilomycin and chloroquine. LC3BII is the lipidated form of LC3B that recognises ubiquitinated proteins and is recruited to autophagosomes as part of the autophagy process. In order for degradation to occur, autophagosomes must fuse with lysosomes and both bafilomycin and chloroquine inhibit this step, causing accumulation of autophagosomes and thereby LC3BII. Therefore the more LC3BII that is present after bafilomycin or chloroquine treatment, the higher the rate of autophagic flux is in the cells. The iCAF accumulated more LC3BII after the drug treatment, indicating that in accordance with the literature they do have higher

levels of autophagy than the iNFs (Fig. 4-13). In this case, it is interesting that in spite of having a decrease in mitochondrial functionality and increased autophagic flux, the iCAFs still maintain the same quantity of mitochondria as the iNFs, as shown by MitoTracker Red (Fig. 4-12a). Normally, dysfunctional mitochondria are separated from the healthy network and degraded through a specific form of autophagy called mitophagy. This suggests that either the CAFs are synthesising new mitochondria to maintain the same amount as the NFs, or that mitophagy is impaired in some way. Interestingly, it has recently been shown that a second target of PDK2 is PARL (presenilin-associated rhomboid-like) (Shi and McQuibban, 2017), which is a key player in one of the canonical mitophagy pathways. The authors showed that in response to mitochondrial depolarisation, PDK2 phosphorylates PARL and prevents it from cleaving PINK-1 (PTEN-induced putative kinase 1). PINK-1 therefore accumulates at the outer mitochondrial membrane and recruits an E3 ubiquitin ligase to stimulate mitophagy. It is therefore possible that the lack of PDK2 in CAFs also reduces the efficacy of this mitophagy pathway, leading to accumulation of dysfunctional mitochondria. However, although PDK2 expression may be involved in the observed differences in autophagy and mitochondrial dysfunction in between CAFs and NFs, it is unlikely that the increased PDH activity in CAFs would affect this pathway. Additionally, the pCAF3s/pNF3s did not show any differences either in mitochondrial content or TMRE labelling, so the differences are not consistent between different fibroblast pairs. Therefore I did not pursue this line of research any further, although it would be interesting to do so in the future.

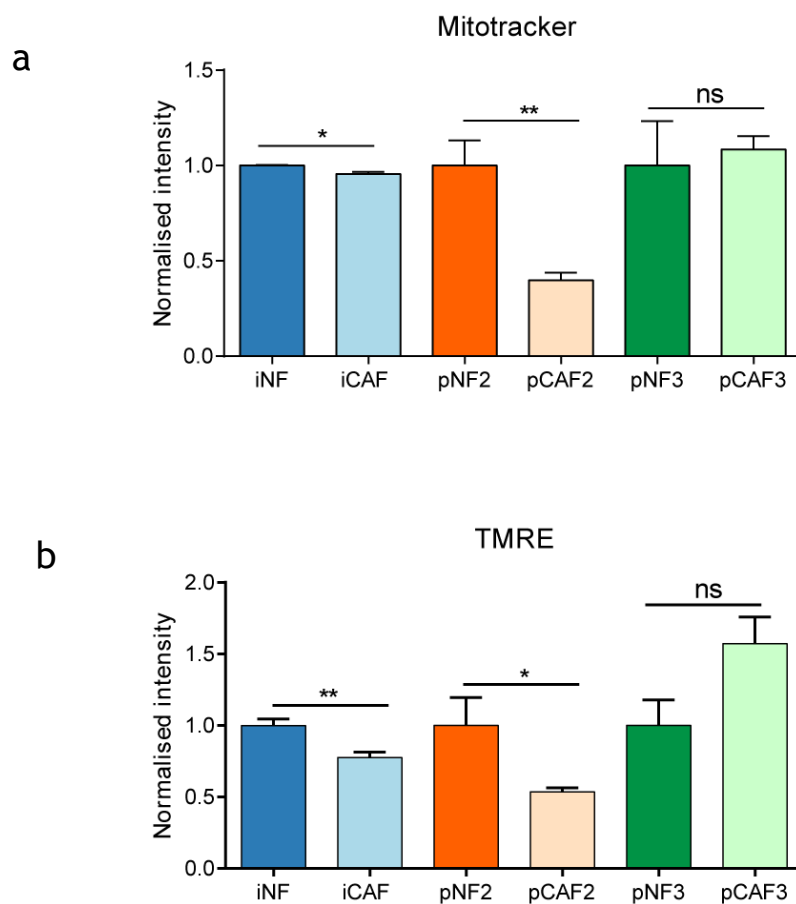


Figure 4-12 Mitochondrial content of CAFs and NFs

a: Intensity of MitoTracker staining as measured by flow cytometry. Intensity was normalised to NF data for each pair of fibroblasts. **b:** Intensity of TMRE staining as measured by flow cytometry. Intensity was normalised to total mitochondrial content as determined by the MitoTracker staining, and to the NF data for each pair.

Significance was calculated using a student's t-test with Welch's correction: * $p \leq 0.05$, ** $p \leq 0.01$, *** $p \leq 0.001$

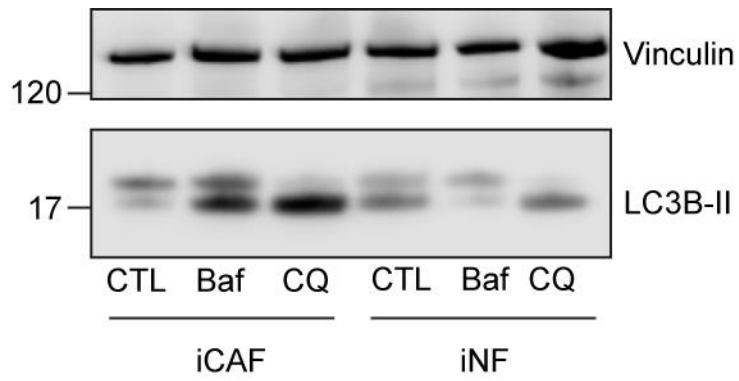


Figure 4-13 LCB-II accumulation in iCAFs and iNFs

Western blot showing accumulation of LC3B-II (lower band) after 4h treatment with bafilomycin (Baf) or chloroquine (CQ) in iCAFs and iNFs. Vinculin was used as a loading control. Molecular weight markers are shown next to the blots

4.2.5 PDH activity does not affect mitochondrial functionality

To further analyse mitochondrial metabolism in CAFs and NFs, I used the Seahorse XF24 Flux analyser. This measures oxygen consumption by cells and thus provides a readout for the rate of oxidative phosphorylation. I grew CAFs and NFs for 24h in Seahorse 24 well culture plates before carrying out the analysis with the Seahorse. Initially the basal oxygen consumption rate was measured, before adding oligomycin to block ATP synthesis and thereby reduce oxygen consumption, followed by CCCP to uncouple the electron transport chain from ATP synthase, forcing the cells to consume oxygen at their maximum capacity. Finally, antimycin A and rotenone were added to inhibit the electron transport chain and block oxygen consumption entirely. I could detect no difference between CAFs and NFs in basal oxygen consumption rate, although the iCAF_s did have a lower mitochondrial capacity than the iNF_s which is consistent with the TMRE staining showing that CAFs have a decrease in mitochondrial functionality (Fig 4-13a). The oxygen consumption rate of the pCAF_s and pNF_s was extremely low and I could detect no differences between CAFs and NFs (Fig 4-14a). To verify that the fibroblasts truly had a low level of oxygen consumption, I compared the rates with that of the MCF7 breast cancer cell line, which is known to have a high level of mitochondrial respiration (Rodriguez-Enriquez et al., 2010). All the fibroblast cell lines had a lower oxygen consumption rate compared to the MCF7 breast cancer cell line (Fig 4-14b). This experiment further supports the metabolomics data showing no differences in mitochondrial metabolism under normal conditions between CAFs and NFs and supports my hypothesis that PDH produced acetyl-coA is not used to increase flux through the TCA cycle in CAFs, especially since the fibroblasts have a low oxygen consumption rate.

To finally show that PDH activity does not impact mitochondrial function, I transfected the iNF_s with siPDK2 or siCtl to reduce PDH phosphorylation and increase its activity, then, 48h after transfection, I used the Seahorse to measure oxygen consumption. I could detect no differences between siCtl and siPDK2 transfected iNF_s in oxygen consumption either at the basal level or in mitochondrial capacity (Fig 4-13c). Therefore it seems that although CAFs do have a decrease in mitochondrial functionality compared to NFs, this does not affect their basal level of oxidative phosphorylation, which is relatively low.

Furthermore, PDH activity has no effect on oxidative metabolism and the evidence from the metabolomics tracing data strongly suggests that the majority of acetyl-coA produced by PDH is exported out of the mitochondria and used elsewhere.

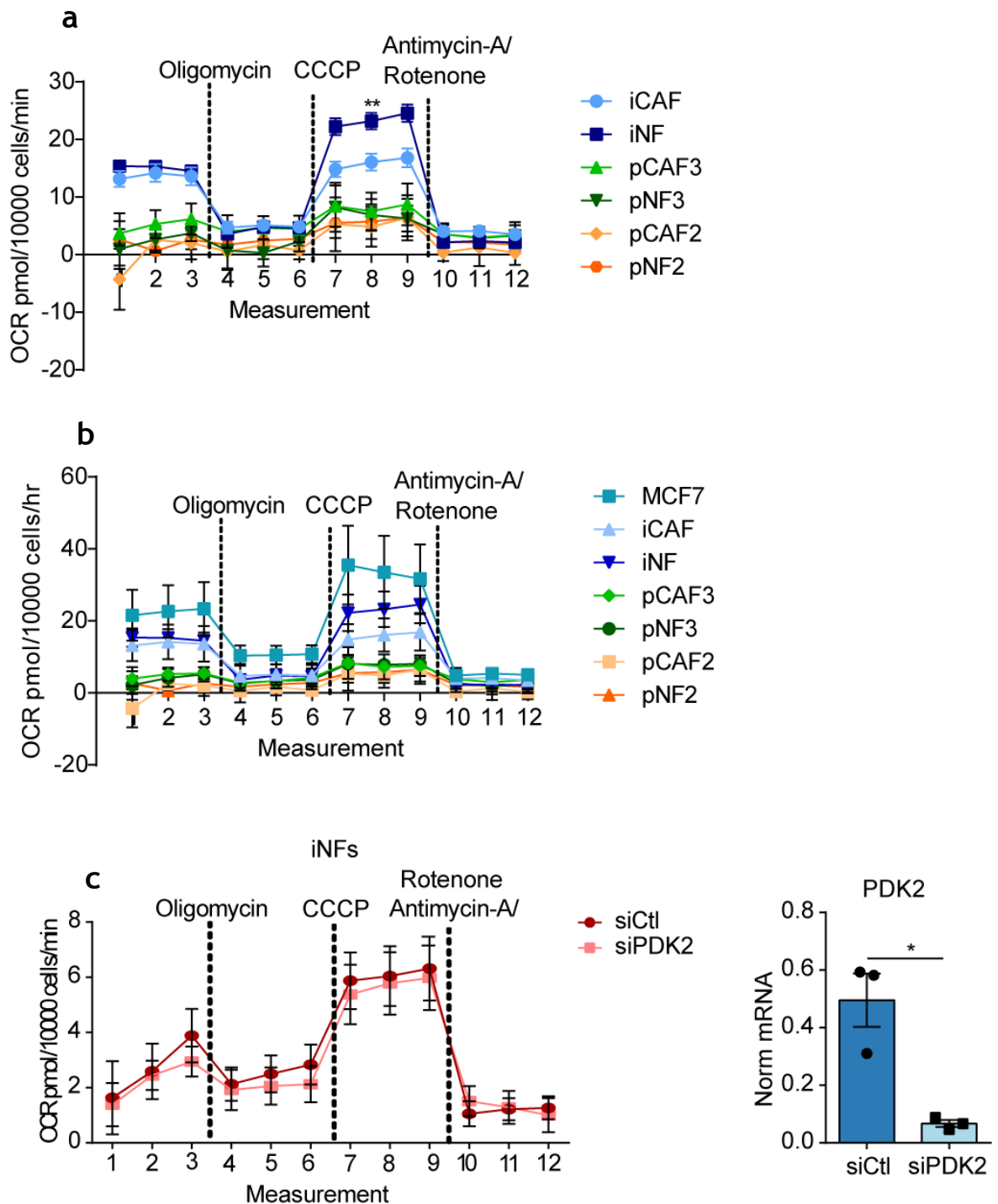


Figure 4-14 Oxygen consumption rate (OCR) of CAFs and NFs

a: OCR as measured by the Seahorse in all CAF and NF cell lines. Time points at which drugs were added are shown with dotted lines. OCR was normalised to cell number. **b:** OCR in CAF and NF cell lines in comparison with that of MCF7 cancer cell line. OCR was normalised to cell number. **c:** OCR of iNFs 24h after transfection with siCtl or siPDK2 and knockdown efficiency as measured by RT-qPCR. OCR was normalised to cell number. PDK2 mRNA was normalised to GAPDH.

Mean and SEM of 3 independent experiments are shown. Significance was calculated using a student's t-test: * $p \leq 0.05$, ** $p \leq 0.01$, *** $p \leq 0.001$

4.3 ATP-citrate lyase is active in CAFs

Acetyl-coA cannot traverse the mitochondrial membrane by itself. The most common way for acetyl-coA to leave the mitochondria is via conversion to citrate, which crosses the mitochondrial membrane via the transporter SLC25A1. Once outside the mitochondria, citrate can be converted back to acetyl-coA by ACLY, which is present both in the cytosol and the nucleus. ACLY is active when phosphorylated on S455 (Potapova et al., 2000). Interestingly, phosphorylation of this site is known to be stimulated by PI3K/Akt signalling, which I found to be a possible upstream pathway regulating PDK2 expression in the previous chapter. This means increased PI3K/Akt signalling in CAFs could doubly enhance acetyl-coA production by both activating PDH and ACLY. I therefore assessed the activation status of ACLY by western blot of lysates from all the CAF and NF cell lines using an antibody against phospho-ACLY (Fig. 4-15). ACLY was more phosphorylated in the iCAF3s and pCAF2s than in their respective NFs, but phosphorylation was decreased between pCAF3 and pNF3. However, this experiment showed that ACLY is more active in two out of the three CAF cell lines I am using, and that activated ACLY is present in all the cell lines, meaning that acetyl-coA exported out of the mitochondria as citrate can be converted back to acetyl-coA in the cytosol and nucleus.

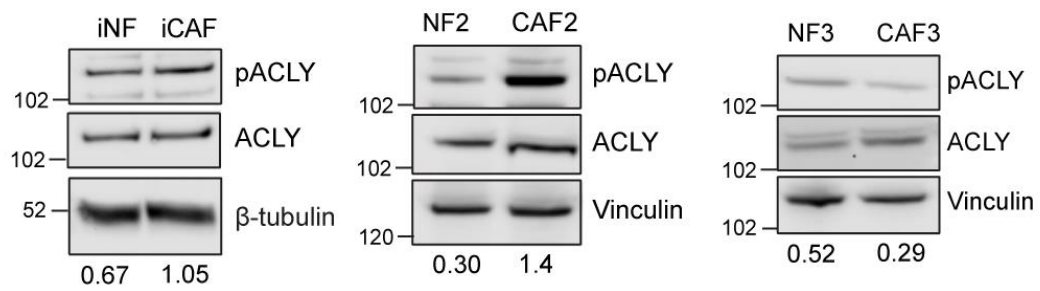


Figure 4-15 p-ACLY levels in NFs and CAFs

Western blot showing levels of phosphorylated and total ACLY in CAFs and NFs. Vinculin and β -tubulin were used as a loading control, and pACLY levels were further normalised to total ACLY levels. Molecular weight markers are shown next to the blots. pACLY quantification is shown under the blots. Representative images of $n \geq 2$ biological replicates are shown

4.4 PDH derived acetyl-coA is not used to fuel increased lipid synthesis

Once outside the mitochondria, acetyl-coA can be used to fuel a variety of metabolic pathways, including synthesis of sterols and fatty acids. There was some evidence from previously acquired proteomic data of the iCAFs and iNFs that several proteins in the cholesterol synthesis pathway were upregulated in iCAFs, so initially I investigated the possibility of increased cholesterol synthesis in CAFs. I labelled the iCAFs and iNFs for 48h with media containing both $^{13}\text{C}_6$ -glucose and $^{13}\text{C}_5$ -glutamine to maximise the amount of labelled carbon being incorporated into cholesterol. Then, in collaboration with Grace McGregor from Dr. Jurre Kamphorst's group, the lipids were extracted from the fibroblasts and the heavy carbon incorporation was detected by GC-MS. We were unable to see any label incorporation in either the iCAFs or the iNFs, and furthermore there was no increase in the total amount of cholesterol in the iCAFs (Fig. 4-16a). In fact, there was slightly more cholesterol in the iNFs. This experiment therefore ruled out the possibility of acetyl-coA fuelling increased cholesterol synthesis in the CAFs.

The next question to be addressed was whether the extra acetyl-coA in the CAFs was being used for fatty acid synthesis. Once again, I labelled the iCAFs and iNFs for 48h with media containing either $^{13}\text{C}_6$ -glucose or $^{13}\text{C}_6$ -glucose and $^{13}\text{C}_5$ -glutamine and in collaboration with Grace McGregor extracted the lipids and determined the label incorporation into palmitate, oleate and stearate, using GC-MS. There was an extremely low rate of incorporation of both glucose and glutamine into the fatty acids, and, as with the cholesterol, there was no detectable incorporation or increase in the total amount of metabolite in the iCAFs (Fig. 4-16b). In fact, I saw a slight decrease in the percentage of the fatty acids labelled in the iCAFs compared to the iNFs. Therefore it does not seem that the increase in acetyl-coA produced by PDH in CAFs is used to fuel increased lipid synthesis.

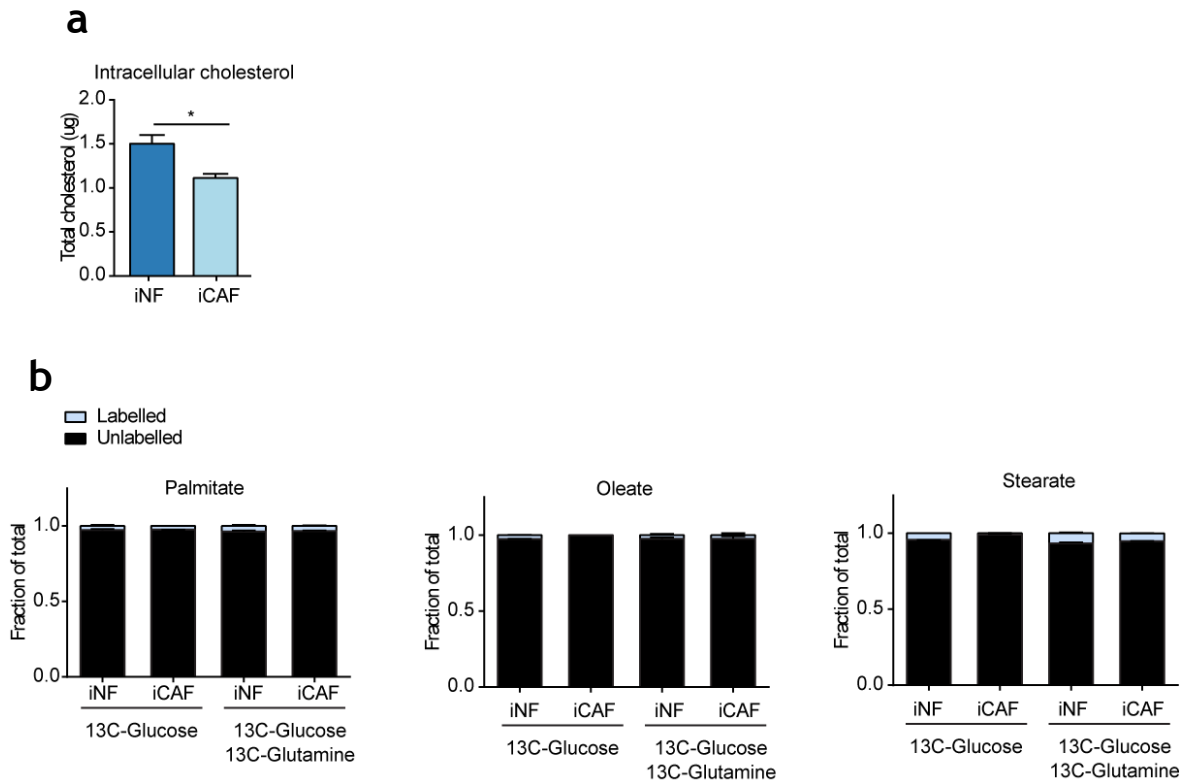


Figure 4-16 Lipid metabolism in iNFs and iCAFs

a: Total intracellular cholesterol in iNFs and iCAFs. **b:** Fraction of intracellular fatty acids labelled with either ^{13}C -glucose or ^{13}C -glucose+ ^{13}C -glutamine after 48h of labelling in iNFs and iCAFs.

Significance was calculated using a student's t-test with Welch's correction: * $p \leq 0.05$, ** $p \leq 0.01$, *** $p \leq 0.001$

4.5 Histones are more acetylated in iCAFs

Acetyl-coA is the substrate for acetylation of lysine residues on proteins. In the mitochondria, where the concentration of acetyl-coA is abnormally high and the environment is alkaline, proteins can be autoacetylated dependent on the amount of acetyl-coA present (Weinert et al., 2014). Outside the mitochondria, higher levels of acetyl-coA can stimulate acetyltransferase enzymes to increase protein acetylation (Choudhary et al., 2014). Acetylation is a common translational modification, and it is increasingly recognised that acetylation has significant impacts on protein functionality. Therefore changes in protein acetylation could have wide ranging effects on the CAF phenotype.

To investigate whether there were differences in protein acetylation between CAFs and NFs, I used MS-proteomics to study the acetylomes of SILAC labelled iCAFs and iNFs. Because such a small fraction of the total proteome is modified, the samples had to be enriched for acetylated peptides. After digesting the lysates from the fibroblasts, agarose beads conjugated to an antibody against acetylated lysine residues were used to bind the acetylated peptides. After eluting the acetylated peptides, the samples were analysed by mass spectrometry using a Q-Exactive HF. MaxQuant software (Cox and Mann, 2008) was used to identify the peptides discovered by the mass spectrometry with the addition of Acetyl(K) as a variable modification, and Perseus software (Tyanova et al., 2016) to carry out statistical analysis on the data. Data from three independent experiments, two of which was carried out by a visiting student, Claudia Boldrini, was analysed in which for each experiment both forward and reverse labelled fibroblasts (i.e. heavy CAFs with light NFs and light CAFs with heavy NFs) were analysed, giving a total of four experiments. The \log_2 SILAC ratios of the acetylated peptides were normalised to the \log_2 SILAC ratios of the total protein in order to normalise for differences in protein levels between iCAFs and iNFs. Acetylation sites that were identified in at least two experiments were considered for the analysis. From a one-sample t-test analysis of the data, there were no significant differences in acetylation between iCAFs and iNFs. However, there was a trend towards histones being more acetylated in the iCAFs (Fig. 4-17). The identified proteins were further annotated with the gene ontology pathways for biological process, cellular compartment and molecular function. A one dimension enrichment analysis (Cox

and Mann, 2012) of the acetylation sites revealed that many of the categories with significantly upregulated acetylation in CAFs were related to histones, histone modifications and the nucleus, further supporting the increase in histone acetylation in the iCAF (Fig. 4-18).

Post translational modification of histones, and particularly on histone tails, is a major epigenetic factor determining which genes are transcribed into mRNA. Although modification of different sites can impact transcription differently, in general, histone acetylation is a marker of increased transcriptional activation. This is thought to be because acetylation of lysine residues neutralises the positive charge on lysine, which normally binds strongly to the negatively charged DNA (Margueron et al., 2005). Thus acetylation frees DNA from being so tightly bound to histones and allows the transcriptional machinery to be recruited. An increase in histone acetylation in CAFs could therefore have an extremely important role in activating transcription of genes required to maintain the activated CAF phenotype.

To see if any of the upregulated histone acetylation sites were known to be involved in regulating transcription, I annotated the dataset using the PhosphoSite Plus database (<https://www.phosphosite.org/homeAction.action>), which is a repository for information on post translational modifications and how they affect protein function. According to this annotation, there were only a few acetylation sites identified in my data which have a known and verified functional impact on a protein (Fig. 4-19). Of these, the only upregulated histone acetylation site was H3K27ac. Acetylated H3K27 is a well characterised marker of activated transcription, and has been shown to be present at 'super enhancer' regions on chromatin (Raisner et al., 2018, Sen et al., 2019). I therefore chose to further investigate the regulation of H3K27 acetylation in relation to PDH activity in CAFs.

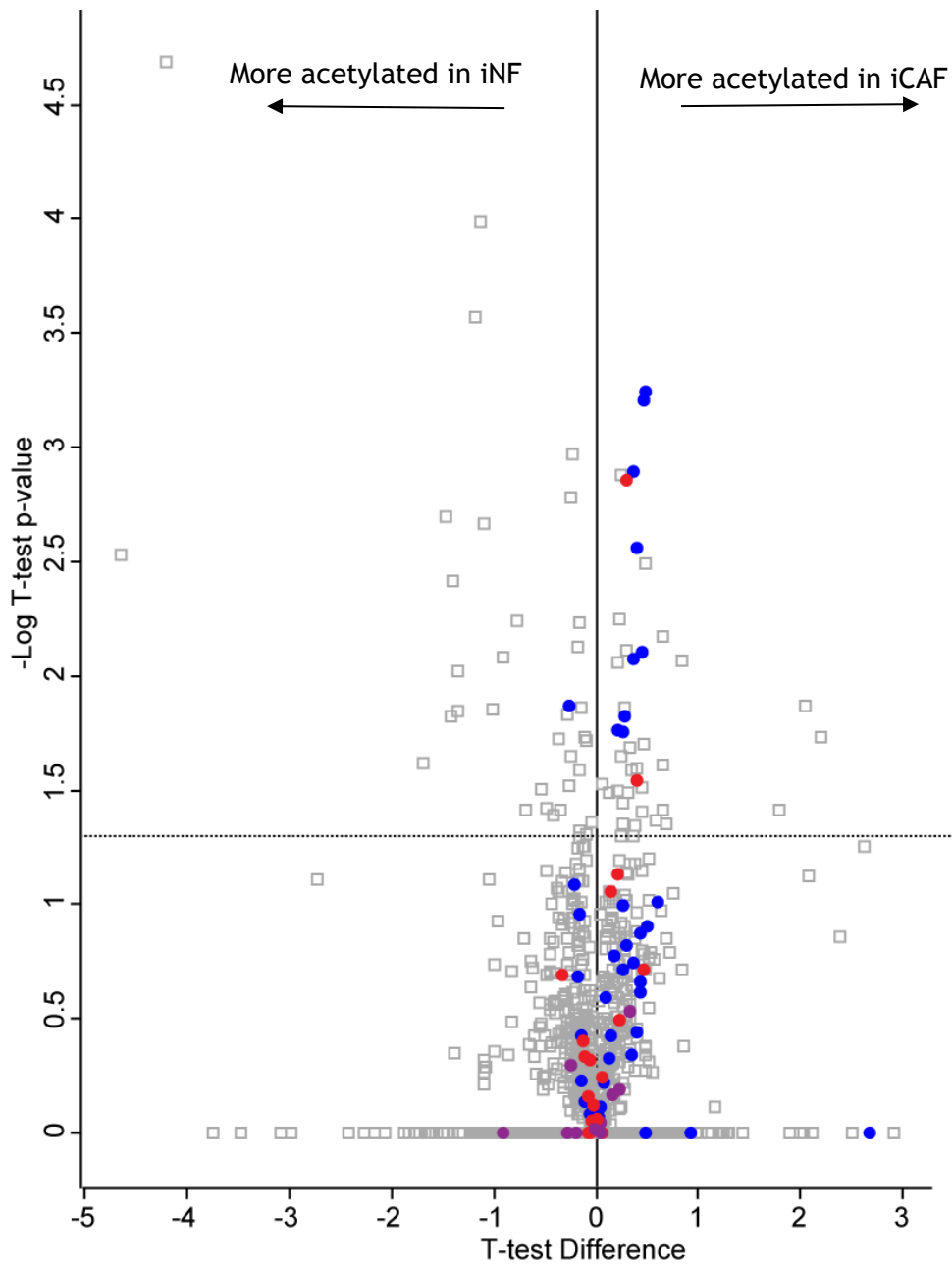


Figure 4-17 iCAF vs iNF acetylome

Volcano plot of a one-sample t-test showing regulation of acetylated peptides in iCAFs compared to iNFs. The x axis indicates the \log_2 SILAC ratio CAF/NF. Each point represents one acetylated peptide. Points above the dotted line have a p value < 0.05. Histone acetylation sites are coloured as follows: **Histone 2**, **Histone 3**, **Histone 4**. Results from 3 independent SILAC experiments with both forward and reverse labelling were used in the analysis

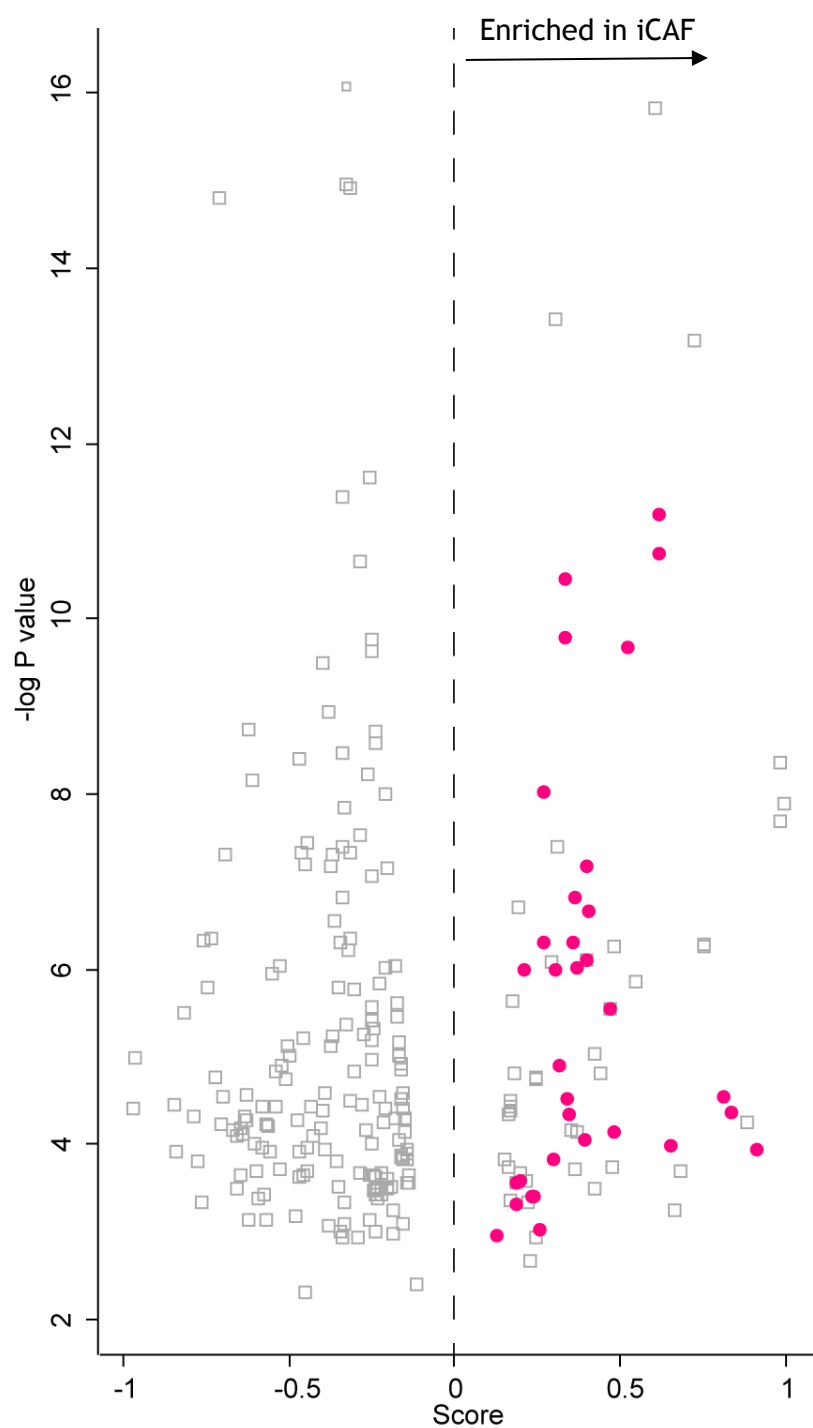


Figure 4-18 One-dimension enrichment analysis of acetylome data

Acetylated proteins were annotated using the gene ontology database and a 1D-enrichment analysis was performed using the annotations. Plot shows significantly enriched and depleted annotations (FDR < 2%) in the dataset. Annotations relating to histones and histone modifications are highlighted in pink.

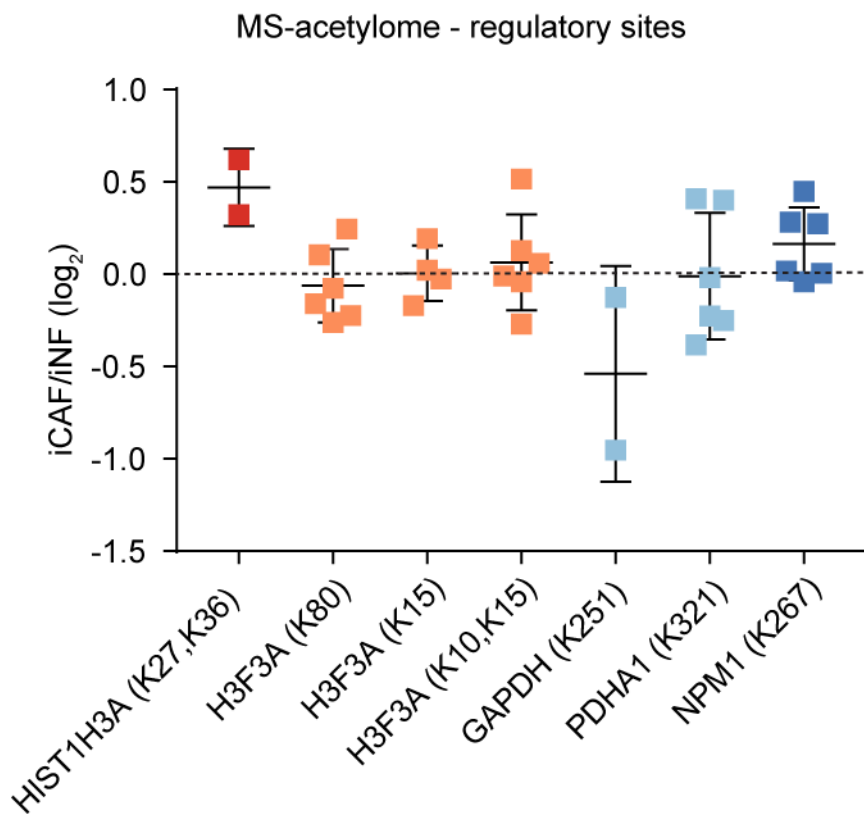


Figure 4-19 Regulatory acetylated sites

Graph shows the log₂ CAF/NF SILAC ratios for acetylated peptides with a known regulatory function identified in the acetylomes of iCAFs and iNFs. Error bars indicate the mean and SEM.

4.6 H3K27 acetylation is regulated by PDH dependent acetyl-coA production

4.6.1 H3K27 is more acetylated in CAFs than NFs

In order to verify the results of the MS-acetylome data of the iCAF and iNF, I confirmed the upregulation of H3K27 acetylation by Western blot using lysates from all the CAF and NF cell lines. All the CAFs had increased H3K27ac levels compared to their respective NFs (Fig 4-20).

4.6.2 H3K27 acetylation is regulated by acetyl-coA availability

Histone acetylation is known to be regulated by the amount of acetyl-coA available in the cytosol and nucleus. ACLY is the main route of export of acetyl-coA from the mitochondria via citrate, and ACLY expression has been shown to influence histone acetylation (Wellen et al., 2009). I had previously shown that ACLY is active in CAFs and that CAFs incorporate a higher proportion of glucose into citrate, therefore I investigated the role of ACLY activity in histone acetylation. To show that export of acetyl-coA from the mitochondria was necessary for H3K27 acetylation in the CAFs, I used an inhibitor against ACLY to prevent exported citrate from being converted back to acetyl-coA outside the mitochondria: BMS303141 (Li et al., 2007). To determine the effectiveness of the drug I used MS-metabolomics to demonstrate that BMS303141 caused an accumulation of citrate in CAFs. The iCAF were treated with 10 or 50 μM BMS303141 in media with $^{13}\text{C}_6$ -glucose for 48h. The intracellular metabolites were then harvested and analysed by LC-MS. (Fig. 4-21a). The peak area was normalised to protein content of the fibroblasts for each samples. The metabolomics data clearly showed an accumulation of labelled citrate in the BMS303141 treated iCAF, implying that the ACLY inhibitor was working because the acetyl-coA was being converted into citrate but was then unable to undergo conversion back to acetyl-coA. There was little effect with the 10 μM dose but a significant effect with the 50 μM dose so I used 50 μM BMS303131 in the following experiments.

To investigate the effect of ACLY inhibition of H3K27 acetylation, I treated CAFs with 50 μ M BMS303141 with or without 2 mM sodium acetate. Acetate can be used by cells as a source of nucleocytosolic acetyl-coA, because it is converted to acetyl-coA by ACSS (Acyl-CoA synthetase short-chain family member) enzymes. By giving the fibroblasts an exogenous supply of acetate I expected to rescue the effect of ACLY inhibition because the cells would still be able to synthesise acetyl-coA outside the mitochondria and use it for histone acetylation. After 48h of treatment, the CAFs were lysed and the levels of H3K27ac were determined by western blot (Fig. 4-21b). BMS303141 did indeed decrease the levels of H3K27ac, and this was rescued by additionally giving the CAFs sodium acetate. This experiment shows that H3K27 acetylation in the CAFs depends on the concentration of acetyl-coA outside the mitochondria.

4.6.3 PDH activity regulates H3K27 acetylation

I have shown that H3K27 acetylation is upregulated in CAFs, and is regulated by the presence of acetyl-coA outside the mitochondria. However, the impact of PDH activity on H3K27 acetylation was still unknown. To connect PDH activity to H3K27 acetylation, I modulated PDK2 expression in the CAFs and NFs to regulate PDH phosphorylation and activity. The iCAF_s were transfected with the enzymatically inactive PDK2^{N255A} or PDK2^{WT}. In contrast, the iNF_s were transfected with siCTL or siPDK2 to decrease PDH phosphorylation, then after 48h the fibroblasts were lysed and the levels of H3K27ac were analysed by western blot (Fig 4-22). PDK2^{WT} overexpression effectively reduced H3K27 acetylation compared to PDK2^{N255A} overexpression, and siPDK2 transfection increased H3K27 acetylation compared to siCtl. I also created shCtl and shPDK2 cell lines using the pNF2 cells by lentiviral transduction. The level of PDK2 knockdown was determined by RT-qPCR, and the shRNA which gave the most efficient knockdown was used for the experiments. By western blot analysis of shCtl and shPDK2 cell lysates, shPDK2 both decreased PDH phosphorylation and increased H3K27 acetylation, in concordance with the siRNA knockdown of PDK2 (Fig. 4-23). Although the shPDK2 knockdown was not as effective as the siRNA knockdown, the level at which it altered PDH phosphorylation and H3K27 acetylation was similar, suggesting that a small change in PDK2 expression in the fibroblasts is sufficient to alter histone acetylation patterns.

In order to rescue the PDK2^{WT} phenotype, the iCAFs were treated with 2 mM sodium acetate, providing a cytosolic supply of the acetyl-coA precursor which could be used to maintain H3K27 acetylation. 48h after transfection with or without acetate treatment, the iCAFs were lysed and the levels of H3K27ac were analysed by western blot (Fig 4-24a). PDK2^{WT} overexpression effectively reduced H3K27 acetylation compared to PDK2^{N255A} overexpression, and this was rescued by the acetate treatment.

Conversely, to reverse the siPDK2 phenotype, the iNFs were treated with 25 μ M c646, which is an EP300 inhibitor. EP300 is a histone acetyltransferase (HAT) known to target H3K27 and has been shown to induce H3K27 acetylation at enhancer regions (Raisner et al., 2018). After 48h with or without c646 treatment, the iNFs were lysed and the levels of H3K27ac were analysed by western blot (Fig 4-24b). The inhibitor c646 reduced PDH activity-induced H3K27 acetylation, as predicted. Therefore acetyl-coA produced by PDH is required for the increase in histone acetylation in CAFs, and modulates H3K27 acetylation. Furthermore I could rescue the effects of modulating PDH activity in the fibroblasts on histone acetylation with either acetate or pharmacological inhibition of c646, which provided me with a good experimental system to further investigate the phenotypic effects of increased PDH activity in the CAFs.

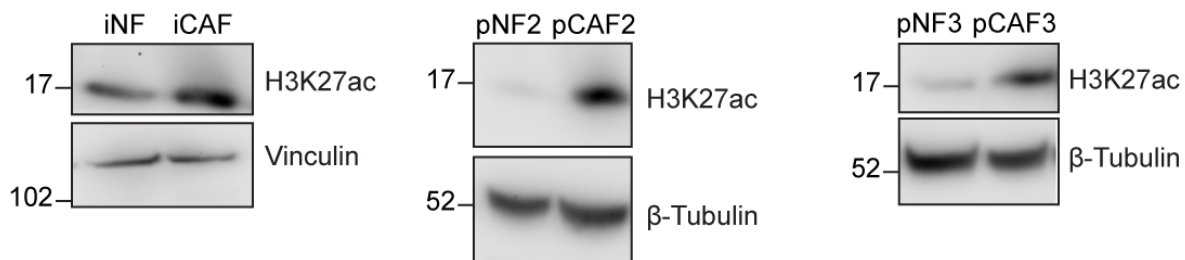


Figure 4-20 H3K27 is more acetylated in CAFs

Representative western blots from $n \geq 2$ independent experiments showing that all CAF cell lines have increased histone acetylation at H3K27 compared to their paired NFs. Vinculin and β -tubulin antibodies were used as a loading control. Molecular weight markers are shown next to the blots.

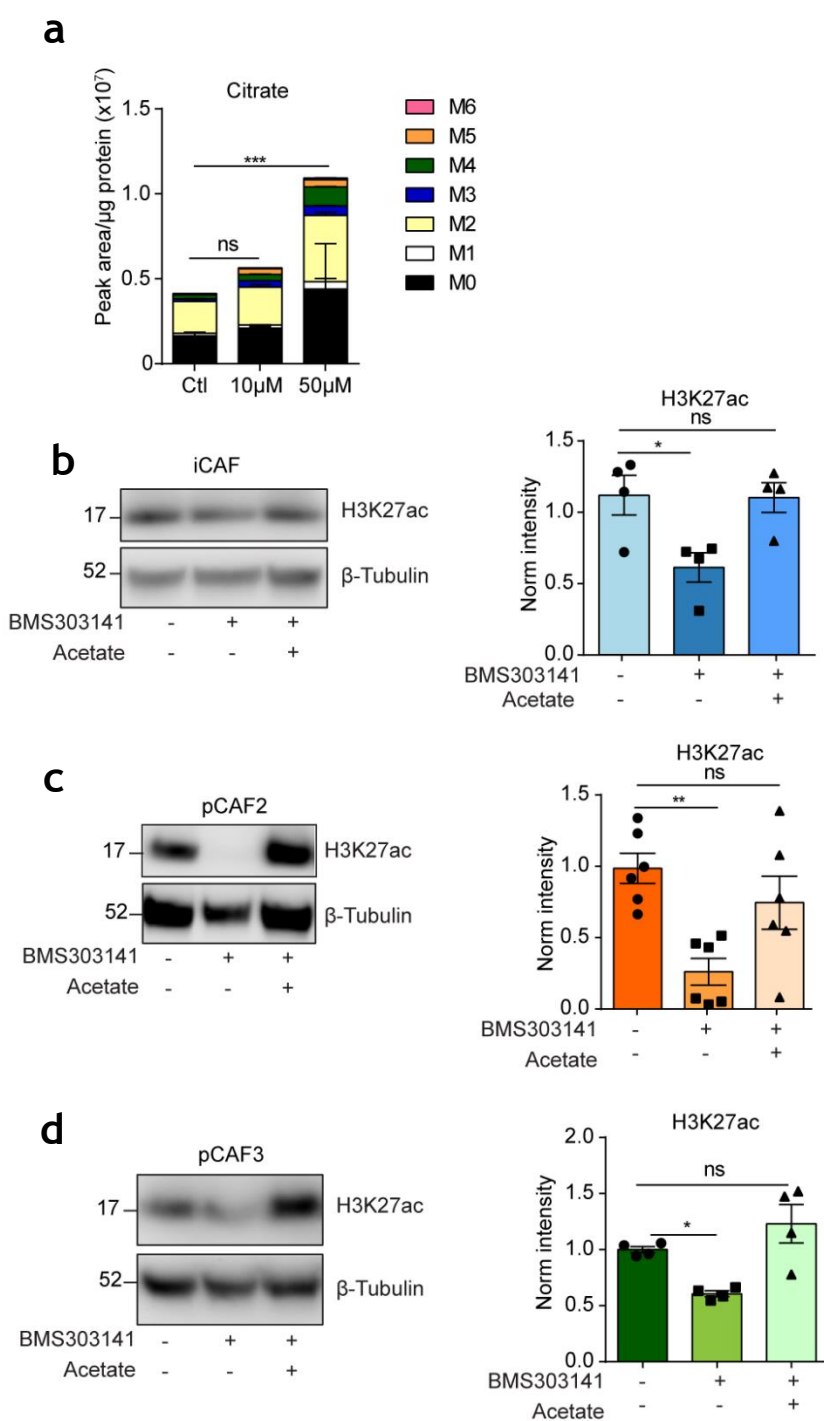
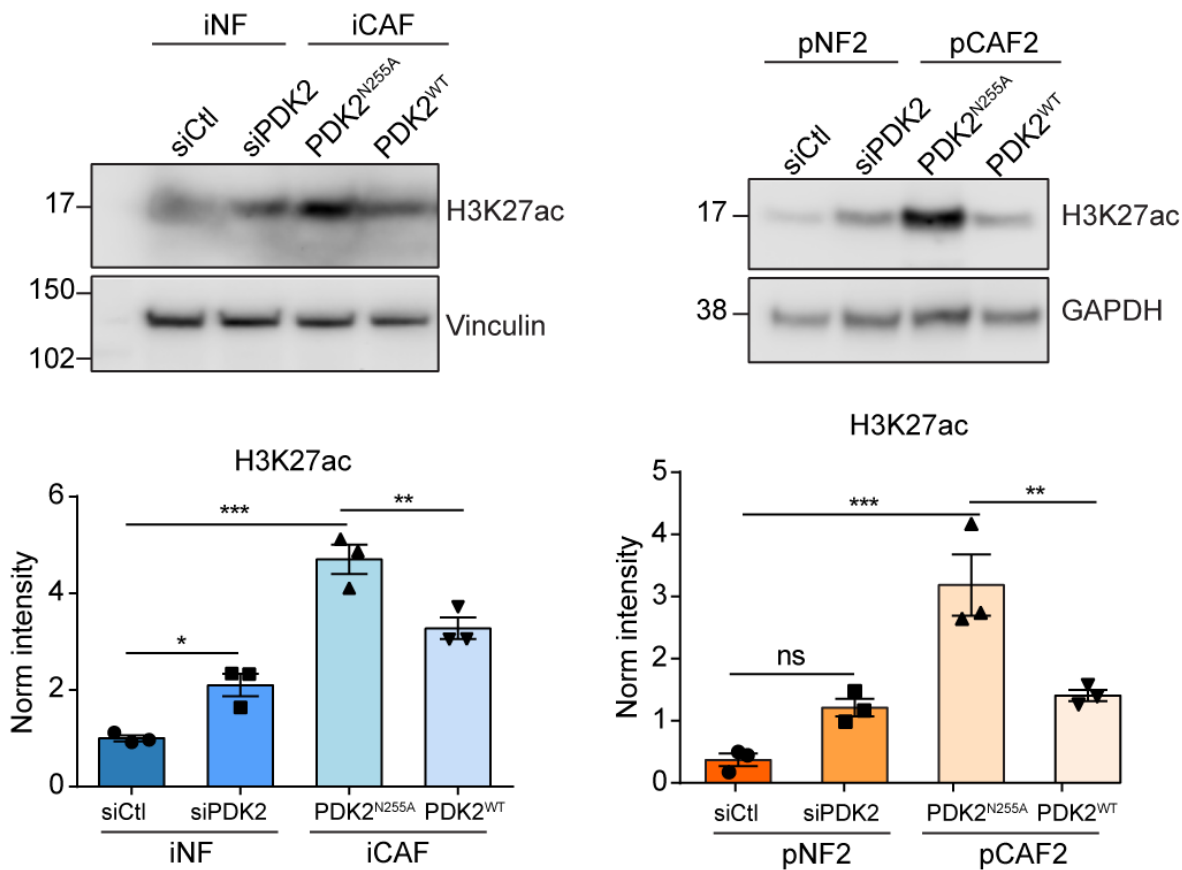


Figure 4-21 H3K27 acetylation is regulated by ACLY inhibition

a: Total citrate with ^{13}C -glucose label incorporation in iCAFs after 48h treatment with DMSO control, 10 μM or 50 μM BMS303141. Graph shows the mean and SEM of 3 experiments. **b,c,d:** Representative western blots and quantification of H3K27ac in iCAFs, pCAF2s and pCAF3s respectively treated with 50 μM BMS303141 +/- 2 mM acetate. β -tubulin was used as a loading control. Molecular weight markers are shown next to the blots. Graphs show the mean and SEM of at least 4 independent experiments. Significance was calculated using one-way ANOVA with Dunnett's multiple comparisons test: * $p \leq 0.05$, ** $p \leq 0.01$, *** $p \leq 0.001$



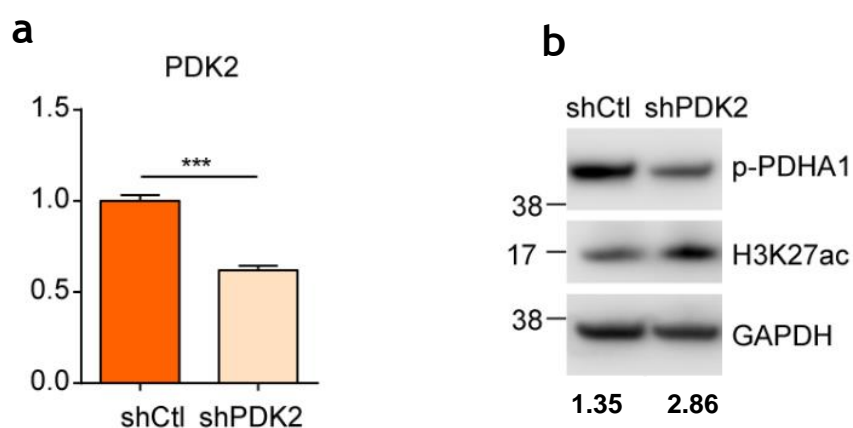


Figure 4-23-shPDK2 increases H3K27 acetylation

a. qPCR for PDK2 expression in shCtl and shPDK2 pNFs. PDK2 mRNA was normalised to 18S mRNA. Graph shows the mean and SEM of 3 independent experiments. Significance was calculated using one-way ANOVA with Dunnett's multiple comparisons test: * $p \leq 0.05$, ** $p \leq 0.01$, *** $p \leq 0.001$. **b.** Western blots of pPDHA1 and H3K27ac in shCtl/shPDK2 pNFs. Quantification of H3K7ac is shown under the blots. GAPDH was used as a loading control. Molecular weight markers are shown next to the blots. Representative image of 2 independent experiments shown.

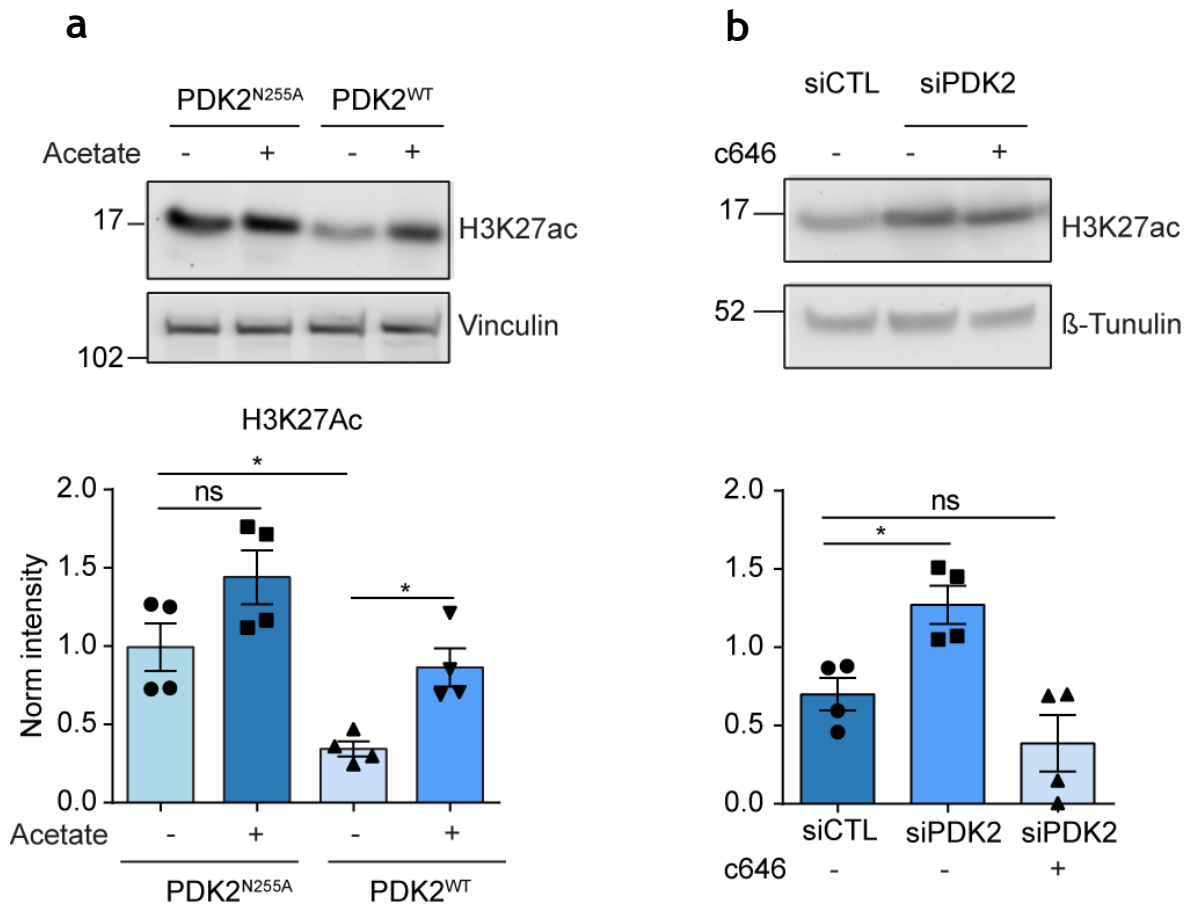


Figure 4-24 H3K27 acetylation is regulated by PDK2 expression

Representative western blots and quantification of H3K27ac in **a**. iCAFs/iNFs and **b**. pCAF2s/pNF2s transfected with siCTL/siPDK2 or PDK2^{N255A}/PKD2^{WT} and treated with 2 mM acetate or 25 μ M c646. Vinculin or β -tubulin was used as a loading control. Molecular weight markers are shown next to the blots. Graphs show the mean and SEM of 4 independent experiments. Significance was calculated using one-way ANOVA with Dunnett's multiple comparisons test: * $p \leq 0.05$, ** $p \leq 0.01$, *** $p \leq 0.001$

4.7 Discussion

In this chapter I set out to discover what the purpose of the increase in intracellular acetyl-coA produced by PDH in CAFs was. Because the majority of pathways involving acetyl-coA are related to metabolism, I first investigated metabolic differences between CAFs and NFs. I was expecting there to be differences in mitochondrial metabolism because I had demonstrated that PDH was localised in the mitochondria, and because PDH had been shown in previous studies to be a key metabolic enzyme controlling entry of glycolysis-derived metabolites to the TCA cycle to support its activity (Kaplon et al., 2013, McFate et al., 2008, Michelakis et al., 2008, Randle, 1986). For this reason, it has been named the 'mitochondrial gatekeeper' (Saunier et al., 2016). Initial experiments showed that there were no differences between CAFs and NFs in the uptake and secretion of four major metabolites: glucose, lactate, glutamine and glutamate. These are the main metabolic sources controlling flux through glycolysis and the TCA cycle. Further metabolic analysis of the CAFs and NFs using MS-metabolomics revealed that there were very few consistent metabolic differences between CAFs and NFs. This was surprising as there are many studies showing that CAFs are reprogrammed metabolically to produce metabolites which fuel tumour cell growth and invasion. However, these studies also highlight the high level of heterogeneity in CAFs. This is consistent with the literature since studies from different tumour types and tissues have discovered different metabolic pathways contributing to the pro-tumourigenic phenotype of the CAFs and their cross talk with the cancer cells. For example, Yang et al. have demonstrated that glutamine and glutamate production is a key metabolic cross talk pathway between ovarian CAFs and cancer cells (Yang et al., 2016), whereas studies in pancreatic cancer have shown that alanine secretion by pancreatic stellate cells, which are the cells that CAFs originate from in the pancreas, is a vital pathway to produce fuel for the cancer cells under nutrient deprived conditions (Sousa et al., 2016, Serrao et al., 2016). Conversely, my mammary CAFs showed increased total levels of proline and asparagine compared to their paired NFs as well as increased production of N-acetylaspartate, none of which have been previously been reported to be upregulated in CAFs. Both asparagine and N-acetylaspartate are products of aspartate metabolism, levels of which were also upregulated in the pCAF cell lines. Since the production of aspartate involves conversion of glutamate to α -KG,

aspartate production could be increased in order to maintain α -KG levels, which were also higher in the CAFs. Since neither asparagine nor N-acetylaspartate can, so far as we know, be used for further metabolic reactions, these metabolites could then be a means of storing the excess aspartate without affecting other metabolic pathways.

However, two themes of CAF metabolism which have been reported in CAFs from several tissues, including breast, is that CAFs are more glycolytic and autophagic (Bonuccelli et al., 2010, Guido et al., 2012, Whitaker-Menezes et al., 2011b, Pavlides et al., 2012, Zhang et al., 2015). None of my extensive metabolic profiling of the CAFs and NFs suggested that the CAFs were more glycolytic than the NFs. As many of the experiments showing that mammary CAFs upregulate glycolysis were done using co-cultures of CAFs and cancer cells (Martinez-Outschoorn et al., 2010a, Whitaker-Menezes et al., 2011b, Martinez-Outschoorn et al., 2010b, Martinez-Outschoorn et al., 2011b), one possibility is that I would need to co-culture my CAFs with cancer cells to see an upregulation in glycolysis. Furthermore, other studies have shown that there is variation in whether mammary CAFs are predominantly glycolytic or oxidative depending on the tumour they are derived from, so it is possible that I derived CAFs from tumours where glycolysis was not upregulated in the stroma (Choi et al., 2013). All of my CAFs and NFs however appear to be highly glycolytic cells as there is little incorporation of glucose into the TCA cycle metabolites from the metabolomics data and the oxygen consumption rate was lower than that of cancer cells, suggesting that fibroblasts in general rely more on glycolysis than oxidative phosphorylation.

While I was investigating mitochondrial differences between the mammary CAF and NF cell lines I did however discover that there were differences in mitochondrial functionality between CAFs and NFs. CAFs had decreased levels of functional mitochondria, decreased mitochondrial capacity and increased autophagic flux compared to NFs. As mentioned previously, several studies have shown that CAFs are more autophagic and that the products of autophagic breakdown are used to fuel tumour cells. For example, Lisanti et al. showed that in co-culture with breast cancer cells, fibroblasts experienced increased oxidative stress and upregulated autophagy and mitophagy via caveolin-1 downregulation (Martinez-Outschoorn et al., 2010a), providing tumour cells with metabolites such

as lactate and ketones. It is interesting to note that in data generated in our lab from proteomic analyses on the iCAFs and iNFs and on the pCAFs and pNFs, caveolin-1 is indeed downregulated in CAFs compared to NFs, suggesting that a similar autophagic pathway could be active in the CAFs used for my studies, although I do not see a corresponding increase in lactate secretion. Dysfunctional mitochondria can be degraded through mitophagy. However, the total levels of mitochondria were consistent between the iCAFs and iNFs, suggesting the dysfunctional mitochondria are not being degraded. This has a possible link to the downregulation of PDK2 in CAFs, as PDK2 has been shown to phosphorylate PARL to stimulate mitophagy. When PDK2 was knocked down in the iNFs, I did not observe the decrease in mitochondrial capacity that I had seen in the iCAFs, however this was a transient knockdown for only 48h and it would be interesting to investigate whether stable knockdown of PDK2 in NFs would decrease mitochondrial capacity in the long term, as this would suggest that it was involved in a mitophagy related pathway.

Despite there being some differences in mitochondrial functionality between CAFs and NFs, I could not find any evidence that the increase in acetyl-coA produced by CAFs was used to increase flux through the TCA cycle. The majority of TCA cycle metabolites were derived from glutamine as shown by metabolic tracing experiments, and apart from citrate there was minimal label incorporation from heavy glucose into TCA cycle metabolites. Furthermore, there was no difference in OXPHOS under basal conditions between CAFs and NFs as shown by the Seahorse analysis, and altering PDH activity by knocking down PDK2 in NFs had no effect on oxygen consumption. Therefore I can conclude that PDH activity does not affect the TCA cycle in the fibroblasts. It is unclear why glucose is incorporated into citrate in both CAFs and NFs, but then makes a minimal contribution to other TCA cycle metabolites. One possibility is that the fibroblasts have a low isocitrate dehydrogenase activity, which would mean that α -ketoglutarate is synthesised mainly from glutamine and is converted through the TCA cycle to citrate, where it is blocked from re-entering the TCA cycle. This could explain why the fibroblasts also have a generally low oxygen consumption rate. Proliferating fibroblasts have previously been shown to have low IDH activity (Lemons et al., 2010). Mitochondrial IDH can be inhibited by acetylation (Zou et al., 2017), however the regulatory site was not identified in my analysis of the acetylomes of the iCAFs

and iNFs. IDH3 downregulation has been reported previously in CAFs as a means to maintain CAF activation through TGF- β and HIF-1 α signalling (Zhang et al., 2015), however, this does not account for the decrease in citrate conversion to α -KG that I also see in the NFs. Therefore, if mitochondrial IDH is downregulated in fibroblasts, the mechanism is yet to be elucidated. It would be interesting to compare the relative activities of citrate synthase and IDH between the fibroblasts and a cell line such as the MCF7 cells which are known to have a functioning TCA cycle.

Since I did see an increase in intracellular citrate labelled by glucose in the CAFs and also significant label incorporation into acetyl-carnitine, both of which are means of exporting acetyl-coA out of the mitochondria, I hypothesised that the acetyl-coA produced by PDH had a cytosolic role. Acetylcarnitine can cycle in and out of the mitochondria, and although it has mostly been studied as a means of transferring acetyl-coA groups derived from beta-oxidation of fatty acids into the mitochondria, it has also been shown to be a means of removing excess acetyl-coA from the mitochondria in order to maintain a steady rate of TCA cycle metabolism. Citrate on the other hand is well known to be the main route of acetyl-coA export from the mitochondria. I demonstrated that ACLY was phosphorylated and therefore active in all the CAF cell lines and furthermore was more phosphorylated than the respective NFs in two out of three pairs. Inhibiting ACLY pharmacologically in the iCAF s caused significant accumulation of glucose-labelled citrate, which must be derived from acetyl-coA, demonstrating that citrate is an important route of acetyl-coA export from the mitochondria.

I therefore investigated the roles of acetyl-coA outside the mitochondria. Metabolically, acetyl-coA is used for lipid synthesis in the cytosol. However, by carrying out further metabolic tracing experiments in the iCAF s and iNF s it was clear that fatty acid and cholesterol synthesis in the fibroblasts is minimal and there is no difference in the rate of synthesis between CAFs and NFs. This is perhaps unsurprising given that the fibroblasts I am using are all derived from mammary tissue, which has a particularly high fat content. Therefore it is unlikely that in a breast tumour these CAFs would need to increase lipid synthesis since they are probably able to take up everything they need from their microenvironment. The increase in acetyl-coA produced by PDH in CAFs does not

seem to be contributing to any metabolic pathways in the CAFs; neither for oxidative phosphorylation in the mitochondria nor for lipid synthesis in the cytosol.

The other major use for acetyl-coA is for protein acetylation. Protein acetylation was first studied in the context of histones, where it generally activates gene transcription by altering chromatin folding to open up DNA for transcription machinery binding and acting as a marker for recruitment of bromodomain containing transcription factors, acetyltransferases, and chromatin remodelling factors. Acetyl-coA availability and concentration has been shown to be a rate limiting factor for histone acetylation (Cai et al., 2011, Galdieri and Vancura, 2012). For example, acetyl-coA production by ACLY, which as I previously discussed is activated in my CAF cell lines, has been shown to be required to link growth factor signalling to regulation of gene expression by histone acetylation (Wellen et al., 2009). However, acetylation has more recently been shown to also be an important post translational modification outside of the nucleus. 63% of mitochondrial proteins contain acetylation sites, and it has been shown that increased concentrations of acetyl-coA in mitochondria causes increased acetylation of proteins (Weinert et al., 2014). Moreover, acetylation can regulate the activity of mitochondrial metabolic enzymes such as succinate dehydrogenase (Cimen et al., 2010). Cytosolic proteins have also been shown to be regulated by acetylation; for example, acetylation of cytoskeletal proteins such as actin can increase fibre stability (Kim et al., 2006b). I therefore wanted to analyse the entire acetylome of the iCAF and iNF and not just histones.

The most accurate method of quantifying global changes in post translational modifications in an unbiased manner is through mass spectrometry (Witze et al., 2007). Using an IP enrichment for acetylated peptides to enable quantification of acetylation sites I analysed the acetylomes of SILAC labelled iCAF and iNF. This revealed a general upregulation of histone acetylation in the iCAF. There was no overall increase of acetylation of mitochondrial proteins in the iCAF, further supporting my previous data showing that acetyl-coA produced by PDH does not affect the mitochondria and that acetyl-coA is preferentially exported out of the mitochondria in CAFs via ACLY. Other nuclear proteins also showed an increase in acetylation in CAFs, including nucleoporins, splicing factors, transcription factors

including BRD8 and the histone acetyl-transferase CREBBP. Of interest, cytoskeletal proteins and ECM proteins including actin, filamin, fibronectin, collagen and myosin 9 showed a trend towards being less acetylated in CAFs. This could indicate increased cytoskeletal turnover since acetylation of cytoskeletal proteins has been shown to increase fibre stability. Glycolytic enzymes such as ALDOA, ENO1 and G6PD also showed decreased acetylation in CAFs. Acetylation of glycolytic enzymes has previously been shown to be inhibitory (Liu and Shyh-Chang, 2017, Nakayasu et al., 2017), which would suggest that the enzymes are more active in CAFs, however, as discussed previously I was unable to discover any significant increase in glycolysis in CAFs. That being said, there is a slight increase in total intracellular glyceraldehyde-3-phosphate and phosphoenolpyruvate, which are produced by ALDOA and ENO1 respectively. G6PD catalyses the first step in the pentose phosphate pathway, however, I did not investigate the production of pentose phosphate metabolites in my experiments so whether the acetylation of this enzyme has a functional output is unknown.

Acetylation is not so well characterised as post translational modifications such as phosphorylation; however, there were few acetylation sites identified in my dataset which have a characterised regulatory function. Of these, the only site upregulated in CAFs was H3K27, which is a hallmark of activated transcription and is found at enhancer regions in chromatin. I demonstrated that H3K27 acetylation is indeed upregulated in all my CAF cell lines compared to their respective NF partners. Acetylation of H3K27 was also dependent on PDH activity in fibroblasts, as regulated by PDK2-mediated phosphorylation, and was further dependent on export of PDH produced acetyl-coA out of the mitochondria via citrate and ACLY. H3K27 is a known target of the HAT EP300, and other sites known to be acetylated by EP300, such as H3K18 and H3K23 were also among the most highly acetylated in the iCAF. This suggests that EP300 activity is required for the increased histone acetylation in CAFs, and my data showed that indeed EP300 inhibition reversed the increase in H3K27ac mediated by PDK2 knockdown in fibroblasts.

Therefore in this chapter I have shown that the increase in acetyl-coA produced by PDH in CAFs does not contribute towards metabolic pathways in CAFs but is instead channelled into increasing histone acetylation, and in particular acetylation of the transcriptional activator H3K27. In CAFs, then, PDH is not a

metabolic regulator but an epigenetic regulator, which is an understudied role of PDH. This could have major implications for how CAFs epigenetically regulate their pro-tumourigenic phenotype and therefore in the following chapter I set out to investigate the phenotypic effects of PDH induced histone acetylation on the CAFs.

Chapter 5 H3K27 acetylation regulates collagen production in CAFs

5.1 MS-proteomic analysis of c646 treated CAFs

Since histone acetylation is generally associated with transcriptional activation, I predicted that modulating histone acetylation levels would affect the proteome of the fibroblasts. As discussed in the previous chapter, the EP300 inhibitor c646 is known to target H3K27 acetylation and treatment of the iNFs with c646 was sufficient to reverse the effects of PDK2 knockdown on H3K27ac levels. Although other EP300 target sites were also regulated in the iCAF and iNF acetylomes, I focussed on H3K27ac as a readout for EP300 activity and histone acetylation since this site is the most highly associated with increased transcriptional activity. I therefore carried out a proteomic analysis of the iCAFs treated with c646 or DMSO control for 72 hours. The efficacy of EP300 on H3K27ac levels was assessed by western blot, which showed that c646 successfully reduced H3K27 acetylation in the iCAFs (Fig. 5-1). Lysates from three independent experiments of iCAFs cultured for 96h with or without c646 treatment were digested and the peptides were analysed using a Q-Exactive HF mass spectrometer. The relative amounts of each protein between samples was determined by label free quantification (LFQ) (Cox et al., 2014). In total, 5480 proteins were identified, and those that were quantified in at least two replicates were included in the analysis. A two tailed t-test analysis revealed that c646 treatment drastically altered the proteome of the iCAFs, in fact, 489 proteins were significantly regulated by c646 which is almost a tenth of the proteins identified. I then considered proteins that were downregulated by c646 treatment as potential candidates for genes regulated, directly or indirectly, by histone acetylation. Strikingly, extracellular matrix (ECM) proteins, especially collagens and fibronectin, were highly downregulated in the c646 treated CAFs (Fig 5-2). Collagen and ECM production is an extremely important aspect of the activated CAF phenotype, as CAFs are the main source of collagen in the tumour microenvironment. Upregulated collagen production by CAFs has been shown to be an important factor contributing to increased tumour growth, progression and metastases. In support of this, proteomic data of SDS soluble ECM derived from the iCAFs previously acquired in our lab showed that

collagens and fibronectin make up the majority of CAF-derived ECM, with collagens alone constituting 40% of the total ECM (Fig. 5-2). I therefore further investigated the regulation of collagen expression in CAFs by histone acetylation.

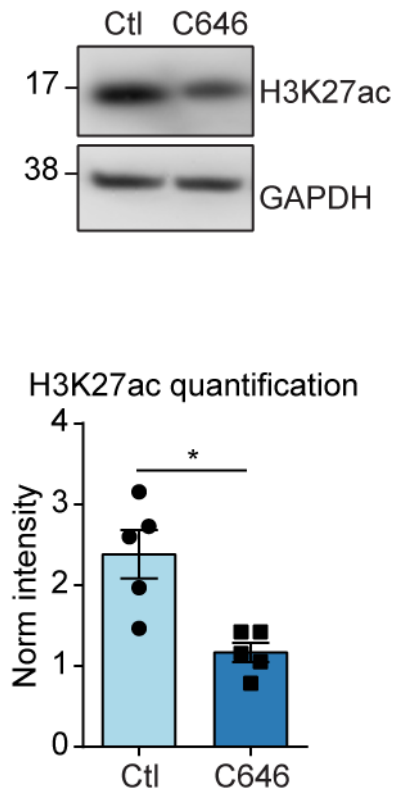


Figure 5-1 c646 reduces H3K27 acetylation

Representative Western blot and quantification of H3K27ac levels in iCAFs treated for 48h with 25 μ M c646 or DMSO control. GAPDH was used as a loading control. Molecular weight markers are shown next to the blots. Graph shows mean and SEM of 5 biological replicates.

Significance was calculated using an unpaired student t-test with Welch's correction: * $p \leq 0.05$

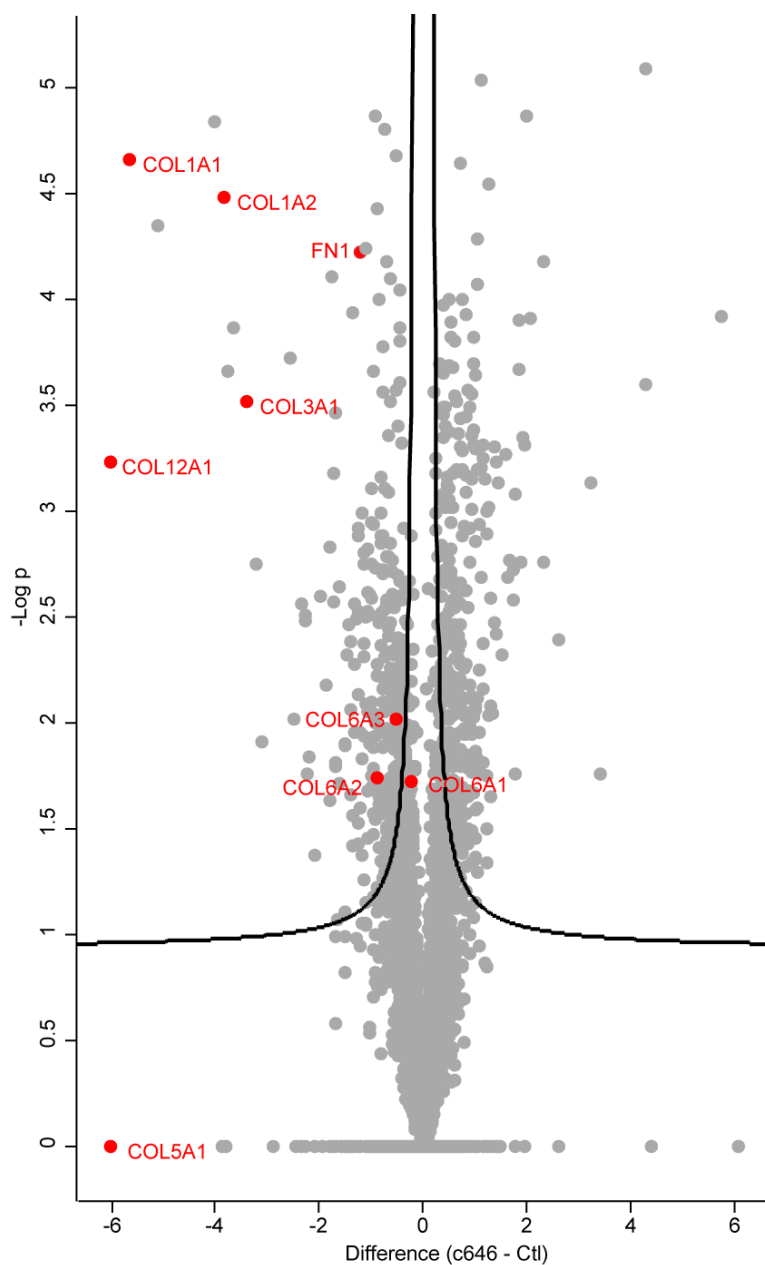


Figure 5-2 c646 downregulates collagen proteins

Volcano plot showing the results of a two-sample t-test comparing the proteomes of control and c646 treated i CAFs. Three independent experiments were included in the analysis. Each dot represents a protein. Proteins above the black line were classed as significantly regulated (cut-off values: $p=0.05$, $S_0=0.1$). All collagens identified in both proteomes are highlighted in red.

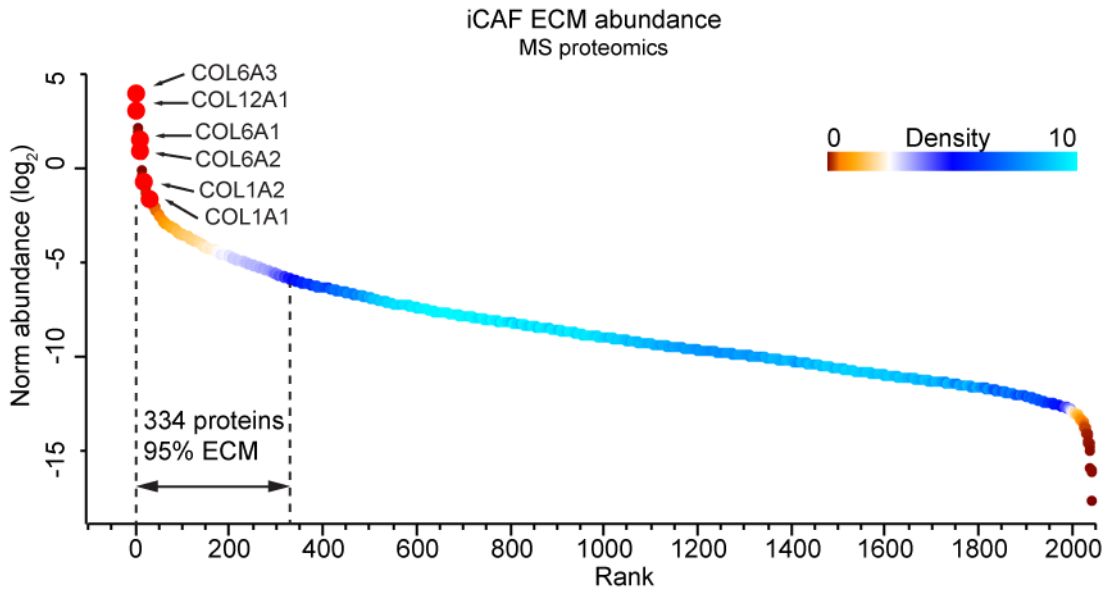


Figure 5-3 Collagens are highly abundant in iCAF ECM

Plot showing all the proteins identified by MS-proteomics in the iCAF ECM and their average abundance, ranked from most abundant to least abundant. Collagens VI, I and XII are highlighted as being among the 10 most abundant ECM proteins.

5.2 c646 regulates collagen expression in CAFs

To corroborate the results of the MS-proteomic data from iCAF treated with c646, I assessed the effects of c646 treatment on collagen expression at the mRNA and protein level. From the MS-proteome of the iCAF ECM, two of the most abundant collagens were collagen VI and collagen I, expression of both of which are known to be increased in breast cancer (Kauppila et al., 1998, Chen et al., 2013) and both of which were downregulated in the proteomes of c646 treated CAFs. Collagen VI is a mediator between the interstitial matrix and basement membrane and has been shown to stimulate tumour growth, angiogenesis and inflammation (Nissen et al., 2019, Chen et al., 2013). Collagen I is the classic structural collagen, with no imperfections in the Gly-X-Y repeats, and has been shown to promote tumour proliferation and metastasis in many tumour types including breast (Nissen et al., 2019). I therefore focussed on the expression of these two collagens in the following experiments. mRNA was extracted from CAFs treated with c646 or DMSO control for 72h and the expression of COL1A1 and COL6A1 was measured by RT-PCR. Both mRNAs were downregulated in both c646 treated iCAF and pCAF3s (Fig. 5-4). This showed that c646 controls collagen expression at the transcriptional level, and strongly points to a role for histone acetylation and particularly H3K27 acetylation in regulating Collagen I and Collagen VI expression.

To show that collagen in the CAF ECM is regulated by EP300 activity, I determined the levels of Collagen VI in ECM from CAFs by western blot analysis. CAFs were seeded at confluence and treated with c646 or DMSO control for 1 week. Subsequently, the CAFs were lysed and removed, leaving the cell-free ECM attached to the dish. The ECM was harvested and the proteins denatured and analysed by western blot (Fig. 5-5). Collagen VI was significantly depleted in ECM from c646 treated CAFs, showing that not only does c646 treatment reduce collagen mRNA expression within the CAFs, but it also affects its abundance in the ECM.

To further demonstrate that EP300 regulates collagen production by CAFs, I used fluorescent microscopy to visualise collagen in the ECM. I used a pan-collagen binding fluorescent protein: CNA35-mCherry. This protein has the advantage of binding all collagen proteins, rather than using an antibody against a specific

collagen, and also binds collagen in live cell cultures or in *in vivo* tissues (Aper et al., 2014). The iCAFs were seeded at confluence on glass coverslips and allowed to produce ECM for 72h, with or without 25 μ M c646 treatment. CNA35-mCherry was then added to the media at a concentration of 1 μ M for two hours, following which the coverslips were fixed in 4% PFA, counterstained with DAPI and imaged (Fig. 5-6). The images clearly showed that collagen was reduced in the c646 treated samples, again showing that inhibition of histone acetylation reduces ECM production in the CAFs.

In order to show that this effect also occurs in CAFs when in the presence of cancer cells, I seeded the pCAF2s in a 1:1 ratio with Cellaria-Wood cancer cells at confluence on glass coverslips. The Cellaria-Wood cell line is a primary breast cancer cell line, derived from an ER+ infiltrating ductal and lobular carcinoma. After 96h of co-culture with or without c646 treatment, CNA35-mCherry was added to the media at a concentration of 1 μ M for two hours, following which the coverslips were fixed, counterstained with DAPI and imaged (Fig. 5-7a). The pCAF2s are GFP positive, so I classed nuclei within the green area as fibroblasts, and nuclei outside the green area as cancer cells. The collagen staining overlapped almost solely with the fibroblasts, confirming that they are the main source of collagen (Fig. 5-7b). In the c646 treated cultures, there was a dramatic decrease in collagen staining, confirming that the c646 treatment is also effective when CAFs are in the presence of cancer cells (Fig. 5-7c). Interestingly, in the control cultures the Cellaria-Wood cells formed large clusters around which the fibroblasts formed a network, whereas in the c646 treated cultures the Cellaria-Wood cells formed much smaller clusters, suggesting that c646 affects interactions between the cells, or that interactions with the CAF-derived ECM is required for the cancer cells to form clusters.

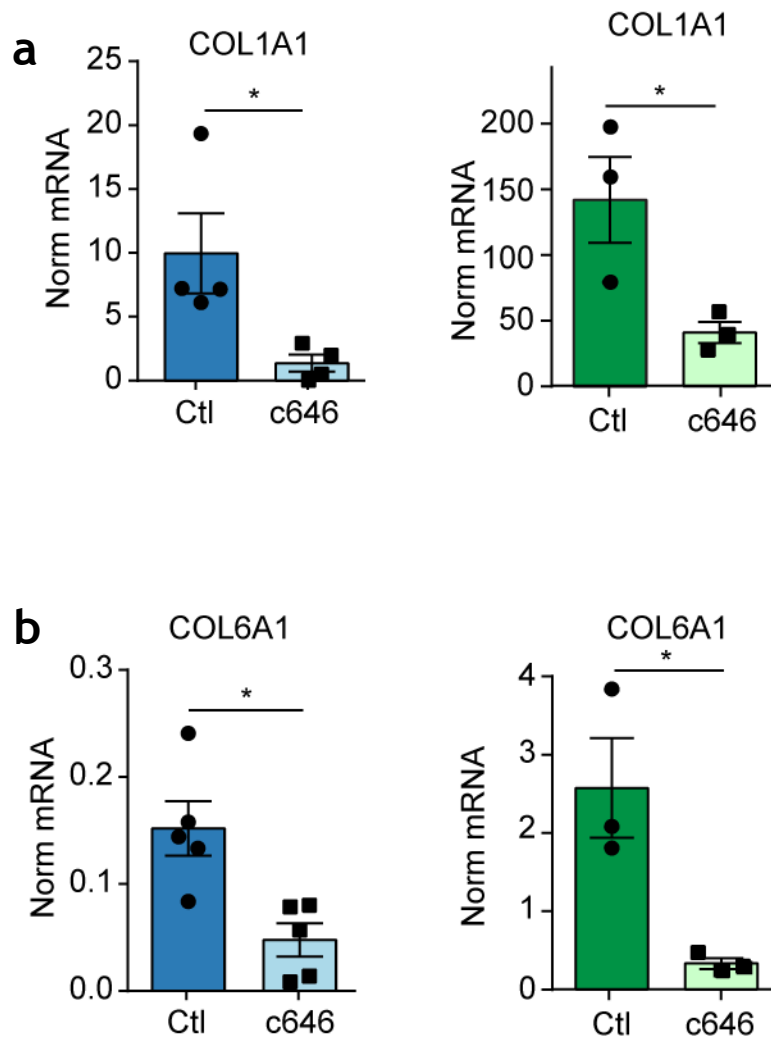


Figure 5-4 c646 reduces collagen expression at the mRNA level

a: COL1A1 mRNA levels in iCAFs (blue) and pCAFs (green) with or without 25 μ M c646 treatment. **b:** COL6A1 mRNA levels in iCAFs (blue) and pCAFs (green) with or without 25 μ M c646 treatment. The mRNA levels were measured by RT-qPCR and collagen mRNA was normalised to TBP2 levels. Graphs show mean and SEM of at least 3 independent experiments. Significance was calculated using an unpaired student t-test with Welch's correction: * $p \leq 0.05$

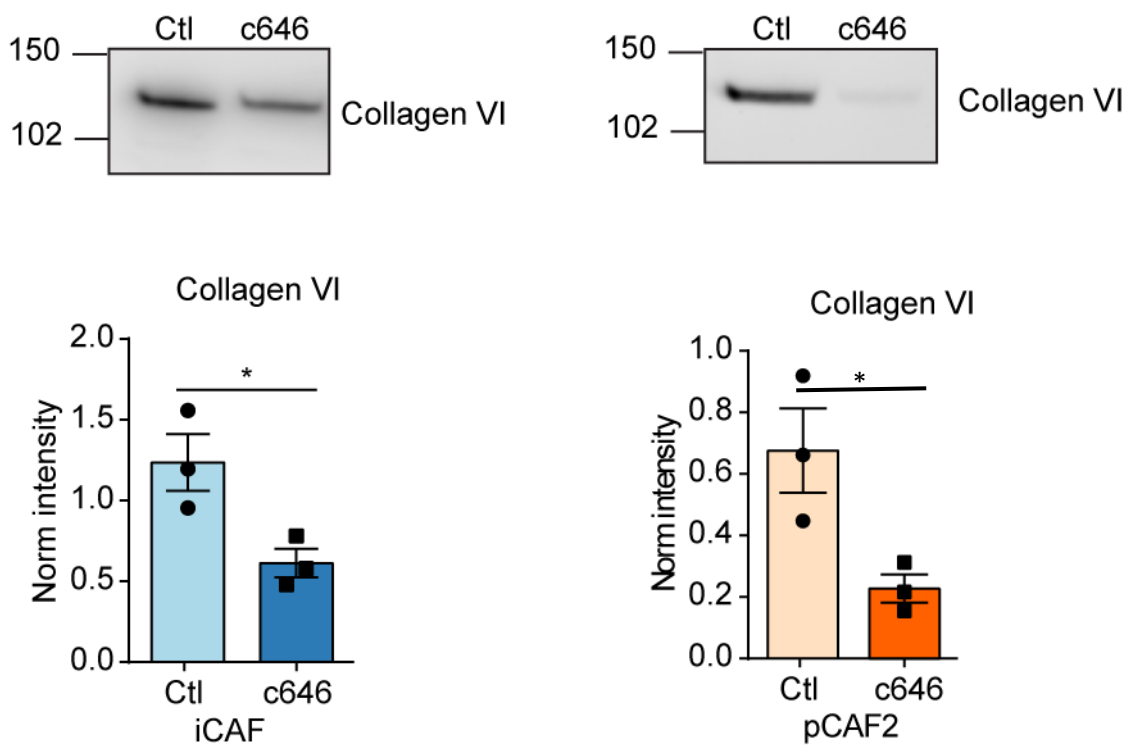


Figure 5-5 c646 reduces collagen levels in the ECM

Representative western blots and quantification of Collagen VI levels in ECM derived from iCAFs or pCAF2s after treatment with 25 μ M c646 or DMSO control. Graphs show mean and SEM of 3 independent experiments. Significance was calculated using an unpaired student t-test with Welch's correction: * $p \leq 0.05$

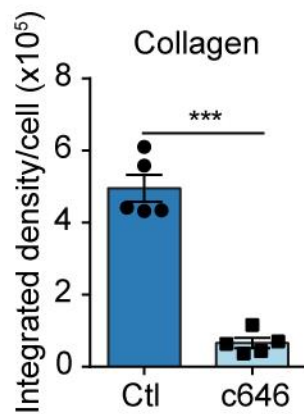
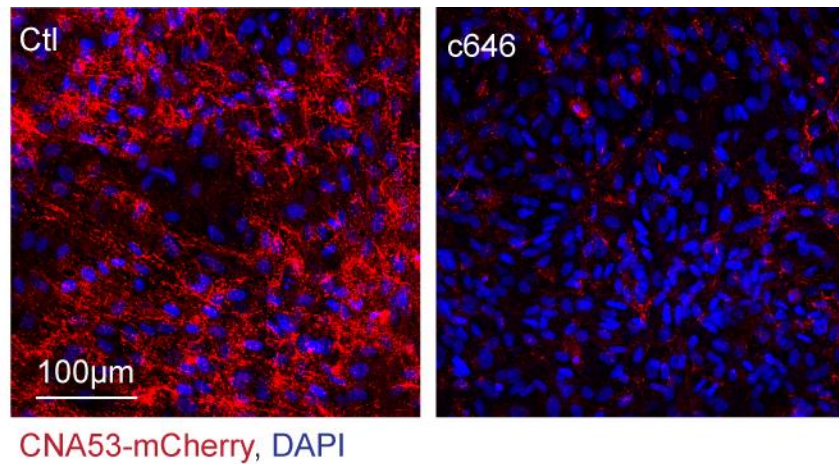


Figure 5-6 c646 reduces collagen production by CAFs

Representative images and quantification of collagen stained with CNA35-mCherry after treatment with 25 μ M c646 or DMSO control. Images were acquired using a Zeiss 710 at 20x magnification and the staining density was calculated using ImageJ software and normalised to cell number. Graph shows mean and SEM of 6 independent experiments. Significance was calculated using an unpaired student t-test with Welch's correction: *** $p \leq 0.001$

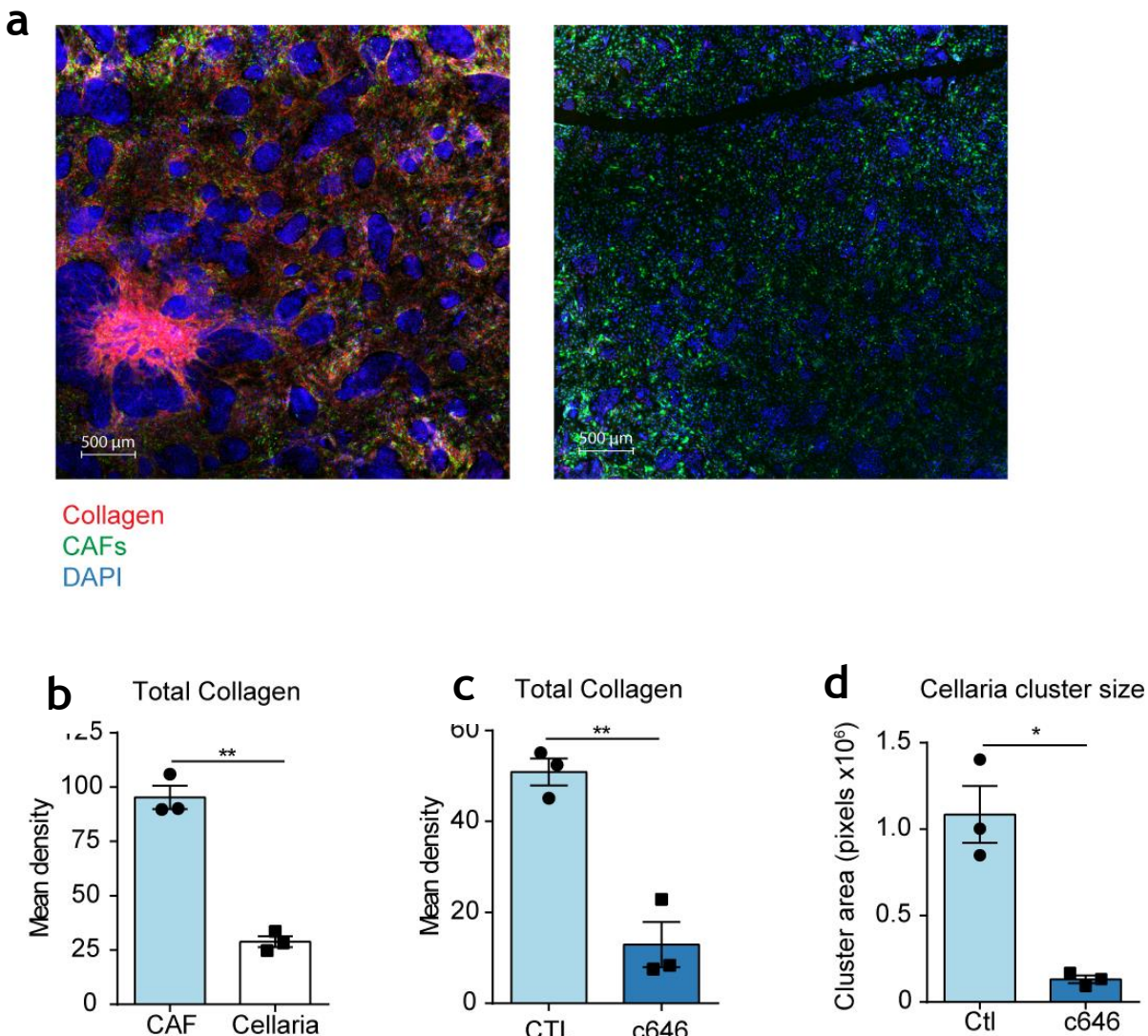


Figure 5-7 c646 reduces collagen production in CAF/Cellaria-Wood co-cultures

a: Representative images of pCAF2 (GFP positive) and Cellaria-Wood cancer cells in 1:1 co-culture after 96h treatment with 25 μ M c646 or DMSO control. Collagen was stained with CNA35-mCherry. Images were acquired as 5x5 tilescan using a Zeiss 710 at 10x magnification. **b:** Graph showing mean density of collagen staining overlapping with CAF or Cellaria cells in the DMSO control treated cultures. **c:** Mean density of total collagen staining in the control vs c646 treated cultures. **d:** Mean area of Cellaria-Wood clusters in the control vs c646 treated cultures. The staining density and cluster size was calculated using ImageJ software. Graphs show mean and SEM of 3 experiments. Significance was calculated using an unpaired student t-test with Welch's correction: ** $p \leq 0.01$

5.3 Acetyl-coA availability regulates collagen production in CAFs

5.3.1 ACLY inhibition reduces collagen production in CAFs

I have shown that c646 treatment, which inhibits EP300 and thereby reduces H3K27 acetylation, decreases collagen production by CAFs. However, although I demonstrated that histone acetylation regulates collagen production, this is not necessarily dependent on acetyl-coA. Therefore, in order to further prove that acetyl-coA availability regulated collagen production by the CAFs, the iCAF were cultured at confluence for seven days and were treated for the duration of the experiment with DMSO or BMS303141, the ACLY inhibitor which, as I showed in the previous chapter, regulates H3K27 acetylation. The ACLY inhibition was rescued by additionally treating the CAFs with 2 mM acetate to provide them with a source of nucleocytosolic acetyl-coA. The CAFs were then lysed and removed, leaving the ECM intact, and the cell-free ECM was harvested, denatured and analysed by Western blot. The level of collagen VI in the CAF-derived ECM was significantly reduced by BMS303141 treatment, and was subsequently rescued by the additional acetate treatment, thus showing that collagen production in CAFs requires a cytosolic and nuclear pool of acetyl-coA (Fig. 5-8).

Again, to further demonstrate that inhibition of ACLY to block acetyl-coA export from the mitochondria reduces collagen production in CAFs, the iCAF were cultured at confluence with Cellaria-Wood cancer cells with or without BMS303141 treatment for 96 h, following which the collagen in the ECM was labelled with CNA35-mCherry and imaged. This clearly showed that ACLY inhibition also reduced collagen deposition by CAFs in the ECM when in the presence of cancer cells (Fig 5-9). Interestingly, BMS303141 also reduced the size of the clusters of Cellaria-Wood cells, as I saw previously with the EP300 inhibitor. This again suggests that blocking histone acetylation also affects some interactions between the cells, which could be related to the decreased ECM production or to an entirely different pathway that is regulated by acetyl-coA dependent histone acetylation.

Finally, in order to show that ACLY inhibition affected collagen production at the gene expression level, mRNA was extracted from CAFs treated with BMS303141

with or without acetate rescue for 72h. The expression of COL1A1 and COL6A1 mRNA was determined by RT-qPCR. This showed that ACLY inhibition reduced expression of the collagens compared to the DMSO treated control, and that this could be rescued by exogenous acetate treatment (Fig. 5-10). Therefore the nucleocytosolic pool of acetyl-coA in the fibroblasts regulates collagen production at the transcriptional level, further supporting my hypothesis that collagen production in CAFs is epigenetically regulated by increased histone acetylation in an acetyl-coA dependent manner.

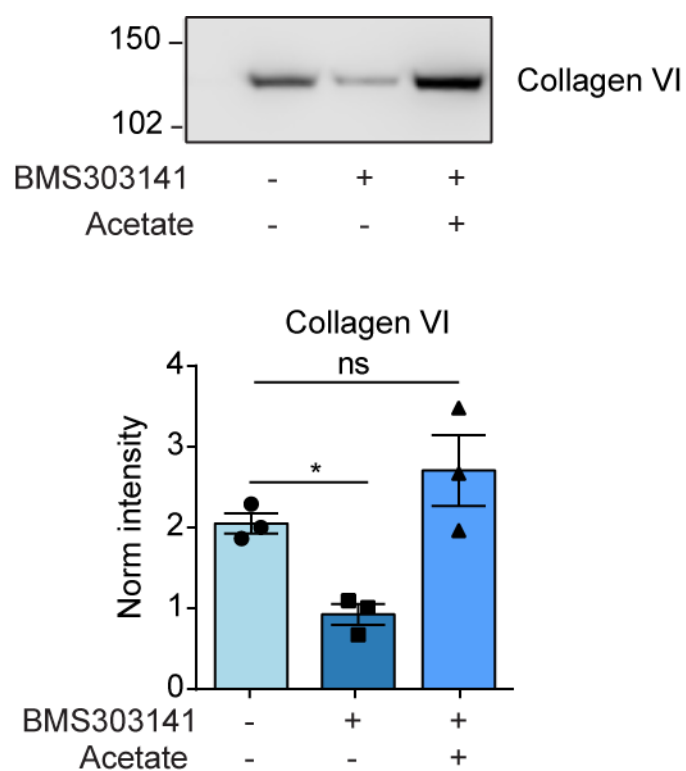


Figure 5-8 BMS303141 reduces collagen in CAF-derived ECM

Representative western blot and quantification of Collagen VI levels in ECM derived from iCAFs after treatment with 50 μ M BMS303141 +/- 2 mM acetate or DMSO control for 72h. Graphs show mean and SEM of 3 independent experiments. Significance was calculated using a one way ANOVA with Dunnett's multiple comparisons test: * $p \leq 0.05$

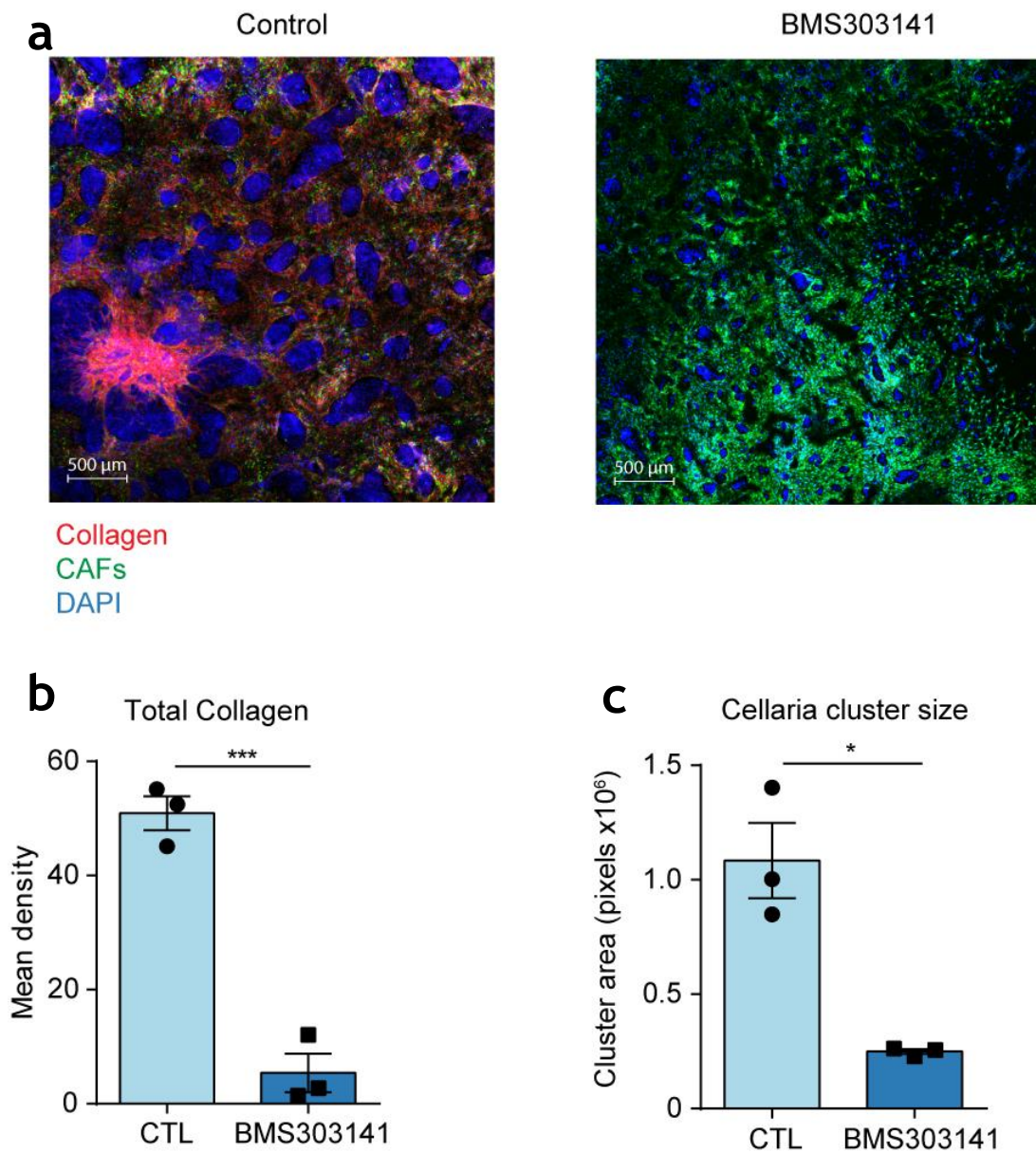


Figure 5-9 BMS303141 reduces collagen production in CAF/Cellaria-Wood co-cultures

a: Representative images and quantification of pCAF2 (GFP positive) and Cellaria-Wood cancer cells in 1:1 co-culture after 96h treatment with 50 μM BMS303141 or DMSO control. Collagen was stained with CNA35-mCherry. Images were acquired as 5x5 tilescans using a Zeiss 710 at 10x magnification. **b:** Graph shows mean density of total collagen staining in the control vs BMS303141 treated cultures. The staining density was calculated using ImageJ software. **c:** Graph shows the mean area of Cellaria-Wood clusters in the control vs BMS303141 treated cultures.

The staining density and cluster size was calculated using ImageJ software. Graphs show mean and SEM of 3 experiments. Significance was calculated using an unpaired student t-test with Welch's correction: ** $p \leq 0.01$

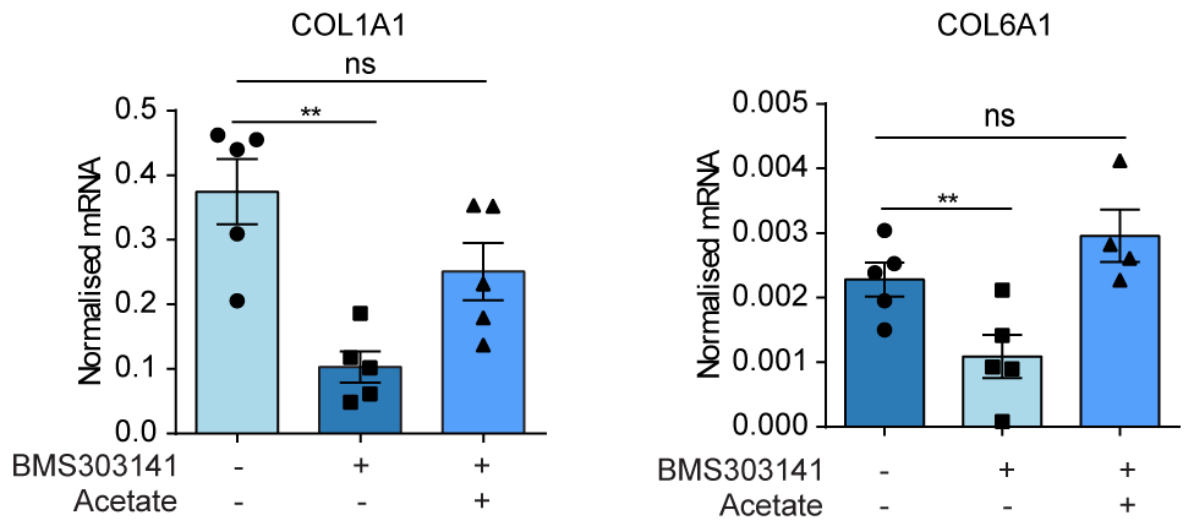


Figure 5-10 BMS303141 reduces collagen expression at the mRNA level

COL1A1 and COL6A1 mRNA levels in iCAFs after 48h of BMS303141 +/- 2 mM acetate or DMSO control treatment.

The mRNA levels were measured by RT-qPCR and collagen mRNA was normalised to TBP2 levels. Graphs show mean and SEM of at 5 independent experiments.

Significance was calculated using a one way ANOVA with Dunnett's multiple comparisons test: ** $p \leq 0.01$

5.3.2 Acetate increases collagen production in NFs

I had shown that reducing the cytosolic and nuclear pool of acetyl-coA decreased collagen production and deposition in CAFs, therefore I also attempted to increase the nucleocytosolic pool of acetyl-coA in NFs in order to activate collagen production. The NFs were treated with exogenous acetate to stimulate acetyl-coA production. After 72h of acetate treatment, the NFs were lysed for either western blot or RT-qPCR analysis. Western blot analysis confirmed that, as in the CAFs, acetate treatment increased H3K27 acetylation (Fig. 5-11). The mRNA was also extracted from NF lysates and the expression of COL1A1 and COL6A1 mRNA was determined by RT-qPCR (Fig. 5-12b). Acetate treatment significantly increased expression of both collagens at the mRNA level, suggesting that increased levels of acetyl-CoA are sufficient to epigenetically increase transcription of collagen genes.

To show that acetate increases collagen deposition in the ECM in NFs, NFs were cultured at confluence with acetate treatment for seven days and then lysed and removed, leaving the ECM behind. The cell-free ECM was then harvested and analysed by Western blot (Fig 5-12a). This showed that Collagen VI levels in NF-derived ECM were upregulated upon acetate treatment, thus connecting the increase in transcription of collagen genes with an increase in production and secretion of the protein.

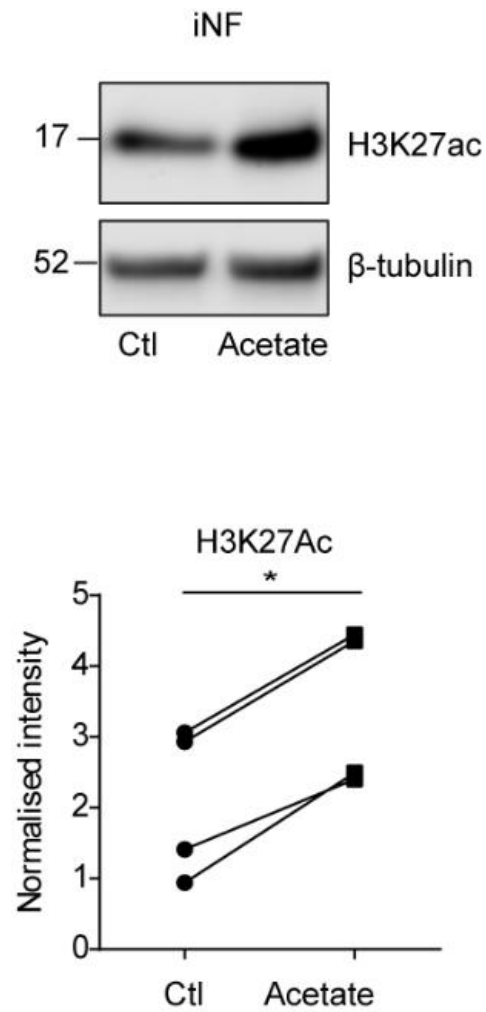


Figure 5-11 Acetate increases H3K27 acetylation in NFs

Representative western blot and quantification of H3K27ac levels in iNFs after treatment with 2 mM acetate or DMSO control for 48h. Graphs show mean and SEM of 4 independent experiments. Significance was calculated using a paired student t-test: * $p \leq 0.05$

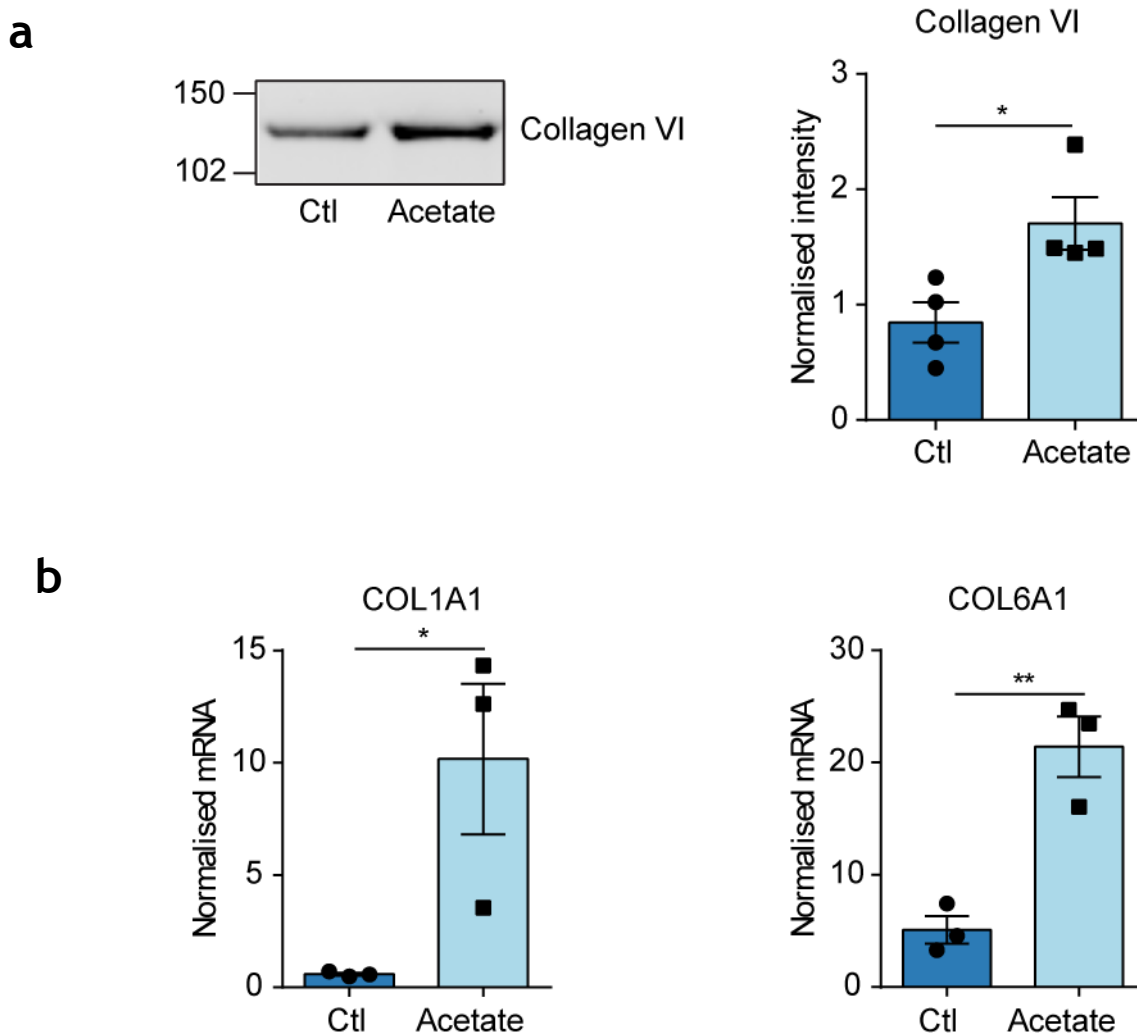


Figure 5-12 Acetate increases collagen expression in NFs

a: Representative western blot and quantification of collagen VI levels in ECM derived from iNFs after treatment with 2 mM acetate or DMSO control for 48h. Graph shows mean and SEM of 4 independent experiments. **b:** Levels of COL1A1 and COL6A1 mRNA in iNFs after treatment with 2 mM acetate or DMSO control for 48h. mRNA levels were measured by RT-qPCR and normalised to TBP2 mRNA. Graphs show mean and SEM of 3 independent experiments. Significance was calculated using an unpaired student t-test with Welch's correction t: * $p \leq 0.05$, ** $p \leq 0.01$

5.4 PDH activity regulates collagen production in fibroblasts

I showed in the previous chapter that PDH activity regulates H3K27 acetylation in the fibroblasts, and in this chapter that pharmacological inhibition of histone acetylation either via EP300 or ACLY regulates collagen production in the CAFs. Therefore, I hypothesised that modulating PDH activity in the fibroblasts would also regulate collagen production and deposition in the ECM. In order to control PDH activity, I modulated the expression of PDK2 to control PDH phosphorylation, either by transfection of NFs with siCtl or siPDK2, or by transfection of CAFs with the enzymatically inactive PDK2^{N255A} or PDK2^{WT}. The transfected fibroblasts were seeded at confluence for 72h to produce ECM, and the ECM was then decellularised. The cell-free ECM was harvested, denatured and analysed by Western blot. As predicted, PDK2 knockdown to decrease PDH phosphorylation in NFs increased collagen VI deposition in the ECM, whereas PDK2 overexpression in CAFs decreased collagen VI in the ECM (Fig. 5-13).

In order to assess the effect of PDK2 expression on collagen expression at the mRNA level, the fibroblasts were transfected as described above, with the addition of EP300 inhibition in the NFs and acetate treatment of the CAFs to reverse the effects of modulating PDK2 expression on H3K27 acetylation. The mRNA was extracted from the fibroblasts 48h after transfection with or without treatment, and the levels of COL1A1 and COL6A1 were assessed by RT-qPCR. In the NFs, siPDK2 increased collagen expression and this was reduced by c646 treatment (Fig. 5-14a). Conversely, collagen mRNA levels were decreased by PDK2 overexpression in CAFs and this was rescued with exogenous acetate (Fig 5-14b). Therefore PDH phosphorylation, as regulated by PDK2 expression, controls acetyl-coA production to epigenetically regulate collagen production by CAFs.

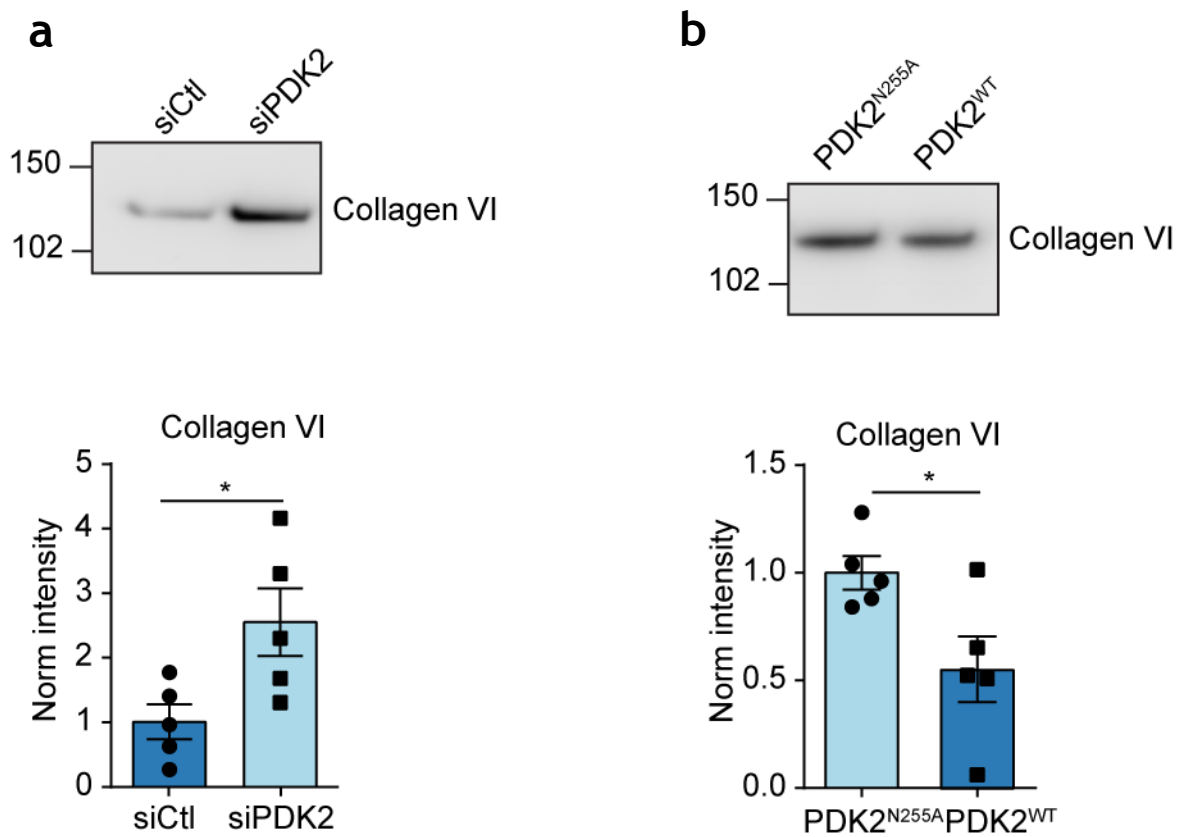
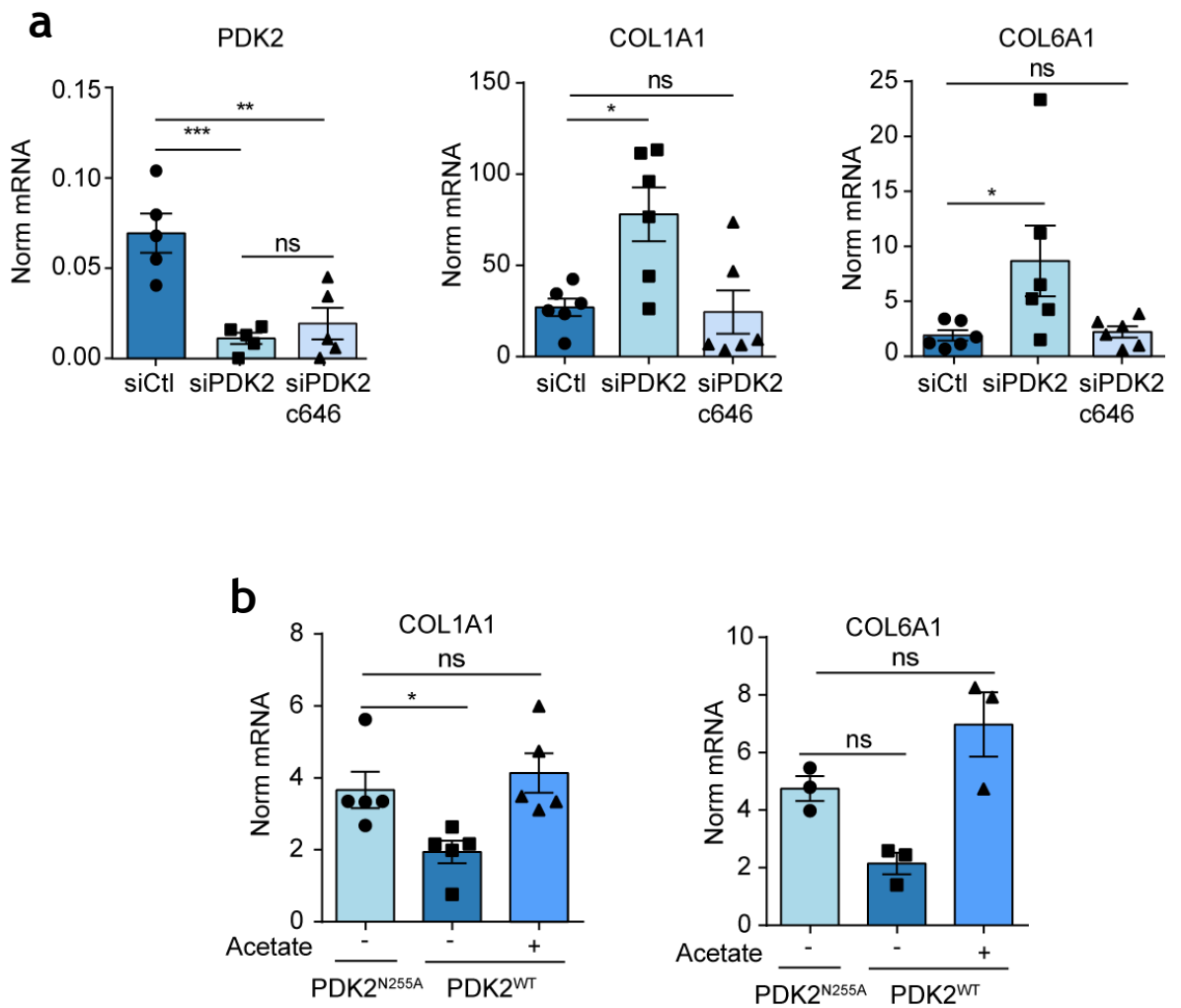


Figure 5-13 PDK2 expression regulates collagen production in fibroblasts

a: Representative western blot and quantification of collagen VI levels in ECM derived from iNFs 48h after transfection with siCtl or siPDK2. **b:** Representative western blot and quantification of collagen VI levels in ECM derived from iCAFs 48h after transfection with PDK2-N255A or PDK2-WT. Graphs show mean and SEM of 6 independent experiments. Significance was calculated using an unpaired student t-test with Welch's correction: * $p \leq 0.05$



5.5 Discussion

The key finding of this chapter is that collagen production in CAFs is epigenetically regulated by histone acetylation, as measured by H3K27 acetylation, and that this in turn is regulated by the increase in acetyl-coA produced by upregulated PDH activity in CAFs. My proteomic analysis of proteins regulated by EP300 inhibition highlighted collagens as a key group of proteins whose expression correlated with EP300 activity, and I then demonstrated that EP300 activity does indeed regulate collagen expression both at the mRNA and protein level. This strongly suggests that collagen production is being controlled at the epigenetic level. I then connected collagen expression at the mRNA and protein level to acetyl-coA availability by pharmacologically controlling the pool of acetyl-coA in the cytosol and nucleus, further demonstrating that collagen expression in CAFs and NFs is dependent on acetyl-coA mediated histone acetylation. Finally, I showed that the increase in collagen expression and production in CAFs is dependent on PDH activity, thus linking for the first time metabolic regulation of acetyl-coA production to an epigenetic regulation of the CAF phenotype.

The proteomic analysis of c646 treated CAFs clearly showed that collagens were a major group of proteins that were significantly downregulated by EP300 inhibition, suggesting that they are under epigenetic control by histone acetylation. Other extracellular matrix proteins such as fibronectin, emilin and laminin were also downregulated, suggesting that there is a general downregulation of ECM production by c646. Another group of proteins that was downregulated by c646 was proteins related to cell adhesion and integrin signalling, including ITGB5, ITGAV, ITGA6, CDH6, CDH11 and IGTA11. Interestingly, ITGA11 is known to be a receptor for collagen and CDH11 has been implicated in regulating collagen synthesis (Row et al., 2016) (Fig. 5-15). It is possible that regulation of these two groups of proteins is connected, as if ECM production is decreased it makes sense to also decrease expression of proteins that bind to and respond to ECM proteins. A third group of proteins to be downregulated by EP300 inhibition was proteins involved in collagen assembly (Fig. 5-16). This included PLOD1 and PLOD3, which are lysyl hydroxylases that convert lysine residues in collagen to hydroxylysine, enabling crosslinking of collagen fibres in the ECM. An increase in cross-linked collagen in the ECM of tumours leads to increased stiffness

of the tumour microenvironment, which has been shown to promote angiogenesis and metastasis. The prolyl hydroxylases P4HA2, P3H3 and P3H1 were also downregulated. Proline hydroxylation is a key part of collagen production and is critical for the correct folding and assembly of collagen. About half of all proline residues in collagen are modified to hydroxyproline. Indeed, proline is a vital amino acid for collagen production since one of the defining features of collagens is a tightly packed triple helix consisting of repeats of the Gly-X-Y motif. X and Y are most commonly proline or hydroxyproline, meaning that about 25% of collagen is comprised of proline or hydroxyproline residues. Interestingly the translation factor EIF5A, which is required for translation of polyproline sequences (Gutierrez et al., 2013, Doerfel et al., 2013) was also downregulated by c646 treatment. Additionally, the enzymes PYCR1 and OAT, which are involved in proline synthesis were downregulated by c646, with PYCR1 being one of the most highly downregulated proteins (Fig. 5-16). This suggested that proline production itself could be a limiting factor in collagen synthesis by CAFs, and I investigated this possibility further in the following chapter. Taken together, these proteomic data from the c646 treated fibroblasts show that collagen production is a major pathway regulated by histone acetylation in CAFs, since not only the collagen proteins but also proteins involved in collagen production and modification to promote its stability and structural assembly in the ECM were similarly regulated.

Increased collagen and ECM production is one of the key aspects of the CAF phenotype. In fact, increased collagen production is a general feature of activated fibroblasts not only in the tumour microenvironment but also in fibrosis and in wound healing. In the context of cancer, the presence of collagen in the ECM drives tumour progression through a plethora of different pathways. It provides a substrate for integrin binding and downstream signalling to promote cell growth, acts as a reservoir for angiogenic factors, drives EMT and promotes focal adhesion assembly to drive cell migration. The finding that histone modification, and particularly H3K27 modification, is a driver of collagen production in fibroblasts is not a novel discovery. In fibroblasts in both cancer and other fibrotic diseases, collagen production has been shown to be epigenetically regulated. For example, BET inhibitors, which bind to BRD proteins and prevent them from binding to acetylated enhancer regions and activating transcription, have been shown to inhibit collagen production in pancreatic stellate cells. The BET inhibitors both

attenuated pancreatic fibrosis and decreased pancreatic tumour growth in a mouse model of pancreatic ductal adenocarcinoma (Kumar et al., 2017). H3K27 trimethylation, the opposing modification to H3K27 acetylation, which decreases transcriptional activation, was shown to decrease collagen expression and fibroblast activation in sclerotic fibrosis (Kramer et al., 2013). Upregulated TGF β signalling, which is one of the hallmarks of fibroblast activation, has been shown to alter histone methylation at the promoters of ECM related genes, including collagens, in fibroblasts (Sun et al., 2010). However, my work is the first study to link fibroblast metabolism with epigenetic regulation of aspects of the CAF phenotype, and particularly with collagen production. Most previous studies on CAF metabolism have focussed on how CAFs upregulated production and secretion of metabolites which can be taken up and used as fuel by the cancer cells. My results show that CAF metabolic rewiring is important for the CAFs themselves to maintain key aspects of their activated phenotype at the epigenetic level.

Pharmacologically, targeting tumours at the epigenetic level has long been investigated as a line of treatment. Aberrant hypomethylation can drive the expression of oncogenes, and the presence of specific histone modifications can be a predictor of patient outcome. For example H3K4me was found to predict the recurrence of prostate cancer (Ellinger et al., 2010). DNA-methyltransferase inhibitors such as azacitadine and decitabine are effective in the treatment of some leukaemias. Azacitadine combined with histone deacetylase (HDAC) inhibition has also been shown to combat non-small cell lung cancer. My data show that epigenetic alterations are also an important feature of the tumour microenvironment, and should be taken into account when considering epigenetic therapies. In particular, HDAC inhibitors would also promote increased histone acetylation in the CAFs which, as I have shown, might increase collagen production which could then lessen the anti-tumour effects of the drug, either by hindering drug delivery or by its positive effects on tumour growth and metastasis.

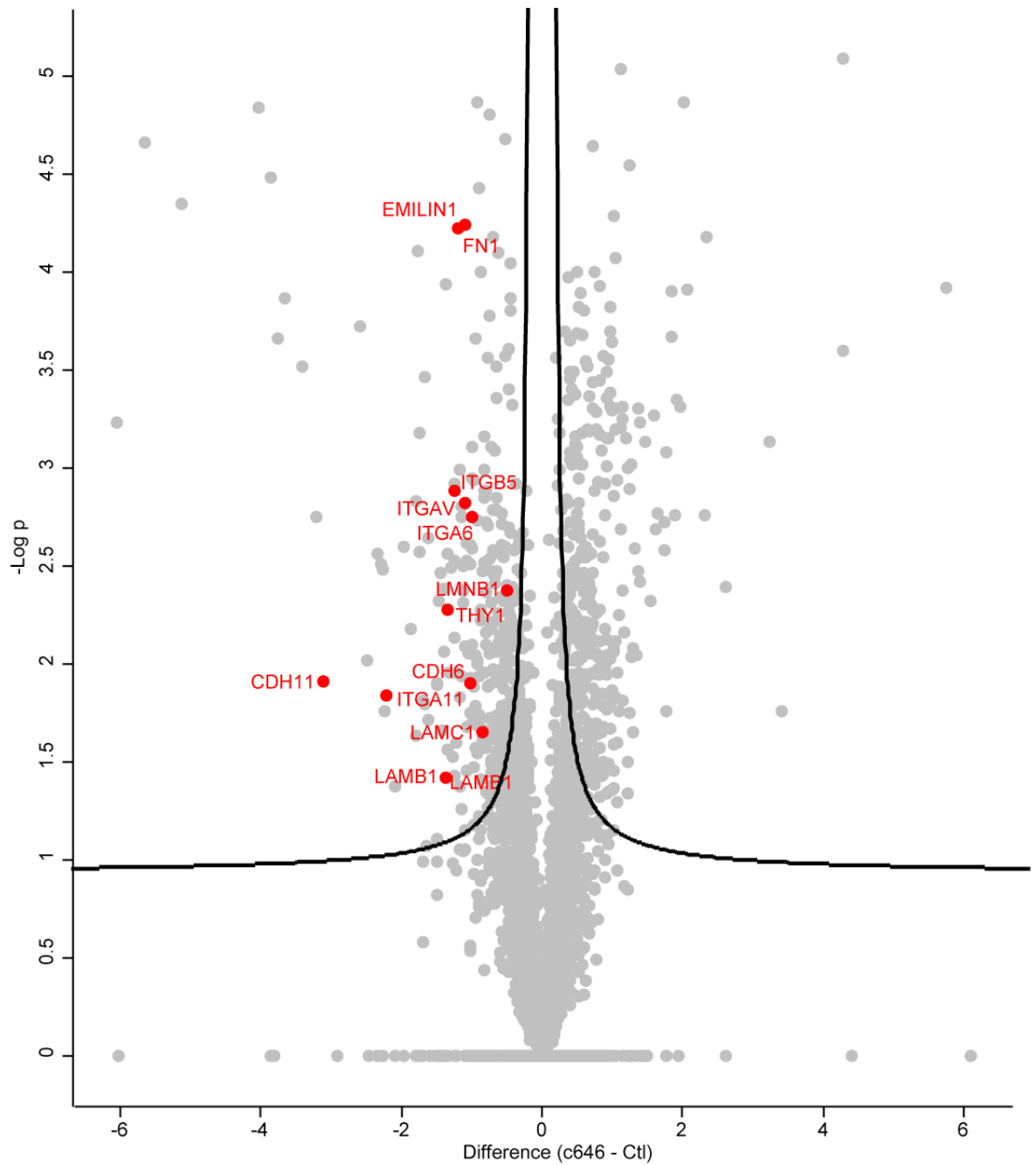


Figure 5-15 c646 downregulates ECM proteins

Volcano plot showing the results of a two-tailed t-test comparing the proteomes of control and c646 treated iCAFs. Three independent experiments were included in the analysis. Each dot represents a protein. Proteins above the black line were classed as significant (cut-off values: $p=0.05$, $S_0=0.1$). All ECM and ECM adhesion proteins which were significantly downregulated by c646 treatment are highlighted in red.

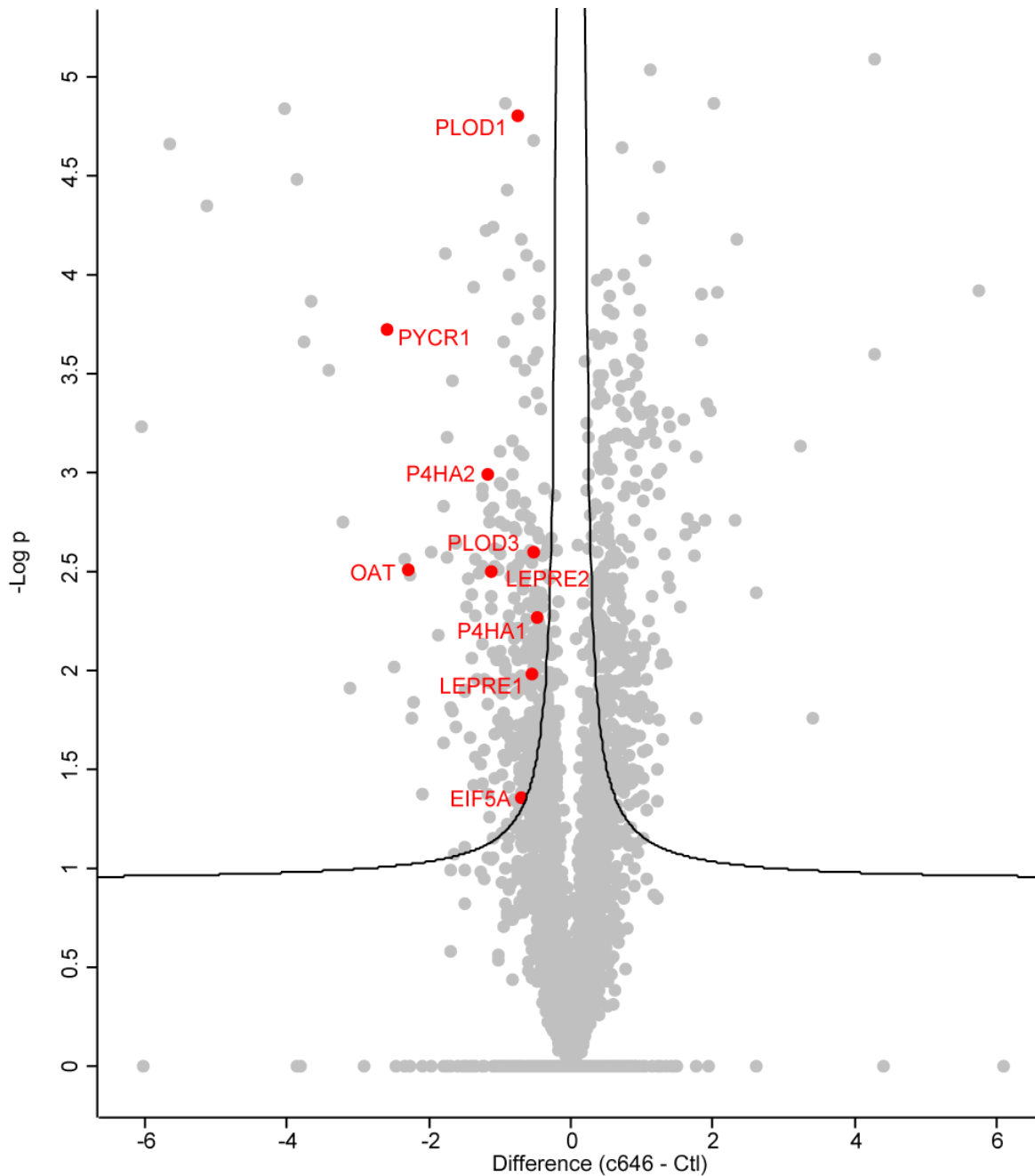


Figure 5-16 c646 downregulates proteins involved in proline and collagen synthesis

Volcano plot showing the results of a two-sample t-test comparing the proteomes of control and c646 treated iCAFs. Three independent experiments were included in the analysis. Each dot represents a protein. Proteins above the black line were classed as significant (cut-off values: $p=0.05$, $S_0=0.1$). All proteins relating to proline synthesis or collagen modification which were significantly downregulated by c646 treatment are highlighted in red.

Chapter 6 6 Upregulated proline synthesis in CAFs promotes collagen production

6.1 c646 regulates PYCR1 expression

As mentioned in chapter 4, one of the few metabolites that was consistently regulated between CAFs and NFs was proline, which was upregulated in CAFs. I have also discussed how two enzymes involved in proline synthesis were downregulated in the proteome of c646 treated iCAF: OAT and PYCR1. In particular, PYCR1 is known to be the rate limiting enzyme for proline synthesis and was one of the most highly downregulated proteins upon inhibition of EP300 with c646. I therefore hypothesised that in addition to regulating collagen expression, the epigenetic control induced by PDH activity in CAFs could also be upregulating proline synthesis by increasing PYCR1 expression. Furthermore, proline makes up a significant proportion of the amino acids in collagen. Collagens are the most abundant proteins in the CAF ECM and most of them are among the top 334 proteins that make up 95% of CAF derived ECM as determined by MS-proteomic analysis of iCAF ECM (Fig. 5-3). Therefore collagens provide a significant proportion of the total amount of proline in the ECM. Therefore it is possible that in order to support the increase in collagen production, CAFs need to increase proline production. In this chapter I investigated the regulation of PYCR1 expression by PDH-mediated histone acetylation and its impact on proline and collagen synthesis.

Firstly, I verified the results of the proteomic data by demonstrating that p300 inhibition by c646 did indeed reduce PYCR1 expression. Expression of PYCR1 in lysates from CAFs treated with 25 μ M c646 for 48h was examined at both the mRNA and the protein level. RT-qPCR for PYCR1 showed that c646 decreased PYCR1 expression at the mRNA level (Fig. 6-1a), and western blot analysis showed that PYCR1 was also downregulated by c646 at the protein level and could therefore be regulated by the increase in histone acetylation in CAFs (Fig. 6-1b). Furthermore, PYCR1 and OAT were both upregulated in tumour associated stroma compared to normal stroma in microdissected sections of TNBC and normal stroma analysed in collaboration with Dr. Morag Park from McGill University, suggesting

that stromal PYCR1 expression and proline synthesis is also relevant in a clinical setting (Fig. 6-2). Conversely, PRODH, the enzyme that degrades proline, was not upregulated.

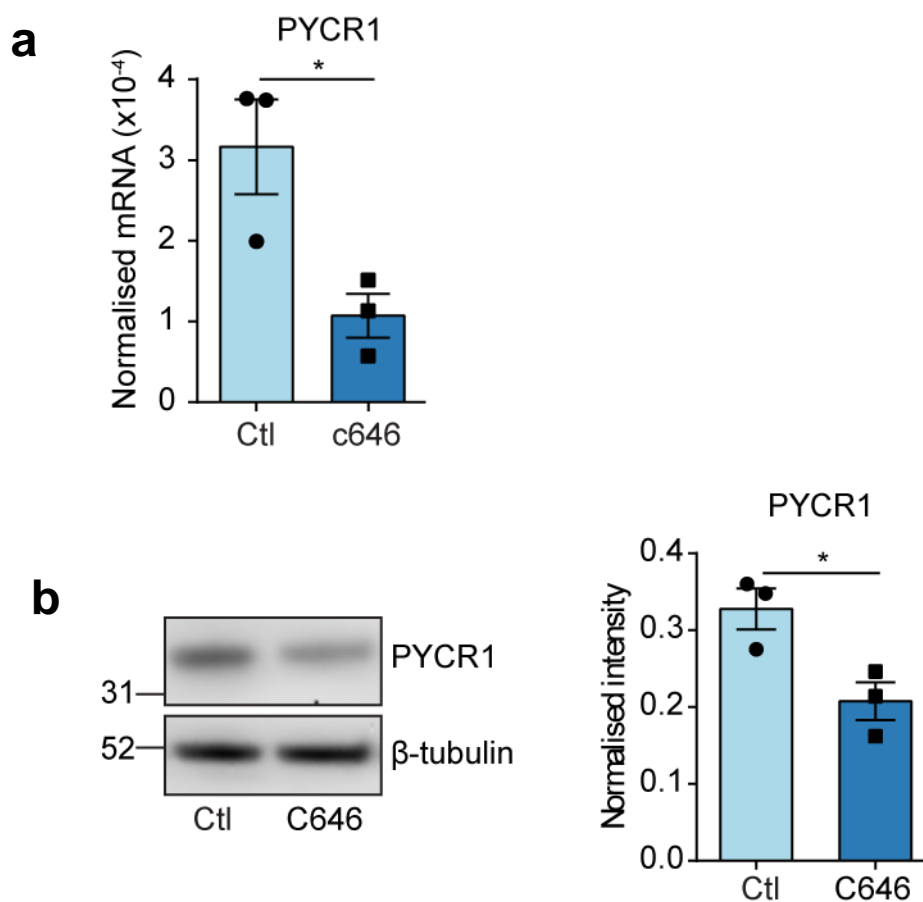


Figure 6-1 c646 reduces PYCR1 expression

a: PYCR1 mRNA levels in iCAFs treated for 48h with 25 μ M c646 or DMSO control. mRNA levels were measured by RT-qPCR and PYCR1 mRNA was normalised to TBP2 levels. **b:** Representative Western blot and quantification of PYCR1 levels in iCAFs treated for 48h with 25 μ M c646 or DMSO control.

Graphs show mean and SEM of at least 3 independent experiments. Significance was calculated using an unpaired Student t-test with Welch's correction: * $p \leq 0.05$

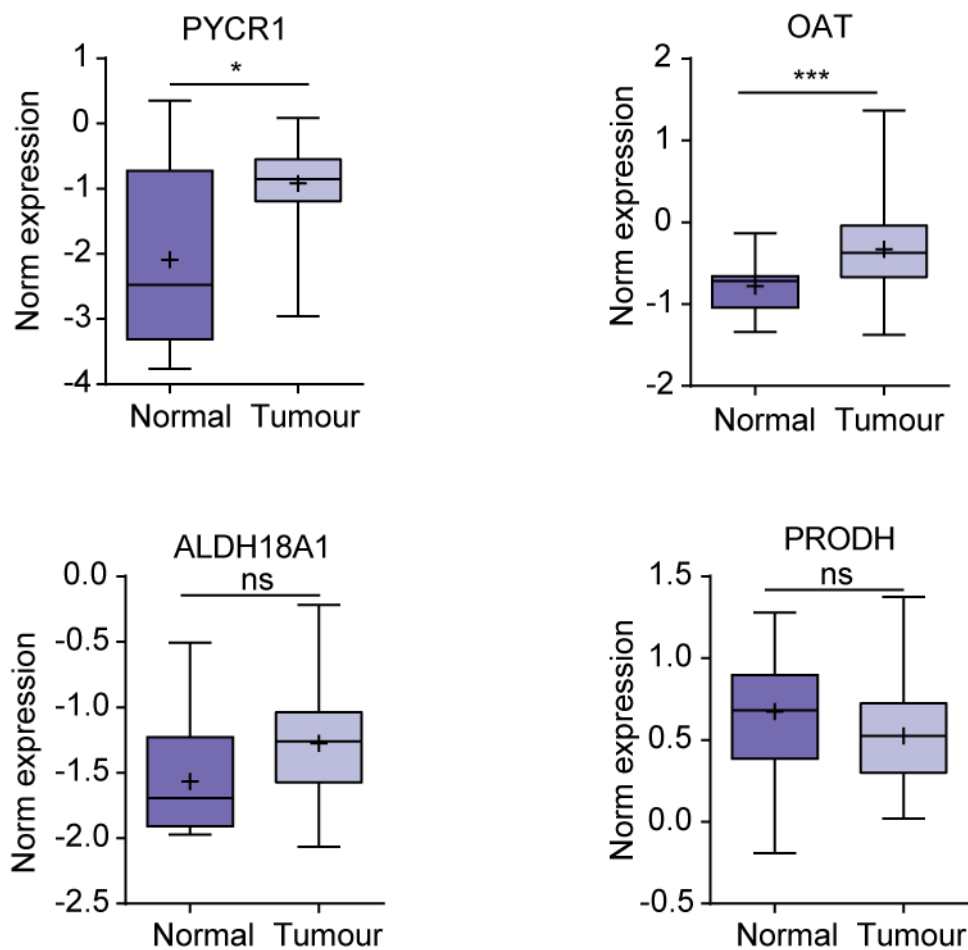


Figure 6-2 Proline synthesis enzymes are upregulated in tumour-associated stroma

PYCR1 and OAT mRNA expression in microdissected sections of stroma from normal and tumour associated stroma from triple negative breast cancer patients. Data was provided by Dr. Morag Park (McGill University). Error bars show mean and SEM. Significance was calculated using an unpaired student t-test: $p \leq 0.05$ *, $p \leq 0.01$ **, $p \leq 0.001$ ***

6.2 PYCR1 expression is regulated by acetyl-coA

In order to determine whether the increase in PYCR1 expression in CAFs is regulated by the extra-mitochondrial pool of acetyl-coA, the CAFs were treated with the ACLY inhibitor BMS303141 for 48h to prevent export of acetyl-coA out of the mitochondria, and given exogenous acetate to replenish the cytosolic and nuclear pool of acetyl-coA. PYCR1 mRNA was downregulated by BMS303141 treatment, and the expression of PYCR1 was restored by the acetate treatment as measured by RT-qPCR in both the iCAF and the pCAF2s (Fig. 6-3a). Similarly, in the iCAF, PYCR1 protein levels were decreased with the BMS303131 treatment and rescued by acetate when analysed by Western blot (Fig. 6-3b). Therefore the increase in PYCR1 mRNA also translated into an increase in PYCR1 protein, suggesting that this could have functional implications regarding proline production.

To further show that the extra-mitochondrial pool of acetyl-coA controls PYCR1 expression, iNFs and pNF2s were treated with 2 mM acetate for 48h. Acetate treatment was sufficient to increase PYCR1 expression at the mRNA level as determined by RT-qPCR (Fig. 6-4). Taken together, these data show that PYCR1 expression at the mRNA level in both CAFs and NFs is dependent on the nucleocytosolic pool of acetyl-coA and is therefore likely to be under epigenetic regulation by histone acetylation.

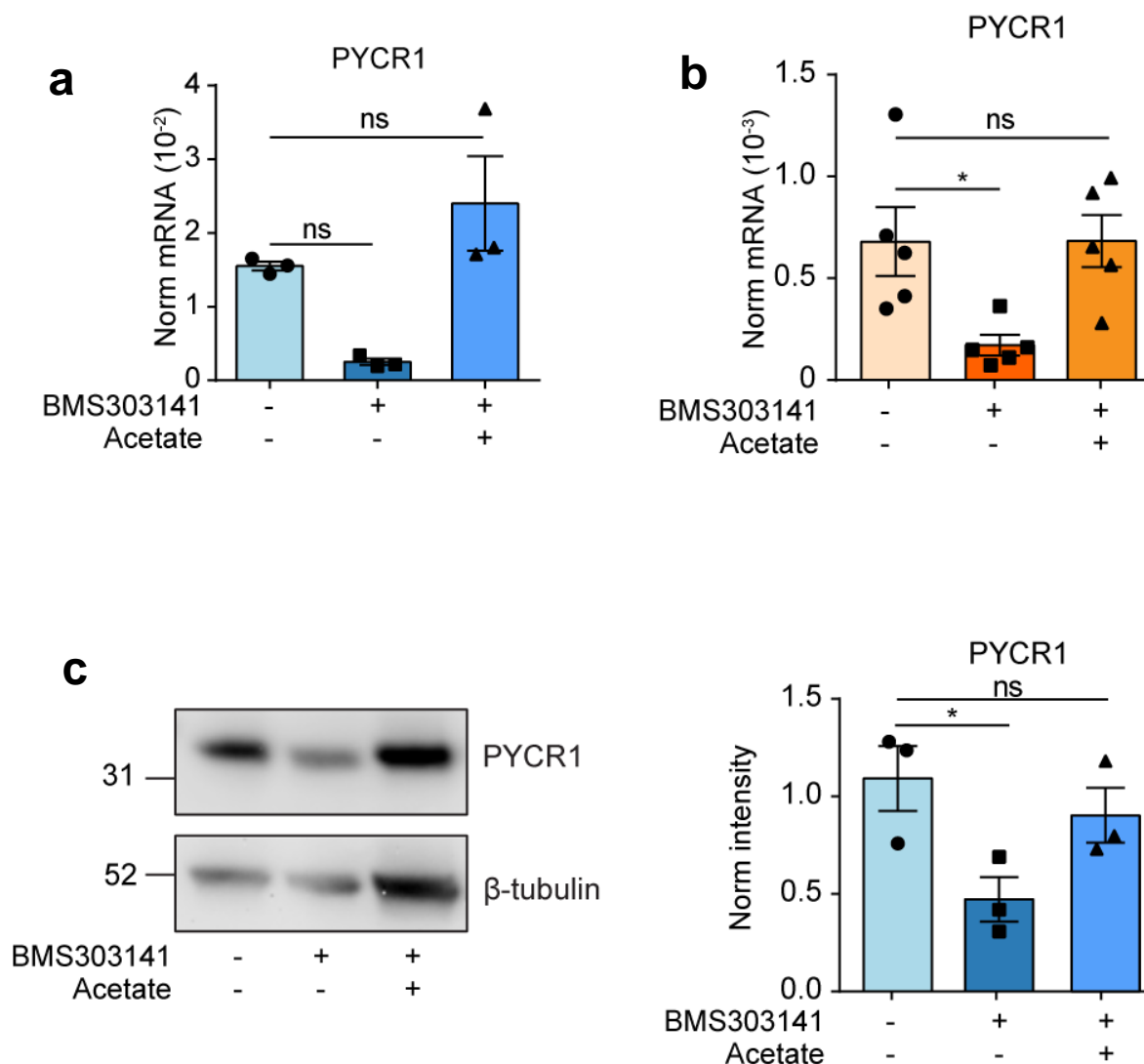


Figure 6-3 PCYR1 expression is regulated by extra-mitochondrial acetyl-coA

a. PYCR1 mRNA expression measured by RT-qPCR in iCAFs treated for 48h with 50 μ M BMS30141 \pm 2 mM acetate. PYCR1 mRNA was normalised to TBP2. **b.** PYCR1 mRNA expression measured by RT-qPCR in pCAF2s treated for 48h with 50 μ M BMS30141 \pm 2mM acetate. PYCR1 mRNA was normalised to TBP2. **c.** Representative Western blot and quantification of PYCR1 levels in iCAFs treated for 48h with 50 μ M BMS30141 \pm 2 mM acetate. β -tubulin was used as a loading control. Molecular weight markers are shown next to the blots.

Error bars show mean and SEM of ≥ 3 biological replicates. Significance was calculated using a one way ANOVA with Dunnett's multiple comparisons test: $p \leq 0.05$ *, $p \leq 0.01$ **, $p \leq 0.001$ ***

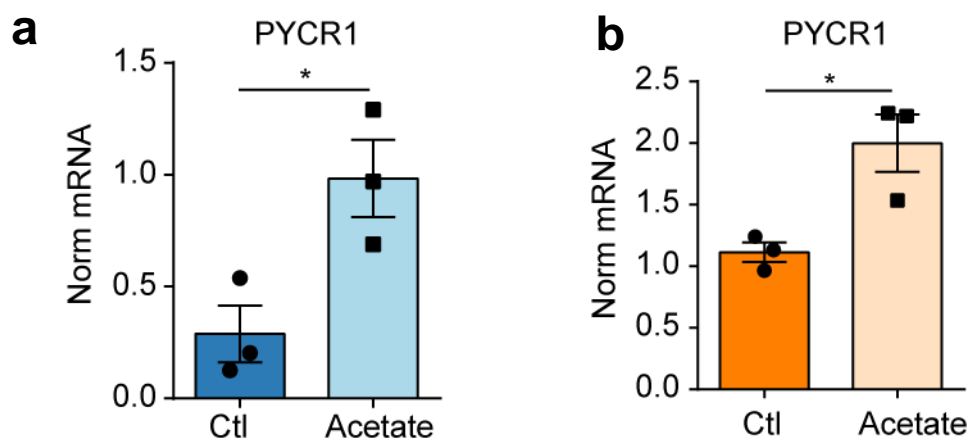


Figure 6-4 PCYR1 expression is regulated by extra-mitochondrial acetyl-coA

a. PYCR1 mRNA expression measured by RT-qPCR in iNFs treated for 48h with 2 mM acetate. PYCR1 mRNA was normalised to TBP2. **b.** PYCR1 mRNA expression measured by RT-qPCR in pCAF2s treated for 48h with 2 mM acetate. PYCR1 mRNA was normalised to TBP2.

Error bars show mean and SEM of 3 biological replicates. Significance was calculated using a Students' t-test with Welch's correction: $p \leq 0.05$ *, $p \leq 0.01$ **, $p \leq 0.001$ ***

6.3 PYCR1 expression is regulated by PDH activity

To investigate the effect of PDH activity on PYCR1 expression in fibroblasts, I again modulated PDK2 expression in order to control PDH phosphorylation and thereby its activity. PDK2 expression was altered either by transfection of NFs with siCtl or siPDK2, or by transfection of CAFs with PDK2^{N255A} or PDK2^{WT}. To further tie PDH activity-induced PYCR1 expression to histone acetylation, I treated the siPDK2 transfected NFs with c646 to reduce histone acetylation. Conversely I treated the PDK2 overexpressing CAFs with 2 mM acetate to replenish the intracellular pool of acetyl-coA and increase histone acetylation. 48h after transfection, the fibroblasts were lysed and the expression of PYCR1 was assessed by RT-qPCR. PDK2 knockdown in the NFs to increase PDH activity increased PYCR1 expression at the mRNA level, and this was successfully reversed by c646 treatment (Fig. 6-5a). In the reverse, overexpression of PDK2 in the CAFs decreased PYCR1 expression at the mRNA level but acetate treatment rescued PYCR1 expression (Fig. 6-5b). This verified that PDH activity is an upstream regulator of PYCR1 expression, and that the increase in acetyl-coA and histone acetylation produced by PDH in CAFs is required for the increase in PYCR1 expression.

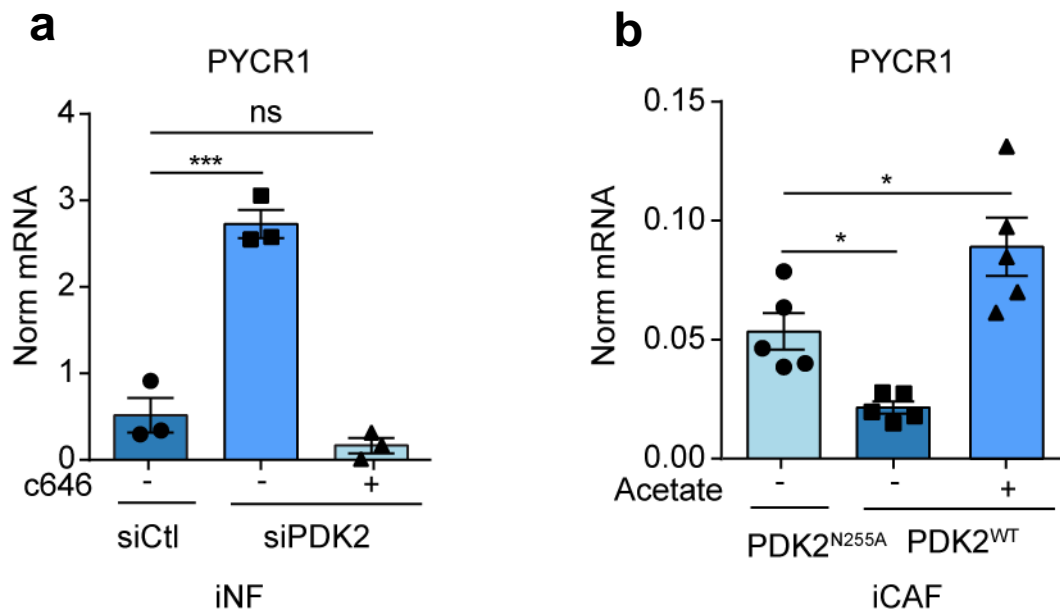


Figure 6-5 PYCR1 expression is regulated by PDK2 levels

a. PYCR1 mRNA expression measured by RT-qPCR in iNFs 48h after transfection with siCtl or siPDK2 \pm 25 μ M c646 treatment. PYCR1 mRNA was normalised to TBP2. **b.** PYCR1 mRNA expression measured by RT-qPCR in iCAFs 48h after transfection with PDK2^{N255A} or PDK2^{WT} \pm 2 mM acetate treatment. PYCR1 mRNA was normalised to TBP2.

Error bars show mean and SEM of 3 biological replicates. Significance was calculated using a one way ANOVA with Dunnett's multiple comparisons test: $p \leq 0.05$ *, $p \leq 0.01$ **, $p \leq 0.001$ ***

6.4 PYCR1 expression regulates proline production

6.4.1 PYCR1 knockdown reduces intracellular proline

Although I had shown that expression of PYCR1 was upregulated by PDH activity in CAF, I had not yet shown that PYCR1 expression affected the intracellular proline levels. As discussed in Chapter 4, CAFs have more total intracellular proline than NFs, and, using ^{13}C -labelled metabolites, I showed that in the fibroblasts proline is mainly derived from glutamine via the TCA cycle. Therefore, using the pCAF2s, I created shCtl and shPYCR1 cell lines via lentiviral transduction with five different shPYCR1 constructs. The level of PYCR1 knockdown in lysates of the shPYCR1 cell lines was assessed both by RT-qPCR and by Western blot. Two out of the five shRNAs against PYCR1 successfully knocked down PYCR1 expression by around 70% at the mRNA level and 50% at the protein level compared to the shCtl CAFs: henceforth called shPYCR1-a and shPYCR1-b (Fig. 6-6a, b). I therefore used these two cell lines for future experiments. To determine whether the shPYCR1 cell lines reduced proline production, the intracellular metabolites from shCtl and shPYCR1 cells were harvested and analysed by LC-MS. The total amount of intracellular proline was calculated by normalising the peak area to the protein content of the cells. Both shPYCR1 cell lines produced significantly less proline than the shCtl cells, demonstrating that PYCR1 activity is required to maintain intracellular proline levels in CAFs (Fig. 6-6c).

There is another pyrroline-5-carboxylate reductase: PYCR2, which shares 84% homology with PYCR1. PYCR2 was not among the proteins regulated by c646 in the proteomic data, but in order to demonstrate that it does not compensate for the reduction in PYCR1 expression, I also assessed the expression of PYCR2 mRNA in the shPYCR1 and shCtl CAFs by RT-qPCR (Fig. 6-7). PYCR2 was not upregulated in the shPYCR1 cells, in fact it was also downregulated, showing that it is not acting as a compensatory mechanism.

To further demonstrate that PYCR1 expression controls proline production, the CAFs were transfected with either siCtl or siPYCR1. The efficacy of the siPYCR1 knockdown was determined by RT-qPCR and significantly reduced PYCR1 mRNA

48h after transfection. The intracellular metabolites were then harvested and analysed by LC-MS. The total amount of intracellular proline was calculated by normalising the peak area to the protein content of the cells. siPYCR1 also significantly reduced proline production by the CAFs (Fig. 6-8).

6.4.2 Acetyl-coA regulates proline production

In order to link proline production to upregulation of PYCR1 expression by acetyl-coA dependent histone acetylation, I treated the iCAF_s with the ACLY inhibitor BMS303131 with or without 2 mM acetate for 48h, which I previously showed regulates both H3K27 acetylation and PYCR1 expression. The intracellular metabolites were then harvested and analysed by LC-MS. The total amount of intracellular proline was calculated by normalising the peak area to the total protein content of the cells. BMS303141 reduced the amount of proline in the cells and this was rescued by the acetate treatment, showing that the extra-mitochondrial pool of acetyl-coA regulates proline production in CAFs (Fig. 6-9).

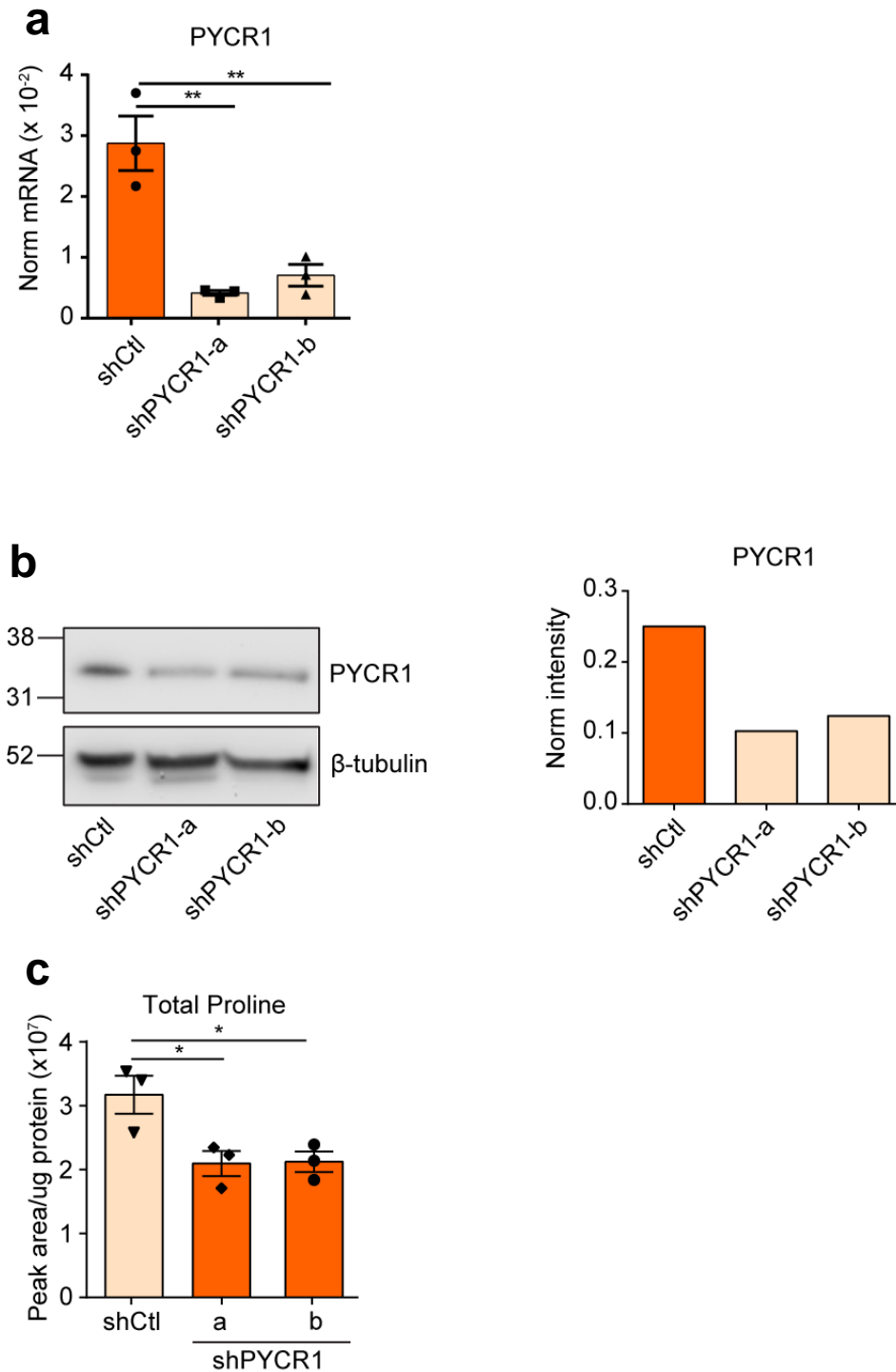


Figure 6-6 Proline synthesis is regulated by PYCR1 expression

a. PYCR1 mRNA expression measured by RT-qPCR in shCtl and shPYCR1 CAFs. PYCR1 mRNA was normalised to TBP2. **b.** Western blot and quantification of PYCR1 levels in shCtl and shPYCR1 CAFs. β -tubulin was used as a loading control. Molecular weight markers are shown next to the blots. **c.** Total proline in shCtl and shPYCR1 cell lines measured by LC-MS and normalised to total proline content.

Error bars show mean and SEM of 3 biological replicates. Significance was calculated using a one way ANOVA with Dunnett's multiple comparisons test: $p \leq 0.05$ *, $p \leq 0.01$ **, $p \leq 0.001$ ***

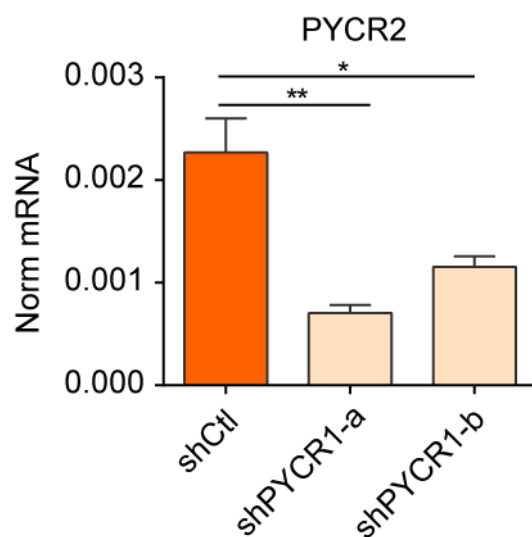


Figure 6-7 PYCR2 does not compensate for PYCR1

PYCR2 mRNA expression measured by RT-qPCR in shCtl and shPYCR1 CAFs. PYCR2 mRNA was normalised to TBP2.

Error bars show mean and SEM of 3 biological replicates. Significance was calculated using a one way ANOVA with Dunnett's multiple comparisons test: $p \leq 0.05$ *, $p \leq 0.01$ **, $p \leq 0.001$ ***

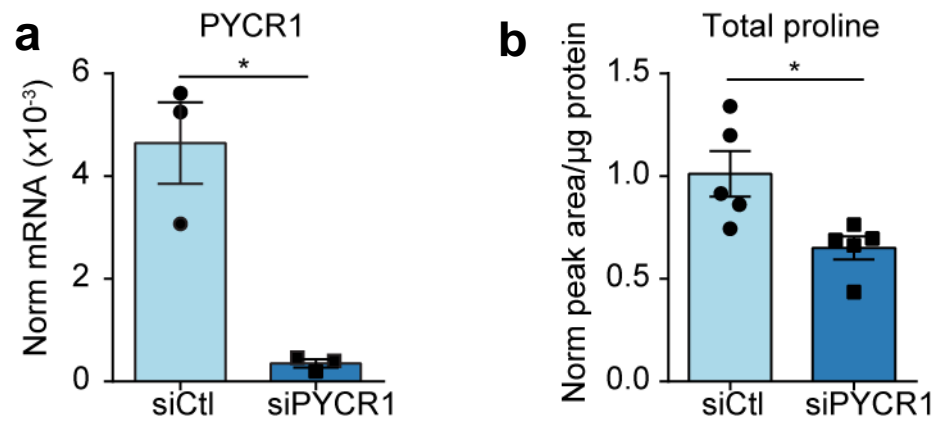


Figure 6-8 Proline synthesis is regulated by PYCR1 expression

a. PYCR1 mRNA expression measured by RT-qPCR in iCAFs 48h after transfection with siCtl or siPYCR1. PYCR1 mRNA was normalised to TBP2. **b.** Total proline in iCAFs 48h after transfection with siCtl or siPYCR1 measured by LC-MS and normalised to total protein content.

Error bars show mean and SEM of ≥ 3 biological replicates. Significance was calculated using a student's t-test with Welch's correction: $p \leq 0.05$ *, $p \leq 0.01$ **, $p \leq 0.001$ ***

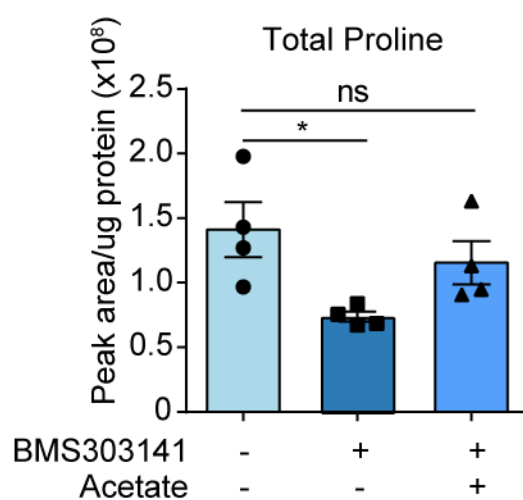


Figure 6-9 Proline synthesis is regulated by acetyl-coA levels

Total proline in iCAFs treated for 48h with 50 μ M BMS30141 \pm 2mM acetate measured by LC-MS and normalised to total protein content.

Error bars show mean and SEM of 4 biological replicates. Significance was calculated using a one way ANOVA with Dunnett's multiple comparisons test: $p \leq 0.05$ *, $p \leq 0.01$ **, $p \leq 0.001$ ***

6.5 PYCR1 produces proline for collagen production

As I had demonstrated that PYCR1 expression does indeed control proline synthesis in cells, I then sought to assess whether, as I had hypothesised, this had a significant impact on collagen production by the fibroblasts. I wanted to show specifically that proline produced by PYCR1 is incorporated into collagen. Since PYCR1 produces proline from glutamate, we hypothesised that by giving the CAFs heavy glutamine we would be able to detect the incorporation of heavy proline into collagen. I therefore seeded the shCtl and shPYCR1 CAFs at confluence and cultured them with medium containing either ^{12}C -glutamine or ^{13}C -glutamine for 72h. I then decellularised the ECM and lysed it. I separated the ECM proteins on an SDS-page gel and cut each sample into 3 bands, which I then processed by in-gel digestion for MS-proteomic analysis. Sergio Lilla in the Proteomics Facility then carried out the data acquisition and analysis using the MaxQuant computational platform to determine the incorporation of heavy proline residues into peptides from ECM proteins. As a proof of principle, we focussed on peptides from COL1A1 for the analysis, because it is highly abundant in the samples. I then compared the LFQ intensities of heavy labelled COL1A1 peptides in shCtl and shPYCR1 ECMs. For this analysis, I only considered peptides in which just proline residues were labelled, since glutamine can be used to produce many amino acids. Furthermore I only considered peptides in which all the proline residues were labelled to avoid complications due to different combinations of sites being quantified. Four quantified peptides fit these criteria. The ^{13}C -proline containing peptides had a high intensity in the ^{13}C -labelled samples while they were not detected in the unlabelled control, demonstrating that proline produced from glutamate via PYCR1 is used to produce collagen (Fig. 6-10a). Furthermore all of the peptides showed a decreased intensity in the shPYCR1 samples compared to the shCtl samples, again showing that proline produced by PYCR1 is required for collagen production in CAFs (Fig. 6-10b).

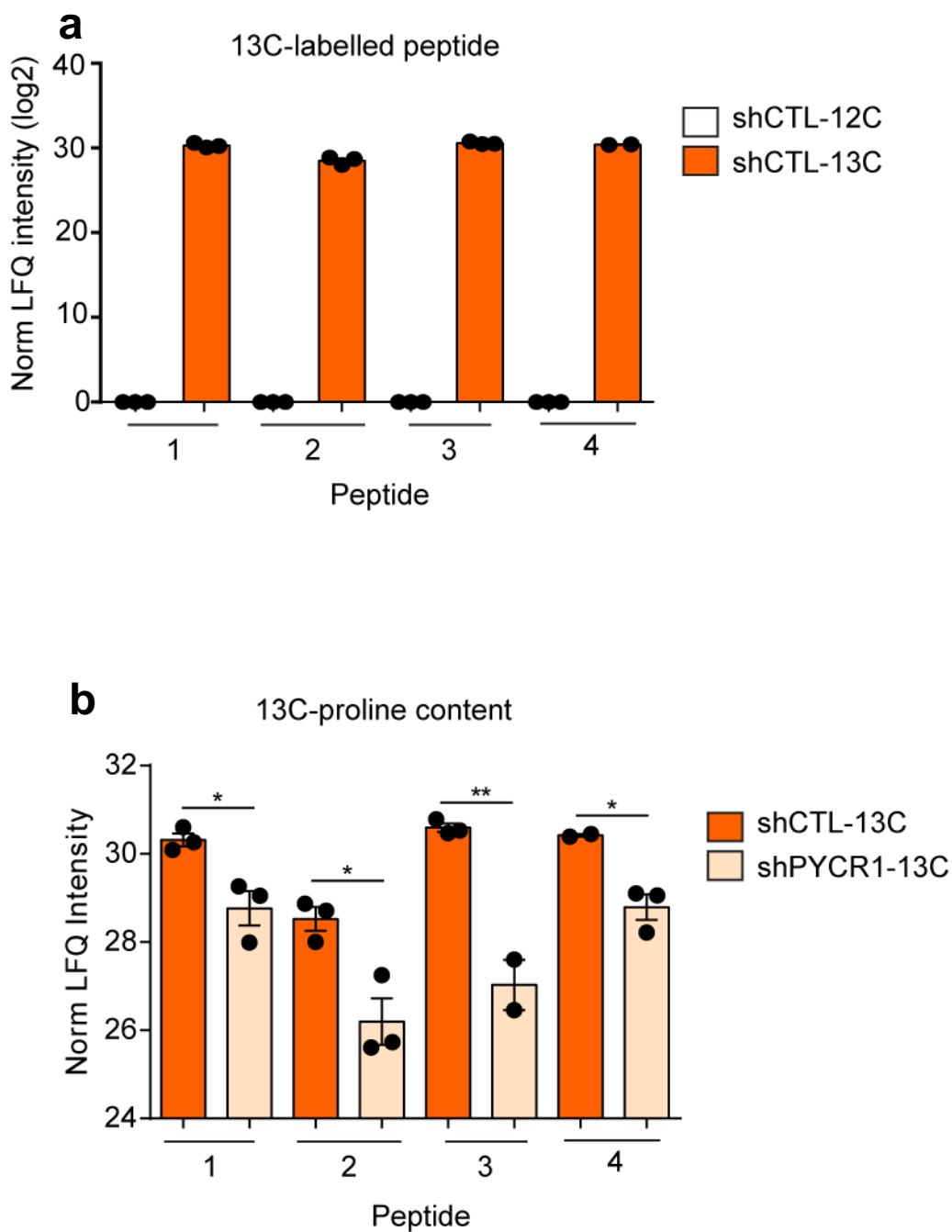


Figure 6-10 PCYR1 produces proline for collagen synthesis

a: Comparison of LFQ intensities for the ¹³C-proline labelled COL1A1 peptides between heavy labelled and unlabelled shCtl CAF-derived ECM. There is a significant incorporation of ¹³C-glutamine-derived proline into collagen in the labelled shCtl CAFs.

b: Comparison of LFQ intensities of ¹³C-proline labelled COL1A1 peptides between shCtl and shPCYR1 CAF-derived ECM.

Graphs show mean and SEM of 3 biological replicates. Significance was calculated using a Students t-test with Welch's correction: $p \leq 0.05$ * $p \leq 0.01$ **, $p \leq 0.001$ ***

6.6 PYCR1 regulates collagen production

I have shown that PYCR1 expression affects both proline synthesis and proline incorporation into collagen in CAFs; next, I wanted to investigate whether this affected the total amount of collagen produced by the fibroblasts. The shCtl, shPYCR1-a and shPYCR1-b CAFs were seeded at confluence and cultured for seven days to produce ECM. Additionally, the shPYCR1 were treated with 500 μ M proline in order to rescue the effects of shPYCR1 loss on proline production. The ECM was then decellularised, and subsequently harvested and analysed by Western blot for collagen VI. shPYCR1 significantly reduced collagen VI in the ECM, and this could be rescued with the exogenous proline (Fig. 6-11).

To confirm that PYCR1 levels regulated collagen accumulation in the ECM, I also transfected i CAFs with siCTL or siPYCR1 to acutely downregulate PYCR1, and the siPYCR1 transfected CAFs were further treated with 500 μ M proline. 72h after transfection, the cells were removed and the ECM harvested and analysed by Western blot. As with the shRNAs against PYCR1, siPYCR1 decreased the amount of collagen VI in the ECM and this was rescued by treating the cells with proline (Fig. 6-12).

To further demonstrate that collagen production by CAFs was dependent on proline levels produced by PYCR1, the shCtl and shPYCR1 CAFs were cultured at confluence on coverslips for seven days with or without proline treatment, following which the collagen in the ECM was stained with CNA35-mCherry. The cells were then fixed and counterstained with DAPI before being imaged (Fig. 6-13). The intensity of the collagen staining was quantified using ImageJ software, and clearly demonstrated a decrease in the amount of collagen produced by the shPYCR1 cells, which was then rescued by the addition of extracellular proline. Therefore the production of collagen in CAFs is proline dependent, and relies on the expression of PYCR1.

To finally link PDH activity to both proline production and collagen synthesis via PYCR1, the iNFs were transfected with siCtl, siPDK2 or both siPDK2 and siPYCR1. 72h after transfection, the cells were removed, leaving the ECM intact and the ECM was harvested and analysed by Western blot. As demonstrated before, siPDK2

was sufficient to increase collagen VI levels in the NF derived ECM, however, the additional silencing of PYCR1 reduced the collagen VI levels back to those in the ECM from the siCtl cells (Fig. 6-14). This experiment showed that the proline produced by PYCR1 is required to support the increase in collagen production that is stimulated by the upregulated PDH activity following silencing of PDK2. Therefore collagen production in CAFs is regulated by a twofold metabolic pathway. First, upregulated PDH activity leads to an increase in acetyl-coA which is used to increase histone acetylation levels and in particular the transcription activation marker H3K27ac. This leads to an upregulation in transcription of collagen genes, but in order to provide sufficient amino acids for the translation of collagen mRNA an increase in proline synthesis is required. This is achieved by simultaneously upregulating PYCR1 expression via the increase in PDH-dependent histone acetylation.

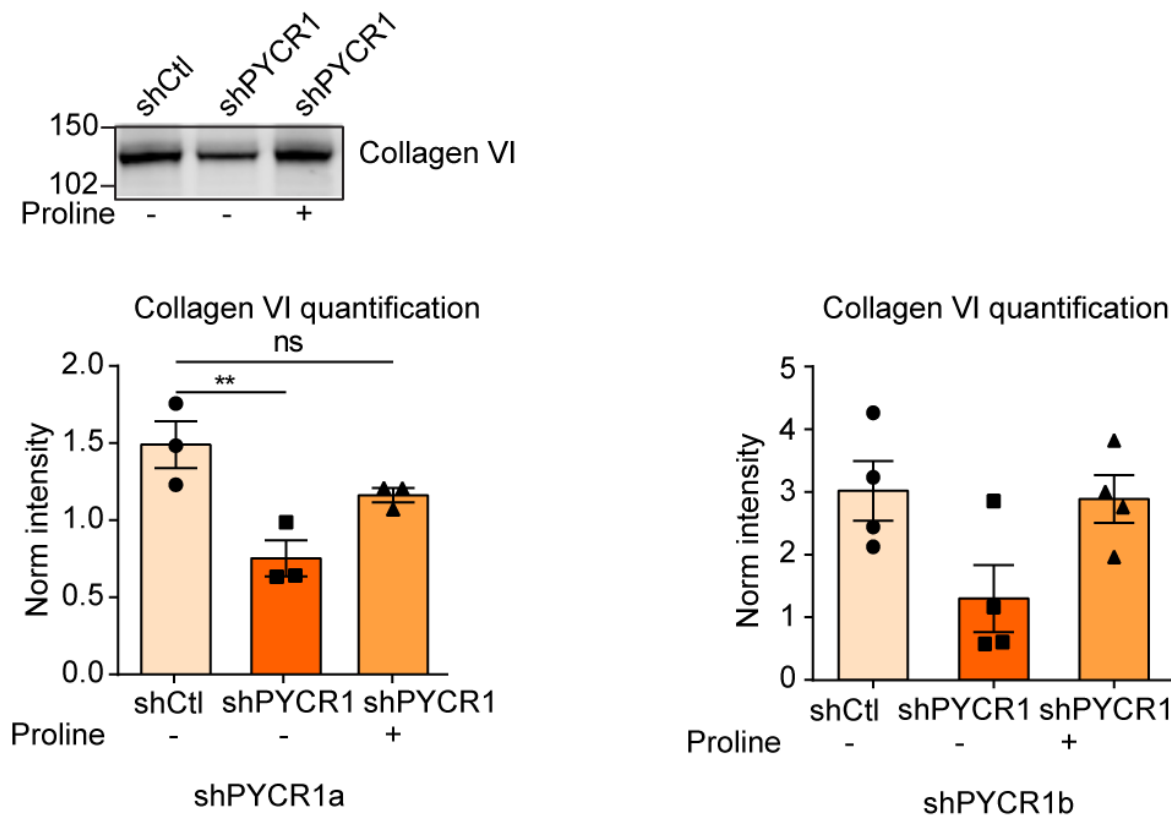


Figure 6-11 Collagen production is regulated by PCYR1 expression

Representative Western blot and quantification of collagen VI in ECM derived from shCtl CAFs compared to shPYCR1-a and shPYCR1-b CAFs \pm 500 μ M proline. Molecular weight markers are shown next to the blot.

Error bars show mean and SEM of ≥ 3 biological replicates. Significance was calculated using a one way ANOVA with Dunnett's multiple comparisons test: $p \leq 0.05$ *, $p \leq 0.01$ **, $p \leq 0.001$ ***

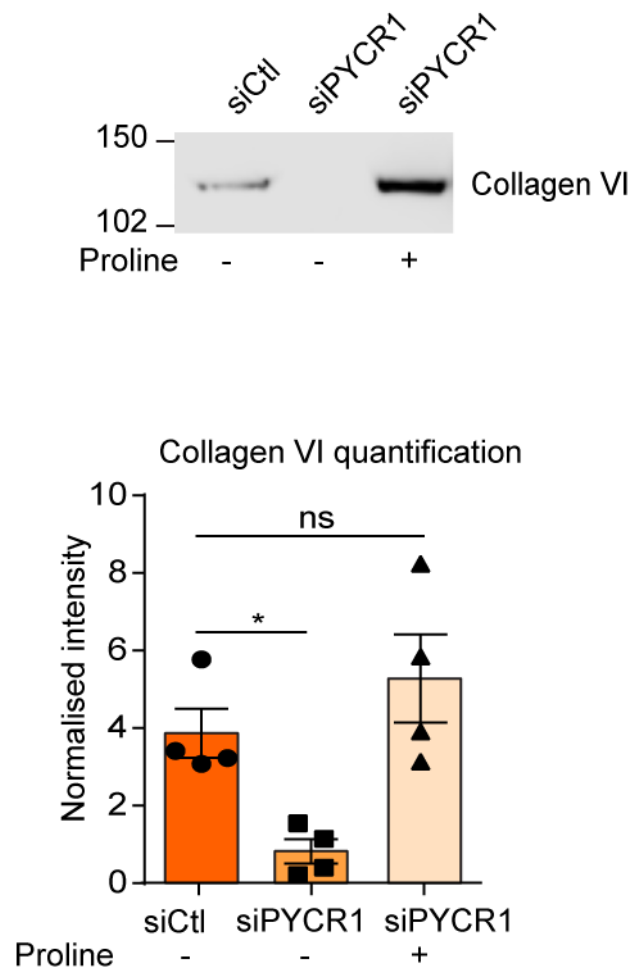


Figure 6-12 Collagen production is regulated by PYCR1 expression

Representative Western blot and quantification of collagen VI in ECM derived from CAFs 72 after transfection with siCtl or siPYCR1 \pm 500 μ M proline. Molecular weight markers are shown next to the blot.

Error bars show mean and SEM of 4 biological replicates. Significance was calculated using a one way ANOVA with Dunnett's multiple comparisons test: $p \leq 0.05$ *

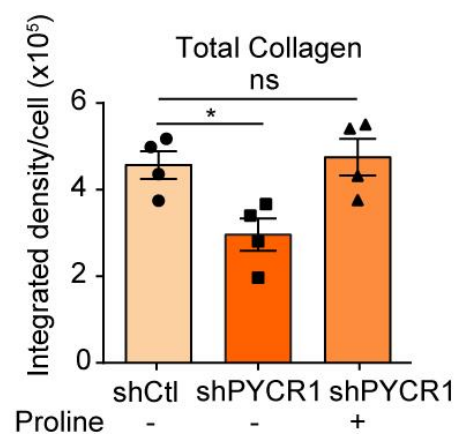
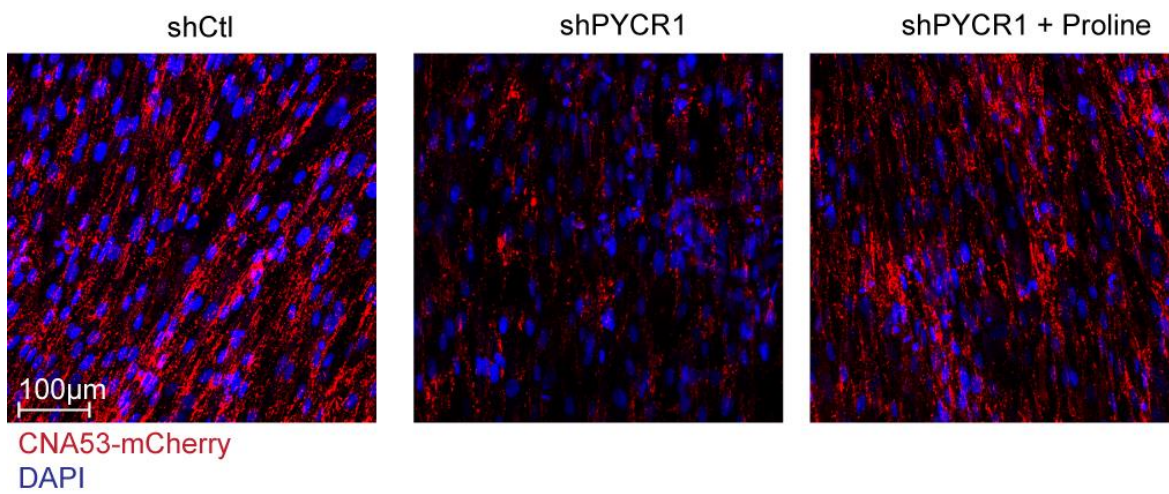


Figure 6-13 Collagen production is regulated by PYCR1 expression

Representative images and quantification of collagen produced over 5 days by shCtl and shPYCR1-b CAFs \pm 500 μ M proline. Collagen was stained with CNA35-mCherry and nuclei were stained with DAPI. Images were acquired using a Zeiss 710 at 20x magnification and the staining density was calculated using ImageJ software and normalised to cell number. Graph shows mean and SEM of 4 independent experiments. Significance was calculated using a one way ANOVA with Dunnett's multiple comparisons test: $*p \leq 0.05$

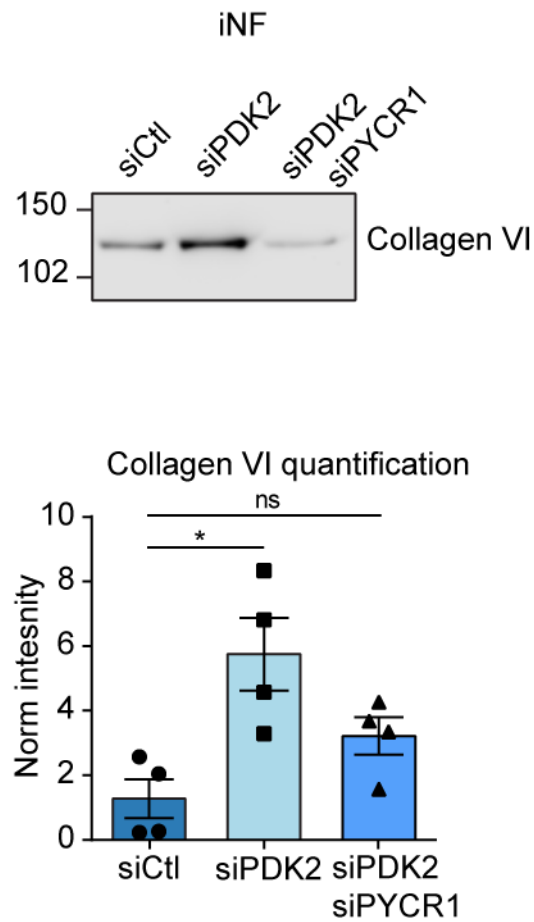


Figure 6-14 PYCR1 is required for PDH activity-induced collagen production

Representative Western blot and quantification of collagen produced by iNFs 72h after transfection with siCtl, siPDK2 or siPDK2 and siPYCR1. Molecular weight markers are shown next to the blot. Graph shows mean and SEM of 4 independent experiments. Significance was calculated using a one way ANOVA with Dunnett's multiple comparisons test: * $p \leq 0.05$

6.7 *in vivo* co-transplantation of CAFs and MCF10DCIS.com cells

In order to validate our findings *in vivo* I investigated the effect of PYCR1 knockdown in CAFs on collagen production and tumour growth. MCF10DCIS.com cells were coinjected subcutaneously with either the shCtl or shPYCR1-b pCAF cell lines into Balb-C nude mice, with a ratio of CAFs to cancer cells at 3:1. Twelve mice were used for each condition. After two weeks, when the tumours started increasing size, half of the mice from each group were culled and the tumours were harvested. We took the tumours at such an early timepoint because, based on the experience of our group (Hernandez-Fernaud et al., 2017) the human CAFs are eventually overtaken by the murine stroma and we wanted to be sure that any effects on the tumours were due to the CAFs which we had transplanted. Even at the two week timepoint, there was already a significant reduction in tumour size in the mice that had been injected with the shPYCR1 CAFs (Fig. 6-15). I then fixed the tumours in 4% PFA and sliced them into 400 μ m sections using a vibratome. The CAFs were GFP positive and were therefore easily detected using fluorescent microscopy. Z-stacks of the tissues were acquired using multi-photon microscopy with single harmonic generation imaging to visualise the collagen. Since collagen can be also produced by cancer cells, or by fibroblasts from the mice that had infiltrated the tumour, to assess whether shCtl and shPYCR1 CAFs deposited different amounts of collagen, I quantified only the collagen surrounding the GFP positive CAFs. There was significantly less collagen surrounding the shPYCR1 CAFs compared to the shCtl CAFs, which provides initial support to my hypothesis that PYCR1 knockdown also reduces collagen production *in vivo* (Fig. 6-16a). Although the amount of GFP positive fibroblasts remaining varied between tumours, there was no overall decrease in the area of GFP positive CAFs in the shPYCR1 tumours compared to the shCtl tumours, suggesting that the difference in collagen production is not due to an increase in cell death or decrease in proliferation caused by the PYCR1 knockdown (Fig. 6-16b). The remaining mice were allowed to reach endpoint before being culled, however there was no significant difference in the time take to reach endpoint between the tumours containing shCtl and shPYCR1 CAFs, probably because by this point the murine fibroblasts had completely taken over from the pCAFs.

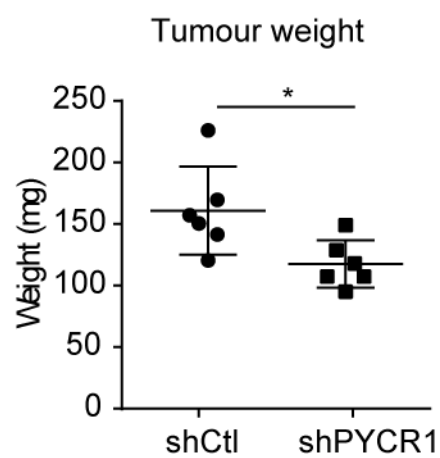


Figure 6-15 Stromal PYCR1 promotes tumour growth

Tumour weight of MCF10DCIS.com xenografts containing shCtl or shPYCR1 CAFs taken two weeks after injection. Graph shows mean and SEM of 6 tumours from one experiment. Significance was calculated using a Students t-test with Welch's correction: $p \leq 0.05$ *

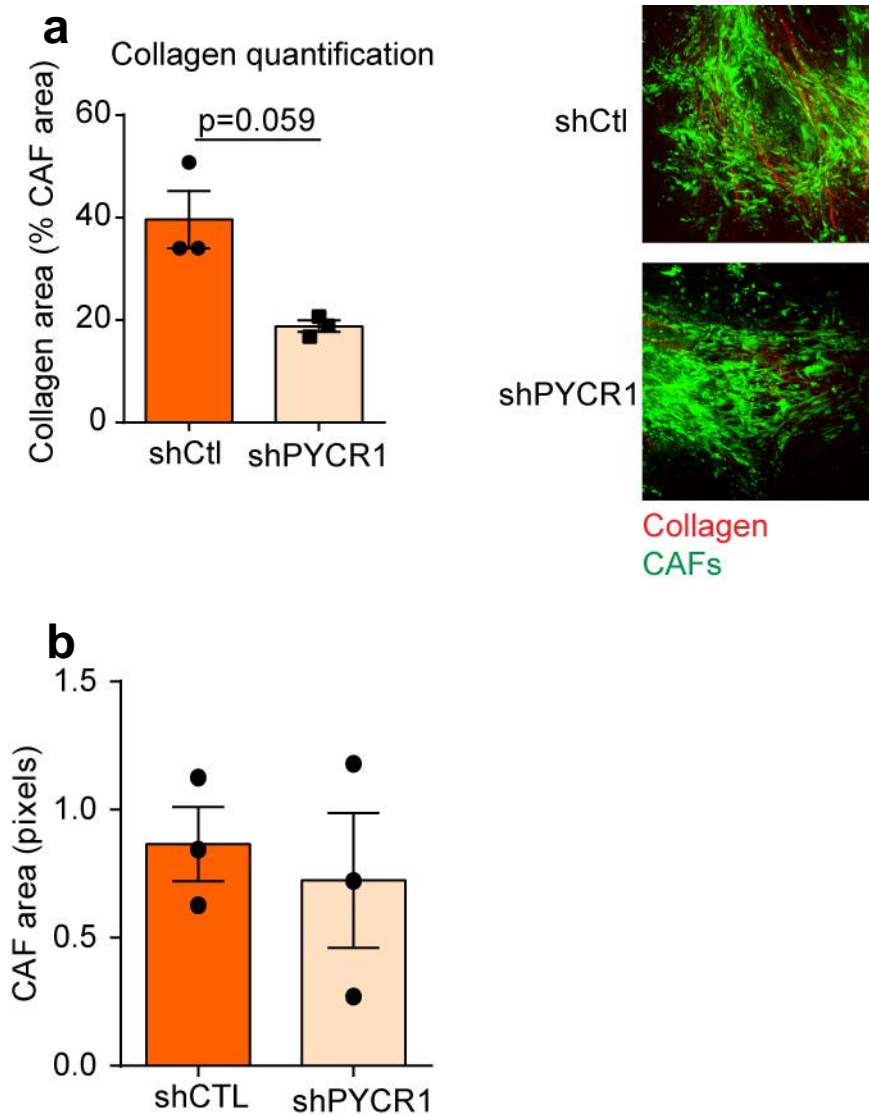


Figure 6-16 PCYR1 promotes collagen production in vivo

a: Representative images and quantification of the proportion of the area of GFP positive CAFs that is also positive for collagen in sections of xenografts containing shCtl or shPYCR1 CAFs. **b:** Quantification of the average CAF area in the images used for **a**.

Graphs show mean and SEM of at 3 biological replicates. Z-stacks of at least two areas from each tumour were acquired using a Zeiss 880 and each plane was analysed separately and the average taken.

Significance was calculated using a Students t-test with Welch's correction

6.8 Discussion

In this chapter I investigated the link between proline synthesis and collagen production. Collagen is a significant proportion of the protein output of CAFs, and is a vital component of the ECM. Proline and hydroxyproline together constitute about 25% of the amino acids in collagen. Therefore when I found that firstly the amount of intracellular proline was higher in CAFs than in NFs and secondly that PYCR1, the rate limiting enzyme for proline synthesis was also upregulated in CAFs and was regulated by c646 suggesting that it was under the control of histone acetylation, I hypothesised that the upregulation of PYCR1 drives an increase in proline production that can be used to support the translation of collagen. Although some studies have correlated the proline synthetic pathway with ECM production in the genetic disorder cutis laxa (Skidmore et al., 2011, Liang et al., 2019), until now there has not been an in depth investigation into whether proline production by PYCR1 affects collagen production.

It is interesting to note that in the MS-proteomics experiment with c646 treated iCAF, several genes related to proline were regulated, including OAT, which catalysed the first step in proline synthesis from ornithine, and EIF5A, which enables polyproline regions of mRNA to be translated. Therefore PYCR1 may not be the only enzyme relating to proline production or incorporation of proline into collagen to be under epigenetic control in CAFs. However, as PYCR1 is the rate limiting enzyme in proline synthesis, it is likely to play the most significant part in this process.

I first demonstrated that PYCR1 is under control of the same pathway as collagen proteins in CAFs. This is the first time that acetyl-coA and proline production have been connected, and demonstrates the importance of acetyl-coA as a central metabolite in regulating diverse pathways. I verified using pharmacological inhibitors that EP300 activity does regulate PYCR1 expression in CAFs, and that PYCR1 expression is also regulated by the pool of extra-mitochondrial acetyl-coA. PYCR1 was regulated both at the mRNA and at the protein level, implying that there is an increase in PYCR1 transcription and therefore that PYCR1 expression may also be epigenetically regulated. Finally, I showed that PYCR1 expression is

also regulated by the activity of PDH, which again corroborates my previous results showing that PDH activity controls the levels of intracellular acetyl-coA and histone acetylation. I then demonstrated that PYCR1 expression does indeed control intracellular proline levels. Furthermore, intracellular proline was also regulated by the extra-mitochondrial pool of acetyl-coA. Therefore production of acetyl-coA regulates production of proline by regulating PYCR1 expression through increased histone acetylation.

I then investigated whether the two pathways of proline synthesis and collagen production are connected, and indeed I demonstrated that collagen levels in fibroblast-derived ECM were regulated by PYCR1 expression. Collagen production was rescued by treating the cells with exogenous proline, showing that it is specifically proline availability that regulates collagen production. Furthermore, PYCR1 was required for PDH activity-induced collagen production, showing that PYCR1 is downstream from PDK2 and PDH activity in the process of collagen synthesis. Therefore, although PDH activity may cause increased transcription of collagen genes, the increased proline produced by PYCR1 is necessary to produce the collagen protein.

The final question of this thesis was whether PYCR1 activity could limit collagen production *in vivo* and whether or not this would have an impact on tumour progression. Xenografts of the human breast cancer cell line MCF10DCIS.com and CAFs expressing shCtl or shPYCR1 showed that tumours with shPYCR1 CAFs grew more slowly and that the shPYCR1 CAFs produced less collagen *in vivo* as well as *in vitro*. Therefore targeting PYCR1 expression has a positive effect on inhibiting the tumour stroma as well as tumour cells, and targeting PYCR1 in patients would be an effective way to metabolically target both tumour and stroma simultaneously. Previously, targeting the tumour stroma has been considered a separate endeavour from targeting tumour cells, with combination therapies to target tumour and stroma separately. This is especially true in the context of metabolism, where many studies have focussed on tumour cells and CAFs having opposing but complimentary metabolism, making targeting tumour metabolism difficult without conversely activating CAFs or vice versa (Guido et al., 2012, Martinez-Outschoorn et al., 2010b, Yang et al., 2016). However, this research has provided a target that is relevant both in tumour and in stroma, at least in breast

cancer. Furthermore, the decrease in fibrosis caused by targeting stromal PYCR1 could increase delivery and uptake of other chemotherapies, since high collagen density in the TME has been shown to impede drug delivery due to increased interstitial pressure and blood vessel compression (Netti et al., 2000, Chauhan et al., 2013)

A connection between PYCR1 and collagen production has been demonstrated before, although not specifically in CAFs. A recent study showing that PYCR1 expression is regulated by mechanotransduction through Kindlin-2 in lung adenocarcinoma also showed that when kindlin-2 expression was ablated in the lungs, there was a decrease in collagen and fibrosis in tumours, and a decrease in α -SMA positive CAFs. This suggests that PYCR1 is also required for CAF functionality (Guo et al., 2019). However, the study focussed on the role of PYCR1 in the cancer cells. Whether there was a direct connection between proline produced by PYCR1 in CAFs and collagen was unexplored, and would be more difficult to prove given that the reduction in the overall number of activated CAFs could account for the decrease in collagen in the tumours.

One question that must be addressed is the relevance of the link between proline and collagen synthesis in the context of a tumour, since proline is present in serum and I have been conducting my experiments in media that does not contain proline, with the exception of the SILAC media. Therefore CAFs may not experience so great a need to produce proline in the context of a tumour. However, the tumour microenvironment is frequently deficient in various nutrients due to the leaky vasculature of the TME and also the high demand of the cancer cells for nutrients to fuel their continual proliferation. Therefore it is reasonable to suppose that proline may be limited in the TME. In support of this, it has been shown that cancer cells take up and degrade collagen from the TME to provide them with a source of proline, showing that they require more proline than they can source from their blood supply (Olivares et al., 2017). Furthermore, the abundance of studies showing that PYCR1 is upregulated in cancer cells and is required for tumour progression also suggests that proline is limited in the TME (Cai et al., 2018, Ding et al., 2017, Hollinshead et al., 2018). From my own in vivo experiment, although some of the collagen in the tumours was produced by endogenous stroma, quantification of collagen surrounding the transplanted CAFs

suggested PYCR1 expression was a limiting factor for collagen production by CAFs in the tumour. This further suggests that CAFs are not able to uptake sufficient proline from the TME to meet their needs, although I did not quantify proline production by these cell lines in vivo.

Since PYCR1 has been shown to be upregulated in many types of tumour, another question is whether PYCR1 and proline synthesis is also upregulated in the stroma of different types of tumour, since in my PhD I have focussed solely on mammary CAFs. We analysed two previously published transcriptome datasets of ovarian fibroblasts. In laser capture microdissected stroma from ovarian cancer tissue compared to normal fibroblasts (Leung et al., 2014) both PYCR1 and ALDH18A1, which is also involved in proline synthesis from glutamate, were upregulated (Fig. 6-17). OAT, which is involved in proline synthesis from ornithine, was not upregulated however, suggesting that the glutamate pathway is more prominent. Similarly, transcriptome profiling of TGF- β treated and normal ovarian fibroblasts showed upregulation of PYCR1 and ALDH18A1, but not OAT (Fig. 6-18) (Yeung et al., 2013). Therefore upregulation of proline synthesis in the stroma is not confined to mammary CAFs and could be a more universal pathway to support collagen synthesis in CAFs. In the future, it would be useful to investigate PYCR1 expression in the stroma of more types of tumour with a high stromal content, such as PDAC, in order to find out how universal this pathway is and also to further stratify which tumours might benefit from treatments targeting PYCR1 to reduce fibrosis.

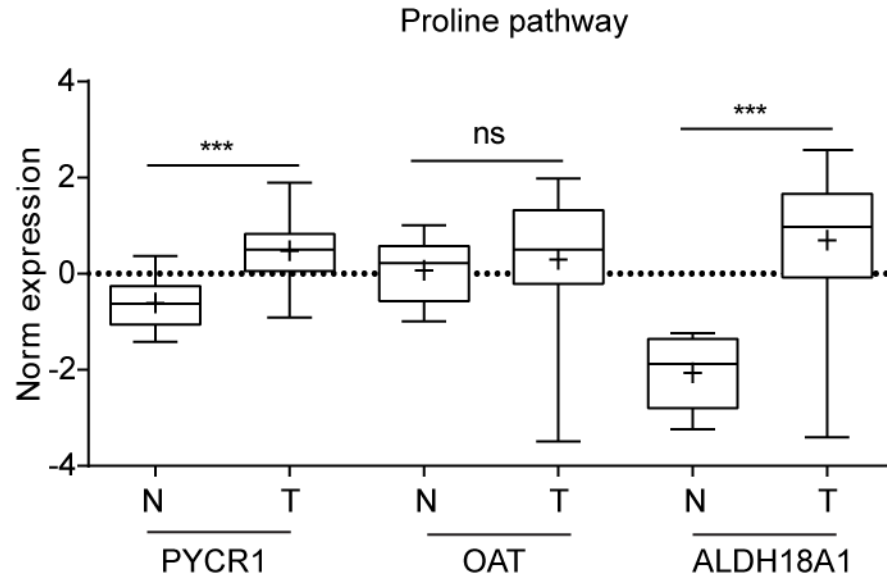


Figure 6-17 Proline synthesis pathway is upregulated in ovarian stroma

Graph shows normalised expression of genes involved in proline synthesis between normal and tumour associated fibroblasts isolated from ovarian tissue samples by laser capture microdissection. Significance was calculated using a Students t-test with Welch's correction: $p \leq 0.05$ *, $p \leq 0.01$ **, $p \leq 0.001$ ***

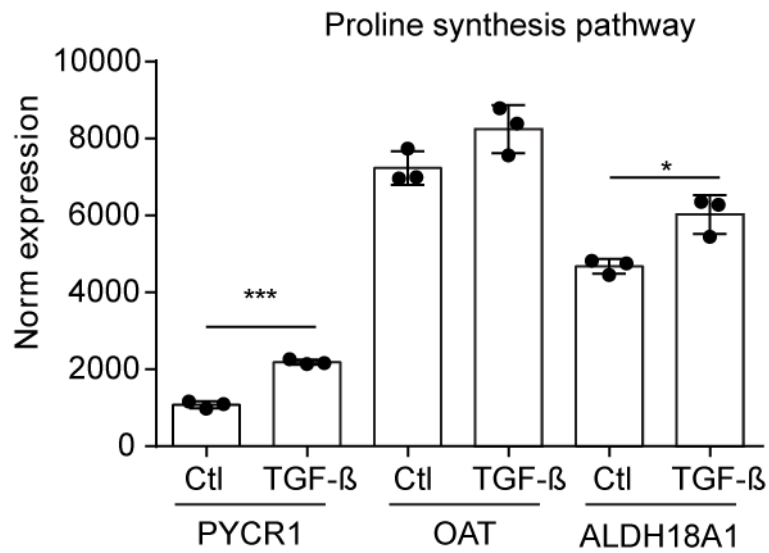


Figure 6-18 Proline synthesis pathway is upregulated in TGF-B treated fibroblasts

Graph shows normalised expression of genes involved in proline synthesis between control and TGF-B treated ovarian fibroblasts. Significance was calculated using a students t-test with Welch's correction: $p \leq 0.05$ *, $p \leq 0.01$ **, $p \leq 0.001$ ***

Chapter 7 Discussion and Future work

7.1 Discussion

In this thesis I investigated the vital role of metabolism in the maintenance of the pro-tumourigenic phenotype in mammary CAFs. Specifically, I showed how CAF metabolism influences collagen production, which is a major output of CAFs in the TME. Collagen has long been known to play an important role in breast cancer. At the clinical level, breast tumours with a high collagen content have a poorer prognosis (Conklin et al., 2011, Kauppila et al., 1998). Collagens promote tumour growth and metastasis, and induce solid stress that impedes drug delivery to tumours (Provenzano et al., 2008, Netti et al., 2000, Kaushik et al., 2016). Indeed, targeting fibrotic collagen production with angiotensin inhibition improved chemotherapy delivery and reduced hypoxia in breast and pancreatic cancer models (Chauhan et al., 2013). Therefore targeting collagen production in breast cancer and other tumour types with a desmoplastic TME would be an effective way to target tumour growth and metastasis, as well as improving the efficiency of conventional anti-cancer therapies. Since CAFs are the major source of collagen in the TME, they are most promising target to reduce collagen in tumours. In this work, using an unbiased approach, I discovered metabolic pathways supporting collagen production in CAFs. Specifically, I uncovered two distinct, but connected, metabolic pathways that support collagen synthesis by CAFs: acetyl-coA synthesis by PDH and proline synthesis by PYCR1. PDH-derived acetyl-coA controls collagen transcription through epigenetic regulation, and PYCR1 supports collagen production by providing building blocks for its translation into protein (Fig. 7-1). The two metabolic pathways that I have identified as regulators of collagen production in CAFs both provide possibilities for developing new ways to therapeutically target collagen production by CAFs to inhibit the formation of a fibrotic TME. This has the potential to reduce the pro-tumourigenic functions of the TME and improve tumour perfusion.

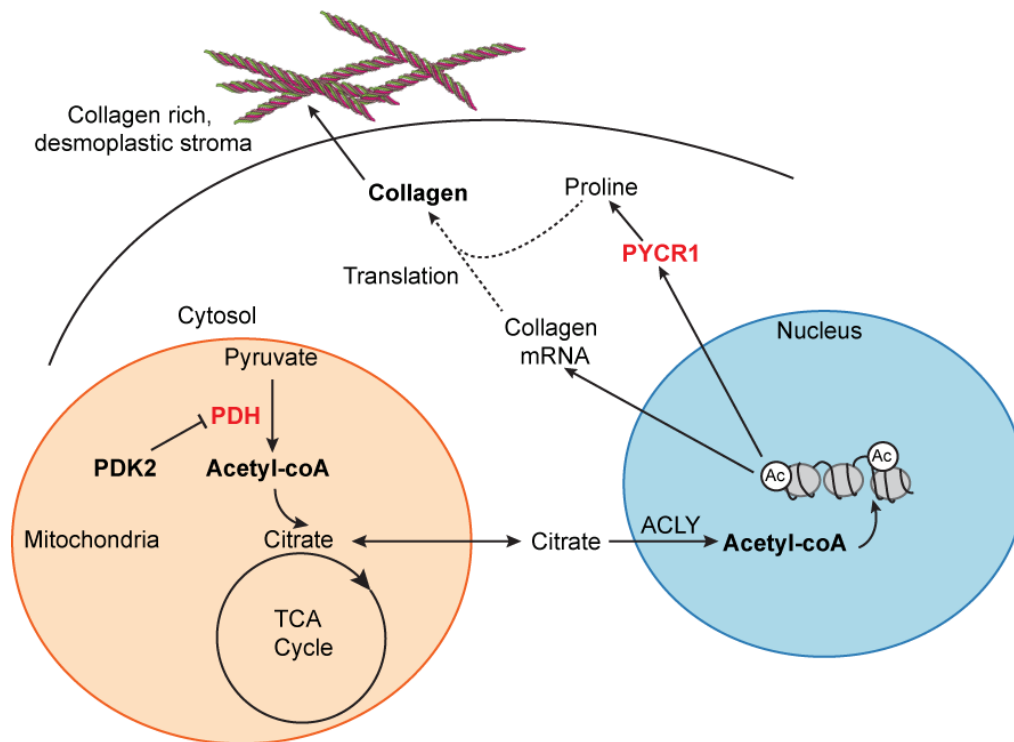


Figure 7-1 Working model

Increased PDH activity leads to increased acetyl-coA production in CAFs. Acetyl-coA is exported out of the mitochondria via citrate, and is converted back to acetyl-coA by ACLY. In the nucleus, acetyl-coA is used for histone acetylation, leading to increased transcription of collagen genes. Simultaneously, PYCR1 expression is also upregulated, enabling increased proline production. Proline is then used to support translation of collagen mRNA, and collagen is secreted into the ECM to create a pro-tumourigenic, desmoplastic stroma.

I used two models of mammary CAFs and NFs for my research: the iCAF/iNFs and pCAF/pNFs. Whereas the iCAFs were activated from immortalised NFs isolated from a healthy individual by an *in vivo* co-culture with cancer cells, the pCAFs and pNFs were derived separately from breast cancer patient tissue samples. All the fibroblasts were immortalised with hTERT (Calvo et al., 2013) to enable in depth characterisation without them becoming senescent. Collagen production and high levels of α SMA expression are defining features of the activated, myofibroblast phenotype (Ronnov-Jessen and Petersen, 1993). My group has previously shown that the iCAF have a myofibroblast phenotype and I ensured that the pCAFs recapitulated the myofibroblast phenotype by monitoring their α SMA expression. All the CAFs expressed high levels of α SMA compared to the NFs, showing that they were activated. Further functional characterisation of the fibroblasts carried out by other members of the lab has shown that the CAF secretome is more pro-invasive and pro-angiogenic than their paired NFs, further supporting that both the iCAFs and pCAFs are relevant models of the activated, myofibroblast phenotype.

The first key finding of my thesis was that PDH phosphorylation at key regulatory sites is reduced in CAFs. I found this was due to the reduced expression of the kinase PDK2 in CAFs. As a consequence of its reduced phosphorylation, PDH was more active in CAFs. Moreover, by increasing or decreasing PDK2 expression in CAFs and NFs I could regulate PDH phosphorylation and acetyl-coA production, thus showing that, although other PDKs can phosphorylate PDH, PDK2 alone is an important regulator of PDH activity in fibroblasts. The role of PDKs and PDH have largely been unexplored in CAF metabolism, despite PDH being a central metabolic enzyme connecting glycolytic, oxidative and lipid metabolism. A comparison of metabolic protein levels by IHC staining in lung tumour and stromal cells showed that PDK expression was low and PDH expression high in stromal cells compared to the tumour cells (Koukourakis et al., 2014). A further study from the same group showed that PDH expression, but not phosphorylation, is upregulated in fibroblasts upon co-culture with lung tumour cells (Koukourakis et al., 2017). While this is slightly different from the results from my mammary fibroblasts, in which PDH expression is unchanged but the phosphorylation is decreased in CAFs, the end result is still that PDH is more active in CAFs. However, neither of these studies investigated the functional consequences of PDH activity in the lung stroma.

Therefore, the discovery that PDH activity was upregulated in mammary CAFs opened up many questions regarding how CAFs might use the resulting acetyl-coA to rewire their metabolism or alter protein acetylation levels.

Extensive metabolic profiling and mitochondrial characterisation of the CAFs and NFs did not immediately reveal differentially regulated pathways that might be affected by PDH activity. Surprisingly, there was no evidence that PDH activity affected TCA cycle flux. In proliferating fibroblasts compared to quiescent fibroblasts, it has been shown that there is a decrease in citrate conversion to alpha-ketoglutarate due to decreased IDH expression, and that citrate is preferentially exported to the cytosol (Lemons et al., 2010). IDH3 expression has also been found to be downregulated in prostate CAFs, which could further exacerbate TCA cycle truncation (Zhang et al., 2015). This is in accordance with my metabolic tracing experiments, in which I saw that in CAFs and NFs, which are both proliferative, glucose was incorporated into citrate but then was incorporated at a much lower ratio into other TCA cycle metabolites. Glutamine is then the main source of TCA cycle metabolites, although there was still evidence of a lack of transmission of labelled carbon atoms from citrate to α -ketoglutarate and of some backwards flux from α -ketoglutarate to citrate (citrate +5 labelled) when cells were labelled with ^{13}C -glutamine (Fig 4-10). Both CAFs and NFs clearly have a truncated TCA cycle, and the increased PDH activity in CAFs exacerbated this effect. CAFs contained significantly higher levels of intracellular citrate than NFs, yet this difference was not reflected in the levels of other TCA cycle metabolites. Furthermore, the increase in citrate in CAFs was also not reflected in total cholesterol levels or fatty acid synthesis. Instead, MS analysis of the global acetylome of CAFs and NFs suggested that the acetyl-coA produced by PDH may be used as an epigenetic regulator to increase histone acetylation. Many histone sites were more acetylated in CAFs, but of these H3K27 was the only site annotated with a known regulatory function: as a potent activator of transcription (Raisner et al., 2018). Since histone acetylation is known to be a general indicator of active transcription, I cannot exclude that the other identified acetylated histone sites also play a role in regulating gene expression in CAFs. For example, H3K18 and H3K23, both of which are also known to be regulated by EP300 and are associated with active transcription, were also more acetylated in CAFs. Further

investigation into deciphering the histone code is required to uncover the specific role of these acetylation sites.

It may therefore be that in proliferating fibroblasts, the mechanism of channelling PDH-produced acetyl-coA into the cytoplasm and thence to the nucleus via citrate to maintain histone acetylation is shared between CAFs and NFs due to the truncated TCA cycle. However, in CAFs this is more pronounced by upregulating PDH activity to increase histone acetylation. Furthermore, there is some evidence that the levels of nucleocytosolic acetyl-coA influence the site specificity of EP300 to alter histone acetylation patterns (Henry et al., 2014, Henry et al., 2013). Therefore in addition to increasing overall histone acetylation, the increased acetyl-coA in CAFs could also regulate which histone sites are more acetylated.

In my thesis I directly connected mitochondrial acetyl-coA production by PDH with histone acetylation. Previous works showing that intracellular acetyl-coA levels induce histone acetylation have focussed on the synthesis of acetyl-coA in the nucleus from acetate or from nuclear PDH rather than mitochondrial PDH (Sutendra et al., 2014, Sivanand et al., 2018, Choudhary et al., 2014). The role of mitochondrial PDH has previously been studied for the most part as a metabolic gatekeeper linking glycolytic, oxidative and lipid metabolism (Randle, 1986, Saunier et al., 2016). PDH activity does not affect these metabolic pathways in CAFs and NFs, at least when kept in normal culture conditions, so while this is undoubtedly a vitally important function of PDH in many cell types, it does not appear to have a prominent role in my mammary CAFs. Mitochondrial acetyl-coA has been shown to contribute to protein acetylation in the mitochondria (Baeza et al., 2016), but whether mitochondrial PDH activity impacts acetylation of proteins outside of the mitochondria has not been largely explored. This is perhaps surprising given that it is well-known that acetyl-coA can be exported out of the mitochondria and it has been shown to impact cytoplasmic metabolic pathways, such as lipid synthesis (Mahmood et al., 2016). Indeed, ACLY, which is crucial for export of acetyl-coA from the mitochondria has been shown to play an important role in protein acetylation (Wellen et al., 2009, Kinnaird et al., 2016). My work therefore shows that protein acetylation and in particular histone acetylation should be considered along with cellular metabolism during future research into the role of PDH in cells. This is especially important when IDH activity is decreased

since low IDH activity prevents acetyl-coA from being channelled into the TCA cycle and therefore promotes export of acetyl-coA from the mitochondria.

My work provides the first evidence that CAF metabolism regulates the CAF epigenetic phenotype through histone acetylation and that a link exists between PDH-mediated acetyl-coA production and collagen synthesis. My proteomic analysis of CAFs with inhibition of the HAT EP300 suggested that histone acetylation in CAFs was involved in activating transcription of ECM genes, which I subsequently confirmed with in vitro assays. There have been several studies showing that epigenetic changes are responsible for the increase in collagen production in myofibroblasts, indicating that a way through which CAFs can maintain a significant increase in collagen production is by increasing the transcription of the corresponding genes. My research has uncovered that PDH activity is an upstream regulator of this mechanism. TGF β signalling is known to induce upregulation of ECM production in CAFs, and studies have shown that TGF β is linked to expression of ECM genes through epigenetic alterations (Sun et al., 2010, Vizoso et al., 2015). Since my work suggests that collagen expression is epigenetically regulated through PDH independently of TGF β signalling, there may therefore be multiple mechanisms that CAFs can use to epigenetically control ECM production. Recently, CAF metabolism was shown to contribute to decreased H3K27 and H3K4 trimethylation through increased expression of nicotinamide N-methyltransferase (NNMT) (Eckert et al., 2019). The decrease in histone methylation was induced by the depletion of S-adenosyl methionine by NNMT and promoted the transcription of markers of CAF activation, including ECM proteins. Furthermore, BET inhibitors, which block the response of BRD transcription factors to acetylated histones, inhibited the fibrotic phenotype in pancreatic cancer-associated stellate cells, suggesting that increased histone acetylation is an important epigenetic regulator of fibroblast activation (Kumar et al., 2017). H3K27 acetylation is a known binding site for BRD4, and a decrease in H3K27me could be accompanied by an increase in H3K27ac, however, H3K27ac was not specifically investigated in these studies. Therefore my results showing that EP300 activity and histone acetylation are increased in CAFs further corroborate the existence of an epigenetic switch in CAFs to promote ECM production. Additionally, also my findings indicate activation of transcription in CAFs, since H3K27ac is a well-known marker of active transcription and is often found at

enhancer regions (Raisner et al., 2018). It is already known that pathways activating transcription factors are upregulated in CAFs, such as TGF β and NF- κ B signalling (Kojima et al., 2010, Pavlides et al., 2010b). Moreover, the CAF phenotype involves high levels of protein secretion (Hernandez-Fernaud et al., 2017). It is therefore likely that overall transcription is upregulated in order to maintain an increased protein output, and my finding that overall histones were more acetylated supports this possibility.

In addition to ECM-related proteins, PDGFR, which is a well-known marker of CAF activation, was also significantly downregulated in the c646-treated CAF proteome. Other proteins that have been previously associated with CAF pro-tumourigenic functions were also downregulated, such as TAGLN, THY1 and ITGA11 (Schliekelman et al., 2017, Navab et al., 2015, Yu et al., 2013). Therefore, in addition to regulating ECM production, histone acetylation may regulate other aspects of the activated CAF phenotype that might be relevant in cancer and therefore interesting to explore in the future.

The second metabolic pathway that I found to regulate collagen production in CAFs was proline synthesis by PYCR1. There is increasing interest in how metabolites affect collagen synthesis. Amino acid availability clearly plays an important role, since glycine synthesis has been recently shown to regulate collagen production in fibrosis by maintaining the levels of glycine, which is highly abundant in collagens (Selvarajah et al., 2019). My work is the first to demonstrate that production and availability of the amino acid proline is important for collagen production. Pyruvate metabolism has also been shown to be important for collagen deposition. Collagen hydroxylation at proline residues is critical for the production of functional collagen molecules, because it stabilises the collagen helix. Pyruvate metabolism has been shown to support proline hydroxylation by providing a source of alpha-ketoglutarate which is a cofactor required for prolyl hydroxylase activity (Elia et al., 2019). Interestingly, the total levels of alpha-ketoglutarate were consistently higher in CAFs than in NFs, suggesting that the CAFs could also metabolically maintain the increased need of prolyl hydroxylase activity for collagen production. Why CAFs have more alpha-ketoglutarate is still an open question. The metabolomics tracing experiments that I performed showed that in CAFs alpha-ketoglutarate was derived mostly from glutamine rather than pyruvate

produced from glucose. I did not assess the contribution of extracellular pyruvate to TCA cycle metabolites, as pyruvate can enter the TCA cycle independently from the acetyl-coA pathway via conversion to oxaloacetate. Therefore tracing experiments using isotope labelled pyruvate should be performed to assess whether pyruvate could be a source of alpha-ketoglutarate in CAFs. Alternatively, the production of acetyl-coA from citrate by ACLY produces oxaloacetate in the cytosol. This oxaloacetate can be then combined with glutamate to make alpha-ketoglutarate and aspartate (Fig. 7-2). It would therefore be interesting to investigate further the roles of extracellular pyruvate and alpha-ketoglutarate metabolism in regulating collagen production in CAFs.

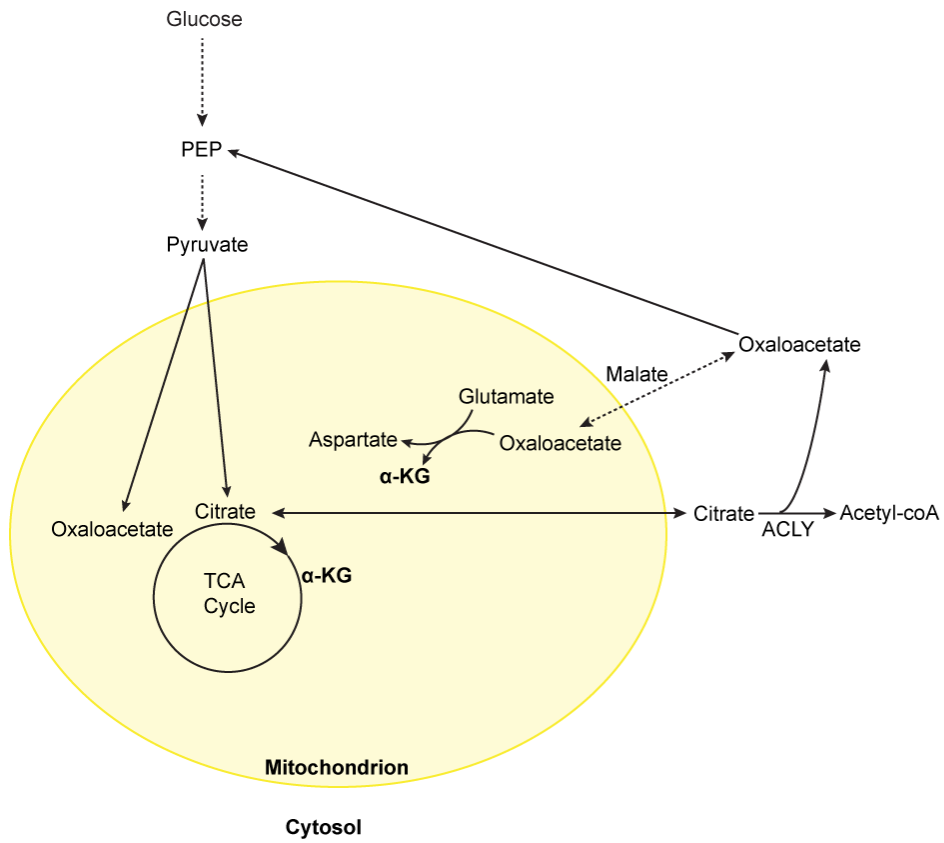


Figure 7-2 Sources of alpha-ketoglutarate

Diagram showing that oxaloacetate and pyruvate are possible sources of alpha-ketoglutarate

By showing that PYCR1 expression is downstream of the PDH-induced histone acetylation in mammary CAFs, and that an increase in acetyl-coA availability corresponds with an increase in the intracellular proline levels, I provided the first link between acetyl-coA production by PDH and the proline synthesis pathway. Moreover, I have shown that EP300 activity is a key linker of these two pathways. However, I have not yet solved the details of the mechanism through which the epigenetic regulation triggered by PDH activity in CAFs coordinates the downstream increase in ECM and PYCR1 expression. Although, as discussed previously, it is already known that collagen synthesis is epigenetically regulated in fibroblasts, the regulation of PYCR1 at the epigenetic level has not been previously studied. Whilst I provided evidence that PYCR1 expression is controlled both by EP300 activity and acetyl-coA availability, it is possible that PYCR1 is not directly regulated by H3K27 acetylation, but is upregulated as part of a feedback mechanism when proline becomes limiting due to the increase demand of proline for collagen synthesis. PYCR1 levels have been shown to be upregulated by a lack of proline precursors (Loayza-Puch et al., 2016) and translation of mRNA transcripts for biosynthetic enzymes in bacteria is known to be inhibited by binding of amino acids to riboswitches, so that, when that amino acid is in short supply, translation of the mRNA is activated (Serganov and Patel, 2009). Transcription factors can also respond to shortages of amino acids, such as the ATF family of transcription factors (Kilberg et al., 2012). Therefore a proline sensing mechanism could be in place, so that when collagen production is increased and proline is used up more rapidly, more PYCR1 is produced. Since I saw upregulation of PYCR1 mRNA expression as well as the protein levels in conditions where histone acetylation is upregulated, it seems likely that there is a transcriptional or epigenetic component upstream of PYCR1 activation.

I have shown that reduced levels of PYCR1 are sufficient to reduce the amount of collagen produced by CAFs, and that treating the cells with exogenous proline rescued the phenotype. This strongly points to the use of proline for translation as a limiting factor in collagen synthesis. A first indication of the importance of this process in vivo was the decreased tumour growth and collagen levels between MCF10DCIS.com breast cancer cells xenografts with shPYCR1 CAFs compared to the shCTL CAFs. This first in vivo experiment was important to show that reduced levels of PYCR1 in CAFs have a positive effect on reducing tumour growth in

xenografts, which provides further support for targeting PYCR1 in breast cancer, since reducing PYCR1 expression in breast cancer cells has already been demonstrated to reduce growth and invasion (Ding et al., 2017). If PYCR1 inhibition also has a beneficial effect in inhibiting the pro-tumourigenic stroma, this could be a very effective strategy for targeting tumours. My data therefore suggest that tumours with both high PYCR1 expression and a significant stromal component would be good candidates for therapy involving PYCR1 inhibition.

Much of the research on PYCR1 activity has focussed on its role in protecting against oxidative stress and apoptosis. In skin fibroblasts taken from cutis laxa patients with mutations leading to decreased levels or activity of PYCR1, there is an increase in mitochondrial dysfunction and ROS-mediated apoptosis due to the loss of protection against oxidative stress given by the activity of the proline cycle. (Cai et al., 2018, Reversade et al., 2009). No studies have yet investigated whether PYCR1 and proline production also protect against oxidative stress in CAFs. CAFs have been shown to have decreased mitochondrial functionality and increased ROS production in several studies (Martinez-Outschoorn et al., 2010b, Pavlides et al., 2010b). PYCR1 activity could therefore be a means of protecting the CAFs from ROS induced apoptosis and alleviating some of the negative effects of increased oxidative stress in CAFs. If PYCR1 activity does affect mitochondrial functionality in CAFs, inhibiting PYCR1 in the stroma could increase apoptosis in CAFs and thus reduce the total amount of pro-tumourigenic stroma in addition to targeting collagen production. Surprisingly, in my experiments the shCTL and shPYCR1 CAFs proliferated similarly in vitro. This suggests that if there are differences in mitochondrial functionality, they do not affect cell survival under standard cell culture conditions. These results are consistent with my data showing that, although there is a decrease in functional mitochondria in the mammary CAFs, this does not affect oxygen consumption rate, mitochondrial metabolism or proliferation under basal cell culture conditions, suggesting that a certain amount of mitochondrial dysfunction is tolerated by the CAFs. Although mitochondrial dysfunction may become a greater vulnerability in the context of the TME where nutrients and oxygen are limited, in the two week period that the shCTL and shPYCR1 CAFs grew together with the cancer cells in xenografts, I did not observe differences in the area of CAFs remaining. This suggests that the shPYCR1 CAFs are neither deficient in growth nor more apoptotic due to the loss

of PYCR1 in vivo. I cannot, however, exclude the possibility that differences would appear over a longer period of time. Further in vivo experiments would be required to confirm this. Another possible reason that I did not see differences in the amount of CAFs in vivo is that the shRNA against PYCR1 reduced PYCR1 levels only by about 50% at the protein level. This reduction could have been sufficient to reduce collagen production in culture, but it might not be enough to cause mitochondrial dysfunction and increased apoptosis as described in PYCR1 mutant cells.

In recent years, the topic of CAF subpopulations and the possibility of targeting specific subpopulations have been studied more closely. I was therefore curious to investigate whether the metabolic pathways that I have identified are similarly regulated in a particular subset of CAFs. Current studies point to at least two subpopulations existing, of which one is pro-inflammatory and one is α SMA high and myofibroblastic (Bartoschek et al., 2018, Ohlund et al., 2017, Costa et al., 2018). I analysed the gene expression data from the study by Ohlund et al., which focusses on two CAF phenotypes isolated from the KPC mouse model, because this study clearly differentiated between the pro-inflammatory and myofibroblastic subpopulations. I found that *Pdk2* was downregulated and *Pycr1* and *Aldh18a1* were upregulated in CAFs from the myofibroblastic subpopulation compared to the inflammatory subpopulation (Fig. 7-3) (Ohlund et al., 2017). This provides further evidence that the mechanism that I have discovered may be a general mechanism activated in myofibroblastic cells and not specific to the mammary CAFs I have studied, and also suggests that this pathway might be best targeted in tumours with a high proportion of α SMA positive CAFs in the stroma.

To conclude, I have discovered an novel mechanism through which two metabolic pathways work together to support increase collagen production in activated CAFs both, at gene and protein expression level. Both of these pathways provide opportunities for targeting the activated CAF phenotype, with different advantages to each. PDH has several times been proposed as a therapeutic target; although until recently this has always been in the context of trying to activate PDH in tumour cells to mitigate the Warburg effect. However, although individual cases have responded to dichloroacetate treatment to inhibit PDK activity, in clinical trials no positive effect has been demonstrated (Dunbar et al., 2014,

Flavin, 2010b, Powell, 2015). Based on my work, activating PDH to reduce cancer cell aggressiveness might conversely increase the pro-tumorigenic and pro-fibrotic activity of the stroma, reducing the efficacy of this strategy. Thus, the effects of targeting PDH on the stroma should also be taken into account, and possibly tumours with a low stromal component would benefit most from PDK inhibitors. Furthermore, since PDH activation has a general effect on upregulating histone acetylation in CAFs, more pathways will be affected by PDH activation or inhibition than just ECM production, the effects of which I have not investigated. Therefore further investigation into which tumours might respond to DCA treatment is required, and probably tumours with a lower stromal component would be a better choice for further clinical testing. The drug CPI-613, which inhibits PDH activity, has had much greater success in clinical trials and, for example, has shown positive results in PDAC (Alistar, 2018), which is known to have a significant stromal component and in which the stroma has been shown to be highly pro-tumourigenic. CPI-613 is currently in clinical trials for other tumour types including breast, leukaemia, lung and liver cancer. It will be interesting both to find out whether CPI-613 is also effective in other tumours with a high stromal content, such as breast cancer, and also to investigate whether CPI-613 reduces the stromal component in mouse models as this would further support my results on the importance of activated PDH in promoting the fibrotic CAF phenotype.

PYCR1 is well known to be upregulated in many tumours, and targeting PYCR1 in cancer cells inhibits tumour growth and metastasis (Cai et al., 2018, Ding et al., 2017, Hollinshead et al., 2018). Here I have shown that PYCR1 is also upregulated and plays a pro-tumourigenic role in the stroma, making it an ideal target to simultaneously inhibit tumour and stromal cells. A small molecule PYCR1 inhibitor has been developed recently (Milne et al., 2019), which will create opportunities to test whether general PYCR1 inhibition, rather than specific ablation in cancer or stromal cells, is well tolerated in vivo and whether it is an effective anti-cancer therapy. The development of an inhibitor is a crucial step in being able to assess the impact of targeting PYCR1 in different tumour models and to verify whether it is an effective treatment strategy.

The standard treatment for most breast cancers is either surgery or radiotherapy, combined with adjuvant or sometimes neoadjuvant chemotherapy or other drug

therapies. Targeting collagen synthesis in CAFs, either through PDH or PYCR1 inhibition, would likely be most effective as a combination therapy with the current standard drug treatments. Reducing stromal collagen could improve tumour perfusion and thereby drug delivery, enhancing the effectiveness of the chemotherapy. Additionally, it could further contribute to reducing growth of the primary tumour in addition to any established metastases. In tumours where there are not yet detectable metastases, inhibiting collagen production by fibroblasts could also reduce the interaction of circulating tumour cells with the pre-metastatic niche, since increased collagen crosslinking has been shown to be important for colony formation by disseminated breast cancer cells (Cox et al., 2015).

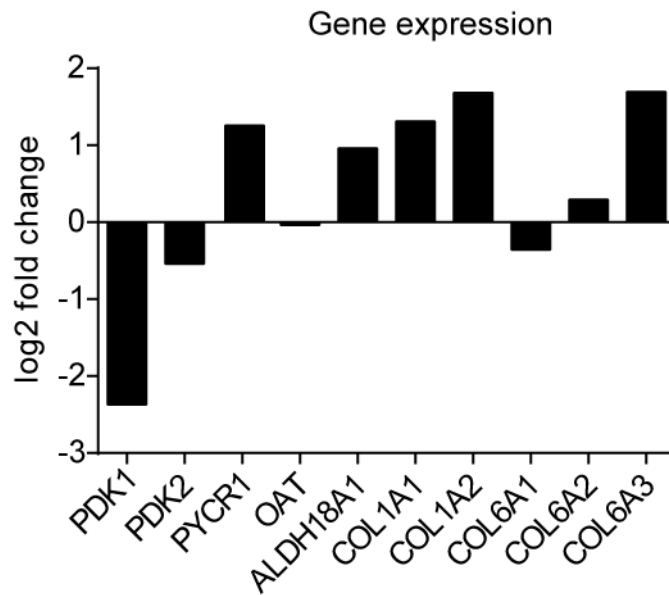


Figure 7-3 Expression of PDK, proline synthesis and collagen genes in CAF subpopulations

Graphs show the log₂ fold change in gene expression of PDK1, PDK2, the proline synthesis pathway and collagens in myfibroblastic CAFs (myCAF) compared to inflammatory CAFs (iCAF). The dataset was taken from Ohlund et al., 2017.

7.2 Future Work

For the future, several questions remain outstanding which merit further research. It would be interesting to discover what lies upstream of PDK2 downregulation in CAFs to understand the trigger of the cascade of events that I have described. CAFs are known to maintain their activation through autocrine signalling feedback loops, such as TGF β (Kojima et al., 2010). Therefore it is possible that interactions with their own ECM stimulate further ECM production by CAFs in another positive feedback loop to maintain CAF activation. My initial experiments suggest that CAF-derived ECM stimulates PDK2 downregulation, possibly via PI3K/Akt signalling. Since integrins mediate a vast proportion of cell-ECM interactions, I would first carry out experiments in which integrins were inhibited to try and narrow down which integrin or integrins might be responsible for this pathway, and to investigate further the role of Akt/PI3K signalling in regulating collagen production by CAFs. I would also investigate the effects of FAK inhibitors on collagen production by CAFs, since FAK mediates integrin signalling and has previously been shown to regulate collagen production in fibroblasts (Kinoshita et al., 2013, Rajshankar et al., 2017). The PI3K/Akt/mTOR signalling pathway has been previously implicated in collagen production during idiopathic pulmonary fibrosis (Mercer et al., 2016). In this study the pathway was under the control of TGF- β signalling. However, TGF- β signalling does not appear to trigger PDK2 regulation, because my data showed that TGF β -1 stimulation did not regulate PDH phosphorylation in CAFs. Further experiments using other TGF- β receptor ligands would reveal whether TGF- β signalling plays any role at all in regulating PDK2 in CAFs. Interestingly, PYCR1 has recently been shown to be upregulated in response to ECM interactions in cancer cells (Guo et al., 2019). Therefore there is a precedent for ECM interactions regulating proline synthesis enzymes, and it will be important to test whether CAF-ECM can also stimulate proline production and PYCR1 expression in fibroblasts as this would further corroborate my results demonstrating a connection between PDH phosphorylation and PYCR1 expression.

In this work I focussed on the role of histone acetylation and proline production in the context of collagen production in CAFs. Interestingly, several other ECM proteins were also downregulated in the MS-proteomic analysis of CAFs with EP300

inhibition by c646, including fibronectin. Fibronectin is known to contribute a significant proportion of CAF-derived ECM and to play important roles in tumour progression (Tang et al., 2016, Pickup et al., 2014). Our analysis of the proline content of ECM proteins showed that, similarly to collagens, fibronectin is also a proline-rich protein. It would therefore be interesting to extend my analysis and investigate the role of PDH and PYCR1 activity in the context of fibronectin production. It would also be important to do ChIP-Seq for H3K27ac in CAFs and NFs or CAFs treated with c646 to uncover which of the proteins that I found to be regulated by EP300 activity in my proteomic study are directly regulated by changes in H3K27 acetylation on enhancer regions of their genes. This would also clarify whether PYCR1 is epigenetically regulated by the same pathway as the collagens or whether it is regulated by other signalling downstream of collagen production. Moreover, since EP300 regulates acetylation of other histone sites and other histone sites were regulated between the acetylomes of CAFs and NFs, an unbiased MS-acetylome analysis of fibroblasts expressing different levels of PDK2 would tell us whether the epigenetic control triggered by PDH activity also involves other histone modifications. c646 is also not completely specific for EP300 (Shrimp et al., 2015), so to verify that my results are EP300 dependent I would need to repeat the key experiments with another EP300 inhibitor, such as A-485, which has been shown to specifically inhibit the ability of EP300 to acetylate H3K27 (Lasko et al., 2017). To explore the mechanism for the epigenetic control of collagen in CAFs in more depth, I would also need to investigate which transcription factors are regulating the epigenetic control of specific genes by EP300. To identify candidate transcription factors, I could use a MS-based proteomic approach and perform immunoprecipitation experiments to determine which factors interact with EP300 and H3K27ac in the fibroblasts with different levels of PDH activity.

The role of proline in maintaining redox homeostasis and protecting against ROS and apoptosis has been investigated in the context of cancer cells (Cai et al., 2018, Hollinshead et al., 2018, Kuo et al., 2016); as yet there have been no studies on proline metabolism and oxidative stress in CAFs. Although I did not observe any differences in survival between shCtl and shPYCR1 fibroblasts, either in vitro or in vivo, it is possible that a stronger depletion of PYCR1 is necessary to see differences. To address this, we are currently isolating mouse embryonic

fibroblasts (MEFs) from *Pycr1* $-/-$ mice which we plan to use for further xenograft experiments where they will be co-transplanted with 4T1 or E0771 cancer cells. The effect of the PYCR1 KO in these fibroblasts will be much stronger than the shPYCR1 cells that I have used for my experiments, so it is possible that we will see greater effects on vulnerability to ROS and survival in vitro and in vivo than we did with the shPYCR1 CAFs.

Changes in the rate of proline production can also affect other metabolic pathways, because a by-product of proline synthesis by PYCR1 is the production of NADP⁺ or NAD⁺. I did not observe any significant differences in the NADH:NAD⁺ ratio between CAFs and NFs in my metabolomic experiments, with the exception of the pCAF3/pNF3 pair (Fig. 4-9). This suggests that the extra NAD⁺ in CAFs is used up in further metabolic reactions. NAD⁺ is required for production of acetyl-coA by PDH, so the NAD⁺ could be used to maintain the increase in PDH activity in CAFs. NAD⁺ can be also be used to fuel glycolysis as it is required for flux through GAPDH. I did see an overall increase in intracellular PEP, which is downstream of GAPDH, in the CAFs, which could imply that there is an increase in flux through this part of the glycolytic pathway. NADP⁺ is required for the pentose phosphate pathway branch of glucose metabolism, which I did not investigate in my metabolomic tracing experiments, and PYCR1 activity has been previously shown to affect flux through the pentose phosphate pathway (Liu et al., 2015). Therefore, to determine whether the CAFs use PYCR1 produced NAD⁺ and NADP⁺ for glycolysis or the pentose phosphate pathway respectively I could use MS-metabolomic tracing experiments to compare the flux through glyceraldehyde-3-phosphate dehydrogenase and enzymes of the pentose phosphate pathway in the shCtl and shPYCR1 CAFs.

Another question that is still not entirely answered is whether the proline residues produced by PYCR1 directly affect the translation of collagen mRNA into protein. I have shown that reducing PYCR1 levels is sufficient to reduce proline production and that the level of intracellular proline correlates with the amount of collagen deposited in the ECM by CAFs. I also demonstrated by MS-proteomics that proline produced by PYCR1 (i.e. ¹³C-proline labelled collagen) is incorporated into collagen, and that there is a decreased amount of collagen produced using glutamine-derived proline in the shPYCR1 CAFs. Whether this result is due to a

lack of proline for translation has not been conclusively shown. To answer this question, we are collaborating with Dr. Fabricio Loayza-Puch from the Deutsches Krebsforschung Zentrum in Heidelberg to measure whether there is an increase in ribosome stalling at proline codons in CAFs when CAFs express lower levels of PYCR1. This will determine whether proline produced by PYCR1 is necessary for protein translation.

Finally, the *in vivo* xenograft experiment provided preliminary evidence that reducing levels of PYCR1 in fibroblasts affects collagen production and tumour growth in a xenograft model. However, the endogenous murine fibroblasts were also present in the stroma of the tumours, making it difficult to conclusively state that the collagen measured was produced by the human pCAFs that we had transplanted. Further experiments are required to answer this question. First, I could isolate the transplanted fibroblasts and use qPCR and Western blot analyses to determine if the shPYCR1 fibroblasts express less collagen *in vivo*. Moreover, I could use a mouse model where PYCR1 is knocked out in the endogenous murine stroma, or perhaps treating tumour bearing mice with the small molecule inhibitor of PYCR1 which has recently been developed (Milne et al., 2019).

Whether PDH inhibition in the stroma *in vivo* would have the same effect as inhibiting PYCR1 has not yet been addressed. We are currently working to create a model with *Pdha1* specifically deleted in fibroblasts through an *Fsp1-Cre* model (Trimboli et al., 2008). In collaboration with the Transgenic Mouse Models team we are carrying out the necessary crosses to generate those mice in FVB and C57Bl/6 backgrounds for syngeneic orthotopic transplantation of breast cancer cells, such as E0771 or lines isolated from the GEM model MMTV-PyMT model. In addition to altering PDHA1 activity genetically, we could also target PDHA1 pharmacologically using the PDH inhibitor CPI-613 in syngeneic orthotopic models or the MMTV-PyMT GEM model. CPI-613 is not specific for PDH as it also inhibits α -ketoglutarate dehydrogenase, however it would be a good starting point to investigate the role of PDH activity on collagen production and tumour progression *in vivo*. If we find that CPI-613 and PYCR1 inhibition significantly decrease the amount of collagen in the stroma, we will test the effects of the inhibitors on tumour perfusion and whether this can improve drug delivery and the efficacy of chemotherapy.

To conclude, in this thesis I have shown that CAFs metabolically regulate collagen production both through increased PDH-mediated acetyl-coA production for epigenetic regulation of collagen genes, and through increased proline production to support production of collagen proteins. My results open up new possibilities for therapeutically targeting the desmoplastic TME to reduce tumour growth and metastasis, and to improve tumour perfusion and drug delivery.

References

- ADAMS, E. & FRANK, L. 1980. Metabolism of proline and the hydroxyprolines. *Annu Rev Biochem*, 49, 1005-61.
- ALBRENGUES, J., BERTERO, T., GRASSET, E., BONAN, S., MAIEL, M., BOURGET, I., PHILIPPE, C., HERRAIZ SERRANO, C., BENAMAR, S., CROCE, O., SANZ-MORENO, V., MENEGUZZI, G., FERAL, C. C., CRISTOFARI, G. & GAGGIOLI, C. 2015. Epigenetic switch drives the conversion of fibroblasts into proinvasive cancer-associated fibroblasts. *Nat Commun*, 6, 10204.
- ALEXANDER, J. & CUKIERMAN, E. 2016. Stromal dynamic reciprocity in cancer: intricacies of fibroblastic-ECM interactions. *Curr Opin Cell Biol*, 42, 80-93.
- ALISTAR, N. 2018. *A Phase I/II Open-Label Dose-Escalation Clinical Trial of CPI-613 in Combination With Gemcitabine in Cancer Patients* [Online]. Available: <https://ClinicalTrials.gov/show/NCT00907166> [Accessed].
- ALLEN, E., MIEVILLE, P., WARREN, C. M., SAGHAFINIA, S., LI, L., PENG, M. W. & HANAHAN, D. 2016. Metabolic Symbiosis Enables Adaptive Resistance to Anti-angiogenic Therapy that Is Dependent on mTOR Signaling. *Cell Rep*, 15, 1144-60.
- ANDERSON, K. A. & HIRSCHEY, M. D. 2012. Mitochondrial protein acetylation regulates metabolism. *Essays Biochem*, 52, 23-35.
- AO, M., BREWER, B. M., YANG, L., FRANCO CORONEL, O. E., HAYWARD, S. W., WEBB, D. J. & LI, D. 2015. Stretching fibroblasts remodels fibronectin and alters cancer cell migration. *Sci Rep*, 5, 8334.
- APER, S. J., VAN SPREEUWEL, A. C., VAN TURNHOUT, M. C., VAN DER LINDEN, A. J., PIETERS, P. A., VAN DER ZON, N. L., DE LA RAMBELJE, S. L., BOUTEN, C. V. & MERKX, M. 2014. Colorful protein-based fluorescent probes for collagen imaging. *PLoS One*, 9, e114983.
- ARAS, S. & ZAIDI, M. R. 2017. TAMEless traitors: macrophages in cancer progression and metastasis. *Br J Cancer*, 117, 1583-1591.
- ASENCIO, C., RODRIGUEZ-HERNANDEZ, M. A., BRIONES, P., MONTOYA, J., CORTES, A., EMPERADOR, S., GAVILAN, A., RUIZ-PESINI, E., YUBERO, D., MONTERO, R., PINEDA, M., O'CALLAGHAN, M. M., ALCAZAR-FABRA, M., SALVIATI, L., ARTUCH, R. & NAVAS, P. 2016. Severe encephalopathy associated to pyruvate dehydrogenase mutations and unbalanced coenzyme Q10 content. *Eur J Hum Genet*, 24, 367-72.
- ATA, R. & ANTONESCU, C. N. 2017. Integrins and Cell Metabolism: An Intimate Relationship Impacting Cancer. *Int J Mol Sci*, 18.
- ATTIA, R. R., CONNNAUGHTON, S., BOONE, L. R., WANG, F., ELAM, M. B., NESS, G. C., COOK, G. A. & PARK, E. A. 2010. Regulation of pyruvate dehydrogenase kinase 4 (PDK4) by thyroid hormone: role of the peroxisome proliferator-activated receptor gamma coactivator (PGC-1 alpha). *J Biol Chem*, 285, 2375-85.
- AUCIELLO, F. R., BULUSU, V., OON, C., TAIT-MULDER, J., BERRY, M., BHATTACHARYYA, S., TUMANOV, S., ALLEN-PETERSEN, B. L., LINK, J., KENDSERSKY, N. D., VRINGER, E., SCHUG, M., NOVO, D., HWANG, R. F., EVANS, R. M., NIXON, C., DORRELL, C., MORTON, J. P., NORMAN, J. C., SEARS, R. C., KAMPHORST, J. J. & SHERMAN, M. H. 2019. A Stromal Lysolipid-Autotaxin Signaling Axis Promotes Pancreatic Tumor Progression. *Cancer Discov*, 9, 617-627.
- AVGUSTINOVA, A., IRAVANI, M., ROBERTSON, D., FEARN, A., GAO, Q., KLINGBEIL, P., HANBY, A. M., SPEIRS, V., SAHAI, E., CALVO, F. & ISACKE, C. M. 2016. Tumour cell-derived Wnt7a recruits and activates fibroblasts to promote tumour aggressiveness. *Nat Commun*, 7, 10305.
- BAE, Y. H., MUI, K. L., HSU, B. Y., LIU, S. L., CRETU, A., RAZINIA, Z., XU, T., PURE, E. & ASSOIAN, R. K. 2014. A FAK-Cas-Rac-lamellipodin signaling module transduces extracellular matrix stiffness into mechanosensitive cell cycling. *Sci Signal*, 7, ra57.
- BAEZA, J., SMALLEGAN, M. J. & DENU, J. M. 2016. Mechanisms and Dynamics of Protein Acetylation in Mitochondria. *Trends Biochem Sci*, 41, 231-244.

- BAGER, C. L., WILLUMSEN, N., LEEMING, D. J., SMITH, V., KARSDAL, M. A., DORNAN, D. & BAY-JENSEN, A. C. 2015. Collagen degradation products measured in serum can separate ovarian and breast cancer patients from healthy controls: A preliminary study. *Cancer Biomark*, 15, 783-8.
- BARTOSCHEK, M., OSKOLKOV, N., BOCCI, M., LOVROT, J., LARSSON, C., SOMMARIN, M., MADSEN, C. D., LINDGREN, D., PEKAR, G., KARLSSON, G., RINGNER, M., BERGH, J., BJORKLUND, A. & PIETRAS, K. 2018. Spatially and functionally distinct subclasses of breast cancer-associated fibroblasts revealed by single cell RNA sequencing. *Nat Commun*, 9, 5150.
- BARTOVA, E., KREJCI, J., HARNICAROVA, A., GALIOVA, G. & KOZUBEK, S. 2008. Histone modifications and nuclear architecture: a review. *J Histochem Cytochem*, 56, 711-21.
- BAUML, J., SEIWERT, T. Y., PFISTER, D. G., WORDEN, F., LIU, S. V., GILBERT, J., SABA, N. F., WEISS, J., WIRTH, L., SUKARI, A., KANG, H., GIBSON, M. K., MASSARELLI, E., POWELL, S., MEISTER, A., SHU, X., CHENG, J. D. & HADDAD, R. 2017. Pembrolizumab for Platinum- and Cetuximab-Refractory Head and Neck Cancer: Results From a Single-Arm, Phase II Study. *J Clin Oncol*, 35, 1542-1549.
- BEYER, C., REICHERT, H., AKAN, H., MALLANO, T., SCHRAMM, A., DEES, C., PALUMBO-ZERR, K., LIN, N. Y., DISTLER, A., GELSE, K., VARGA, J., DISTLER, O., SCHETT, G. & DISTLER, J. H. 2013. Blockade of canonical Wnt signalling ameliorates experimental dermal fibrosis. *Ann Rheum Dis*, 72, 1255-8.
- BHOOGAL, R. K., STOICA, C. M., MCGAHA, T. L. & BONA, C. A. 2005. Molecular aspects of regulation of collagen gene expression in fibrosis. *J Clin Immunol*, 25, 592-603.
- BHOWMICK, N. A., NEILSON, E. G. & MOSES, H. L. 2004. Stromal fibroblasts in cancer initiation and progression. *Nature*, 432, 332-7.
- BOIRE, A., COVIC, L., AGARWAL, A., JACQUES, S., SHERIFI, S. & KULIOPULOS, A. 2005. PAR1 is a matrix metalloprotease-1 receptor that promotes invasion and tumorigenesis of breast cancer cells. *Cell*, 120, 303-13.
- BONNET, S., ARCHER, S. L., ALLALUNIS-TURNER, J., HAROMY, A., BEAULIEU, C., THOMPSON, R., LEE, C. T., LOPASCHUK, G. D., PUTTAGUNTA, L., BONNET, S., HARRY, G., HASHIMOTO, K., PORTER, C. J., ANDRADE, M. A., THEBAUD, B. & MICHELAKIS, E. D. 2007. A mitochondria-K⁺ channel axis is suppressed in cancer and its normalization promotes apoptosis and inhibits cancer growth. *Cancer Cell*, 11, 37-51.
- BONUCCELLI, G., WHITAKER-MENEZES, D., CASTELLO-CROS, R., PAVLIDES, S., PESTELL, R. G., FATATIS, A., WITKIEWICZ, A. K., VANDER HEIDEN, M. G., MIGNECO, G., CHIAVARINA, B., FRANK, P. G., CAPOZZA, F., FLOMENBERG, N., MARTINEZ-OUTSCHOORN, U. E., SOTGIA, F. & LISANTI, M. P. 2010. The reverse Warburg effect: glycolysis inhibitors prevent the tumor promoting effects of caveolin-1 deficient cancer associated fibroblasts. *Cell Cycle*, 9, 1960-71.
- BOOT-HANDFORD, R. P. & TUCKWELL, D. S. 2003. Fibrillar collagen: the key to vertebrate evolution? A tale of molecular incest. *Bioessays*, 25, 142-51.
- BOWKER-KINLEY, M. M., DAVIS, W. I., WU, P., HARRIS, R. A. & POPOV, K. M. 1998. Evidence for existence of tissue-specific regulation of the mammalian pyruvate dehydrogenase complex. *Biochem J*, 329 (Pt 1), 191-6.
- BRAUER, H. A., MAKOWSKI, L., HOADLEY, K. A., CASBAS-HERNANDEZ, P., LANG, L. J., ROMAN-PEREZ, E., D'ARCY, M., FREEMERMAN, A. J., PEROU, C. M. & TROESTER, M. A. 2013. Impact of tumor microenvironment and epithelial phenotypes on metabolism in breast cancer. *Clin Cancer Res*, 19, 571-85.
- BREDFELDT, J. S., LIU, Y., CONKLIN, M. W., KEELY, P. J., MACKIE, T. R. & ELICEIRI, K. W. 2014. Automated quantification of aligned collagen for human breast carcinoma prognosis. *J Pathol Inform*, 5, 28.
- BUSCH, S., RYDEN, L., STAL, O., JIRSTROM, K. & LANDBERG, G. 2012. Low ERK phosphorylation in cancer-associated fibroblasts is associated with tamoxifen resistance in pre-menopausal breast cancer. *PLoS One*, 7, e45669.

- CAI, F., MIAO, Y., LIU, C., WU, T., SHEN, S., SU, X. & SHI, Y. 2018. Pyrroline-5-carboxylate reductase 1 promotes proliferation and inhibits apoptosis in non-small cell lung cancer. *Oncol Lett*, 15, 731-740.
- CAI, L., SUTTER, B. M., LI, B. & TU, B. P. 2011. Acetyl-CoA induces cell growth and proliferation by promoting the acetylation of histones at growth genes. *Mol Cell*, 42, 426-37.
- CALVO, F., EGE, N., GRANDE-GARCIA, A., HOOPER, S., JENKINS, R. P., CHAUDHRY, S. I., HARRINGTON, K., WILLIAMSON, P., MOEENDARBARY, E., CHARRAS, G. & SAHAI, E. 2013. Mechanotransduction and YAP-dependent matrix remodelling is required for the generation and maintenance of cancer-associated fibroblasts. *Nat Cell Biol*, 15, 637-46.
- CAO, W., YACOUB, S., SHIVERICK, K. T., NAMIKI, K., SAKAI, Y., PORVASNIK, S., URBANEK, C. & ROSSER, C. J. 2008. Dichloroacetate (DCA) sensitizes both wild-type and over expressing Bcl-2 prostate cancer cells in vitro to radiation. *Prostate*, 68, 1223-31.
- CAPPARELLI, C., GUIDO, C., WHITAKER-MENEZES, D., BONUCCELLI, G., BALLIET, R., PESTELL, T. G., GOLDBERG, A. F., PESTELL, R. G., HOWELL, A., SNEDDON, S., BIRBE, R., TSIRIGOS, A., MARTINEZ-OUTSCHOORN, U., SOTGIA, F. & LISANTI, M. P. 2012. Autophagy and senescence in cancer-associated fibroblasts metabolically supports tumor growth and metastasis via glycolysis and ketone production. *Cell Cycle*, 11, 2285-302.
- CARITO, V., BONUCCELLI, G., MARTINEZ-OUTSCHOORN, U. E., WHITAKER-MENEZES, D., CAROLEO, M. C., CIONE, E., HOWELL, A., PESTELL, R. G., LISANTI, M. P. & SOTGIA, F. 2012. Metabolic remodeling of the tumor microenvironment: migration stimulating factor (MSF) reprograms myofibroblasts toward lactate production, fueling anabolic tumor growth. *Cell Cycle*, 11, 3403-14.
- CARMELIET, P. 2005. VEGF as a key mediator of angiogenesis in cancer. *Oncology*, 69 Suppl 3, 4-10.
- CARMELIET, P. & JAIN, R. K. 2000. Angiogenesis in cancer and other diseases. *Nature*, 407, 249-257.
- CASTELLO-CROS, R., BONUCCELLI, G., MOLCHANSKY, A., CAPOZZA, F., WITKIEWICZ, A. K., BIRBE, R. C., HOWELL, A., PESTELL, R. G., WHITAKER-MENEZES, D., SOTGIA, F. & LISANTI, M. P. 2011. Matrix remodeling stimulates stromal autophagy, "fueling" cancer cell mitochondrial metabolism and metastasis. *Cell Cycle*, 10, 2021-34.
- CASTRICONI, R., CANTONI, C., DELLA CHIESA, M., VITALE, M., MARCENARO, E., CONTE, R., BIASSONI, R., BOTTINO, C., MORETTA, L. & MORETTA, A. 2003. Transforming growth factor beta 1 inhibits expression of NKp30 and NKG2D receptors: consequences for the NK-mediated killing of dendritic cells. *Proc Natl Acad Sci U S A*, 100, 4120-5.
- CATE, R. L. & ROCHE, T. E. 1978. A unifying mechanism for stimulation of mammalian pyruvate dehydrogenase(a) kinase by reduced nicotinamide adenine dinucleotide, dihydrolipoamide, acetyl coenzyme A, or pyruvate. *J Biol Chem*, 253, 496-503.
- CERNIGLIA, G. J., DEY, S., GALLAGHER-COLOMBO, S. M., DAURIO, N. A., TUTTLE, S., BUSCH, T. M., LIN, A., SUN, R., ESIPOVA, T. V., VINOGRADOV, S. A., DENKO, N., KOUMENIS, C. & MAITY, A. 2015. The PI3K/Akt Pathway Regulates Oxygen Metabolism via Pyruvate Dehydrogenase (PDH)-E1alpha Phosphorylation. *Mol Cancer Ther*, 14, 1928-38.
- CHAE, Y. C., VAIRA, V., CAINO, M. C., TANG, H. Y., SEO, J. H., KOSENKOV, A. V., OTTOBRINI, L., MARTELLI, C., LUCIGNANI, G., BERTOLINI, I., LOCATELLI, M., BRYANT, K. G., GHOSH, J. C., LISANTI, S., KU, B., BOSARI, S., LANGUINO, L. R., SPEICHER, D. W. & ALTIERI, D. C. 2016. Mitochondrial Akt Regulation of Hypoxic Tumor Reprogramming. *Cancer Cell*, 30, 257-272.
- CHANG, P. H., HWANG-VERSLUES, W. W., CHANG, Y. C., CHEN, C. C., HSIAO, M., JENG, Y. M., CHANG, K. J., LEE, E. Y., SHEW, J. Y. & LEE, W. H. 2012. Activation of Robo1 signaling of breast cancer cells by Slit2 from stromal fibroblast restrains tumorigenesis via blocking PI3K/Akt/beta-catenin pathway. *Cancer Res*, 72, 4652-61.

- CHAUHAN, V. P., MARTIN, J. D., LIU, H., LACORRE, D. A., JAIN, S. R., KOZIN, S. V., STYLIANOPOULOS, T., MOUSA, A. S., HAN, X., ADSTAMONGKONKUL, P., POPOVIĆ, Z., HUANG, P., BAWENDI, M. G., BOUCHER, Y. & JAIN, R. K. 2013. Angiotensin inhibition enhances drug delivery and potentiates chemotherapy by decompressing tumour blood vessels. *Nature Communications*, 4.
- CHEN, J., GUCCINI, I., DI MITRI, D., BRINA, D., REVANDKAR, A., SARTI, M., PASQUINI, E., ALAJATI, A., PINTON, S., LOSA, M., CIVENNI, G., CATAPANO, C. V., SGRIGNANI, J., CAVALLI, A., D'ANTUONO, R., ASARA, J. M., MORANDI, A., CHIARUGI, P., CROTTI, S., AGOSTINI, M., MONTOPOLI, M., MASGRAS, I., RASOLA, A., GARCIA-ESCUADERO, R., DELALEU, N., RINALDI, A., BERTONI, F., BONO, J., CARRACEDO, A. & ALIMONTI, A. 2018. Compartmentalized activities of the pyruvate dehydrogenase complex sustain lipogenesis in prostate cancer. *Nat Genet*, 50, 219-228.
- CHEN, P., CESCONE, M. & BONALDO, P. 2013. Collagen VI in cancer and its biological mechanisms. *Trends Mol Med*, 19, 410-7.
- CHEN, Y., ZENG, C., ZHAN, Y., WANG, H., JIANG, X. & LI, W. 2017. Aberrant low expression of p85alpha in stromal fibroblasts promotes breast cancer cell metastasis through exosome-mediated paracrine Wnt10b. *Oncogene*, 36, 4692-4705.
- CHENG, B., GAO, F., MAISSY, E. & XU, P. 2019. Repurposing suramin for the treatment of breast cancer lung metastasis with glycol chitosan-based nanoparticles. *Acta Biomater*, 84, 378-390.
- CHERNOV, A. V., BARANOVSKAYA, S., GOLUBKOV, V. S., WAKEMAN, D. R., SNYDER, E. Y., WILLIAMS, R. & STRONGIN, A. Y. 2010. Microarray-based transcriptional and epigenetic profiling of matrix metalloproteinases, collagens, and related genes in cancer. *J Biol Chem*, 285, 19647-59.
- CHIAVARINA, B., WHITAKER-MENEZES, D., MIGNECO, G., MARTINEZ-OUTSCHOORN, U. E., PAVLIDES, S., HOWELL, A., TANOWITZ, H. B., CASIMIRO, M. C., WANG, C., PESTELL, R. G., GRIESHABER, P., CARO, J., SOTGIA, F. & LISANTI, M. P. 2010. HIF1-alpha functions as a tumor promoter in cancer associated fibroblasts, and as a tumor suppressor in breast cancer cells: Autophagy drives compartment-specific oncogenesis. *Cell Cycle*, 9, 3534-51.
- CHOI, J., KIM, D. H., JUNG, W. H. & KOO, J. S. 2013. Metabolic interaction between cancer cells and stromal cells according to breast cancer molecular subtype. *Breast Cancer Res*, 15, R78.
- CHOUHARY, C., WEINERT, B. T., NISHIDA, Y., VERDIN, E. & MANN, M. 2014. The growing landscape of lysine acetylation links metabolism and cell signalling. *Nat Rev Mol Cell Biol*, 15, 536-50.
- CIMEN, H., HAN, M. J., YANG, Y., TONG, Q., KOC, H. & KOC, E. C. 2010. Regulation of succinate dehydrogenase activity by SIRT3 in mammalian mitochondria. *Biochemistry*, 49, 304-11.
- COHEN, N., SHANI, O., RAZ, Y., SHARON, Y., HOFFMAN, D., ABRAMOVITZ, L. & EREZ, N. 2017. Fibroblasts drive an immunosuppressive and growth-promoting microenvironment in breast cancer via secretion of Chitinase 3-like 1. *Oncogene*, 36, 4457-4468.
- COLAK, S. & TEN DIJKE, P. 2017. Targeting TGF-beta Signaling in Cancer. *Trends Cancer*, 3, 56-71.
- COMITO, G., GIANNONI, E., SEGURA, C. P., BARCELLOS-DE-SOUZA, P., RASPOLINI, M. R., BARONI, G., LANCIOTTI, M., SERNI, S. & CHIARUGI, P. 2014. Cancer-associated fibroblasts and M2-polarized macrophages synergize during prostate carcinoma progression. *Oncogene*, 33, 2423-31.
- CONKLIN, M. W., EICKHOFF, J. C., RICHING, K. M., PEHLKE, C. A., ELICEIRI, K. W., PROVENZANO, P. P., FRIEDL, A. & KEELY, P. J. 2011. Aligned collagen is a prognostic signature for survival in human breast carcinoma. *Am J Pathol*, 178, 1221-32.
- CONNAUGHTON, S., CHOWDHURY, F., ATTIA, R. R., SONG, S., ZHANG, Y., ELAM, M. B., COOK, G. A. & PARK, E. A. 2010. Regulation of pyruvate dehydrogenase kinase

- isoform 4 (PDK4) gene expression by glucocorticoids and insulin. *Mol Cell Endocrinol*, 315, 159-67.
- CONTRACTOR, T. & HARRIS, C. R. 2012. p53 negatively regulates transcription of the pyruvate dehydrogenase kinase Pdk2. *Cancer Res*, 72, 560-7.
- COSTA, A., KIEFFER, Y., SCHOLER-DAHIREL, A., PELON, F., BOURACHOT, B., CARDON, M., SIRVEN, P., MAGAGNA, I., FUHRMANN, L., BERNARD, C., BONNEAU, C., KONDRATOVA, M., KUPERSTEIN, I., ZINOVYEV, A., GIVEL, A. M., PARRINI, M. C., SOUMELIS, V., VINCENT-SALOMON, A. & MECHTA-GRIGORIOU, F. 2018. Fibroblast Heterogeneity and Immunosuppressive Environment in Human Breast Cancer. *Cancer Cell*, 33, 463-479 e10.
- COX, J., HEIN, M. Y., LUBER, C. A., PARON, I., NAGARAJ, N. & MANN, M. 2014. Accurate Proteome-wide Label-free Quantification by Delayed Normalization and Maximal Peptide Ratio Extraction, Termed MaxLFQ. *Molecular & Cellular Proteomics*, 13, 2513-2526.
- COX, J. & MANN, M. 2008. MaxQuant enables high peptide identification rates, individualized p.p.b.-range mass accuracies and proteome-wide protein quantification. *Nat Biotechnol*, 26, 1367-72.
- COX, J. & MANN, M. 2012. 1D and 2D annotation enrichment: a statistical method integrating quantitative proteomics with complementary high-throughput data. *BMC Bioinformatics*, 13 Suppl 16, S12.
- COX, T. R., RUMNEY, R. M. H., SCHOOF, E. M., PERRYMAN, L., HOYE, A. M., AGRAWAL, A., BIRD, D., LATIF, N. A., FORREST, H., EVANS, H. R., HUGGINS, I. D., LANG, G., LINDING, R., GARTLAND, A. & ERLER, J. T. 2015. The hypoxic cancer secretome induces pre-metastatic bone lesions through lysyl oxidase. *Nature*, 522, 106-110.
- DAMIANO, J. S. 2002. Integrins as novel drug targets for overcoming innate drug resistance. *Curr Cancer Drug Targets*, 2, 37-43.
- DARBY, I. A., LAVERDET, B., BONTE, F. & DESMOULIERE, A. 2014. Fibroblasts and myofibroblasts in wound healing. *Clin Cosmet Investig Dermatol*, 7, 301-11.
- DAVIES, M. N., KJALARSDOTTIR, L., THOMPSON, J. W., DUBOIS, L. G., STEVENS, R. D., ILKAYEVA, O. R., BROSNAN, M. J., ROLPH, T. P., GRIMSRUD, P. A. & MUOIO, D. M. 2016. The Acetyl Group Buffering Action of Carnitine Acetyltransferase Offsets Macronutrient-Induced Lysine Acetylation of Mitochondrial Proteins. *Cell Rep*, 14, 243-54.
- DE INGENIIS, J., RATNIKOV, B., RICHARDSON, A. D., SCOTT, D. A., AZA-BLANC, P., DE, S. K., KAZANOV, M., PELLECCIA, M., RONAI, Z., OSTERMAN, A. L. & SMITH, J. W. 2012. Functional specialization in proline biosynthesis of melanoma. *PLoS One*, 7, e45190.
- DE KRUIJF, E. M., VAN NES, J. G., VAN DE VELDE, C. J., PUTTER, H., SMIT, V. T., LIEFERS, G. J., KUPPEN, P. J., TOLLENAAR, R. A. & MESKER, W. E. 2011. Tumor-stroma ratio in the primary tumor is a prognostic factor in early breast cancer patients, especially in triple-negative carcinoma patients. *Breast Cancer Res Treat*, 125, 687-96.
- DE PAZ-LUGO, P., LUPIANEZ, J. A. & MELENDEZ-HEVIA, E. 2018. High glycine concentration increases collagen synthesis by articular chondrocytes in vitro: acute glycine deficiency could be an important cause of osteoarthritis. *Amino Acids*, 50, 1357-1365.
- DEAN, R. A., COX, J. H., BELLAC, C. L., DOUCET, A., STARR, A. E. & OVERALL, C. M. 2008. Macrophage-specific metalloelastase (MMP-12) truncates and inactivates ELR+ CXC chemokines and generates CCL2, -7, -8, and -13 antagonists: potential role of the macrophage in terminating polymorphonuclear leukocyte influx. *Blood*, 112, 3455-64.
- DEES, C., ZERR, P., TOMCIK, M., BEYER, C., HORN, A., AKHMETSHINA, A., PALUMBO, K., REICH, N., ZWERINA, J., STICHERLING, M., MATTSON, M. P., DISTLER, O., SCHETT, G. & DISTLER, J. H. 2011. Inhibition of Notch signaling prevents experimental fibrosis and induces regression of established fibrosis. *Arthritis Rheum*, 63, 1396-404.

- DEGENHARDT, T., SARMAKI, A., MALINEN, M., RIECK, M., VAISANEN, S., HUOTARI, A., HERZIG, K. H., MULLER, R. & CARLBERG, C. 2007. Three members of the human pyruvate dehydrogenase kinase gene family are direct targets of the peroxisome proliferator-activated receptor beta/delta. *J Mol Biol*, 372, 341-55.
- DEL RIO, A., PEREZ-JIMENEZ, R., LIU, R., ROCA-CUSACHS, P., FERNANDEZ, J. M. & SHEETZ, M. P. 2009. Stretching single talin rod molecules activates vinculin binding. *Science*, 323, 638-41.
- DERYUGINA, E. I. & QUIGLEY, J. P. 2015. Tumor angiogenesis: MMP-mediated induction of intravasation- and metastasis-sustaining neovasculature. *Matrix Biol*, 44-46, 94-112.
- DIMANCHE-BOITREL, M. T., VAKAET, L., JR., PUJUGUET, P., CHAUFFERT, B., MARTIN, M. S., HAMMANN, A., VAN ROY, F., MAREEL, M. & MARTIN, F. 1994. In vivo and in vitro invasiveness of a rat colon-cancer cell line maintaining E-cadherin expression: an enhancing role of tumor-associated myofibroblasts. *Int J Cancer*, 56, 512-21.
- DING, J., KUO, M. L., SU, L., XUE, L., LUH, F., ZHANG, H., WANG, J., LIN, T. G., ZHANG, K., CHU, P., ZHENG, S., LIU, X. & YEN, Y. 2017. Human mitochondrial pyrroline-5-carboxylate reductase 1 promotes invasiveness and impacts survival in breast cancers. *Carcinogenesis*, 38, 519-531.
- DING, N., YU, R. T., SUBRAMANIAM, N., SHERMAN, M. H., WILSON, C., RAO, R., LEBLANC, M., COULTER, S., HE, M., SCOTT, C., LAU, S. L., ATKINS, A. R., BARISH, G. D., GUNTON, J. E., LIDDLE, C., DOWNES, M. & EVANS, R. M. 2013. A vitamin D receptor/SMAD genomic circuit gates hepatic fibrotic response. *Cell*, 153, 601-13.
- DING, W. X. & YIN, X. M. 2012. Mitophagy: mechanisms, pathophysiological roles, and analysis. *Biol Chem*, 393, 547-64.
- DING, X., JI, J., JIANG, J., CAI, Q., WANG, C., SHI, M., YU, Y., ZHU, Z. & ZHANG, J. 2018. HGF-mediated crosstalk between cancer-associated fibroblasts and MET-unamplified gastric cancer cells activates coordinated tumorigenesis and metastasis. *Cell Death Dis*, 9, 867.
- DOERFEL, L. K., WOHLGEMUTH, I., KOTHE, C., PESKE, F., URLAUB, H. & RODNINA, M. V. 2013. EF-P is essential for rapid synthesis of proteins containing consecutive proline residues. *Science*, 339, 85-8.
- DONNARUMMA, E., FIORE, D., NAPPA, M., ROSCIGNO, G., ADAMO, A., IABONI, M., RUSSO, V., AFFINITO, A., PUOTI, I., QUINTAVALLE, C., RIENZO, A., PISCUOGLIO, S., THOMAS, R. & CONDORELLI, G. 2017. Cancer-associated fibroblasts release exosomal microRNAs that dictate an aggressive phenotype in breast cancer. *Oncotarget*, 8, 19592-19608.
- DROR, S., SANDER, L., SCHWARTZ, H., SHEINBOIM, D., BARZILAI, A., DISHON, Y., APCHER, S., GOLAN, T., GREENBERGER, S., BARSHACK, I., MALCOV, H., ZILBERBERG, A., LEVIN, L., NESSLING, M., FRIEDMANN, Y., IGRAS, V., BARZILAY, O., VAKNINE, H., BRENNER, R., ZINGER, A., SCHROEDER, A., GONEN, P., KHALED, M., EREZ, N., HOHEISEL, J. D. & LEVY, C. 2016. Melanoma miRNA trafficking controls tumour primary niche formation. *Nat Cell Biol*, 18, 1006-17.
- DUNBAR, E. M., COATS, B. S., SHROADS, A. L., LANGAEE, T., LEW, A., FORDER, J. R., SHUSTER, J. J., WAGNER, D. A. & STACPOOLE, P. W. 2014. Phase 1 trial of dichloroacetate (DCA) in adults with recurrent malignant brain tumors. *Invest New Drugs*, 32, 452-64.
- DUNNWARD, L. K., ROSSING, M. A. & LI, C. I. 2007. Hormone receptor status, tumor characteristics, and prognosis: a prospective cohort of breast cancer patients. *Breast Cancer Res*, 9, R6.
- DURAN, R. V., MACKENZIE, E. D., BOULAHBEL, H., FREZZA, C., HEISERICH, L., TARDITO, S., BUSSOLATI, O., ROCHA, S., HALL, M. N. & GOTTLIEB, E. 2013. HIF-independent role of prolyl hydroxylases in the cellular response to amino acids. *Oncogene*, 32, 4549-56.
- DVORAK, H. F. 2015. Tumors: wounds that do not heal-redux. *Cancer Immunol Res*, 3, 1-11.
- DVORAK, K. M., PETTEE, K. M., RUBINIC-MINOTTI, K., SU, R., NESTOR-KALINOSKI, A. & EISENMANN, K. M. 2018. Carcinoma associated fibroblasts (CAFs) promote breast

- cancer motility by suppressing mammalian Diaphanous-related formin-2 (mDia2). *PLoS One*, 13, e0195278.
- ECKERT, M. A., COSCIA, F., CHRYPLEWICZ, A., CHANG, J. W., HERNANDEZ, K. M., PAN, S., TIENDA, S. M., NAHOTKO, D. A., LI, G., BLAŽENOVIC, I., LASTRA, R. R., CURTIS, M., YAMADA, S. D., PERETS, R., MCGREGOR, S. M., ANDRADE, J., FIEHN, O., MOELLERING, R. E., MANN, M. & LENGYEL, E. 2019. Proteomics reveals NNMT as a master metabolic regulator of cancer-associated fibroblasts. *Nature*, 569, 723-728.
- EDWARDS, J. R., YARYCHKIVSKA, O., BOULARD, M. & BESTOR, T. H. 2017. DNA methylation and DNA methyltransferases. *Epigenetics Chromatin*, 10, 23.
- EGEBLAD, M., NAKASONE, E. S. & WERB, Z. 2010. Tumors as organs: complex tissues that interface with the entire organism. *Dev Cell*, 18, 884-901.
- EKE, I., DEUSE, Y., HEHLGANS, S., GURTNER, K., KRAUSE, M., BAUMANN, M., SHEVCHENKO, A., SANDFORT, V. & CORDES, N. 2012. beta(1)Integrin/FAK/cortactin signaling is essential for human head and neck cancer resistance to radiotherapy. *J Clin Invest*, 122, 1529-40.
- ELIA, I., BROEKAERT, D., CHRISTEN, S., BOON, R., RADAELLI, E., ORTH, M. F., VERFAILLIE, C., GRUNEWALD, T. G. P. & FENDT, S. M. 2017. Proline metabolism supports metastasis formation and could be inhibited to selectively target metastasizing cancer cells. *Nat Commun*, 8, 15267.
- ELIA, I., ROSSI, M., STEGEN, S., BROEKAERT, D., DOGLIONI, G., VAN GORSEL, M., BOON, R., ESCALONA-NOGUERO, C., TORREKENS, S., VERFAILLIE, C., VERBEKEN, E., CARMELIET, G. & FENDT, S. M. 2019. Breast cancer cells rely on environmental pyruvate to shape the metastatic niche. *Nature*, 568, 117-121.
- ELLINGER, J., KAHL, P., VON DER GATHEN, J., ROGENHOFER, S., HEUKAMP, L. C., GUTGEMANN, I., WALTER, B., HOFSTADTER, F., BUTTNER, R., MULLER, S. C., BASTIAN, P. J. & VON RUECKER, A. 2010. Global levels of histone modifications predict prostate cancer recurrence. *Prostate*, 70, 61-9.
- ENGLER, A. J., SEN, S., SWEENEY, H. L. & DISCHER, D. E. 2006. Matrix elasticity directs stem cell lineage specification. *Cell*, 126, 677-89.
- ESBONA, K., INMAN, D., SAHA, S., JEFFERY, J., SCHEDIN, P., WILKE, L. & KEELY, P. 2016. COX-2 modulates mammary tumor progression in response to collagen density. *Breast Cancer Res*, 18, 35.
- FAN, J., SHAN, C., KANG, H. B., ELF, S., XIE, J., TUCKER, M., GU, T. L., AGUIAR, M., LONNING, S., CHEN, H., MOHAMMADI, M., BRITTON, L. M., GARCIA, B. A., ALECKOVIC, M., KANG, Y., KALUZ, S., DEVI, N., VAN MEIR, E. G., HITOSUGI, T., SEO, J. H., LONIAL, S., GADDH, M., ARELLANO, M., KHOURY, H. J., KHURI, F. R., BOGGON, T. J., KANG, S. & CHEN, J. 2014. Tyr phosphorylation of PDP1 toggles recruitment between ACAT1 and SIRT3 to regulate the pyruvate dehydrogenase complex. *Mol Cell*, 53, 534-48.
- FANG, T., LV, H., LV, G., LI, T., WANG, C., HAN, Q., YU, L., SU, B., GUO, L., HUANG, S., CAO, D., TANG, L., TANG, S., WU, M., YANG, W. & WANG, H. 2018. Tumor-derived exosomal miR-1247-3p induces cancer-associated fibroblast activation to foster lung metastasis of liver cancer. *Nat Commun*, 9, 191.
- FANG, W. B., MAFUVADZE, B., YAO, M., ZOU, A., PORTSCHE, M. & CHENG, N. 2015. TGF-beta Negatively Regulates CXCL1 Chemokine Expression in Mammary Fibroblasts through Enhancement of Smad2/3 and Suppression of HGF/c-Met Signaling Mechanisms. *PLoS One*, 10, e0135063.
- FEIG, C., JONES, J. O., KRAMAN, M., WELLS, R. J., DEONARINE, A., CHAN, D. S., CONNELL, C. M., ROBERTS, E. W., ZHAO, Q., CABALLERO, O. L., TEICHMANN, S. A., JANOWITZ, T., JODRELL, D. I., TUVESON, D. A. & FEARON, D. T. 2013. Targeting CXCL12 from FAP-expressing carcinoma-associated fibroblasts synergizes with anti-PD-L1 immunotherapy in pancreatic cancer. *Proc Natl Acad Sci U S A*, 110, 20212-7.
- FENG, X. H. & DERYNCK, R. 2005. Specificity and versatility in tgf-beta signaling through Smads. *Annu Rev Cell Dev Biol*, 21, 659-93.

- FERRARA, N. 2010. Pathways mediating VEGF-independent tumor angiogenesis. *Cytokine Growth Factor Rev*, 21, 21-6.
- FERRARI, KARIN J., SCELFO, A., JAMMULA, S., CUOMO, A., BAROZZI, I., STÜTZER, A., FISCHLE, W., BONALDI, T. & PASINI, D. 2014. Polycomb-Dependent H3K27me1 and H3K27me2 Regulate Active Transcription and Enhancer Fidelity. *Molecular Cell*, 53, 49-62.
- FINAK, G., BERTOS, N., PEPIN, F., SADEKOVA, S., SOULEIMANOVA, M., ZHAO, H., CHEN, H., OMEROGU, G., METERISSIAN, S., OMEROGU, A., HALLETT, M. & PARK, M. 2008. Stromal gene expression predicts clinical outcome in breast cancer. *Nat Med*, 14, 518-27.
- FISHER, M. T. 2006. Proline to the rescue. *Proc Natl Acad Sci U S A*, 103, 13265-6.
- FLAVIN, D. 2010a. Medullary thyroid carcinoma relapse reversed with dichloroacetate: A case report. *Oncol Lett*, 1, 889-891.
- FLAVIN, D. F. 2010b. Non-Hodgkin's Lymphoma Reversal with Dichloroacetate. *J Oncol*, 2010.
- FLORIO, R., DE LELLIS, L., VESCHI, S., VERGINELLI, F., DI GIACOMO, V., GALLORINI, M., PERCONTI, S., SANNA, M., MARIANI-COSTANTINI, R., NATALE, A., ARDUINI, A., AMOROSO, R., CATALDI, A. & CAMA, A. 2018. Effects of dichloroacetate as single agent or in combination with GW6471 and metformin in paraganglioma cells. *Sci Rep*, 8, 13610.
- FRANCO-BARRAZA, J., FRANCESCONE, R., LUONG, T., SHAH, N., MADHANI, R., CUKIERMAN, G., DULAIMI, E., DEVARAJAN, K., EGLESTON, B. L., NICOLAS, E., KATHERINE ALPAUGH, R., MALIK, R., UZZO, R. G., HOFFMAN, J. P., GOLEMIS, E. A. & CUKIERMAN, E. 2017. Matrix-regulated integrin alphavbeta5 maintains alpha5beta1-dependent desmoplastic traits prognostic of neoplastic recurrence. *Elife*, 6.
- FRANTZ, C., STEWART, K. M. & WEAVER, V. M. 2010. The extracellular matrix at a glance. *J Cell Sci*, 123, 4195-200.
- FRANZKE, C. W., TASANEN, K., SCHUMANN, H. & BRUCKNER-TUDERMAN, L. 2003. Collagenous transmembrane proteins: collagen XVII as a prototype. *Matrix Biol*, 22, 299-309.
- FUKUMURA, D., XAVIER, R., SUGIURA, T., CHEN, Y., PARK, E. C., LU, N., SELIG, M., NIELSEN, G., TAKSIR, T., JAIN, R. K. & SEED, B. 1998. Tumor induction of VEGF promoter activity in stromal cells. *Cell*, 94, 715-25.
- FURUYAMA, T., KITAYAMA, K., YAMASHITA, H. & MORI, N. 2003. Forkhead transcription factor FOXO1 (FKHR)-dependent induction of PDK4 gene expression in skeletal muscle during energy deprivation. *Biochem J*, 375, 365-71.
- GAGGIOLI, C., HOOPER, S., HIDALGO-CARCEDO, C., GROSSE, R., MARSHALL, J. F., HARRINGTON, K. & SAHAI, E. 2007. Fibroblast-led collective invasion of carcinoma cells with differing roles for RhoGTPases in leading and following cells. *Nat Cell Biol*, 9, 1392-400.
- GALDIERI, L. & VANCURA, A. 2012. Acetyl-CoA carboxylase regulates global histone acetylation. *J Biol Chem*, 287, 23865-76.
- GANDHI, L., RODRIGUEZ-ABREU, D., GADGEEL, S., ESTEBAN, E., FELIP, E., DE ANGELIS, F., DOMINE, M., CLINGAN, P., HOCHMAIR, M. J., POWELL, S. F., CHENG, S. Y., BISCHOFF, H. G., PELED, N., GROSSI, F., JENNENS, R. R., RECK, M., HUI, R., GARON, E. B., BOYER, M., RUBIO-VIQUEIRA, B., NOVELLO, S., KURATA, T., GRAY, J. E., VIDA, J., WEI, Z., YANG, J., RAFTOPOULOS, H., PIETANZA, M. C., GARASSINO, M. C. & INVESTIGATORS, K.-. 2018. Pembrolizumab plus Chemotherapy in Metastatic Non-Small-Cell Lung Cancer. *N Engl J Med*, 378, 2078-2092.
- GARON, E. B., CHRISTOFK, H. R., HOSMER, W., BRITTEN, C. D., BAHNG, A., CRABTREE, M. J., HONG, C. S., KAMRANPOUR, N., PITTS, S., KABBINAVAR, F., PATEL, C., VON EUW, E., BLACK, A., MICHELAKIS, E. D., DUBINETT, S. M. & SLAMON, D. J. 2014. Dichloroacetate should be considered with platinum-based chemotherapy in hypoxic tumors rather than as a single agent in advanced non-small cell lung cancer. *J Cancer Res Clin Oncol*, 140, 443-52.

- GE, J., CUI, H., XIE, N., BANERJEE, S., GUO, S., DUBEY, S., BARNES, S. & LIU, G. 2018. Glutaminolysis Promotes Collagen Translation and Stability via alpha-Ketoglutarate-mediated mTOR Activation and Proline Hydroxylation. *Am J Respir Cell Mol Biol*, 58, 378-390.
- GE, S., MAO, Y., YI, Y., XIE, D., CHEN, Z. & XIAO, Z. 2012. Comparative proteomic analysis of secreted proteins from nasopharyngeal carcinoma-associated stromal fibroblasts and normal fibroblasts. *Exp Ther Med*, 3, 857-860.
- GEHLER, S., BALDASSARRE, M., LAD, Y., LEIGHT, J. L., WOZNIAK, M. A., RICHING, K. M., ELICEIRI, K. W., WEAVER, V. M., CALDERWOOD, D. A. & KEELY, P. J. 2009. Filamin A-beta1 integrin complex tunes epithelial cell response to matrix tension. *Mol Biol Cell*, 20, 3224-38.
- GIANNONI, E., BIANCHINI, F., MASIERI, L., SERNI, S., TORRE, E., CALORINI, L. & CHIARUGI, P. 2010. Reciprocal activation of prostate cancer cells and cancer-associated fibroblasts stimulates epithelial-mesenchymal transition and cancer stemness. *Cancer Res*, 70, 6945-56.
- GILMORE, A. P., METCALFE, A. D., ROMER, L. H. & STREULI, C. H. 2000. Integrin-mediated survival signals regulate the apoptotic function of Bax through its conformation and subcellular localization. *J Cell Biol*, 149, 431-46.
- GLENTIS, A., OERTLE, P., MARIANI, P., CHIKINA, A., EL MARJOU, F., ATTIEH, Y., ZACCARINI, F., LAE, M., LOEW, D., DINGLI, F., SIRVEN, P., SCHOUMACHER, M., GURCHENKOV, B. G., PLODINEC, M. & VIGNJEVIC, D. M. 2017. Cancer-associated fibroblasts induce metalloprotease-independent cancer cell invasion of the basement membrane. *Nat Commun*, 8, 924.
- GOETZ, J. G., MINGUET, S., NAVARRO-LERIDA, I., LAZCANO, J. J., SAMANIEGO, R., CALVO, E., TELLO, M., OSTESO-IBANEZ, T., PELLINEN, T., ECHARRI, A., CEREZO, A., KLEIN-SZANTO, A. J., GARCIA, R., KEELY, P. J., SANCHEZ-MATEOS, P., CUKIERMAN, E. & DEL POZO, M. A. 2011. Biomechanical remodeling of the microenvironment by stromal caveolin-1 favors tumor invasion and metastasis. *Cell*, 146, 148-63.
- GOMES, F. G., NEDEL, F., ALVES, A. M., NOR, J. E. & TARQUINIO, S. B. 2013. Tumor angiogenesis and lymphangiogenesis: tumor/endothelial crosstalk and cellular/microenvironmental signaling mechanisms. *Life Sci*, 92, 101-7.
- GORDON, M. K. & HAHN, R. A. 2010. Collagens. *Cell Tissue Res*, 339, 247-57.
- GORRES, K. L. & RAINES, R. T. 2010. Prolyl 4-hydroxylase. *Crit Rev Biochem Mol Biol*, 45, 106-24.
- GOTZE, S., SCHUMACHER, E. C., KORDES, C. & HAUSSINGER, D. 2015. Epigenetic Changes during Hepatic Stellate Cell Activation. *PLoS One*, 10, e0128745.
- GOUIRAND, V. & VASSEUR, S. 2018. Fountain of youth of pancreatic cancer cells: the extracellular matrix. *Cell Death Discov*, 4, 1.
- GRASSIAN, A. R., METALLO, C. M., COLOFF, J. L., STEPHANOPOULOS, G. & BRUGGE, J. S. 2011. Erk regulation of pyruvate dehydrogenase flux through PDK4 modulates cell proliferation. *Genes Dev*, 25, 1716-33.
- GROESSL, M., SLANY, A., BILECK, A., GLOESSMANN, K., KREUTZ, D., JAEGER, W., PFEILER, G. & GERNER, C. 2014. Proteome profiling of breast cancer biopsies reveals a wound healing signature of cancer-associated fibroblasts. *J Proteome Res*, 13, 4773-82.
- GUIDO, C., WHITAKER-MENEZES, D., CAPPARELLI, C., BALLIET, R., LIN, Z., PESTELL, R. G., HOWELL, A., AQUILA, S., ANDO, S., MARTINEZ-OUTSCHOORN, U., SOTGIA, F. & LISANTI, M. P. 2012. Metabolic reprogramming of cancer-associated fibroblasts by TGF-beta drives tumor growth: connecting TGF-beta signaling with "Warburg-like" cancer metabolism and L-lactate production. *Cell Cycle*, 11, 3019-35.
- GUO, L., CUI, C., ZHANG, K., WANG, J., WANG, Y., LU, Y., CHEN, K., YUAN, J., XIAO, G., TANG, B., SUN, Y. & WU, C. 2019. Kindlin-2 links mechano-environment to proline synthesis and tumor growth. *Nat Commun*, 10, 845.
- GUTIERREZ, E., SHIN, B. S., WOOLSTENHULME, C. J., KIM, J. R., SAINI, P., BUSKIRK, A. R. & DEVER, T. E. 2013. eIF5A promotes translation of polyproline motifs. *Mol Cell*, 51, 35-45.

- HAGEDORN, C. H. & PHANG, J. M. 1983. Transfer of reducing equivalents into mitochondria by the interconversions of proline and delta 1-pyrroline-5-carboxylate. *Arch Biochem Biophys*, 225, 95-101.
- HANSFORD, R. G. 1976. Studies on the effects of coenzyme A-SH: acetyl coenzyme A, nicotinamide adenine dinucleotide: reduced nicotinamide adenine dinucleotide, and adenosine diphosphate: adenosine triphosphate ratios on the interconversion of active and inactive pyruvate dehydrogenase in isolated rat heart mitochondria. *J Biol Chem*, 251, 5483-9.
- HARRIS, R. A., HUANG, B. & WU, P. 2001. Control of pyruvate dehydrogenase kinase gene expression. *Adv Enzyme Regul*, 41, 269-88.
- HAZLEHURST, L. A. & DALTON, W. S. 2001. Mechanisms associated with cell adhesion mediated drug resistance (CAM-DR) in hematopoietic malignancies. *Cancer Metastasis Rev*, 20, 43-50.
- HELDIN, C. H., RUBIN, K., PIETRAS, K. & OSTMAN, A. 2004. High interstitial fluid pressure - an obstacle in cancer therapy. *Nat Rev Cancer*, 4, 806-13.
- HENRY, R. A., KUO, Y.-M. & ANDREWS, A. J. 2013. Differences in Specificity and Selectivity Between CBP and p300 Acetylation of Histone H3 and H3/H4. *Biochemistry*, 52, 5746-5759.
- HENRY, R. A., KUO, Y.-M., BHATTACHARJEE, V., YEN, T. J. & ANDREWS, A. J. 2014. Changing the Selectivity of p300 by Acetyl-CoA Modulation of Histone Acetylation. *ACS Chemical Biology*, 10, 146-156.
- HERNANDEZ-FERNAUD, J. R., RUENGELER, E., CASAZZA, A., NEILSON, L. J., PULLEINE, E., SANTI, A., ISMAIL, S., LILLA, S., DHAYADE, S., MACPHERSON, I. R., MCNEISH, I., ENNIS, D., ALI, H., KUGERATSKI, F. G., AL KHAMICI, H., VAN DEN BIGGELAAR, M., VAN DEN BERGHE, P. V., CLOIX, C., MCDONALD, L., MILLAN, D., HOYLE, A., KUCHNIO, A., CARMELIET, P., VALENZUELA, S. M., BLYTH, K., YIN, H., MAZZONE, M., NORMAN, J. C. & ZANIVAN, S. 2017. Secreted CLIC3 drives cancer progression through its glutathione-dependent oxidoreductase activity. *Nat Commun*, 8, 14206.
- HIRAKAWA, T., YASHIRO, M., DOI, Y., KINOSHITA, H., MORISAKI, T., FUKUOKA, T., HASEGAWA, T., KIMURA, K., AMANO, R. & HIRAKAWA, K. 2016. Pancreatic Fibroblasts Stimulate the Motility of Pancreatic Cancer Cells through IGF1/IGF1R Signaling under Hypoxia. *PLoS One*, 11, e0159912.
- HOLLINSHEAD, K. E. R., MUNFORD, H., EALES, K. L., BARDELLA, C., LI, C., ESCRIBANO-GONZALEZ, C., THAKKER, A., NONNENMACHER, Y., KLUCKOVA, K., JEEVES, M., MURREN, R., CUOZZO, F., YE, D., LAURENTI, G., ZHU, W., HILLER, K., HODSON, D. J., HUA, W., TOMLINSON, I. P., LUDWIG, C., MAO, Y. & TENNANT, D. A. 2018. Oncogenic IDH1 Mutations Promote Enhanced Proline Synthesis through PYCR1 to Support the Maintenance of Mitochondrial Redox Homeostasis. *Cell Rep*, 22, 3107-3114.
- HOLNESS, M. J. & SUGDEN, M. C. 2003. Regulation of pyruvate dehydrogenase complex activity by reversible phosphorylation. *Biochem Soc Trans*, 31, 1143-51.
- HSIEH, M. C., DAS, D., SAMBANDAM, N., ZHANG, M. Q. & NAHLE, Z. 2008. Regulation of the PDK4 isozyme by the Rb-E2F1 complex. *J Biol Chem*, 283, 27410-7.
- HU, B., GHARAEE-KERMANI, M., WU, Z. & PHAN, S. H. 2010. Epigenetic regulation of myofibroblast differentiation by DNA methylation. *Am J Pathol*, 177, 21-8.
- HU, M., YAO, J., CAI, L., BACHMAN, K. E., VAN DEN BRULE, F., VELCULESCU, V. & POLYAK, K. 2005. Distinct epigenetic changes in the stromal cells of breast cancers. *Nat Genet*, 37, 899-905.
- HUANG, B., GUDI, R., WU, P., HARRIS, R. A., HAMILTON, J. & POPOV, K. M. 1998. Isoenzymes of pyruvate dehydrogenase phosphatase. DNA-derived amino acid sequences, expression, and regulation. *J Biol Chem*, 273, 17680-8.
- HUANG, B., WU, P., BOWKER-KINLEY, M. M. & HARRIS, R. A. 2002. Regulation of pyruvate dehydrogenase kinase expression by peroxisome proliferator-activated receptor-alpha ligands, glucocorticoids, and insulin. *Diabetes*, 51, 276-83.
- HUANG, C., PARK, C. C., HILSENBECK, S. G., WARD, R., RIMAWI, M. F., WANG, Y. C., SHOU, J., BISSELL, M. J., OSBORNE, C. K. & SCHIFF, R. 2011. beta1 integrin

- mediates an alternative survival pathway in breast cancer cells resistant to lapatinib. *Breast Cancer Res*, 13, R84.
- HUANG, G., GE, G., IZZI, V. & GREENSPAN, D. S. 2017. alpha3 Chains of type V collagen regulate breast tumour growth via glypican-1. *Nat Commun*, 8, 14351.
- HURWITZ, H. 2004. Integrating the anti-VEGF-A humanized monoclonal antibody bevacizumab with chemotherapy in advanced colorectal cancer. *Clin Colorectal Cancer*, 4 Suppl 2, S62-8.
- HYNES, R. O. 2009. The extracellular matrix: not just pretty fibrils. *Science*, 326, 1216-9.
- ISHII, G., SANGAI, T., ODA, T., AOYAGI, Y., HASEBE, T., KANOMATA, N., ENDOH, Y., OKUMURA, C., OKUHARA, Y., MAGAE, J., EMURA, M., OCHIYA, T. & OCHIAI, A. 2003. Bone-marrow-derived myofibroblasts contribute to the cancer-induced stromal reaction. *Biochem Biophys Res Commun*, 309, 232-40.
- IWANO, M., PLIETH, D., DANOFF, T. M., XUE, C., OKADA, H. & NEILSON, E. G. 2002. Evidence that fibroblasts derive from epithelium during tissue fibrosis. *J Clin Invest*, 110, 341-50.
- IYENGAR, P., ESPINA, V., WILLIAMS, T. W., LIN, Y., BERRY, D., JELICKS, L. A., LEE, H., TEMPLE, K., GRAVES, R., POLLARD, J., CHOPRA, N., RUSSELL, R. G., SASISEKHARAN, R., TROCK, B. J., LIPPMAN, M., CALVERT, V. S., PETRICOIN, E. F., 3RD, LIOTTA, L., DADACHOVA, E., PESTELL, R. G., LISANTI, M. P., BONALDO, P. & SCHERER, P. E. 2005. Adipocyte-derived collagen VI affects early mammary tumor progression in vivo, demonstrating a critical interaction in the tumor/stroma microenvironment. *J Clin Invest*, 115, 1163-76.
- JACOB, A. & PREKERIS, R. 2015. The regulation of MMP targeting to invadopodia during cancer metastasis. *Front Cell Dev Biol*, 3, 4.
- JANG, I. & BENINGO, K. A. 2019. Integrins, CAFs and Mechanical Forces in the Progression of Cancer. *Cancers (Basel)*, 11.
- JIANG, L., GONDA, T. A., GAMBLE, M. V., SALAS, M., SESHAN, V., TU, S., TWADDELL, W. S., HEGYI, P., LAZAR, G., STEELE, I., VARRO, A., WANG, T. C. & TYCKO, B. 2008. Global hypomethylation of genomic DNA in cancer-associated myofibroblasts. *Cancer Res*, 68, 9900-8.
- JONES, P. A. 2012. Functions of DNA methylation: islands, start sites, gene bodies and beyond. *Nat Rev Genet*, 13, 484-92.
- JOTZU, C., ALT, E., WELTE, G., LI, J., HENNESSY, B. T., DEVARAJAN, E., KRISHNAPPA, S., PINILLA, S., DROLL, L. & SONG, Y. H. 2010. Adipose tissue-derived stem cells differentiate into carcinoma-associated fibroblast-like cells under the influence of tumor-derived factors. *Anal Cell Pathol (Amst)*, 33, 61-79.
- JOYCE, J. A. 2005. Therapeutic targeting of the tumor microenvironment. *Cancer Cell*, 7, 513-20.
- KADLER, K. E., BALDOCK, C., BELLA, J. & BOOT-HANDFORD, R. P. 2007. Collagens at a glance. *J Cell Sci*, 120, 1955-8.
- KAI, F., DRAIN, A. P. & WEAVER, V. M. 2019. The Extracellular Matrix Modulates the Metastatic Journey. *Developmental Cell*, 49, 332-346.
- KALINSKI, P. 2012. Regulation of immune responses by prostaglandin E2. *J Immunol*, 188, 21-8.
- KALLURI, R. 2016. The biology and function of fibroblasts in cancer. *Nat Rev Cancer*, 16, 582-98.
- KAMARAJUGADDA, S., STEMBOROSKI, L., CAI, Q., SIMPSON, N. E., NAYAK, S., TAN, M. & LU, J. 2012. Glucose oxidation modulates anoikis and tumor metastasis. *Mol Cell Biol*, 32, 1893-907.
- KAPLON, J., ZHENG, L., MEISSL, K., CHANETON, B., SELIVANOV, V. A., MACKAY, G., VAN DER BURG, S. H., VERDEGAAL, E. M., CASCANTE, M., SHLOMI, T., GOTTLIEB, E. & PEEPER, D. S. 2013. A key role for mitochondrial gatekeeper pyruvate dehydrogenase in oncogene-induced senescence. *Nature*, 498, 109-12.
- KARDOS, G. R., WASTYK, H. C. & ROBERTSON, G. P. 2015. Disruption of Proline Synthesis in Melanoma Inhibits Protein Production Mediated by the GCN2 Pathway. *Mol Cancer Res*, 13, 1408-20.

- KATANOV, C., LERRER, S., LIUBOMIRSKI, Y., LEIDER-TREJO, L., MESHEL, T., BAR, J., FENIGER-BARISH, R., KAMER, I., SORIA-ARTZI, G., KAHANI, H., BANERJEE, D. & BEN-BARUCH, A. 2015. Regulation of the inflammatory profile of stromal cells in human breast cancer: prominent roles for TNF-alpha and the NF-kappaB pathway. *Stem Cell Res Ther*, 6, 87.
- KAUPPILA, S., STENBACK, F., RISTELI, J., JUUKOLA, A. & RISTELI, L. 1998. Aberrant type I and type III collagen gene expression in human breast cancer in vivo. *J Pathol*, 186, 262-8.
- KAUSHIK, S., PICKUP, M. W. & WEAVER, V. M. 2016. From transformation to metastasis: deconstructing the extracellular matrix in breast cancer. *Cancer and Metastasis Reviews*, 35, 655-667.
- KESSENBROCK, K., PLAKS, V. & WERB, Z. 2010. Matrix metalloproteinases: regulators of the tumor microenvironment. *Cell*, 141, 52-67.
- KILBERG, M. S., BALASUBRAMANIAN, M., FU, L. & SHAN, J. 2012. The Transcription Factor Network Associated With the Amino Acid Response in Mammalian Cells. *Advances in Nutrition*, 3, 295-306.
- KIM, J. W., GAO, P., LIU, Y. C., SEMENZA, G. L. & DANG, C. V. 2007. Hypoxia-inducible factor 1 and dysregulated c-Myc cooperatively induce vascular endothelial growth factor and metabolic switches hexokinase 2 and pyruvate dehydrogenase kinase 1. *Mol Cell Biol*, 27, 7381-93.
- KIM, J. W., TCHERNYSHYOV, I., SEMENZA, G. L. & DANG, C. V. 2006a. HIF-1-mediated expression of pyruvate dehydrogenase kinase: a metabolic switch required for cellular adaptation to hypoxia. *Cell Metab*, 3, 177-85.
- KIM, M. Y., CHO, W. D., HONG, K. P., CHOI DA, B., HONG, J. W., KIM, S., MOON, Y. R., SON, S. M., LEE, O. J., LEE, H. C. & SONG, H. G. 2016. Novel monoclonal antibody against beta 1 integrin enhances cisplatin efficacy in human lung adenocarcinoma cells. *J Biomed Res*, 30, 217-24.
- KIM, S. C., SPRUNG, R., CHEN, Y., XU, Y., BALL, H., PEI, J., CHENG, T., KHO, Y., XIAO, H., XIAO, L., GRISHIN, N. V., WHITE, M., YANG, X. J. & ZHAO, Y. 2006b. Substrate and functional diversity of lysine acetylation revealed by a proteomics survey. *Mol Cell*, 23, 607-18.
- KIM, W., SEOK KANG, Y., SOO KIM, J., SHIN, N. Y., HANKS, S. K. & SONG, W. K. 2008. The integrin-coupled signaling adaptor p130Cas suppresses Smad3 function in transforming growth factor-beta signaling. *Mol Biol Cell*, 19, 2135-46.
- KIM, Y. I., LEE, F. N., CHOI, W. S., LEE, S. & YOUN, J. H. 2006c. Insulin regulation of skeletal muscle PDK4 mRNA expression is impaired in acute insulin-resistant states. *Diabetes*, 55, 2311-7.
- KIMMELMAN, A. C. 2011. The dynamic nature of autophagy in cancer. *Genes Dev*, 25, 1999-2010.
- KINNAIRD, A., ZHAO, S., WELLEN, K. E. & MICHELAKIS, E. D. 2016. Metabolic control of epigenetics in cancer. *Nat Rev Cancer*, 16, 694-707.
- KINOSHITA, K., AONO, Y., AZUMA, M., KISHI, J., TAKEZAKI, A., KISHI, M., MAKINO, H., OKAZAKI, H., UEHARA, H., IZUMI, K., SONE, S. & NISHIOKA, Y. 2013. Antifibrotic effects of focal adhesion kinase inhibitor in bleomycin-induced pulmonary fibrosis in mice. *Am J Respir Cell Mol Biol*, 49, 536-43.
- KLYUYEVA, A., TUGANOVA, A., KEDISHVILI, N. & POPOV, K. M. 2019. Tissue-specific kinase expression and activity regulate flux through the pyruvate dehydrogenase complex. *J Biol Chem*, 294, 838-851.
- KO, Y. A., MOHTAT, D., SUZUKI, M., PARK, A. S., IZQUIERDO, M. C., HAN, S. Y., KANG, H. M., SI, H., HOSTETTER, T., PULLMAN, J. M., FAZZARI, M., VERMA, A., ZHENG, D., GREALLY, J. M. & SUSZTAK, K. 2013. Cytosine methylation changes in enhancer regions of core pro-fibrotic genes characterize kidney fibrosis development. *Genome Biol*, 14, R108.
- KOJIMA, Y., ACAR, A., EATON, E. N., MELLODY, K. T., SCHEEL, C., BEN-PORATH, I., ONDER, T. T., WANG, Z. C., RICHARDSON, A. L., WEINBERG, R. A. & ORIMO, A. 2010. Autocrine TGF-beta and stromal cell-derived factor-1 (SDF-1) signaling

- drives the evolution of tumor-promoting mammary stromal myofibroblasts. *Proc Natl Acad Sci U S A*, 107, 20009-14.
- KORTLEVER, R. M., SODIR, N. M., WILSON, C. H., BURKHART, D. L., PELLEGRINET, L., BROWN SWIGART, L., LITTLEWOOD, T. D. & EVAN, G. I. 2017. Myc Cooperates with Ras by Programming Inflammation and Immune Suppression. *Cell*, 171, 1301-1315 e14.
- KOUKOURAKIS, M. I., GIATROMANOLAKI, A., BOUGIOUKAS, G. & SIVRIDIS, E. 2014. Lung cancer: An organized cellular and metabolic domain. *Cancer Biology & Therapy*, 6, 1472-1475.
- KOUKOURAKIS, M. I., KALAMIDA, D., MITRAKAS, A. G., LIOUSIA, M., POULILIOU, S., SIVRIDIS, E. & GIATROMANOLAKI, A. 2017. Metabolic cooperation between co-cultured lung cancer cells and lung fibroblasts. *Lab Invest*, 97, 1321-1331.
- KOYAMA, S., AKBAY, E. A., LI, Y. Y., AREF, A. R., SKOULIDIS, F., HERTER-SPRIE, G. S., BUCZKOWSKI, K. A., LIU, Y., AWAD, M. M., DENNING, W. L., DIAO, L., WANG, J., PARRA-CUENTAS, E. R., WISTUBA, II, SOUCHERAY, M., THAI, T., ASAHINA, H., KITAJIMA, S., ALTABEF, A., CAVANAUGH, J. D., RHEE, K., GAO, P., ZHANG, H., FECCI, P. E., SHIMAMURA, T., HELLMANN, M. D., HEYMACH, J. V., HODI, F. S., FREEMAN, G. J., BARBIE, D. A., DRANOFF, G., HAMMERMAN, P. S. & WONG, K. K. 2016. STK11/LKB1 Deficiency Promotes Neutrophil Recruitment and Proinflammatory Cytokine Production to Suppress T-cell Activity in the Lung Tumor Microenvironment. *Cancer Res*, 76, 999-1008.
- KRAMER, C. J. H., VANGANGELT, K. M. H., VAN PELT, G. W., DEKKER, T. J. A., TOLLENAAR, R. & MESKER, W. E. 2019. The prognostic value of tumour-stroma ratio in primary breast cancer with special attention to triple-negative tumours: a review. *Breast Cancer Res Treat*, 173, 55-64.
- KRAMER, M., DEES, C., HUANG, J., SCHLOTTMANN, I., PALUMBO-ZERR, K., ZERR, P., GELSE, K., BEYER, C., DISTLER, A., MARQUEZ, V. E., DISTLER, O., SCHETT, G. & DISTLER, J. H. 2013. Inhibition of H3K27 histone trimethylation activates fibroblasts and induces fibrosis. *Ann Rheum Dis*, 72, 614-20.
- KRETZ, R., BOZORGMEHR, B., KARIMINEJAD, M. H., ROHRBACH, M., HAUSSER, I., BAUMER, A., BAUMGARTNER, M., GIUNTA, C., KARIMINEJAD, A. & HABERLE, J. 2011. Defect in proline synthesis: pyrroline-5-carboxylate reductase 1 deficiency leads to a complex clinical phenotype with collagen and elastin abnormalities. *J Inherit Metab Dis*, 34, 731-9.
- KRISHNAN, N., DICKMAN, M. B. & BECKER, D. F. 2008. Proline modulates the intracellular redox environment and protects mammalian cells against oxidative stress. *Free Radic Biol Med*, 44, 671-81.
- KUGERATSKI, F. G., ATKINSON, S. J., NEILSON, L. J., LILLA, S., KNIGHT, J. R. P., SERNEELS, J., JUIN, A., ISMAIL, S., BRYANT, D. M., MARKERT, E. K., MACHESKY, L. M., MAZZONE, M., SANSOM, O. J. & ZANIVAN, S. 2019. Hypoxic cancer-associated fibroblasts increase NCBP2-AS2/HIAR to promote endothelial sprouting through enhanced VEGF signaling. *Sci Signal*, 12.
- KUMAR, A., KANT, S. & SINGH, S. M. 2013a. Antitumor and chemosensitizing action of dichloroacetate implicates modulation of tumor microenvironment: a role of reorganized glucose metabolism, cell survival regulation and macrophage differentiation. *Toxicol Appl Pharmacol*, 273, 196-208.
- KUMAR, D., NEW, J., VISHWAKARMA, V., JOSHI, R., ENDERS, J., LIN, F., DASARI, S., GUTIERREZ, W. R., LEEF, G., PONNURANGAM, S., CHAVAN, H., GANADEN, L., THORNTON, M. M., DAI, H., TAWFIK, O., STRAUB, J., SHNAYDER, Y., KAKARALA, K., TSUE, T. T., GIROD, D. A., VAN HOUTEN, B., ANANT, S., KRISHNAMURTHY, P. & THOMAS, S. M. 2018. Cancer-Associated Fibroblasts Drive Glycolysis in a Targetable Signaling Loop Implicated in Head and Neck Squamous Cell Carcinoma Progression. *Cancer Res*, 78, 3769-3782.
- KUMAR, K., DECANT, B. T., GRIPPO, P. J., HWANG, R. F., BENTREM, D. J., EBINE, K. & MUNSHI, H. G. 2017. BET inhibitors block pancreatic stellate cell collagen I production and attenuate fibrosis in vivo. *JCI Insight*, 2, e88032.

- KUMAR, K., WIGFIELD, S., GEE, H. E., DEVLIN, C. M., SINGLETON, D., LI, J. L., BUFFA, F., HUFFMAN, M., SINN, A. L., SILVER, J., TURLEY, H., LEEK, R., HARRIS, A. L. & IVAN, M. 2013b. Dichloroacetate reverses the hypoxic adaptation to bevacizumab and enhances its antitumor effects in mouse xenografts. *J Mol Med (Berl)*, 91, 749-58.
- KUO, M. L., LEE, M. B., TANG, M., DEN BESTEN, W., HU, S., SWEREDOSKI, M. J., HESS, S., CHOU, C. M., CHANGOU, C. A., SU, M., JIA, W., SU, L. & YEN, Y. 2016. PYCR1 and PYCR2 Interact and Collaborate with RRM2B to Protect Cells from Overt Oxidative Stress. *Sci Rep*, 6, 18846.
- KUPERWASSER, C., CHAVARRIA, T., WU, M., MAGRANE, G., GRAY, J. W., CAREY, L., RICHARDSON, A. & WEINBERG, R. A. 2004. Reconstruction of functionally normal and malignant human breast tissues in mice. *Proc Natl Acad Sci U S A*, 101, 4966-71.
- LAMAR, Z. 2016. *CPI-613, Bendamustine Hydrochloride, and Rituximab in Treating Patients With Relapsed or Refractory B-Cell Non-Hodgkin Lymphoma* [Online]. Available: <https://ClinicalTrials.gov/show/NCT02168907> [Accessed].
- LANNING, N. J., CASTLE, J. P., SINGH, S. J., LEON, A. N., TOVAR, E. A., SANGHERA, A., MACKEIGAN, J. P., FILIPP, F. V. & GRAVEEL, C. R. 2017. Metabolic profiling of triple-negative breast cancer cells reveals metabolic vulnerabilities. *Cancer Metab*, 5, 6.
- LASKO, L. M., JAKOB, C. G., EDALJI, R. P., QIU, W., MONTGOMERY, D., DIGIAMMARINO, E. L., HANSEN, T. M., RISI, R. M., FREY, R., MANAVES, V., SHAW, B., ALGIRE, M., HESSLER, P., LAM, L. T., UZIEL, T., FAIVRE, E., FERGUSON, D., BUCHANAN, F. G., MARTIN, R. L., TORRENT, M., CHIANG, G. G., KARUKURICHI, K., LANGSTON, J. W., WEINERT, B. T., CHOUDHARY, C., DE VRIES, P., KLUGE, A. F., PATANE, M. A., VAN DRIE, J. H., WANG, C., MCELLIGOTT, D., KESICKI, E., MARMORSTEIN, R., SUN, C., COLE, P. A., ROSENBERG, S. H., MICHAELIDES, M. R., LAI, A. & BROMBERG, K. D. 2017. Discovery of a selective catalytic p300/CBP inhibitor that targets lineage-specific tumours. *Nature*, 550, 128-132.
- LAWRENCE, M., DAUJAT, S. & SCHNEIDER, R. 2016. Lateral Thinking: How Histone Modifications Regulate Gene Expression. *Trends Genet*, 32, 42-56.
- LEASK, A. 2010. Potential therapeutic targets for cardiac fibrosis: TGFbeta, angiotensin, endothelin, CCN2, and PDGF, partners in fibroblast activation. *Circ Res*, 106, 1675-80.
- LEBLEU, V. S. & KALLURI, R. 2018. A peek into cancer-associated fibroblasts: origins, functions and translational impact. *Dis Model Mech*, 11.
- LEE, J. E., PARK, Y. K., PARK, S., JANG, Y., WARING, N., DEY, A., OZATO, K., LAI, B., PENG, W. & GE, K. 2017. Brd4 binds to active enhancers to control cell identity gene induction in adipogenesis and myogenesis. *Nat Commun*, 8, 2217.
- LEIGHT, J. L., WOZNIAK, M. A., CHEN, S., LYNCH, M. L. & CHEN, C. S. 2012. Matrix rigidity regulates a switch between TGF-beta1-induced apoptosis and epithelial-mesenchymal transition. *Mol Biol Cell*, 23, 781-91.
- LEMONS, J. M., FENG, X. J., BENNETT, B. D., LEGESSE-MILLER, A., JOHNSON, E. L., RAITMAN, I., POLLINA, E. A., RABITZ, H. A., RABINOWITZ, J. D. & COLLIER, H. A. 2010. Quiescent fibroblasts exhibit high metabolic activity. *PLoS Biol*, 8, e1000514.
- LEUNG, C. S., YEUNG, T. L., YIP, K. P., PRADEEP, S., BALASUBRAMANIAN, L., LIU, J., WONG, K. K., MANGALA, L. S., ARMAIZ-PENA, G. N., LOPEZ-BERESTEIN, G., SOOD, A. K., BIRRER, M. J. & MOK, S. C. 2014. Calcium-dependent FAK/CREB/TNNC1 signalling mediates the effect of stromal MFAP5 on ovarian cancer metastatic potential. *Nat Commun*, 5, 5092.
- LEVENTAL, K. R., YU, H., KASS, L., LAKINS, J. N., EGEBLAD, M., ERLER, J. T., FONG, S. F., CSISZAR, K., GIACCIA, A., WENINGER, W., YAMAUCHI, M., GASSER, D. L. & WEAVER, V. M. 2009. Matrix crosslinking forces tumor progression by enhancing integrin signaling. *Cell*, 139, 891-906.
- LEWIS, J. M., TRUONG, T. N. & SCHWARTZ, M. A. 2002. Integrins regulate the apoptotic response to DNA damage through modulation of p53. *Proc Natl Acad Sci U S A*, 99, 3627-32.

- LI, J., JIA, Z., KONG, J., ZHANG, F., FANG, S., LI, X., LI, W., YANG, X., LUO, Y., LIN, B. & LIU, T. 2016. Carcinoma-Associated Fibroblasts Lead the Invasion of Salivary Gland Adenoid Cystic Carcinoma Cells by Creating an Invasive Track. *PLoS One*, 11, e0150247.
- LI, J. J., WANG, H. X., TINO, J. A., ROBL, J. A., HERPIN, T. F., LAWRENCE, R. M., BILLER, S., JAMIL, H., PONTICIELLO, R., CHEN, L. P., CHU, C., FLYNN, N., CHENG, D., ZHAO, R. L., CHEN, B. C., SCHNUR, D., OBERMEIER, M. T., SASSEVILLE, V., PADMANABHA, R., PIKE, K. & HARRITY, T. 2007. 2-Hydroxy-N-arylbenzenesulfonamides as ATP-citrate lyase inhibitors. *Bioorganic & Medicinal Chemistry Letters*, 17, 3208-3211.
- LI, M. O. & FLAVELL, R. A. 2008. TGF-beta: a master of all T cell trades. *Cell*, 134, 392-404.
- LI, W., GERMAIN, R. N. & GERNER, M. Y. 2017. Multiplex, quantitative cellular analysis in large tissue volumes with clearing-enhanced 3D microscopy (Ce3D). *Proc Natl Acad Sci U S A*, 114, E7321-E7330.
- LIANG, S. T., AUDIRA, G., JUNIARDI, S., CHEN, J. R., LAI, Y. H., DU, Z. C., LIN, D. S. & HSIAO, C. D. 2019. Zebrafish Carrying pycr1 Gene Deficiency Display Aging and Multiple Behavioral Abnormalities. *Cells*, 8.
- LIAO, D., LUO, Y., MARKOWITZ, D., XIANG, R. & REISFELD, R. A. 2009. Cancer associated fibroblasts promote tumor growth and metastasis by modulating the tumor immune microenvironment in a 4T1 murine breast cancer model. *PLoS One*, 4, e7965.
- LINGASAMY, P., TOBI, A., HAUGAS, M., HUNT, H., PAISTE, P., ASSER, T., RATSEP, T., KOTAMRAJU, V. R., BJERKVIG, R. & TEESALU, T. 2019. Bi-specific tenascin-C and fibronectin targeted peptide for solid tumor delivery. *Biomaterials*, 219, 119373.
- LITTLEPAGE, L. E., STERNLICHT, M. D., ROUGIER, N., PHILLIPS, J., GALLO, E., YU, Y., WILLIAMS, K., BRENOT, A., GORDON, J. I. & WERB, Z. 2010. Matrix metalloproteinases contribute distinct roles in neuroendocrine prostate carcinogenesis, metastasis, and angiogenesis progression. *Cancer Res*, 70, 2224-34.
- LIU, J., LIAO, S., DIOP-FRIMPONG, B., CHEN, W., GOEL, S., NAXEROVA, K., ANCUKIEWICZ, M., BOUCHER, Y., JAIN, R. K. & XU, L. 2012a. TGF-beta blockade improves the distribution and efficacy of therapeutics in breast carcinoma by normalizing the tumor stroma. *Proc Natl Acad Sci U S A*, 109, 16618-23.
- LIU, T. M. & SHYH-CHANG, N. 2017. SIRT2 and glycolytic enzyme acetylation in pluripotent stem cells. *Nat Cell Biol*, 19, 412-414.
- LIU, W., HANCOCK, C. N., FISCHER, J. W., HARMAN, M. & PHANG, J. M. 2015. Proline biosynthesis augments tumor cell growth and aerobic glycolysis: involvement of pyridine nucleotides. *Sci Rep*, 5, 17206.
- LIU, W., LE, A., HANCOCK, C., LANE, A. N., DANG, C. V., FAN, T. W. & PHANG, J. M. 2012b. Reprogramming of proline and glutamine metabolism contributes to the proliferative and metabolic responses regulated by oncogenic transcription factor c-MYC. *Proc Natl Acad Sci U S A*, 109, 8983-8.
- LIU, X., ZHANG, Y., NI, M., CAO, H., SIGNER, R. A. J., LI, D., LI, M., GU, Z., HU, Z., DICKERSON, K. E., WEINBERG, S. E., CHANDEL, N. S., DEBERARDINIS, R. J., ZHOU, F., SHAO, Z. & XU, J. 2017. Regulation of mitochondrial biogenesis in erythropoiesis by mTORC1-mediated protein translation. *Nat Cell Biol*, 19, 626-638.
- LOAYZA-PUCH, F., ROOIJERS, K., BUIL, L. C., ZIJLSTRA, J., OUDE VRIELINK, J. F., LOPES, R., UGALDE, A. P., VAN BREUGEL, P., HOFLAND, I., WESSELING, J., VAN TELLINGEN, O., BEX, A. & AGAMI, R. 2016. Tumour-specific proline vulnerability uncovered by differential ribosome codon reading. *Nature*, 530, 490-4.
- LOMBARD, D. B., ALT, F. W., CHENG, H. L., BUNKENBORG, J., STREPPER, R. S., MOSTOSLAVSKY, R., KIM, J., YANCOPOULOS, G., VALENZUELA, D., MURPHY, A., YANG, Y., CHEN, Y., HIRSCHHEY, M. D., BRONSON, R. T., HAIGIS, M., GUARENTE, L. P., FARESE, R. V., JR., WEISSMAN, S., VERDIN, E. & SCHWER, B. 2007. Mammalian

- Sir2 homolog SIRT3 regulates global mitochondrial lysine acetylation. *Mol Cell Biol*, 27, 8807-14.
- LOZOYA, O. A., WANG, T., GRENET, D., WOLFGANG, T. C., SOBHANY, M., GANINI DA SILVA, D., RIADI, G., CHANDEL, N., WOYCHIK, R. P. & SANTOS, J. H. 2019. Mitochondrial acetyl-CoA reversibly regulates locus-specific histone acetylation and gene expression. *Life Sci Alliance*, 2.
- LU, C. W., LIN, S. C., CHEN, K. F., LAI, Y. Y. & TSAI, S. J. 2008. Induction of pyruvate dehydrogenase kinase-3 by hypoxia-inducible factor-1 promotes metabolic switch and drug resistance. *J Biol Chem*, 283, 28106-14.
- LU, C. W., LIN, S. C., CHIEN, C. W., LIN, S. C., LEE, C. T., LIN, B. W., LEE, J. C. & TSAI, S. J. 2011. Overexpression of pyruvate dehydrogenase kinase 3 increases drug resistance and early recurrence in colon cancer. *Am J Pathol*, 179, 1405-14.
- LU, P., WEAVER, V. M. & WERB, Z. 2012. The extracellular matrix: a dynamic niche in cancer progression. *J Cell Biol*, 196, 395-406.
- LUCERO, H. A. & KAGAN, H. M. 2006. Lysyl oxidase: an oxidative enzyme and effector of cell function. *Cell Mol Life Sci*, 63, 2304-16.
- LUGA, V., ZHANG, L., VILORIA-PETIT, A. M., OGUNJIMI, A. A., INANLOU, M. R., CHIU, E., BUCHANAN, M., HOSEIN, A. N., BASIK, M. & WRANA, J. L. 2012. Exosomes mediate stromal mobilization of autocrine Wnt-PCP signaling in breast cancer cell migration. *Cell*, 151, 1542-56.
- LYNG, H., BROVIG, R. S., SVENDSRUD, D. H., HOLM, R., KAALHUS, O., KNUTSTAD, K., OKSEFJELL, H., SUNDFOR, K., KRISTENSEN, G. B. & STOKKE, T. 2006. Gene expressions and copy numbers associated with metastatic phenotypes of uterine cervical cancer. *BMC Genomics*, 7, 268.
- MACKAY, G. M., ZHENG, L., VAN DEN BROEK, N. J. & GOTTLIEB, E. 2015. Analysis of Cell Metabolism Using LC-MS and Isotope Tracers. *Methods Enzymol*, 561, 171-96.
- MACKENZIE, E. D., SELAK, M. A., TENNANT, D. A., PAYNE, L. J., CROSBY, S., FREDERIKSEN, C. M., WATSON, D. G. & GOTTLIEB, E. 2007. Cell-permeating alpha-ketoglutarate derivatives alleviate pseudohypoxia in succinate dehydrogenase-deficient cells. *Mol Cell Biol*, 27, 3282-9.
- MADSEN, C. D., PEDERSEN, J. T., VENNING, F. A., SINGH, L. B., MOEENDARBARY, E., CHARRAS, G., COX, T. R., SAHAI, E. & ERLER, J. T. 2015. Hypoxia and loss of PHD2 inactivate stromal fibroblasts to decrease tumour stiffness and metastasis. *EMBO Rep*, 16, 1394-408.
- MAEDA, T., SAKABE, T., SUNAGA, A., SAKAI, K., RIVERA, A. L., KEENE, D. R., SASAKI, T., STAVNEZER, E., IANNOTTI, J., SCHWEITZER, R., ILIC, D., BASKARAN, H. & SAKAI, T. 2011. Conversion of mechanical force into TGF-beta-mediated biochemical signals. *Curr Biol*, 21, 933-41.
- MAHMOOD, S., BIRKAYA, B., RIDEOUT, T. C. & PATEL, M. S. 2016. Lack of mitochondria-generated acetyl-CoA by pyruvate dehydrogenase complex downregulates gene expression in the hepatic de novo lipogenic pathway. *Am J Physiol Endocrinol Metab*, 311, E117-27.
- MARGUERON, R., TROJER, P. & REINBERG, D. 2005. The key to development: interpreting the histone code? *Curr Opin Genet Dev*, 15, 163-76.
- MARIATHASAN, S., TURLEY, S. J., NICKLES, D., CASTIGLIONI, A., YUEN, K., WANG, Y., KADEL, E. E., III, KOEPPEN, H., ASTARITA, J. L., CUBAS, R., JHUNJHUNWALA, S., BANCHEREAU, R., YANG, Y., GUAN, Y., CHALOUNI, C., ZIAI, J., SENBABA OGLU, Y., SANTORO, S., SHEINSON, D., HUNG, J., GILTNER, J. M., PIERCE, A. A., MESH, K., LIANOGLU, S., RIEGLER, J., CARANO, R. A. D., ERIKSSON, P., HOGLUND, M., SOMARRIBA, L., HALLIGAN, D. L., VAN DER HEIJDEN, M. S., LORIOT, Y., ROSENBERG, J. E., FONG, L., MELLMAN, I., CHEN, D. S., GREEN, M., DERLETH, C., FINE, G. D., HEGDE, P. S., BOURGON, R. & POWLES, T. 2018. TGFbeta attenuates tumour response to PD-L1 blockade by contributing to exclusion of T cells. *Nature*, 554, 544-548.
- MARTINEZ-OUTSCHOORN, U. E., BALLIET, R. M., LIN, Z., WHITAKER-MENEZES, D., HOWELL, A., SOTGIA, F. & LISANTI, M. P. 2012. Hereditary ovarian cancer and two-compartment tumor metabolism: epithelial loss of BRCA1 induces hydrogen

- peroxide production, driving oxidative stress and NFkappaB activation in the tumor stroma. *Cell Cycle*, 11, 4152-66.
- MARTINEZ-OUTSCHOORN, U. E., GOLDBERG, A., LIN, Z., KO, Y. H., FLOMENBERG, N., WANG, C., PAVLIDES, S., PESTELL, R. G., HOWELL, A., SOTGIA, F. & LISANTI, M. P. 2011a. Anti-estrogen resistance in breast cancer is induced by the tumor microenvironment and can be overcome by inhibiting mitochondrial function in epithelial cancer cells. *Cancer Biol Ther*, 12, 924-38.
- MARTINEZ-OUTSCHOORN, U. E., LIN, Z., TRIMMER, C., FLOMENBERG, N., WANG, C., PAVLIDES, S., PESTELL, R. G., HOWELL, A., SOTGIA, F. & LISANTI, M. P. 2011b. Cancer cells metabolically "fertilize" the tumor microenvironment with hydrogen peroxide, driving the Warburg effect: implications for PET imaging of human tumors. *Cell Cycle*, 10, 2504-20.
- MARTINEZ-OUTSCHOORN, U. E., PAVLIDES, S., WHITAKER-MENEZES, D., DAUMER, K. M., MILLIMAN, J. N., CHIAVARINA, B., MIGNECO, G., WITKIEWICZ, A. K., MARTINEZ-CANTARIN, M. P., FLOMENBERG, N., HOWELL, A., PESTELL, R. G., LISANTI, M. P. & SOTGIA, F. 2010a. Tumor cells induce the cancer associated fibroblast phenotype via caveolin-1 degradation: implications for breast cancer and DCIS therapy with autophagy inhibitors. *Cell Cycle*, 9, 2423-33.
- MARTINEZ-OUTSCHOORN, U. E., TRIMMER, C., LIN, Z., WHITAKER-MENEZES, D., CHIAVARINA, B., ZHOU, J., WANG, C., PAVLIDES, S., MARTINEZ-CANTARIN, M. P., CAPOZZA, F., WITKIEWICZ, A. K., FLOMENBERG, N., HOWELL, A., PESTELL, R. G., CARO, J., LISANTI, M. P. & SOTGIA, F. 2010b. Autophagy in cancer associated fibroblasts promotes tumor cell survival: Role of hypoxia, HIF1 induction and NFkappaB activation in the tumor stromal microenvironment. *Cell Cycle*, 9, 3515-33.
- MAUDE, S. L. 2018. Tisagenlecleucel in pediatric patients with acute lymphoblastic leukemia. *Clin Adv Hematol Oncol*, 16, 664-666.
- MCFATE, T., MOHYELDIN, A., LU, H., THAKAR, J., HENRIQUES, J., HALIM, N. D., WU, H., SCHELL, M. J., TSANG, T. M., TEAHAN, O., ZHOU, S., CALIFANO, J. A., JEOUNG, N. H., HARRIS, R. A. & VERMA, A. 2008. Pyruvate dehydrogenase complex activity controls metabolic and malignant phenotype in cancer cells. *J Biol Chem*, 283, 22700-8.
- MCLEAN, P., KUNJARA, S., GREENBAUM, A. L., GUMAA, K., LOPEZ-PRADOS, J., MARTINLOMAS, M. & RADEMACHER, T. W. 2008. Reciprocal control of pyruvate dehydrogenase kinase and phosphatase by inositol phosphoglycans. Dynamic state set by "push-pull" system. *J Biol Chem*, 283, 33428-36.
- MERCER, P. F., WOODCOCK, H. V., ELEY, J. D., PLATE, M., SULIKOWSKI, M. G., DURRENBERGER, P. F., FRANKLIN, L., NANTHAKUMAR, C. B., MAN, Y., GENOVESE, F., MCANULTY, R. J., YANG, S., MAHER, T. M., NICHOLSON, A. G., BLANCHARD, A. D., MARSHALL, R. P., LUKEY, P. T. & CHAMBERS, R. C. 2016. Exploration of a potent PI3 kinase/mTOR inhibitor as a novel anti-fibrotic agent in IPF. *Thorax*, 71, 701-11.
- MEYAARD, L. 2008. The inhibitory collagen receptor LAIR-1 (CD305). *J Leukoc Biol*, 83, 799-803.
- MIAO, L., WANG, Y., LIN, C. M., XIONG, Y., CHEN, N., ZHANG, L., KIM, W. Y. & HUANG, L. 2015. Nanoparticle modulation of the tumor microenvironment enhances therapeutic efficacy of cisplatin. *J Control Release*, 217, 27-41.
- MICHELAKIS, E. D., WEBSTER, L. & MACKAY, J. R. 2008. Dichloroacetate (DCA) as a potential metabolic-targeting therapy for cancer. *Br J Cancer*, 99, 989-94.
- MILNE, K., SUN, J., ZAAL, E. A., MOWAT, J., CELIE, P. H. N., FISH, A., BERKERS, C. R., FORLANI, G., LOAYZA-PUCH, F., JAMIESON, C. & AGAMI, R. 2019. A fragment-like approach to PYCR1 inhibition. *Bioorg Med Chem Lett*.
- MOORE-SMITH, L. D., ISAYEVA, T., LEE, J. H., FROST, A. & PONNAZHAGAN, S. 2017. Silencing of TGF-beta1 in tumor cells impacts MMP-9 in tumor microenvironment. *Sci Rep*, 7, 8678.

- MOORMAN, A. M., VINK, R., HEIJMANS, H. J., VAN DER PALEN, J. & KOUWENHOVEN, E. A. 2012. The prognostic value of tumour-stroma ratio in triple-negative breast cancer. *Eur J Surg Oncol*, 38, 307-13.
- NABA, A., CLAUSER, K. R., LAMAR, J. M., CARR, S. A. & HYNES, R. O. 2014. Extracellular matrix signatures of human mammary carcinoma identify novel metastasis promoters. *Elife*, 3, e01308.
- NAGASAKI, T., HARA, M., NAKANISHI, H., TAKAHASHI, H., SATO, M. & TAKEYAMA, H. 2014. Interleukin-6 released by colon cancer-associated fibroblasts is critical for tumour angiogenesis: anti-interleukin-6 receptor antibody suppressed angiogenesis and inhibited tumour-stroma interaction. *Br J Cancer*, 110, 469-78.
- NAKAI, N., OBAYASHI, M., NAGASAKI, M., SATO, Y., FUJITSUKA, N., YOSHIMURA, A., MIYAZAKI, Y., SUGIYAMA, S. & SHIMOMURA, Y. 2000. The abundance of mRNAs for pyruvate dehydrogenase kinase isoenzymes in brain regions of young and aged rats. *Life Sci*, 68, 497-503.
- NAKAYASU, E. S., BURNET, M. C., WALUKIEWICZ, H. E., WILKINS, C. S., SHUKLA, A. K., BROOKS, S., PLUTZ, M. J., LEE, B. D., SCHILLING, B., WOLFE, A. J., MULLER, S., KIRBY, J. R., RAO, C. V., CORT, J. R. & PAYNE, S. H. 2017. Ancient Regulatory Role of Lysine Acetylation in Central Metabolism. *MBio*, 8.
- NAVAB, R., STRUMPF, D., TO, C., PASKO, E., KIM, K. S., PARK, C. J., HAI, J., LIU, J., JONKMAN, J., BARCZYK, M., BANDARCHI, B., WANG, Y. H., VENKAT, K., IBRAHIMOV, E., PHAM, N. A., NG, C., RADULOVICH, N., ZHU, C. Q., PINTILIE, M., WANG, D., LU, A., JURISICA, I., WALKER, G. C., GULLBERG, D. & TSAO, M. S. 2015. Integrin $\alpha 11\beta 1$ regulates cancer stromal stiffness and promotes tumorigenicity and metastasis in non-small cell lung cancer. *Oncogene*, 35, 1899-1908.
- NETTI, P. A., BERK, D. A., SWARTZ, M. A., GRODZINSKY, A. J. & JAIN, R. K. 2000. Role of extracellular matrix assembly in interstitial transport in solid tumors. *Cancer Res*, 60, 2497-503.
- NIGDELIOGLU, R., HAMANAKA, R. B., MELITON, A. Y., O'LEARY, E., WITT, L. J., CHO, T., SUN, K., BONHAM, C., WU, D., WOODS, P. S., HUSAIN, A. N., WOLFGEHER, D., DULIN, N. O., CHANDEL, N. S. & MUTLU, G. M. 2016. Transforming Growth Factor (TGF)-beta Promotes de Novo Serine Synthesis for Collagen Production. *J Biol Chem*, 291, 27239-27251.
- NIJHUIS, A., BIANCHERI, P., LEWIS, A., BISHOP, C. L., GIUFFRIDA, P., CHAN, C., FEAKINS, R., POULSOM, R., DI SABATINO, A., CORAZZA, G. R., MACDONALD, T. T., LINDSAY, J. O. & SILVER, A. R. 2014. In Crohn's disease fibrosis-reduced expression of the miR-29 family enhances collagen expression in intestinal fibroblasts. *Clin Sci (Lond)*, 127, 341-50.
- NILSSON, R., JAIN, M., MADHUSUDHAN, N., SHEPPARD, N. G., STRITTMATTER, L., KAMPF, C., HUANG, J., ASPLUND, A. & MOOTHA, V. K. 2014. Metabolic enzyme expression highlights a key role for MTHFD2 and the mitochondrial folate pathway in cancer. *Nat Commun*, 5, 3128.
- NISSEN, N. I., KARSDAL, M. & WILLUMSEN, N. 2019. Collagens and Cancer associated fibroblasts in the reactive stroma and its relation to Cancer biology. *J Exp Clin Cancer Res*, 38, 115.
- NURAL-GUVENER, H., ZAKHAROVA, L., FEEHERY, L., SLJUKIC, S. & GABALLA, M. 2015. Anti-Fibrotic Effects of Class I HDAC Inhibitor, Mocetinostat Is Associated with IL-6/Stat3 Signaling in Ischemic Heart Failure. *Int J Mol Sci*, 16, 11482-99.
- O'CONNELL, F. C. & MARTIN, F. 2000. Laminin-rich extracellular matrix association with mammary epithelial cells suppresses Brca1 expression. *Cell Death Differ*, 7, 360-7.
- O'CONNOR, R. S., HAO, X., SHEN, K., BASHOUR, K., AKIMOVA, T., HANCOCK, W. W., KAM, L. C. & MILONE, M. C. 2012. Substrate rigidity regulates human T cell activation and proliferation. *J Immunol*, 189, 1330-9.
- OHLUND, D., HANDLY-SANTANA, A., BIFFI, G., ELYADA, E., ALMEIDA, A. S., PONZ-SARVISE, M., CORBO, V., ONI, T. E., HEARN, S. A., LEE, E. J., CHIO, II, HWANG, C. I., TIRIAC, H., BAKER, L. A., ENGLE, D. D., FEIG, C., KULTTI, A., EGEGLAD, M., FEARON, D. T., CRAWFORD, J. M., CLEVERS, H., PARK, Y. & TUVESON, D. A. 2017. Distinct

- populations of inflammatory fibroblasts and myofibroblasts in pancreatic cancer. *J Exp Med*, 214, 579-596.
- OLIVARES, O., MAYERS, J. R., GOUIRAND, V., TORRENCE, M. E., GICQUEL, T., BORGE, L., LAC, S., ROQUES, J., LAVAUT, M. N., BERTHEZENE, P., RUBIS, M., SECQ, V., GARCIA, S., MOUTARDIER, V., LOMBARDO, D., IOVANNA, J. L., TOMASINI, R., GUILLAUMOND, F., VANDER HEIDEN, M. G. & VASSEUR, S. 2017. Collagen-derived proline promotes pancreatic ductal adenocarcinoma cell survival under nutrient limited conditions. *Nat Commun*, 8, 16031.
- OLUMI, A. F., GROSSFELD, G. D., HAYWARD, S. W., CARROLL, P. R., TLSTY, T. D. & CUNHA, G. R. 1999. Carcinoma-associated fibroblasts direct tumor progression of initiated human prostatic epithelium. *Cancer Res*, 59, 5002-11.
- ORIMO, A., GUPTA, P. B., SGROI, D. C., ARENZANA-SEISDEDOS, F., DELAUNAY, T., NAEEM, R., CAREY, V. J., RICHARDSON, A. L. & WEINBERG, R. A. 2005. Stromal fibroblasts present in invasive human breast carcinomas promote tumor growth and angiogenesis through elevated SDF-1/CXCL12 secretion. *Cell*, 121, 335-48.
- OZDEMIR, B. C., PENTCHEVA-HOANG, T., CARSTENS, J. L., ZHENG, X., WU, C. C., SIMPSON, T. R., LAKLAI, H., SUGIMOTO, H., KAHLERT, C., NOVITSKIY, S. V., DE JESUS-ACOSTA, A., SHARMA, P., HEIDARI, P., MAHMOOD, U., CHIN, L., MOSES, H. L., WEAVER, V. M., MAITRA, A., ALLISON, J. P., LEBLEU, V. S. & KALLURI, R. 2014. Depletion of carcinoma-associated fibroblasts and fibrosis induces immunosuppression and accelerates pancreas cancer with reduced survival. *Cancer Cell*, 25, 719-34.
- OZDEN, O., PARK, S. H., WAGNER, B. A., SONG, H. Y., ZHU, Y., VASSILOPOULOS, A., JUNG, B., BUETTNER, G. R. & GIUS, D. 2014. SIRT3 deacetylates and increases pyruvate dehydrogenase activity in cancer cells. *Free Radic Biol Med*, 76, 163-172.
- PAN, X., CHEN, Z., HUANG, R., YAO, Y. & MA, G. 2013. Transforming growth factor beta1 induces the expression of collagen type I by DNA methylation in cardiac fibroblasts. *PLoS One*, 8, e60335.
- PANG, W., SU, J., WANG, Y., FENG, H., DAI, X., YUAN, Y., CHEN, X. & YAO, W. 2015. Pancreatic cancer-secreted miR-155 implicates in the conversion from normal fibroblasts to cancer-associated fibroblasts. *Cancer Sci*, 106, 1362-9.
- PAPANDREOU, I., CAIRNS, R. A., FONTANA, L., LIM, A. L. & DENKO, N. C. 2006. HIF-1 mediates adaptation to hypoxia by actively downregulating mitochondrial oxygen consumption. *Cell Metab*, 3, 187-97.
- PARDEE, T. S., ANDERSON, R. G., PLADNA, K. M., ISOM, S., GHIRALDELI, L. P., MILLER, L. D., CHOU, J. W., JIN, G., ZHANG, W., ELLIS, L. R., BERENZON, D., HOWARD, D. S., HURD, D. D., MANUEL, M., DRALLE, S., LYERLY, S. & POWELL, B. L. 2018. A Phase I Study of CPI-613 in Combination with High-Dose Cytarabine and Mitoxantrone for Relapsed or Refractory Acute Myeloid Leukemia. *Clin Cancer Res*, 24, 2060-2073.
- PATE, K. T., STRINGARI, C., SPROWL-TANIO, S., WANG, K., TESLAA, T., HOVERTER, N. P., MCQUADE, M. M., GARNER, C., DIGMAN, M. A., TEITELL, M. A., EDWARDS, R. A., GRATTON, E. & WATERMAN, M. L. 2014. Wnt signaling directs a metabolic program of glycolysis and angiogenesis in colon cancer. *EMBO J*, 33, 1454-73.
- PATEL, M. S. & KOROTCHKINA, L. G. 2001. Regulation of mammalian pyruvate dehydrogenase complex by phosphorylation: complexity of multiple phosphorylation sites and kinases. *Exp Mol Med*, 33, 191-7.
- PATEL, M. S. & KOROTCHKINA, L. G. 2006. Regulation of the pyruvate dehydrogenase complex. *Biochem Soc Trans*, 34, 217-22.
- PATEL, N. R., BOLE, M., CHEN, C., HARDIN, C. C., KHO, A. T., MIH, J., DENG, L., BUTLER, J., TSCHUMPERLIN, D., FREDBERG, J. J., KRISHNAN, R. & KOZIEL, H. 2012. Cell elasticity determines macrophage function. *PLoS One*, 7, e41024.
- PAULSSON, J., SJOBLUM, T., MICKE, P., PONTEN, F., LANDBERG, G., HELDIN, C. H., BERGH, J., BRENNAN, D. J., JIRSTROM, K. & OSTMAN, A. 2009. Prognostic significance of stromal platelet-derived growth factor beta-receptor expression in human breast cancer. *Am J Pathol*, 175, 334-41.

- PAVLIDES, S., TSIRIGOS, A., MIGNECO, G., WHITAKER-MENEZES, D., CHIAVARINA, B., FLOMENBERG, N., FRANK, P. G., CASIMIRO, M. C., WANG, C., PESTELL, R. G., MARTINEZ-OUTSCHOORN, U. E., HOWELL, A., SOTGIA, F. & LISANTI, M. P. 2010a. The autophagic tumor stroma model of cancer: Role of oxidative stress and ketone production in fueling tumor cell metabolism. *Cell Cycle*, 9, 3485-505.
- PAVLIDES, S., TSIRIGOS, A., VERA, I., FLOMENBERG, N., FRANK, P. G., CASIMIRO, M. C., WANG, C., FORTINA, P., ADDYA, S., PESTELL, R. G., MARTINEZ-OUTSCHOORN, U. E., SOTGIA, F. & LISANTI, M. P. 2010b. Loss of stromal caveolin-1 leads to oxidative stress, mimics hypoxia and drives inflammation in the tumor microenvironment, conferring the "reverse Warburg effect": a transcriptional informatics analysis with validation. *Cell Cycle*, 9, 2201-19.
- PAVLIDES, S., TSIRIGOS, A., VERA, I., FLOMENBERG, N., FRANK, P. G., CASIMIRO, M. C., WANG, C., PESTELL, R. G., MARTINEZ-OUTSCHOORN, U. E., HOWELL, A., SOTGIA, F. & LISANTI, M. P. 2010c. Transcriptional evidence for the "Reverse Warburg Effect" in human breast cancer tumor stroma and metastasis: similarities with oxidative stress, inflammation, Alzheimer's disease, and "Neuron-Glia Metabolic Coupling". *Aging (Albany NY)*, 2, 185-99.
- PAVLIDES, S., VERA, I., GANDARA, R., SNEDDON, S., PESTELL, R. G., MERCIER, I., MARTINEZ-OUTSCHOORN, U. E., WHITAKER-MENEZES, D., HOWELL, A., SOTGIA, F. & LISANTI, M. P. 2012. Warburg meets autophagy: cancer-associated fibroblasts accelerate tumor growth and metastasis via oxidative stress, mitophagy, and aerobic glycolysis. *Antioxid Redox Signal*, 16, 1264-84.
- PAVLIDES, S., WHITAKER-MENEZES, D., CASTELLO-CROS, R., FLOMENBERG, N., WITKIEWICZ, A. K., FRANK, P. G., CASIMIRO, M. C., WANG, C., FORTINA, P., ADDYA, S., PESTELL, R. G., MARTINEZ-OUTSCHOORN, U. E., SOTGIA, F. & LISANTI, M. P. 2009. The reverse Warburg effect: aerobic glycolysis in cancer associated fibroblasts and the tumor stroma. *Cell Cycle*, 8, 3984-4001.
- PEROU, C. M., SORLIE, T., EISEN, M. B., VAN DE RIJN, M., JEFFREY, S. S., REES, C. A., POLLACK, J. R., ROSS, D. T., JOHNSEN, H., AKSLEN, L. A., FLUGE, O., PERGAMENSHIKOV, A., WILLIAMS, C., ZHU, S. X., LONNING, P. E., BORRESENDALE, A. L., BROWN, P. O. & BOTSTEIN, D. 2000. Molecular portraits of human breast tumours. *Nature*, 406, 747-52.
- PERRI, R. T., KAY, N. E., MCCARTHY, J., VESSELLA, R. L., JACOB, H. S. & FURCHT, L. T. 1982. Fibronectin enhances in vitro monocyte-macrophage-mediated tumoricidal activity. *Blood*, 60, 430-5.
- PETERSEN, O. W., LIND NIELSEN, H., GUDJONSSON, T., VILLADSEN, R., RONNOV-JESSEN, L. & BISSELL, M. J. 2001. The plasticity of human breast carcinoma cells is more than epithelial to mesenchymal conversion. *Breast Cancer Res*, 3, 213-7.
- PICKUP, M. W., MOUW, J. K. & WEAVER, V. M. 2014. The extracellular matrix modulates the hallmarks of cancer. *EMBO Rep*, 15, 1243-53.
- PIDSLEY, R., LAWRENCE, M. G., ZOTENKO, E., NIRANJAN, B., STATHAM, A., SONG, J., CHABANON, R. M., QU, W., WANG, H., RICHARDS, M., NAIR, S. S., ARMSTRONG, N. J., NIM, H. T., PAPARGIRIS, M., BALANATHAN, P., FRENCH, H., PETERS, T., NORDEN, S., RYAN, A., PEDERSEN, J., KENCH, J., DALY, R. J., HORVATH, L. G., STRICKER, P., FRYDENBERG, M., TAYLOR, R. A., STIRZAKER, C., RISBRIDGER, G. P. & CLARK, S. J. 2018. Enduring epigenetic landmarks define the cancer microenvironment. *Genome Res*, 28, 625-638.
- PIETROCOLA, F., GALLUZZI, L., BRAVO-SAN PEDRO, J. M., MADEO, F. & KROEMER, G. 2015. Acetyl coenzyme A: a central metabolite and second messenger. *Cell Metab*, 21, 805-21.
- PILEGAARD, H. & NEUFER, P. D. 2004. Transcriptional regulation of pyruvate dehydrogenase kinase 4 in skeletal muscle during and after exercise. *Proc Nutr Soc*, 63, 221-6.
- POSSEMATO, R., MARKS, K. M., SHAUL, Y. D., PACOLD, M. E., KIM, D., BIRSOY, K., SETHUMADHAVAN, S., WOO, H. K., JANG, H. G., JHA, A. K., CHEN, W. W., BARRETT, F. G., STRANSKY, N., TSUN, Z. Y., COWLEY, G. S., BARRETINA, J., KALAANY, N. Y., HSU, P. P., OTTINA, K., CHAN, A. M., YUAN, B., GARRAWAY, L.

- A., ROOT, D. E., MINO-KENUDSON, M., BRACHTEL, E. F., DRIGGERS, E. M. & SABATINI, D. M. 2011. Functional genomics reveal that the serine synthesis pathway is essential in breast cancer. *Nature*, 476, 346-50.
- POTAPOVA, I. A., EL-MAGHRABI, M. R., DORONIN, S. V. & BENJAMIN, W. B. 2000. Phosphorylation of recombinant human ATP:citrate lyase by cAMP-dependent protein kinase abolishes homotropic allosteric regulation of the enzyme by citrate and increases the enzyme activity. Allosteric activation of ATP:citrate lyase by phosphorylated sugars. *Biochemistry*, 39, 1169-79.
- POWELL, S. 2015. *Study of DCA (Dichloroacetate) in Combination With Cisplatin and Definitive Radiation in Head and Neck Carcinoma* [Online]. Available: <https://ClinicalTrials.gov/show/NCT01386632> [Accessed].
- PRATT, M. L. & ROCHE, T. E. 1979. Mechanism of pyruvate inhibition of kidney pyruvate dehydrogenase kinase and synergistic inhibition by pyruvate and ADP. *J Biol Chem*, 254, 7191-6.
- PROVENZANO, P. P., INMAN, D. R., ELICEIRI, K. W., KNITTEL, J. G., YAN, L., RUEDEN, C. T., WHITE, J. G. & KEELY, P. J. 2008. Collagen density promotes mammary tumor initiation and progression. *BMC Med*, 6, 11.
- PROVENZANO, P. P. & KEELY, P. J. 2011. Mechanical signaling through the cytoskeleton regulates cell proliferation by coordinated focal adhesion and Rho GTPase signaling. *J Cell Sci*, 124, 1195-205.
- QUANTE, M., TU, S. P., TOMITA, H., GONDA, T., WANG, S. S., TAKASHI, S., BAIK, G. H., SHIBATA, W., DIPRETE, B., BETZ, K. S., FRIEDMAN, R., VARRO, A., TYCKO, B. & WANG, T. C. 2011. Bone marrow-derived myofibroblasts contribute to the mesenchymal stem cell niche and promote tumor growth. *Cancer Cell*, 19, 257-72.
- RABINOVICH, G. A., GABRILOVICH, D. & SOTOMAYOR, E. M. 2007. Immunosuppressive strategies that are mediated by tumor cells. *Annu Rev Immunol*, 25, 267-96.
- RAISNER, R., KHARBANDA, S., JIN, L., JENG, E., CHAN, E., MERCHANT, M., HAVERTY, P. M., BAINER, R., CHEUNG, T., ARNOTT, D., FLYNN, E. M., ROMERO, F. A., MAGNUSON, S. & GASCOIGNE, K. E. 2018. Enhancer Activity Requires CBP/P300 Bromodomain-Dependent Histone H3K27 Acetylation. *Cell Rep*, 24, 1722-1729.
- RAJAGOPALAN, K. N., EGNATCHIK, R. A., CALVARUSO, M. A., WASTI, A. T., PADANAD, M. S., BOROUGHS, L. K., KO, B., HENSLEY, C. T., ACAR, M., HU, Z., JIANG, L., PASCUAL, J. M., SCAGLIONI, P. P. & DEBERARDINIS, R. J. 2015. Metabolic plasticity maintains proliferation in pyruvate dehydrogenase deficient cells. *Cancer Metab*, 3, 7.
- RAJSHANKAR, D., WANG, Y. & MCCULLOCH, C. A. 2017. Osteogenesis requires FAK-dependent collagen synthesis by fibroblasts and osteoblasts. *FASEB J*, 31, 937-953.
- RANDLE, P. J. 1986. Fuel selection in animals. *Biochem Soc Trans*, 14, 799-806.
- RAZ, Y., COHEN, N., SHANI, O., BELL, R. E., NOVITSKIY, S. V., ABRAMOVITZ, L., LEVY, C., MILYAVSKY, M., LEIDER-TREJO, L., MOSES, H. L., GRISARU, D. & EREZ, N. 2018. Bone marrow-derived fibroblasts are a functionally distinct stromal cell population in breast cancer. *The Journal of Experimental Medicine*, 215, 3075-3093.
- REN, J., GUO, H., WU, H., TIAN, T., DONG, D., ZHANG, Y., SUI, Y., ZHANG, Y., ZHAO, D., WANG, S., LI, Z., ZHANG, X., LIU, R., QIAN, J., WEI, H., JIANG, W., LIU, Y. & LI, Y. 2015. GPER in CAFs regulates hypoxia-driven breast cancer invasion in a CTGF-dependent manner. *Oncol Rep*, 33, 1929-37.
- REVERSADE, B., ESCANDE-BEILLARD, N., DIMOPOULOU, A., FISCHER, B., CHNG, S. C., LI, Y., SHBOUL, M., THAM, P. Y., KAYSERILI, H., AL-GAZALI, L., SHAHWAN, M., BRANCATI, F., LEE, H., O'CONNOR, B. D., SCHMIDT-VON KEGLER, M., MERRIMAN, B., NELSON, S. F., MASRI, A., ALKAZALEH, F., GUERRA, D., FERRARI, P., NANDA, A., RAJAB, A., MARKIE, D., GRAY, M., NELSON, J., GRIX, A., SOMMER, A., SAVARIRAYAN, R., JANECKE, A. R., STEICHEN, E., SILLENCE, D., HAUSSER, I., BUDDE, B., NURNBERG, G., NURNBERG, P., SEEMANN, P., KUNKEL, D., ZAMBRUNO, G., DALLAPICCOLA, B., SCHUELKE, M., ROBERTSON, S., HAMAMY, H., WOLLNIK, B., VAN MALDERGEM, L., MUNDLOS, S. & KORNAK, U. 2009. Mutations in PYCR1 cause cutis laxa with progeroid features. *Nat Genet*, 41, 1016-21.

- RHIM, A. D., OBERSTEIN, P. E., THOMAS, D. H., MIREK, E. T., PALERMO, C. F., SASTRA, S. A., DEKLEVA, E. N., SAUNDERS, T., BECERRA, C. P., TATTERSALL, I. W., WESTPHALEN, C. B., KITAJEWSKI, J., FERNANDEZ-BARRENA, M. G., FERNANDEZ-ZAPICO, M. E., IACOBUZIO-DONAHUE, C., OLIVE, K. P. & STANGER, B. Z. 2014. Stromal elements act to restrain, rather than support, pancreatic ductal adenocarcinoma. *Cancer Cell*, 25, 735-47.
- RICE, A. J., CORTES, E., LACHOWSKI, D., CHEUNG, B. C. H., KARIM, S. A., MORTON, J. P. & DEL RIO HERNANDEZ, A. 2017. Matrix stiffness induces epithelial-mesenchymal transition and promotes chemoresistance in pancreatic cancer cells. *Oncogenesis*, 6, e352.
- RICHARDSON, A. D., YANG, C., OSTERMAN, A. & SMITH, J. W. 2008. Central carbon metabolism in the progression of mammary carcinoma. *Breast Cancer Res Treat*, 110, 297-307.
- RODEMANN, H. P. & MULLER, G. A. 1991. Characterization of human renal fibroblasts in health and disease: II. In vitro growth, differentiation, and collagen synthesis of fibroblasts from kidneys with interstitial fibrosis. *Am J Kidney Dis*, 17, 684-6.
- RODRIGUEZ-ENRIQUEZ, S., CARRENO-FUENTES, L., GALLARDO-PEREZ, J. C., SAAVEDRA, E., QUEZADA, H., VEGA, A., MARIN-HERNANDEZ, A., OLIN-SANDOVAL, V., TORRES-MARQUEZ, M. E. & MORENO-SANCHEZ, R. 2010. Oxidative phosphorylation is impaired by prolonged hypoxia in breast and possibly in cervix carcinoma. *Int J Biochem Cell Biol*, 42, 1744-51.
- RONNOV-JESSEN, L. & PETERSEN, O. W. 1993. Induction of alpha-smooth muscle actin by transforming growth factor-beta 1 in quiescent human breast gland fibroblasts. Implications for myofibroblast generation in breast neoplasia. *Lab Invest*, 68, 696-707.
- ROSS, D. T., SCHERF, U., EISEN, M. B., PEROU, C. M., REES, C., SPELLMAN, P., IYER, V., JEFFREY, S. S., VAN DE RIJN, M., WALTHAM, M., PERGAMENSCHIKOV, A., LEE, J. C., LASHKARI, D., SHALON, D., MYERS, T. G., WEINSTEIN, J. N., BOTSTEIN, D. & BROWN, P. O. 2000. Systematic variation in gene expression patterns in human cancer cell lines. *Nat Genet*, 24, 227-35.
- ROSWALL, P., BOCCI, M., BARTOSCHEK, M., LI, H., KRISTIANSEN, G., JANSSON, S., LEHN, S., SJOLUND, J., REID, S., LARSSON, C., ERIKSSON, P., ANDERBERG, C., CORTEZ, E., SAAL, L. H., ORSMARK-PIETRAS, C., CORDERO, E., HALLER, B. K., HAKKINEN, J., BURVENICH, I. J. G., LIM, E., ORIMO, A., HOGLUND, M., RYDEN, L., MOCH, H., SCOTT, A. M., ERIKSSON, U. & PIETRAS, K. 2018. Microenvironmental control of breast cancer subtype elicited through paracrine platelet-derived growth factor-CC signaling. *Nat Med*, 24, 463-473.
- ROW, S., LIU, Y., ALIMPERTI, S., AGARWAL, S. K. & ANDREADIS, S. T. 2016. Cadherin-11 is a novel regulator of extracellular matrix synthesis and tissue mechanics. *J Cell Sci*, 129, 2950-61.
- ROZENCHAN, P. B., CARRARO, D. M., BRENTANI, H., DE CARVALHO MOTA, L. D., BASTOS, E. P., E FERREIRA, E. N., TORRES, C. H., KATAYAMA, M. L., ROELA, R. A., LYRA, E. C., SOARES, F. A., FOLGUEIRA, M. A., GOES, J. C. & BRENTANI, M. M. 2009. Reciprocal changes in gene expression profiles of cocultured breast epithelial cells and primary fibroblasts. *Int J Cancer*, 125, 2767-77.
- SADLER, T., SCARPA, M., RIEDER, F., WEST, G. & STYLIANOU, E. 2013. Cytokine-induced chromatin modifications of the type I collagen alpha 2 gene during intestinal endothelial-to-mesenchymal transition. *Inflamm Bowel Dis*, 19, 1354-64.
- SAMUEL, D., KUMAR, T. K., GANESH, G., JAYARAMAN, G., YANG, P. W., CHANG, M. M., TRIVEDI, V. D., WANG, S. L., HWANG, K. C., CHANG, D. K. & YU, C. 2000. Proline inhibits aggregation during protein refolding. *Protein Sci*, 9, 344-52.
- SANDLER, A., GRAY, R., PERRY, M. C., BRAHMER, J., SCHILLER, J. H., DOWLATI, A., LILENBAUM, R. & JOHNSON, D. H. 2006. Paclitaxel-carboplatin alone or with bevacizumab for non-small-cell lung cancer. *N Engl J Med*, 355, 2542-50.
- SANSONE, P., SAVINI, C., KURELAC, I., CHANG, Q., AMATO, L. B., STRILLACCI, A., STEPANOVA, A., IOMMARINI, L., MASTROLEO, C., DALY, L., GALKIN, A., THAKUR, B. K., SOPLOP, N., URYU, K., HOSHINO, A., NORTON, L., BONAFE, M., CRICCA, M.,

- GASPARRE, G., LYDEN, D. & BROMBERG, J. 2017. Packaging and transfer of mitochondrial DNA via exosomes regulate escape from dormancy in hormonal therapy-resistant breast cancer. *Proc Natl Acad Sci U S A*, 114, E9066-E9075.
- SAPPINO, A. P., SKALLI, O., JACKSON, B., SCHURCH, W. & GABBIANI, G. 1988. Smooth-muscle differentiation in stromal cells of malignant and non-malignant breast tissues. *Int J Cancer*, 41, 707-12.
- SAUNIER, E., ANTONIO, S., REGAZZETTI, A., AUZEIL, N., LAPREVOTE, O., SHAY, J. W., COUMOUL, X., BAROUKI, R., BENELLI, C., HUC, L. & BORTOLI, S. 2017. Resveratrol reverses the Warburg effect by targeting the pyruvate dehydrogenase complex in colon cancer cells. *Sci Rep*, 7, 6945.
- SAUNIER, E., BENELLI, C. & BORTOLI, S. 2016. The pyruvate dehydrogenase complex in cancer: An old metabolic gatekeeper regulated by new pathways and pharmacological agents. *Int J Cancer*, 138, 809-17.
- SAWADA, Y., TAMADA, M., DUBIN-THALER, B. J., CHERNIAVSKAYA, O., SAKAI, R., TANAKA, S. & SHEETZ, M. P. 2006. Force sensing by mechanical extension of the Src family kinase substrate p130Cas. *Cell*, 127, 1015-26.
- SCHLIEKELMAN, M. J., CREIGHTON, C. J., BAIRD, B. N., CHEN, Y., BANERJEE, P., BOTA-RABASEDAS, N., AHN, Y.-H., ROYBAL, J. D., CHEN, F., ZHANG, Y., MISHRA, D. K., KIM, M. P., LIU, X., MINO, B., VILLALOBOS, P., RODRIGUEZ-CANALES, J., BEHRENS, C., WISTUBA, I. I., HANASH, S. M. & KURIE, J. M. 2017. Thy-1+ Cancer-associated Fibroblasts Adversely Impact Lung Cancer Prognosis. *Scientific Reports*, 7.
- SCHMIDT, E. V. 2019. Developing combination strategies using PD-1 checkpoint inhibitors to treat cancer. *Semin Immunopathol*, 41, 21-30.
- SCHNEIDER, R., BANNISTER, A. J., MYERS, F. A., THORNE, A. W., CRANE-ROBINSON, C. & KOUZARIDES, T. 2004. Histone H3 lysine 4 methylation patterns in higher eukaryotic genes. *Nat Cell Biol*, 6, 73-7.
- SCHUSTER, S. J. & INVESTIGATORS, J. 2019. Tisagenlecleucel in Diffuse Large B-Cell Lymphoma. Reply. *N Engl J Med*, 380, 1586.
- SCHWARTZ, M. A. & ASSOIAN, R. K. 2001. Integrins and cell proliferation: regulation of cyclin-dependent kinases via cytoplasmic signaling pathways. *J Cell Sci*, 114, 2553-60.
- SCOTT, L. E., WEINBERG, S. H. & LEMMON, C. A. 2019. Mechanochemical Signaling of the Extracellular Matrix in Epithelial-Mesenchymal Transition. *Front Cell Dev Biol*, 7, 135.
- SEGUIN, L., DESGROSELLIER, J. S., WEIS, S. M. & CHERESH, D. A. 2015. Integrins and cancer: regulators of cancer stemness, metastasis, and drug resistance. *Trends Cell Biol*, 25, 234-40.
- SELAK, M. A., ARMOUR, S. M., MACKENZIE, E. D., BOULAHBEL, H., WATSON, D. G., MANSFIELD, K. D., PAN, Y., SIMON, M. C., THOMPSON, C. B. & GOTTLIEB, E. 2005. Succinate links TCA cycle dysfunction to oncogenesis by inhibiting HIF-alpha prolyl hydroxylase. *Cancer Cell*, 7, 77-85.
- SELVARAJAH, B., AZUELOS, I., PLATE, M., GUILLOTIN, D., FORTY, E. J., CONTENTO, G., WOODCOCK, H. V., REDDING, M., TAYLOR, A., BRUNORI, G., DURRENBERGER, P. F., RONZONI, R., BLANCHARD, A. D., MERCER, P. F., ANASTASIOU, D. & CHAMBERS, R. C. 2019. mTORC1 amplifies the ATF4-dependent de novo serine-glycine pathway to supply glycine during TGF-beta1-induced collagen biosynthesis. *Sci Signal*, 12.
- SEN, P., LAN, Y., LI, C. Y., SIDOLI, S., DONAHUE, G., DOU, Z., FREDERICK, B., CHEN, Q., LUENSE, L. J., GARCIA, B. A., DANG, W., JOHNSON, F. B., ADAMS, P. D., SCHULTZ, D. C. & BERGER, S. L. 2019. Histone Acetyltransferase p300 Induces De Novo Super-Enhancers to Drive Cellular Senescence. *Mol Cell*, 73, 684-698 e8.
- SERGANOV, A. & PATEL, D. J. 2009. Amino acid recognition and gene regulation by riboswitches. *Biochim Biophys Acta*, 1789, 592-611.
- SERRAO, E. M., KETTUNEN, M. I., RODRIGUES, T. B., DZIEN, P., WRIGHT, A. J., GOPINATHAN, A., GALLAGHER, F. A., LEWIS, D. Y., FRESE, K. K., ALMEIDA, J., HOWAT, W. J., TUVESON, D. A. & BRINDLE, K. M. 2016. MRI with hyperpolarised [1-13C]pyruvate detects advanced pancreatic preneoplasia prior to invasive disease in a mouse model. *Gut*, 65, 465-75.

- SEWELL-LOFTIN, M. K., BAYER, S. V. H., CRIST, E., HUGHES, T., JOISON, S. M., LONGMORE, G. D. & GEORGE, S. C. 2017. Cancer-associated fibroblasts support vascular growth through mechanical force. *Sci Rep*, 7, 12574.
- SHAH, S. H., MILLER, P., GARCIA-CONTRERAS, M., AO, Z., MACHLIN, L., ISSA, E. & EL-ASHRY, D. 2015. Hierarchical paracrine interaction of breast cancer associated fibroblasts with cancer cells via hMAPK-microRNAs to drive ER-negative breast cancer phenotype. *Cancer Biol Ther*, 16, 1671-81.
- SHAN, C., KANG, H. B., ELF, S., XIE, J., GU, T. L., AGUIAR, M., LONNING, S., HITOSUGI, T., CHUNG, T. W., ARELLANO, M., KHOURY, H. J., SHIN, D. M., KHURI, F. R., BOGGON, T. J. & FAN, J. 2014. Tyr-94 phosphorylation inhibits pyruvate dehydrogenase phosphatase 1 and promotes tumor growth. *J Biol Chem*, 289, 21413-22.
- SHAN, T., CHEN, S., CHEN, X., LIN, W. R., LI, W., MA, J., WU, T., CUI, X., JI, H., LI, Y. & KANG, Y. 2017. Cancer-associated fibroblasts enhance pancreatic cancer cell invasion by remodeling the metabolic conversion mechanism. *Oncol Rep*, 37, 1971-1979.
- SHERMAN, M. H., YU, R. T., ENGLE, D. D., DING, N., ATKINS, A. R., TIRIAC, H., COLLISSON, E. A., CONNOR, F., VAN DYKE, T., KOZLOV, S., MARTIN, P., TSENG, T. W., DAWSON, D. W., DONAHUE, T. R., MASAMUNE, A., SHIMOSEGAWA, T., APTE, M. V., WILSON, J. S., NG, B., LAU, S. L., GUNTON, J. E., WAHL, G. M., HUNTER, T., DREBIN, J. A., O'DWYER, P. J., LIDDLE, C., TUVESON, D. A., DOWNES, M. & EVANS, R. M. 2014. Vitamin D receptor-mediated stromal reprogramming suppresses pancreatitis and enhances pancreatic cancer therapy. *Cell*, 159, 80-93.
- SHI, G. & MCQUIBBAN, G. A. 2017. The Mitochondrial Rhomboid Protease PARL Is Regulated by PDK2 to Integrate Mitochondrial Quality Control and Metabolism. *Cell Rep*, 18, 1458-1472.
- SHI, W. Y., YANG, X., HUANG, B., SHEN, W. H. & LIU, L. 2017. NOK mediates glycolysis and nuclear PDC associated histone acetylation. *Front Biosci (Landmark Ed)*, 22, 1792-1804.
- SHOULDERS, M. D. & RAINES, R. T. 2009. Collagen structure and stability. *Annu Rev Biochem*, 78, 929-58.
- SHRIMP, J. H., SORUM, A. W., GARLICK, J. M., GUASCH, L., NICKLAUS, M. C. & MEIER, J. L. 2015. Characterizing the Covalent Targets of a Small Molecule Inhibitor of the Lysine Acetyltransferase P300. *ACS Medicinal Chemistry Letters*, 7, 151-155.
- SIMIAN, M., HIRAI, Y., NAVRE, M., WERB, Z., LOCHTER, A. & BISSELL, M. J. 2001. The interplay of matrix metalloproteinases, morphogens and growth factors is necessary for branching of mammary epithelial cells. *Development*, 128, 3117-31.
- SINI, V., CASSANO, A., CORSI, D., DE LAURENTIIS, M., GAMUCCI, T., MAURI, M., NASO, G., ROSELLI, M., RUGGERI, E. M., TONINI, G., VICI, P., ZAMPA, G. & MARCHETTI, P. 2016. Bevacizumab as first-line treatment in HER2-negative advanced breast cancer: pros and cons. *Tumori*, 102, 472-480.
- SIVANAND, S., VINEY, I. & WELLEN, K. E. 2018. Spatiotemporal Control of Acetyl-CoA Metabolism in Chromatin Regulation. *Trends Biochem Sci*, 43, 61-74.
- SKIDMORE, D. L., CHITAYAT, D., MORGAN, T., HINEK, A., FISCHER, B., DIMOPOULOU, A., SOMERS, G., HALLIDAY, W., BLASER, S., DIAMBOMBA, Y., LEMIRE, E. G., KORNAK, U. & ROBERTSON, S. P. 2011. Further expansion of the phenotypic spectrum associated with mutations in ALDH18A1, encoding Delta(1)-pyrroline-5-carboxylate synthase (P5CS). *Am J Med Genet A*, 155A, 1848-56.
- SMITH, N. R., BAKER, D., FARREN, M., POMMIER, A., SWANN, R., WANG, X., MISTRY, S., MCDAID, K., KENDREW, J., WOMACK, C., WEDGE, S. R. & BARRY, S. T. 2013. Tumor stromal architecture can define the intrinsic tumor response to VEGF-targeted therapy. *Clin Cancer Res*, 19, 6943-56.
- SONVEAUX, P., VEGRAN, F., SCHROEDER, T., WERGIN, M. C., VERRAX, J., RABBANI, Z. N., DE SAEDELEER, C. J., KENNEDY, K. M., DIEPART, C., JORDAN, B. F., KELLEY, M. J., GALLEZ, B., WAHL, M. L., FERON, O. & DEWHIRST, M. W. 2008. Targeting lactate-fueled respiration selectively kills hypoxic tumor cells in mice. *J Clin Invest*, 118, 3930-42.

- SORLIE, T., PEROU, C. M., TIBSHIRANI, R., AAS, T., GEISLER, S., JOHNSEN, H., HASTIE, T., EISEN, M. B., VAN DE RIJN, M., JEFFREY, S. S., THORSEN, T., QUIST, H., MATESE, J. C., BROWN, P. O., BOTSTEIN, D., LONNING, P. E. & BORRESEN-DALE, A. L. 2001. Gene expression patterns of breast carcinomas distinguish tumor subclasses with clinical implications. *Proc Natl Acad Sci U S A*, 98, 10869-74.
- SOUSA, C. M., BIANCUR, D. E., WANG, X., HALBROOK, C. J., SHERMAN, M. H., ZHANG, L., KREMER, D., HWANG, R. F., WITKIEWICZ, A. K., YING, H., ASARA, J. M., EVANS, R. M., CANTLEY, L. C., LYSSIOTIS, C. A. & KIMMELMAN, A. C. 2016. Pancreatic stellate cells support tumour metabolism through autophagic alanine secretion. *Nature*, 536, 479-83.
- STANISAVLJEVIC, J., LOUBAT-CASANOVAS, J., HERRERA, M., LUQUE, T., PENA, R., LLUCH, A., ALBANELL, J., BONILLA, F., ROVIRA, A., PENA, C., NAVAJAS, D., ROJO, F., GARCIA DE HERREROS, A. & BAULIDA, J. 2015. Snail1-expressing fibroblasts in the tumor microenvironment display mechanical properties that support metastasis. *Cancer Res*, 75, 284-95.
- STEGEN, S., LAPERRE, K., EELEN, G., RINALDI, G., FRAISL, P., TORREKENS, S., VAN LOOVEREN, R., LOOPMANS, S., BULTYNCK, G., VINCKIER, S., MEERSMAN, F., MAXWELL, P. H., RAI, J., WEIS, M., EYRE, D. R., GHESQUIERE, B., FENDT, S. M., CARMELIET, P. & CARMELIET, G. 2019. HIF-1alpha metabolically controls collagen synthesis and modification in chondrocytes. *Nature*, 565, 511-515.
- STRAUSSMAN, R., MORIKAWA, T., SHEE, K., BARZILY-ROKNI, M., QIAN, Z. R., DU, J., DAVIS, A., MONGARE, M. M., GOULD, J., FREDERICK, D. T., COOPER, Z. A., CHAPMAN, P. B., SOLIT, D. B., RIBAS, A., LO, R. S., FLAHERTY, K. T., OGINO, S., WARGO, J. A. & GOLUB, T. R. 2012. Tumour micro-environment elicits innate resistance to RAF inhibitors through HGF secretion. *Nature*, 487, 500-4.
- SUN, G., REDDY, M. A., YUAN, H., LANTING, L., KATO, M. & NATARAJAN, R. 2010. Epigenetic histone methylation modulates fibrotic gene expression. *J Am Soc Nephrol*, 21, 2069-80.
- SUN, K., TANG, S., HOU, Y., XI, L., CHEN, Y., YIN, J., PENG, M., ZHAO, M., CUI, X. & LIU, M. 2019. Oxidized ATM-mediated glycolysis enhancement in breast cancer-associated fibroblasts contributes to tumor invasion through lactate as metabolic coupling. *EBioMedicine*, 41, 370-383.
- SUN, K. H., CHANG, Y., REED, N. I. & SHEPPARD, D. 2016. alpha-Smooth muscle actin is an inconsistent marker of fibroblasts responsible for force-dependent TGFbeta activation or collagen production across multiple models of organ fibrosis. *Am J Physiol Lung Cell Mol Physiol*, 310, L824-36.
- SUROWIAK, P., MURAWA, D., MATERNA, V., MACIEJCZYK, A., PUDELKO, M., CIESLA, S., BREBOROWICZ, J., MURAWA, P., ZABEL, M., DIETEL, M. & LAGE, H. 2007. Occurrence of stromal myofibroblasts in the invasive ductal breast cancer tissue is an unfavourable prognostic factor. *Anticancer Res*, 27, 2917-24.
- SUTENDRA, G., DROMPARIS, P., KINNAIRD, A., STENSON, T. H., HAROMY, A., PARKER, J. M., MCMURTRY, M. S. & MICHELAKIS, E. D. 2013. Mitochondrial activation by inhibition of PDKII suppresses HIF1a signaling and angiogenesis in cancer. *Oncogene*, 32, 1638-50.
- SUTENDRA, G., KINNAIRD, A., DROMPARIS, P., PAULIN, R., STENSON, T. H., HAROMY, A., HASHIMOTO, K., ZHANG, N., FLAIM, E. & MICHELAKIS, E. D. 2014. A nuclear pyruvate dehydrogenase complex is important for the generation of acetyl-CoA and histone acetylation. *Cell*, 158, 84-97.
- TAKAHASHI, H., SAKAKURA, K., KUDO, T., TOYODA, M., KAIRA, K., OYAMA, T. & CHIKAMATSU, K. 2017. Cancer-associated fibroblasts promote an immunosuppressive microenvironment through the induction and accumulation of protumoral macrophages. *Oncotarget*, 8, 8633-8647.
- TAKEDA, Y., TSUJINO, K., KIJIMA, T. & KUMANOGOH, A. 2014. Efficacy and safety of pirfenidone for idiopathic pulmonary fibrosis. *Patient Prefer Adherence*, 8, 361-70.

- TANAKA, H., OKADA, T., KONISHI, H. & TSUJI, T. 1993. The effect of reactive oxygen species on the biosynthesis of collagen and glycosaminoglycans in cultured human dermal fibroblasts. *Arch Dermatol Res*, 285, 352-5.
- TANG, L., ZENG, J., GENG, P., FANG, C., WANG, Y., SUN, M., WANG, C., WANG, J., YIN, P., HU, C., GUO, L., YU, J., GAO, P., LI, E., ZHUANG, Z., XU, G. & LIU, Y. 2018. Global Metabolic Profiling Identifies a Pivotal Role of Proline and Hydroxyproline Metabolism in Supporting Hypoxic Response in Hepatocellular Carcinoma. *Clin Cancer Res*, 24, 474-485.
- TANG, X., HOU, Y., YANG, G., WANG, X., TANG, S., DU, Y. E., YANG, L., YU, T., ZHANG, H., ZHOU, M., WEN, S., XU, L. & LIU, M. 2016. Stromal miR-200s contribute to breast cancer cell invasion through CAF activation and ECM remodeling. *Cell Death Differ*, 23, 132-45.
- TANG, X., PENG, R., REN, Y., APPARSUNDARAM, S., DEGUZMAN, J., BAUER, C. M., HOFFMAN, A. F., HAMILTON, S., LIANG, Z., ZENG, H., FUENTES, M. E., DEMARTINO, J. A., KITSON, C., STEVENSON, C. S. & BUDD, D. C. 2013. BET bromodomain proteins mediate downstream signaling events following growth factor stimulation in human lung fibroblasts and are involved in bleomycin-induced pulmonary fibrosis. *Mol Pharmacol*, 83, 283-93.
- TANNER, J. J., FENDT, S.-M. & BECKER, D. F. 2018. The Proline Cycle As a Potential Cancer Therapy Target. *Biochemistry*, 57, 3433-3444.
- TEN DIJKE, P. & ARTHUR, H. M. 2007. Extracellular control of TGFbeta signalling in vascular development and disease. *Nat Rev Mol Cell Biol*, 8, 857-69.
- THAPA, D., ZHANG, M., MANNING, J. R., GUIMARAES, D. A., STONER, M. W., O'DOHERTY, R. M., SHIVA, S. & SCOTT, I. 2017. Acetylation of mitochondrial proteins by GCN5L1 promotes enhanced fatty acid oxidation in the heart. *Am J Physiol Heart Circ Physiol*, 313, H265-H274.
- TOMASEK, J. J., GABBIANI, G., HINZ, B., CHAPONNIER, C. & BROWN, R. A. 2002. Myofibroblasts and mechano-regulation of connective tissue remodelling. *Nat Rev Mol Cell Biol*, 3, 349-63.
- TORRES, S., BARTOLOME, R. A., MENDES, M., BARDERAS, R., FERNANDEZ-ACENERO, M. J., PELAEZ-GARCIA, A., PENA, C., LOPEZ-LUCENDO, M., VILLAR-VAZQUEZ, R., DE HERREROS, A. G., BONILLA, F. & CASAL, J. I. 2013. Proteome profiling of cancer-associated fibroblasts identifies novel proinflammatory signatures and prognostic markers for colorectal cancer. *Clin Cancer Res*, 19, 6006-19.
- TOULLEC, A., GERALD, D., DESPOUY, G., BOURACHOT, B., CARDON, M., LEFORT, S., RICHARDSON, M., RIGAILL, G., PARRINI, M. C., LUCCHESI, C., BELLANGER, D., STERN, M. H., DUBOIS, T., SASTRE-GARAU, X., DELATTRE, O., VINCENT-SALOMON, A. & MECHTA-GRIGORIOU, F. 2010. Oxidative stress promotes myofibroblast differentiation and tumour spreading. *EMBO Mol Med*, 2, 211-30.
- TRIMBOLI, A. J., FUKINO, K., DE BRUIN, A., WEI, G., SHEN, L., TANNER, S. M., CREASAP, N., ROSOL, T. J., ROBINSON, M. L., ENG, C., OSTROWSKI, M. C. & LEONE, G. 2008. Direct evidence for epithelial-mesenchymal transitions in breast cancer. *Cancer Res*, 68, 937-45.
- TYAN, S. W., KUO, W. H., HUANG, C. K., PAN, C. C., SHEW, J. Y., CHANG, K. J., LEE, E. Y. & LEE, W. H. 2011. Breast cancer cells induce cancer-associated fibroblasts to secrete hepatocyte growth factor to enhance breast tumorigenesis. *PLoS One*, 6, e15313.
- TYANOVA, S., TEMU, T., SINITCYN, P., CARLSON, A., HEIN, M. Y., GEIGER, T., MANN, M. & COX, J. 2016. The Perseus computational platform for comprehensive analysis of (prote)omics data. *Nat Methods*, 13, 731-40.
- UDABAGE, L., BROWNLEE, G. R., WALTHAM, M., BLICK, T., WALKER, E. C., HELDIN, P., NILSSON, S. K., THOMPSON, E. W. & BROWN, T. J. 2005. Antisense-mediated suppression of hyaluronan synthase 2 inhibits the tumorigenesis and progression of breast cancer. *Cancer Res*, 65, 6139-50.
- UNGER, C., KRAMER, N., UNTERLEUTHNER, D., SCHERZER, M., BURIAN, A., RUDISCH, A., STADLER, M., SCHLEDERER, M., LENHARDT, D., RIEDL, A., WALTER, S., WERNITZNIG, A., KENNER, L., HENGSTSCHLAGER, M., SCHULER, J.,

- SOMMERGRUBER, W. & DOLZNIG, H. 2017. Stromal-derived IGF2 promotes colon cancer progression via paracrine and autocrine mechanisms. *Oncogene*, 36, 5341-5355.
- VALENCIA, T., KIM, J. Y., ABU-BAKER, S., MOSCAT-PARDOS, J., AHN, C. S., REINA-CAMPOS, M., DURAN, A., CASTILLA, E. A., METALLO, C. M., DIAZ-MECO, M. T. & MOSCAT, J. 2014. Metabolic reprogramming of stromal fibroblasts through p62-mTORC1 signaling promotes inflammation and tumorigenesis. *Cancer Cell*, 26, 121-135.
- VETTESE-DADEY, M., GRANT, P. A., HEBBES, T. R., CRANE-ROBINSON, C., ALLIS, C. D. & WORKMAN, J. L. 1996. Acetylation of histone H4 plays a primary role in enhancing transcription factor binding to nucleosomal DNA in vitro. *EMBO J*, 15, 2508-18.
- VIZOSO, M., PUIG, M., CARMONA, F. J., MAQUEDA, M., VELASQUEZ, A., GOMEZ, A., LABERNADIE, A., LUGO, R., GABASA, M., RIGAT-BRUGAROLAS, L. G., TREPAT, X., RAMIREZ, J., MORAN, S., VIDAL, E., REGUART, N., PERERA, A., ESTELLER, M. & ALCARAZ, J. 2015. Aberrant DNA methylation in non-small cell lung cancer-associated fibroblasts. *Carcinogenesis*, 36, 1453-63.
- WANG, L., ZOU, X., BERGER, A. D., TWISS, C., PENG, Y., LI, Y., CHIU, J., GUO, H., SATAGOPAN, J., WILTON, A., GERALD, W., BASCH, R., WANG, Z., OSMAN, I. & LEE, P. 2009. Increased expression of histone deacetylases (HDACs) and inhibition of prostate cancer growth and invasion by HDAC inhibitor SAHA. *Am J Transl Res*, 1, 62-71.
- WANG, W., KRYCZEK, I., DOSTAL, L., LIN, H., TAN, L., ZHAO, L., LU, F., WEI, S., MAJ, T., PENG, D., HE, G., VATAN, L., SZELIGA, W., KUICK, R., KOTARSKI, J., TARKOWSKI, R., DOU, Y., RATTAN, R., MUNKARAH, A., LIU, J. R. & ZOU, W. 2016. Effector T Cells Abrogate Stroma-Mediated Chemoresistance in Ovarian Cancer. *Cell*, 165, 1092-1105.
- WATSON, C. J., HORGAN, S., NEARY, R., GLEZEVA, N., TEA, I., CORRIGAN, N., MCDONALD, K., LEDWIDGE, M. & BAUGH, J. 2016. Epigenetic Therapy for the Treatment of Hypertension-Induced Cardiac Hypertrophy and Fibrosis. *J Cardiovasc Pharmacol Ther*, 21, 127-37.
- WEAVER, V. M., LELIEVRE, S., LAKINS, J. N., CHRENEK, M. A., JONES, J. C., GIANCOTTI, F., WERB, Z. & BISSELL, M. J. 2002. beta4 integrin-dependent formation of polarized three-dimensional architecture confers resistance to apoptosis in normal and malignant mammary epithelium. *Cancer Cell*, 2, 205-16.
- WEI, S. C., FATTET, L. & YANG, J. 2015. The forces behind EMT and tumor metastasis. *Cell Cycle*, 14, 2387-8.
- WEINERT, B. T., IESMANTAVICIUS, V., MOUSTAFA, T., SCHOLZ, C., WAGNER, S. A., MAGNES, C., ZECHNER, R. & CHOUDHARY, C. 2014. Acetylation dynamics and stoichiometry in *Saccharomyces cerevisiae*. *Mol Syst Biol*, 10, 716.
- WELLEN, K. E., HATZIVASSILIOU, G., SACHDEVA, U. M., BUI, T. V., CROSS, J. R. & THOMPSON, C. B. 2009. ATP-citrate lyase links cellular metabolism to histone acetylation. *Science*, 324, 1076-80.
- WEN, S., HOU, Y., FU, L., XI, L., YANG, D., ZHAO, M., QIN, Y., SUN, K., TENG, Y. & LIU, M. 2019. Cancer-associated fibroblast (CAF)-derived IL32 promotes breast cancer cell invasion and metastasis via integrin beta3-p38 MAPK signalling. *Cancer Lett*, 442, 320-332.
- WESLEY, R. B., 2ND, MENG, X., GODIN, D. & GALIS, Z. S. 1998. Extracellular matrix modulates macrophage functions characteristic to atheroma: collagen type I enhances acquisition of resident macrophage traits by human peripheral blood monocytes in vitro. *Arterioscler Thromb Vasc Biol*, 18, 432-40.
- WHITAKER-MENEZES, D., MARTINEZ-OUTSCHOORN, U. E., FLOMENBERG, N., BIRBE, R. C., WITKIEWICZ, A. K., HOWELL, A., PAVLIDES, S., TSIRIGOS, A., ERTEL, A., PESTELL, R. G., BRODA, P., MINETTI, C., LISANTI, M. P. & SOTGIA, F. 2011a. Hyperactivation of oxidative mitochondrial metabolism in epithelial cancer cells in situ: visualizing the therapeutic effects of metformin in tumor tissue. *Cell Cycle*, 10, 4047-64.
- WHITAKER-MENEZES, D., MARTINEZ-OUTSCHOORN, U. E., LIN, Z., ERTEL, A., FLOMENBERG, N., WITKIEWICZ, A. K., BIRBE, R. C., HOWELL, A., PAVLIDES, S., GANDARA, R., PESTELL, R. G., SOTGIA, F., PHILP, N. J. & LISANTI, M. P. 2011b.

- Evidence for a stromal-epithelial "lactate shuttle" in human tumors: MCT4 is a marker of oxidative stress in cancer-associated fibroblasts. *Cell Cycle*, 10, 1772-83.
- WITZE, E. S., OLD, W. M., RESING, K. A. & AHN, N. G. 2007. Mapping protein post-translational modifications with mass spectrometry. *Nat Methods*, 4, 798-806.
- WONDRAK, G. T., JACOBSON, M. K. & JACOBSON, E. L. 2005. Identification of quenchers of photoexcited States as novel agents for skin photoprotection. *J Pharmacol Exp Ther*, 312, 482-91.
- WU, G., BAZER, F. W., BURGHARDT, R. C., JOHNSON, G. A., KIM, S. W., KNABE, D. A., LI, P., LI, X., MCKNIGHT, J. R., SATTERFIELD, M. C. & SPENCER, T. E. 2011. Proline and hydroxyproline metabolism: implications for animal and human nutrition. *Amino Acids*, 40, 1053-63.
- WYSOCKA, J. 2006. Identifying novel proteins recognizing histone modifications using peptide pull-down assay. *Methods*, 40, 339-43.
- XIONG, C., MASUCCI, M. V., ZHOU, X., LIU, N., ZANG, X., TOLBERT, E., ZHAO, T. C. & ZHUANG, S. 2016. Pharmacological targeting of BET proteins inhibits renal fibroblast activation and alleviates renal fibrosis. *Oncotarget*, 7, 69291-69308.
- YAMAGUCHI, H., YOSHIDA, N., TAKANASHI, M., ITO, Y., FUKAMI, K., YANAGIHARA, K., YASHIRO, M. & SAKAI, R. 2014. Stromal fibroblasts mediate extracellular matrix remodeling and invasion of scirrhous gastric carcinoma cells. *PLoS One*, 9, e85485.
- YAN, W., WU, X., ZHOU, W., FONG, M. Y., CAO, M., LIU, J., LIU, X., CHEN, C. H., FADARE, O., PIZZO, D. P., WU, J., LIU, L., LIU, X., CHIN, A. R., REN, X., CHEN, Y., LOCASALE, J. W. & WANG, S. E. 2018. Cancer-cell-secreted exosomal miR-105 promotes tumour growth through the MYC-dependent metabolic reprogramming of stromal cells. *Nat Cell Biol*, 20, 597-609.
- YANG, L., ACHREJA, A., YEUNG, T. L., MANGALA, L. S., JIANG, D., HAN, C., BADDOUR, J., MARINI, J. C., NI, J., NAKAHARA, R., WAHLIG, S., CHIBA, L., KIM, S. H., MORSE, J., PRADEEP, S., NAGARAJA, A. S., HAEMMERLE, M., KYUNGHEE, N., DERICHSWEILER, M., PLACKEMEIER, T., MERCADO-URIBE, I., LOPEZ-BERESTEIN, G., MOSS, T., RAM, P. T., LIU, J., LU, X., MOK, S. C., SOOD, A. K. & NAGRATH, D. 2016. Targeting Stromal Glutamine Synthetase in Tumors Disrupts Tumor Microenvironment-Regulated Cancer Cell Growth. *Cell Metab*, 24, 685-700.
- YAO, J., IRWIN, R. W., ZHAO, L., NILSEN, J., HAMILTON, R. T. & BRINTON, R. D. 2009. Mitochondrial bioenergetic deficit precedes Alzheimer's pathology in female mouse model of Alzheimer's disease. *Proc Natl Acad Sci U S A*, 106, 14670-5.
- YEAMAN, S. J., HUTCHESON, E. T., ROCHE, T. E., PETTIT, F. H., BROWN, J. R., REED, L. J., WATSON, D. C. & DIXON, G. H. 1978. Sites of phosphorylation on pyruvate dehydrogenase from bovine kidney and heart. *Biochemistry*, 17, 2364-70.
- YEUNG, T. L., LEUNG, C. S., WONG, K. K., SAMIMI, G., THOMPSON, M. S., LIU, J., ZAID, T. M., GHOSH, S., BIRRER, M. J. & MOK, S. C. 2013. TGF-beta modulates ovarian cancer invasion by upregulating CAF-derived versican in the tumor microenvironment. *Cancer Res*, 73, 5016-28.
- YONASHIRO, R., EGUCHI, K., WAKE, M., TAKEDA, N. & NAKAYAMA, K. 2018. Pyruvate Dehydrogenase PDH-E1beta Controls Tumor Progression by Altering the Metabolic Status of Cancer Cells. *Cancer Res*, 78, 1592-1603.
- YU, B., CHEN, X., LI, J., QU, Y., SU, L., PENG, Y., HUANG, J., YAN, J., YU, Y., GU, Q., ZHU, Z. & LIU, B. 2013. Stromal fibroblasts in the microenvironment of gastric carcinomas promote tumor metastasis via upregulating TAGLN expression. *BMC Cell Biology*, 14.
- YU, T., YANG, G., HOU, Y., TANG, X., WU, C., WU, X. A., GUO, L., ZHU, Q., LUO, H., DU, Y. E., WEN, S., XU, L., YIN, J., TU, G. & LIU, M. 2017. Cytoplasmic GPER translocation in cancer-associated fibroblasts mediates cAMP/PKA/CREB/glycolytic axis to confer tumor cells with multidrug resistance. *Oncogene*, 36, 2131-2145.
- YU, Y., XIAO, C. H., TAN, L. D., WANG, Q. S., LI, X. Q. & FENG, Y. M. 2014. Cancer-associated fibroblasts induce epithelial-mesenchymal transition of breast cancer cells through paracrine TGF-beta signalling. *Br J Cancer*, 110, 724-32.

- ZEISBERG, E. M., POTENTA, S., XIE, L., ZEISBERG, M. & KALLURI, R. 2007. Discovery of endothelial to mesenchymal transition as a source for carcinoma-associated fibroblasts. *Cancer Res*, 67, 10123-8.
- ZHANG, D., WANG, Y., SHI, Z., LIU, J., SUN, P., HOU, X., ZHANG, J., ZHAO, S., ZHOU, B. P. & MI, J. 2015. Metabolic reprogramming of cancer-associated fibroblasts by IDH3alpha downregulation. *Cell Rep*, 10, 1335-48.
- ZHANG, X., JI, R., LIAO, X., CASTILLERO, E., KENNEL, P. J., BRUNJES, D. L., FRANZ, M., MOBIUS-WINKLER, S., DROSATOS, K., GEORGE, I., CHEN, E. I., COLOMBO, P. C. & SCHULZE, P. C. 2018. MicroRNA-195 Regulates Metabolism in Failing Myocardium Via Alterations in Sirtuin 3 Expression and Mitochondrial Protein Acetylation. *Circulation*, 137, 2052-2067.
- ZHANG, Y., MA, K., SADANA, P., CHOWDHURY, F., GAILLARD, S., WANG, F., MCDONNELL, D. P., UNTERMAN, T. G., ELAM, M. B. & PARK, E. A. 2006. Estrogen-related receptors stimulate pyruvate dehydrogenase kinase isoform 4 gene expression. *J Biol Chem*, 281, 39897-906.
- ZHAO, G., JEOUNG, N. H., BURGESS, S. C., ROSAAEN-STOWE, K. A., INAGAKI, T., LATIF, S., SHELTON, J. M., MCANALLY, J., BASSEL-DUBY, R., HARRIS, R. A., RICHARDSON, J. A. & KLIEWER, S. A. 2008. Overexpression of pyruvate dehydrogenase kinase 4 in heart perturbs metabolism and exacerbates calcineurin-induced cardiomyopathy. *Am J Physiol Heart Circ Physiol*, 294, H936-43.
- ZHAO, H., YANG, L., BADDOUR, J., ACHREJA, A., BERNARD, V., MOSS, T., MARINI, J. C., TUDAWE, T., SEVIOUR, E. G., SAN LUCAS, F. A., ALVAREZ, H., GUPTA, S., MAITI, S. N., COOPER, L., PEEHL, D., RAM, P. T., MAITRA, A. & NAGRATH, D. 2016. Tumor microenvironment derived exosomes pleiotropically modulate cancer cell metabolism. *Elife*, 5, e10250.
- ZHENG, Y., DE LA CRUZ, C. C., SAYLES, L. C., ALLEYNE-CHIN, C., VAKA, D., KNAAK, T. D., BIGOS, M., XU, Y., HOANG, C. D., SHRAGER, J. B., FEHLING, H. J., FRENCH, D., FORREST, W., JIANG, Z., CARANO, R. A., BARCK, K. H., JACKSON, E. L. & SWEET-CORDERO, E. A. 2013. A rare population of CD24(+)ITGB4(+)Notch(hi) cells drives tumor propagation in NSCLC and requires Notch3 for self-renewal. *Cancer Cell*, 24, 59-74.
- ZIANI, L., CHOUAIB, S. & THIERY, J. 2018. Alteration of the Antitumor Immune Response by Cancer-Associated Fibroblasts. *Front Immunol*, 9, 414.
- ZOU, X., ZHU, Y., PARK, S. H., LIU, G., O'BRIEN, J., JIANG, H. & GIUS, D. 2017. SIRT3-Mediated Dimerization of IDH2 Directs Cancer Cell Metabolism and Tumor Growth. *Cancer Res*, 77, 3990-3999.